TECHNISCHE UNIVERSITÄT DARMSTADT

Asymptotic Analysis and Numerical Approximation of some Partial Differential Equations on Networks

Vom Fachbereich Mathematik
der Technischen Universität Darmstadt
zur Erlangung des Grades eines
Doktors der Naturwissenschaften
(Dr. rer. nat.)
genehmigte Dissertation

von

Nora Marie Philippi, M.Sc.

aus Wiesbaden

Referent: Prof. Dr. Herbert Egger

1. Korreferent: Prof. Dr. Jan Giesselmann

2. Korreferent: Prof. Dr. Günter Leugering

Tag der Einreichung: 5. Juli 2023

Tag der mündlichen Prüfung: 28. August 2023

Darmstadt 2023
D17

Asymptotic Analysis and Numerical Approximation of some Partial Differential Equations on Networks

Accepted doctoral thesis by Nora Marie Philippi, M.Sc.

Darmstadt, Technische Universität Darmstadt

Date of thesis defense: August 28, 2023
Year of publication on TUprints: 2023

Abstract

In this thesis, we consider three different model problems on one-dimensional networks with applications in gas, water supply, and district heating networks, as well as bacterial chemotaxis. On each edge of the graph representing the network, the dynamics are described by partial differential equations. Additional coupling conditions at network junctions are needed to ensure basic physical principles and to obtain well-posed systems. Each of the model problems under consideration contains an asymptotic parameter $\varepsilon > 0$, which is assumed to be small, describing either a singular perturbation, different modeling scales, or different physical regimes. A central objective of this work is the investigation of the asymptotic behavior of solutions for $\varepsilon \to 0$. Moreover, we focus on suitable numerical approximations based on Galerkin methods that are still viable in the asymptotic limit $\varepsilon = 0$ and preserve the structure and basic properties of the underlying problems.

In the first part, we consider singularly perturbed convection-diffusion equations on networks as well as the corresponding pure transport equations arising in the vanishing diffusion limit $\varepsilon \to 0$, in which the coupling conditions change in number and type. This gives rise to interior boundary layers at network junctions. On a single interval, corresponding asymptotic estimates are well-established. A main contribution is the transfer of these results to networks. For an appropriate numerical approximation, we propose a hybrid discontinuous Galerkin method which is particularly suitable for dominating convection and coupling at network junctions. An approximation strategy is developed based on layer-adapted meshes, leading to ε-uniform error estimates.

The second part is dedicated to a kinetic model of chemotaxis on networks describing the movement of bacteria being influenced by the presence of a chemical substance. Via a suitable scaling the classical Keller-Segel equations can be derived in the diffusion limit. We propose a proper set of coupling conditions that ensure the conservation of mass and lead to a well-posed problem. The local existence of solutions uniformly in the scaling can be established via fixed point arguments. Appropriate a-priori estimates then enable us to rigorously show the convergence of solutions to the diffusion limit. Via asymptotic expansions, we also establish a quantitative asymptotic estimate.

In the last part, we focus on models for gas transport in pipe networks starting from the non-isothermal Euler equations with friction and heat exchange with the surroundings. An appropriate rescaling of the equations accounting for the large friction, large heat transfer, and low Mach regime leads to simplified isothermal models in the limit $\varepsilon \to 0$. We propose a fully discrete approximation of the isothermal Euler equations using a mixed finite element approach. Based on a reformulation of the equations and relative energy estimates, we derive convergence estimates that hold uniformly in the scaling to a parabolic gas model. We finally extend some ideas and results also to the non-isothermal regime.

Zusammenfassung

In dieser Arbeit betrachten wir drei verschiedene Modellprobleme auf eindimensionalen Netzwerken mit Anwendung in Gas-, Wasser-, und Fernwärmenetzwerken sowie in bakterieller Chemotaxis. Auf jeder Kante des Graphen, welcher das Netzwerk beschreibt, ist die Dynamik durch eine partielle Differentialgleichung beschrieben. Zusätzliche Kopplungsbedingungen an inneren Knoten werden zur Erhaltung von physikalischen Grundprinzipien gebraucht. Jedes der drei Modellprobleme enthält einen asymptotischen Parameter $\varepsilon > 0$, der entweder eine singuläre Störung, verschiedene Größenskalen oder physikalische Regimes beschreibt. Zentrales Ziel der Arbeit ist die Untersuchung des asymptotischen Verhaltens von Lösungen für $\varepsilon \to 0$. Darüber hinaus betrachten wir geeignete numerische Approximationen basierend auf Galerkin Verfahren, die auch für $\varepsilon = 0$ gültig sind und die Struktur sowie grundlegende Eigenschaften der Probleme erhalten.

Im ersten Teil befassen wir uns mit singulär gestörten Konvektions-Diffusionsgleichungen auf Netzwerken und die dazugehörigen Transportgleichungen, die wir im Grenzwert $\varepsilon \to 0$ für verschwindene Diffusion erhalten. Die Anzahl und der Typ von Kopplungsbedingungen ändern sich, was zu Grenzschichten an inneren Netzwerkknoten führt. Auf einem Intervall sind zugehörige asymptotische Abschätzungen wohlbekannt. Ein wesentlicher Beitrag unserer Arbeit ist die Erweiterung auf Netzwerke. Für die numerische Approximation schlagen wir eine hybride Discontinuous Galerkin Methode vor, die besonders für dominierende Konvektion sowie die Kopplung an Netzwerkknoten geeignet ist. Eine adaptive Approximationsstrategie auf layer-adapted Gittern liefert ε-uniforme Fehlerschranken.

Im zweiten Teil der Arbeit geht es um ein kinetisches Modell für Chemotaxis auf Netzwerken, welches die Fortbewegung von Bakterien unter Einfluss einer chemischen Substanz beschreibt. Mittels einer geeigneten Reskalierung erhalten wir das klassische Keller-Segel Modell im Diffusionsgrenzwert. Wir schlagen geeignete Kopplungsbedingungen an Netzwerkknoten vor, die zu einem wohlgestellten Problem führen. Die lokale Existenz von Lösungen uniform in ε kann mittels Fixpunktargumenten gezeigt werden. A-priori Schranken erlauben es uns dann die Konvergenz von Lösungen zum Diffusiongrenzwert zu zeigen. Wir leiten außerdem eine quantitative asymptotische Abschätzung her.

Im letzten Teil der Arbeit untersuchen wir Modelle für den Gastransport in Rohrnetzwerken. Ausgehend von den nicht-isothermen Eulergleichungen mit Reibung und Wärmeaustausch mit der Umgebung führt eine geeignete Reskalierung hinsichtlich großer Reibung, hohem Wärmeaustausch und kleiner Geschwindigkeiten zu vereinfachten isothermen Modellen im Grenzwert $\varepsilon \to 0$. Wir analysieren eine gemischte Finite Elemente Methode für den isothermen Gastransport. Mittels relativen Energieabschätzungen können wir Konvergenz des Verfahrens mit Raten uniform in ε zeigen. Schließlich erweitern wir unsere Betrachtungen auf den nicht-isothermen Fall.

Acknowledgments

First and foremost I would like to thank my supervisor Prof. Herbert Egger for his support and guidance throughout my time as his PhD student. I am very grateful to have had him as my mentor and teacher. He always took time for questions and discussions and I learned so much from him.

Moreover, I want to express my gratitude to my co-workers Prof. Jan Giesselmann, Kathrin Hellmuth, Teresa Kunkel, and Prof. Matthias Schlottbom. I genuinely enjoyed doing math together, learning from each other, and having plenty of fruitful discussions.

I am very thankful for the financial support from the German Research Foundation (DFG) via the CRC TRR 154 "Mathematical modelling, simulation and optimization using the example of gas network" in subproject C04. Being part of this project offered me a vibrant research environment and gave me the opportunity to meet many interesting people. In particular, I would like to thank my mentor Prof. Volker Mehrmann.

I also want to thank Elisa, Kathrin, and Teresa for proofreading this thesis.

Special thanks go to my colleagues and friends from Darmstadt and Linz, in particular to my office mate Bogdan, who accompanied me on this journey and made it an unforgettable one! I enjoyed the mathematical and non-mathematical discussions, the many lunches and dinners, the board game nights, and all the laughs we shared.

Last but not least, I want to thank my parents and friends for their support throughout this time. And N for always being by my side.

Contents

Introduction **1**

1. Transport and convection-diffusion equations on networks **5**
1.1. Model problems . . . 9
1.1.1. Notation and function spaces . . . 9
1.1.2. Transport problem . . . 10
1.1.3. Convection-diffusion problem . . . 15
1.2. Asymptotic analysis . . . 18
1.2.1. Auxiliary results . . . 19
1.2.2. Proof of Theorem 1.7 . . . 22
1.3. Numerical approximation . . . 25
1.3.1. Mesh and approximation spaces . . . 26
1.3.2. Semi-discrete hybrid-dG method . . . 27
1.3.3. Fully discrete hybrid-dG method . . . 32
1.3.4. ε-Uniform error estimates . . . 37
1.4. Numerical illustration . . . 40
1.4.1. Contaminant transport in water supply networks . . . 40
1.4.2. Transport of gas mixtures in pipe networks . . . 43
1.5. Discussion and outlook . . . 45

2. Kinetic chemotaxis and diffusion limits on networks **47**
2.1. Model problem . . . 51
2.1.1. Notation and function spaces . . . 51
2.1.2. Kinetic model for chemotaxis on networks . . . 53
2.2. Existence of solutions . . . 55
2.2.1. Linearized problem for the chemoattractant . . . 56
2.2.2. Linearized kinetic problem . . . 57
2.2.3. Proof of Theorem 2.3 . . . 60
2.3. Asymptotic analysis . . . 64
2.3.1. The limit problem . . . 64
2.3.2. Convergence to the limit problem . . . 66
2.3.3. Quantitative convergence estimates . . . 70
2.4. Discussion and outlook . . . 75

3. Gas transport in pipe networks **77**
3.1. Isothermal gas transport . . . 81
3.1.1. Preliminaries . . . 81
3.1.2. Model problem . . . 83
3.1.3. Weak formulation . . . 84
3.1.4. Basic properties . . . 85
3.1.5. Main assumptions . . . 86
3.1.6. Relative energy . . . 86
3.1.7. Asymptotic analysis . . . 88
3.2. Numerical approximation of the isothermal gas transport . . . 89
3.2.1. Mesh and approximation spaces . . . 90
3.2.2. Structure-preserving discretization scheme . . . 90
3.2.3. Uniform error estimate . . . 92
3.2.4. Proof of the uniform error estimate . . . 92
3.2.5. Proof of the technical results . . . 95
3.3. Non-isothermal gas transport . . . 102
3.3.1. Preliminaries . . . 102
3.3.2. Model problem . . . 103
3.3.3. Weak formulation . . . 105
3.3.4. Basic properties . . . 106
3.4. Numerical approximation of the non-isothermal gas transport . . . 109
3.4.1. Mesh and approximation spaces . . . 109
3.4.2. Structure-preserving discretization scheme . . . 111
3.4.3. Discrete balance laws . . . 112
3.5. Numerical illustration . . . 116
3.5.1. Isothermal gas transport . . . 117
3.5.2. Non-isothermal gas transport . . . 119
3.6. Discussion and outlook . . . 121

Conclusion **123**

A. Appendix **125**
A.1. Verification of (E1)–(E3) in the proof of Theorem 3.5 . . . 125
A.2. Discrete Grönwall lemma . . . 127

Bibliography **129**

Introduction

Partial differential equations on networks model a variety of processes of interest. In this thesis, we consider three different model problems with applications to gas networks, water supply and district heating networks, and bacterial chemotaxis on networks. Part of this work was developed within the Collaborative Research Center *TRR 154 on Mathematical modelling, simulation, and optimization using the example of gas networks.*

A network is described as a one-dimensional graph that consists of vertices connected by edges. On each edge, the dynamics of interest is modeled by partial differential equations. In order to obtain a well-posed problem, additional coupling conditions at interior vertices connecting the solutions in the edges are needed. The derivation of a proper set of conditions ensuring that basic physical principles hold, in particular conservation of mass, is crucial. The main focus of this work is on asymptotic aspects, i.e., all model problems contain a scaling parameter $\varepsilon > 0$, which is assumed to be small, describing either a singular perturbation, different length or time scales, or different physical regimes. We are interested in the well-posedness of the problems, i.e., in the existence and uniqueness of solutions as well as the stability with respect to data, uniformly in the scaling parameter ε. The investigation of the asymptotic behavior of solutions for $\varepsilon \to 0$ is a central objective of this work. We also focus on the appropriate numerical approximation of the model problems based on Galerkin methods that, in particular, preserve the underlying structure and basic properties. This enables us to exploit techniques from the continuous analysis for the error estimation of the methods. Special emphasis is on the asymptotic behavior and stability, in particular, the schemes should still be viable in the asymptotic limit $\varepsilon = 0$.

Let us now give a brief overview of the content and main contributions of each chapter. A self-contained and thorough introduction to each of the three model problems under consideration is given at the beginning of the corresponding chapter.

Chapter 1: Transport and convection-diffusion equations on networks

In the first chapter, we consider singularly perturbed convection-diffusion equations on networks and the corresponding pure transport equations that arise in the vanishing diffusion limit $\varepsilon \to 0$. Applications can be found in the context of water supply, district heating, and gas networks. The well-posedness of both problems can be established via semigroup theory. We are particularly interested in the asymptotic behavior of solutions. An essential feature of this problem is that coupling conditions at network junctions change in number and type in the limit $\varepsilon = 0$ leading to additional interior layers. On a single interval and for

appropriate initial conditions, it is well-known that solutions to the convection-diffusion problem converge to the limiting transport problem with order $\mathcal{O}(\sqrt{\varepsilon})$ in the $L^\infty(L^2)$-norm [8]. A main contribution of our work is the extension of this observation to networks. Our results were published together with a complete analysis of the pure transport and the convection-diffusion problem in

> H. Egger and N. Philippi. On the transport limit of singularly perturbed convection-diffusion problems on networks. *Math. Methods Appl. Sci.*, 2021.

The second part of this chapter is dedicated to an appropriate numerical approximation. We propose a hybrid discontinuous Galerkin (dG) method that is particularly well-suited for convection-dominated problems and can handle the coupling conditions at network junctions. Moreover, it yields a viable approximation for the transport limit $\varepsilon = 0$. The hybrid-dG scheme for the pure transport problem was first presented in

> H. Egger and N. Philippi. A hybrid discontinuous Galerkin method for transport equations on networks. In *Finite volumes for complex applications IX—methods, theoretical aspects, examples—FVCA 9, Bergen, Norway, June 2020*, volume 323 of *Springer Proc. Math. Stat.*, Springer, Cham, 2020.

A complete analysis on the continuous level, as well as error estimates for the method, are given therein. In a second publication

> H. Egger and N. Philippi. A hybrid-dG method for singularly perturbed convection-diffusion equations on pipe networks. *ESAIM: M2AN*, 2023.

we then investigated the hybrid-dG semi-discretization for singularly perturbed convection-diffusion equations on networks. We proposed a suitable approximation strategy on layer-adapted meshes, which are a well-known tool to handle boundary layers [109], and we provided ε-uniform error estimates. As a new aspect in this thesis, we give a complete analysis of the fully discretized problem using a dG approach for the time discretization, leading to high-order approximations for all values of $\varepsilon \geq 0$.

Chapter 2: Kinetic chemotaxis and diffusion limits on networks

The second chapter is concerned with chemotaxis on networks describing the movement of bacteria or cells that is influenced by the presence of a chemical substance. Applications can be found in dermal wound healing and the growth of slime molds. A way to model these processes is by kinetic equations where variables additionally depend on the velocity [99]. In the diffusion limit, chemotaxis can be described by the classical Keller-Segel equations [66, 69], which can be derived from the kinetic model by an appropriate scaling and asymptotic expansions [19]. On networks, coupling conditions at interior vertices ensuring the conservation of mass are needed. We propose suitable conditions that converge to the corresponding ones for the Keller-Segel system on networks; see e.g. [9, 113]. The main focus of this chapter is the asymptotic analysis of the kinetic model and its diffusion limit on networks. We show the local existence of solutions uniformly in the scaling via Banach's

fixed point theorem and standard arguments. Suitable a-priori estimates enable us to show that solutions converge to weak solutions of the Keller-Segel system on networks in the diffusion limit $\varepsilon \to 0$. Moreover, by exploiting asymptotic expansions [27], we derive a quantitative asymptotic estimate stating that solutions to the kinetic model converge to the diffusion limit with order $\mathcal{O}(\sqrt{\varepsilon})$ in the $L^\infty(L^2)$-norm. The content of this chapter is joint work with *Herbert Egger, Kathrin Hellmuth,* and *Matthias Schlottbom.* A publication is in preparation.

Chapter 3: Gas Transport in pipe networks

In the last chapter, we focus on models for gas transport in pipe networks starting from the non-isothermal Euler system with quadratic friction law and heat exchange with the surroundings. A suitable rescaling of the equations to the relevant scales in gas networks, i.e., long pipes and time scales, large friction and heat transfer, as well as small velocities (low Mach), leads to simplified models [15]. In the limit $\varepsilon \to 0$, we obtain a parabolic gas transport model that is widely used and has been thoroughly investigated [3, 105], whereas an intermediate simplification is given by the isothermal Euler equations with friction.

In the first part of this chapter, we consider the isothermal gas transport in pipe networks. The stability and, in particular, the asymptotic behavior of solutions has recently been investigated in [37]. The analysis therein is based on a suitable reformulation of the model equations having an "energy structure" that allows the use of relative energy estimates [26] for measuring the distance between (perturbed) solutions. Here, we present a suitable numerical approximation of the isothermal gas transport model based on a mixed finite element approach in space and an implicit Euler time discretization that, in particular, yields a viable approximation method for the parabolic problem in the limit $\varepsilon = 0$ and preserves the underlying structure of the system. This in turn allows us to use the relative energy for deriving rigorous error estimates with convergence rates that are uniform in the scaling parameter ε and hold under the assumption that sufficiently regular subsonic solutions bounded away from vacuum exist. This result was published in

> H. Egger, J. Giesselmann, T. Kunkel, and N. Philippi. An asymptotic-preserving discretization scheme for gas transport in pipe networks. *IMA Journal of Numerical Analysis*, 2022.

The second part of this chapter is dedicated to the extension of the main ideas to the non-isothermal gas transport in pipe networks. Suitable coupling conditions at junctions that ensure basic physical principles are introduced. Moreover, we propose a structure-preserving discretization scheme that extends the mixed finite element method for the isothermal gas transport and is complemented with a hybrid discontinuous Galerkin approach for the additional entropy transport. This method fulfills global balance laws and can be shown to dissipate energy under the assumption of subsonic flow bounded away from vacuum. A rigorous asymptotic analysis as well as the derivation of error estimates for the proposed method might be possible with similar techniques as for the isothermal gas transport but is left for future research. The results concerning the non-isothermal gas transport are first presented in this thesis.

1

Transport and convection-diffusion equations on networks

Transport processes in network structures model various physical phenomena including the transport of gas mixtures in pipe networks [78], the contaminant transport in water supply networks [85] or networks of 1D cracks [96], as well as the heat transport in district heating networks [64]. Related problems also appear in the modeling of traffic flow [55]. This chapter is devoted to the analysis and the numerical treatment of transport and convection-diffusion problems on finite networks described by one-dimensional graphs. In the following, we give an overview of the content and highlight the main contributions.

Problem setting

Let us first consider a single edge or interval on which the transport is described by

$$a(x)\partial_t u(x,t) + b\partial_x u(x,t) = 0, \qquad x \in (0,\ell),\ t > 0 \tag{1.1}$$

with u being the quantity of interest, e.g., the fraction of one gas component in the gas mixture, the concentration of the contaminant solved in the water flow, or the water temperature. The parameters $a > 0$ and $b > 0$ then model the network topology and the background flow. Equation (1.1) has to be complemented by suitable initial as well as boundary data at the inflow boundary $x = 0$ of the edge, i.e.,

$$u(0,t) = \hat{g}(t), \qquad t > 0. \tag{1.2}$$

Adding diffusion to (1.1) leads to the following problem

$$a(x)\partial_t u^\varepsilon(x,t) + b\partial_x u^\varepsilon(x,t) = \varepsilon\partial_{xx} u^\varepsilon(x,t), \qquad x \in (0,\ell),\ t > 0, \tag{1.3}$$

$$u^\varepsilon(x,t) = \hat{g}(t), \qquad x \in \{0,\ell\},\ t > 0 \tag{1.4}$$

with diffusion parameter $\varepsilon > 0$ that is assumed to be small. In contrast to the pure transport problem, boundary data now has to be prescribed at both ends of the edge.

Asymptotic analysis

We are particularly interested in the behavior of solutions to (1.3)–(1.4) for vanishing diffusion $\varepsilon \to 0$. It is well-known that the obsolete boundary condition at the outflow boundary $x = \ell$ in the limit problem (1.1)–(1.2) leads to a boundary layer. Initial layers are also possible but can be avoided by appropriate compatibility conditions on the boundary and initial data. Moreover, the derivatives of the convection-diffusion solution blow up within the boundary layer, i.e.,

$$|\partial_t^n \partial_x^k u^\varepsilon(x,t)| \leq C(1 + \varepsilon^{-k} e^{b(\ell - x)/\varepsilon}), \tag{1.5}$$

see [77, 104]. In contrast to the limiting pure transport problem (1.1)–(1.2), where solutions are smooth but violate the boundary condition at the outflow boundary $x = \ell$. It is well-known that the following asymptotic estimate holds

$$\|u^\varepsilon(t) - u(t)\|_{L^2(0,\ell)} \leq C\sqrt{\varepsilon}. \tag{1.6}$$

The proof is based on the construction of suitable boundary layer functions. We refer to [8] for the original reference and to [109, Ch. II.2] for a complete investigation of the asymptotic behaviour on a single interval.

Extension to networks

In this chapter, we consider transport problems on networks described by finite, connected, and directed graphs, and assume that (1.1) and (1.3) are satisfied on all edges which are identified by intervals. Additional coupling conditions at interior vertices are needed in order to connect the solutions in the individual edges and to ensure the conservation of mass. The well-posedness of both problems on networks can be established using semigroup theory. We refer to [46, 100] for a comprehensive overview. Semigroup methods for flow problems on networks have been widely investigated in the literature; see [94] for a thorough study of general evolution problems. Transport processes similar to (1.1) on networks were considered in [33, 79], wave and diffusion phenomena in [80], and convection-diffusion problems similar to (1.3) on networks in [96]. As the change in the number of boundary conditions on a single interval indicates, we also have a change in the number, but also in the type, of coupling conditions at network junctions in the asymptotic limit of vanishing diffusion $\varepsilon \to 0$. This leads to additional interior layers at junctions, more precisely at the outflow boundary of each edge. As a main result of this chapter, we show that the asymptotic estimate (1.6), as well as the bounds on the derivatives (1.5), carry over to networks. Related singularly perturbed problems on networks have been considered by other authors, we refer to [60] for the study of a general class of coupling conditions and to [4] for results concerning the optimal control. Singularly perturbed stationary reaction-diffusion problems on networks have been investigated in [82], and, very recently, a singularly perturbed stationary convection-diffusion problem on networks with non-constant coefficients has been analyzed in [83]. Vanishing diffusion approximations for scalar conservation laws in the context of traffic flow have been considered in [21].

Numerical approximation

The numerical approximation of pure transport and singularly perturbed convection-diffusion equations on networks is another main focus of this chapter. We first consider the spatial semi-discretization and apply a hybrid discontinuous Galerkin approach. Discontinuous Galerkin (dG) methods are well-suited for convection-dominated problems due to the build-in upwind mechanism for the transport part. We refer to [29] for a comprehensive overview. The hybrid variant of the dG method introduces additional hybrid variables at all grid points. Neighboring elements then only couple via these hybrid variables; see [20] for the original reference and [45, 53] for the application of a hybrid-dG method to convection-diffusion problems in dimension $d = 2, 3$. It turns out that this method allows for a very natural handling of the coupling conditions at network junctions. Moreover, by formally setting $\varepsilon = 0$ we obtain a viable method for the limiting transport problem. In order to obtain a fully discrete scheme, we need a suitable time discretization. For a balanced approximation order in space and time, we employ a high order dG method; see [48, 117].

Error analysis

We are particularly interested in the case of vanishing diffusion $\varepsilon \to 0$, where we know from (1.5) that the derivatives of the convection-diffusion solution blow up within the boundary and interior layers. Hence, a straightforward error analysis as elaborated in [29, 117] does not yield ε-uniform convergence on uniform grids. A standard way to overcome this issue is the use of layer-adapted meshes. We refer to [109] for a profound survey. Various numerical methods on such meshes were studied in the literature. Finite element approximations on layer-adapted meshes were widely investigated, e.g., by [24, 34, 107] and in the context of higher-order methods by [110]. Discontinuous Galerkin schemes on different layer-adapter meshes were considered by [114, 122]. In [83], an upwind finite difference method for a singularly perturbed stationary convection-diffusion problem on networks with a suitably set up Shishkin mesh on each edge was analyzed. In this work, we utilize a layer-adapted mesh similar to the one proposed by Gartland in [56] and later investigated in [108]. By defining a transition point $x^*(\varepsilon) \approx \varepsilon \log(1/\varepsilon)$, we split each edge into two parts, a smooth part $(0, x^*(\varepsilon))$ away from the boundary layer where the derivatives of u^ε up to a desired order are bounded, and a layer part $(x^*(\varepsilon), \ell)$. The spatial mesh is then chosen to be uniform in the smooth part and geometrically refined in the layer part. The choice of this transition point simplifies the error analysis on this layer-adapted mesh significantly, compared to the classical analysis on Shishkin-type meshes; see e.g. [110]. Since we know from the asymptotic estimate (1.6) that the solution to the pure transport problem is already a good approximation for small ε, we define the approximation $\tilde{u}_h^\varepsilon$ to the convection-diffusion problem adaptively as

$$\tilde{u}_h^\varepsilon = \begin{cases} u_h^\varepsilon, & \varepsilon \geq h^{2k}, \\ u_h^0, & \varepsilon < h^{2k} \end{cases} \tag{1.7}$$

with u_h^ε being the solution to the hybrid-dG method for $\varepsilon > 0$ on the layer-adapted mesh, u_h^0 being the corresponding solution for $\varepsilon = 0$ on a uniform mesh, and k being the polynomial approximation order. This choice enables us to show the following ε-uniform error estimate

$$\|u^\varepsilon(t^n) - \tilde{u}_h^\varepsilon(t^n)\|_{L^2} \leq C \max(h^{k+1}, \min(\sqrt{\varepsilon}, h^k)) + C'\tau^{k+1/2}, \tag{1.8}$$

which holds under verifiable smoothness assumptions on the solution u^ε. Here, t^n are the time grid points. For this approximation strategy, we can verify that the number of elements in the layer-adapted mesh is of optimal order $\mathcal{O}(h^{-1})$. Let us note that the convergence rate in time in (1.8) is suboptimal by a factor $1/2$ in comparison to the results for the dG time-stepping obtained in [48, 117]. The numerical tests presented at the end of this chapter, however, indicate an optimal order convergence in time. It might be possible to prove this by other techniques in the context of Runge-Kutta methods since the dG time-stepping can be shown to be equivalent to the Radau IIA Runge-Kutta scheme; see [1, 119]. Finally, let us stress that all results are valid for single intervals as well as finite networks of general topology which can also include cycles.

Main contributions

Before going into the details, let us briefly summarize the main contributions presented in this chapter.

- We extend the well-known asymptotic estimate (1.6) for single intervals to networks. The main difficulty in the analysis is the additional boundary layers at the interior vertices of the network that arise from the change in the number and type of coupling conditions. Since the values of the solution at network junctions are not known a-priori, the asymptotic analysis requires a delicate choice of boundary layer functions in order to handle the interior layers. This result was published together with a complete analysis of the pure transport and the convection-diffusion problem in

  > H. Egger and N. Philippi. On the transport limit of singularly perturbed convection-diffusion problems on networks. *Math. Methods Appl. Sci.*, 2021.

- We propose a hybrid-dG method that is particularly well-suited for convection-dominated problems and can handle the coupling conditions at network junctions. The hybrid-dG scheme for the pure transport problem was first presented in

  > H. Egger and N. Philippi. A hybrid discontinuous Galerkin method for transport equations on networks. In *Finite volumes for complex applications IX—methods, theoretical aspects, examples—FVCA 9, Bergen, Norway, June 2020*, volume 323 of *Springer Proc. Math. Stat.*, pages 487–495. Springer, Cham, 2020.

  A complete analysis of the transport problem on the continuous level and an error estimate on uniform meshes has been given therein. The hybrid-dG semi-discretization

for the singularly perturbed convection-diffusion problem on networks, the corresponding approximation strategy (1.7) on the layer-adapted mesh, and the uniform error estimate (1.8) were proposed and investigated in

> H. Egger and N. Philippi. A hybrid-dG method for singularly perturbed convection-diffusion equations on pipe networks. *ESAIM: M2AN*, 2023.

As a new aspect not contained in this publication, we give a complete analysis of the fully discretized problem using a dG approach for the time discretization.

Outline

In Section 1.1 we present the pure transport and the convection-diffusion problem on networks and establish their well-posedness via semigroup theory. Section 1.2 is dedicated to the asymptotic analysis. The main result is the extension of the asymptotic estimate (1.6) to networks. Further, we derive bounds on the derivatives similar to (1.5), which will later be needed for the error analysis of our numerical scheme. The numerical approximation is discussed in Section 1.3. We first investigate the spatial semi-discretization via a hybrid-dG approach, before we consider the full discretization using the dG time-stepping method. The main result of this section is the uniform error estimate (1.8) employing the adaptive approximation strategy (1.7) on a layer-adapted spatial mesh. In Section 1.4 we illustrate our theoretical findings with some numerical tests. We conclude this chapter with a short discussion and an outlook.

1.1. Model problems

The first section is based on our publication [40]. We present the pure transport problem and the convection-diffusion problem on networks. Suitable coupling conditions at network junctions are proposed leading to well-posed problems. We start by introducing the basic notation that will be used throughout this chapter.

1.1.1. Notation and function spaces

Following the notation from previous publications, see e.g. [39], a network is described by a finite, connected, and directed graph $\mathcal{G} = (\mathcal{V}, \mathcal{E})$ with vertices $\mathcal{V} = \{v_1, \dots, v_m\}$ and edges $\mathcal{E} = \{e_1, \dots, e_l\} \subset \mathcal{V} \times \mathcal{V}$. Let us note that networks can include cycles. For each vertex $v \in \mathcal{V}$ we define the set of incident edges by $\mathcal{E}(v) = \{e \in \mathcal{E} : e = (v, \cdot) \text{ or } e = (\cdot, v)\}$. We further distinguish between boundary vertices $\mathcal{V}_\partial = \{v \in \mathcal{V} : |\mathcal{E}(v)| = 1\}$ and interior vertices $\mathcal{V}_0 = \mathcal{V} \backslash \mathcal{V}_\partial$ with $|\mathcal{E}(v)|$ denoting the cardinality of the set $\mathcal{E}(v)$. In order to indicate the start and end vertex of an edge $e = (v_i, v_j)$, let us introduce the outward normal on the network by $n_e(v_i) = -1,\ n_e(v_j) = 1$, and $n_e(v) = 0$ for $v \in \mathcal{V} \backslash \{v_i, v_j\}$. An illustration of the notation for a simple network is given in Figure 1.1. Each edge $e \in \mathcal{E}$ is

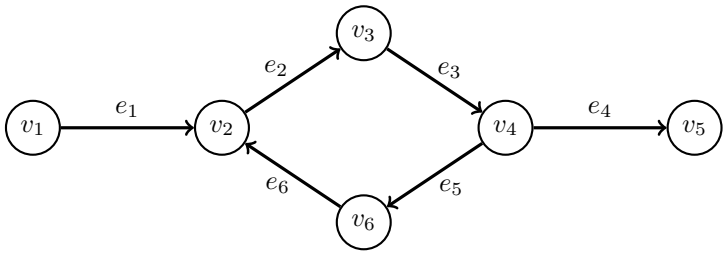

Figure 1.1.: A network with edges $e_1 = (v_1, v_2)$, $e_2 = (v_2, v_3)$, $e_3 = (v_3, v_4)$, $e_4 = (v_4, v_5)$, $e_5 = (v_4, v_6)$, and $e_6 = (v_6, v_2)$, boundary vertices $\mathcal{V}_\partial = \{v_1, v_5\}$, and interior vertices $\mathcal{V}_0 = \{v_2, v_3, v_4, v_6\}$. The incident edges to the vertex v_2 are collected in the set $\mathcal{E}(v_2) = \{e_1, e_2, e_6\}$, which can be split into the sets $\mathcal{E}^{in}(v_2) = \{e_1, e_6\}$ and $\mathcal{E}^{out}(v_2) = \{e_2\}$ of edges carrying flow into or out of the vertex v_2. The inflow and outflow boundary vertices of the network are given by $\mathcal{V}_\partial^{in} = \{v_1\}$ and $\mathcal{V}_\partial^{out} = \{v_5\}$.

identified by an interval $e \simeq (0, \ell_e)$ with $\ell_e > 0$ being the length of the edge. The space of square-integrable functions on the network can then be defined by

$$L^2(\mathcal{E}) = L^2(e_1) \times \cdots \times L^2(e_l) = \{u : u_e \in L^2(0, \ell_e) \text{ for all } e \in \mathcal{E}\}$$

with $u_e = u|_e$ denoting the restriction of a function u onto the edge e. The associated scalar product and norm are given by

$$(u, w)_{L^2(\mathcal{E})} = \sum\nolimits_{e \in \mathcal{E}} (u, w)_{L^2(e)} \qquad \text{and} \qquad \|u\|^2_{L^2(\mathcal{E})} = (u, u)_{L^2(\mathcal{E})}.$$

In a similar way, we can define the broken Sobolev spaces of piecewise smooth functions on the network by

$$H^k_{pw}(\mathcal{E}) = \{u : u_e \in H^k(e) \text{ for all } e \in \mathcal{E}\}.$$

Let us note that functions in $H^k_{pw}(\mathcal{E})$ are continuous along edges for $k \geq 1$ but may be discontinuous at junctions. We thus denote by $H^1(\mathcal{E})$ the space of functions in $H^1_{pw}(\mathcal{E})$ that are additionally continuous across junctions. Each $u \in H^1(\mathcal{E})$ takes a unique value $u(v)$ at $v \in \mathcal{V}$ which belongs to the space $\ell_2(\mathcal{V})$ of possible vertex values.

1.1.2. Transport problem

We are now in the position to introduce the transport problem on a network $\mathcal{G} = (\mathcal{V}, \mathcal{E})$. On each edge $e \in \mathcal{E}$ the dynamics is described by

$$a_e(x)\partial_t u_e(x,t) + b_e \partial_x u_e(x,t) = 0, \qquad x \in (0, \ell_e),\ t > 0. \tag{1.9}$$

Like on a single interval, we need one boundary condition at the inflow boundary of each edge. We thus introduce for each interior vertex $v \in \mathcal{V}_0$ the sets of edges carrying flow into or out of the vertex by

$$\mathcal{E}^{in}(v) = \{e \in \mathcal{E}(v) : b_e n_e(v) > 0\} \quad \text{and} \quad \mathcal{E}^{out}(v) = \{e \in \mathcal{E}(v) : b_e n_e(v) < 0\},$$

respectively. Moreover, the spaces of inflow and outflow boundary vertices are defined by

$$\mathcal{V}_\partial^{in} = \{v \in \mathcal{V}_\partial : b_e n_e(v) < 0\} \quad \text{and} \quad \mathcal{V}_\partial^{out} = \{v \in \mathcal{V}_\partial : b_e n_e(v) > 0\};$$

see Figure 1.1 for an illustration where the flow and the edge direction coincide. We prescribe Dirichlet conditions at the network inflow boundary, i.e.,

$$u_e(v,t) = \hat{g}_v(t), \qquad v \in \mathcal{V}_\partial^{in},\ e \in \mathcal{E}(v),\ t > 0. \tag{1.10}$$

At interior vertices, however, we need additional conditions that couple the solutions in incident edges. Since one boundary condition is required for each outflow edge, we set

$$u_e(v,t) = \hat{u}_v(t), \qquad v \in \mathcal{V}_0,\ e \in \mathcal{E}^{out}(v),\ t > 0 \tag{1.11}$$

with mixing value $\hat{u}_v$ determined by the solutions in inflow edges, i.e.,

$$\hat{u}_v(t) = \frac{\sum_{e\in\mathcal{E}^{in}(v)} b_e u_e(v,t)}{\sum_{e\in\mathcal{E}^{in}(v)} b_e}, \qquad v \in \mathcal{V}_0,\ t > 0. \tag{1.12}$$

We call $\hat{u}_v$ *hybrid variable* in the sequel. The transport problem on networks is now fully described by (1.9)–(1.12) when complemented by suitable initial data.

Let us now state some assumptions on the parameters a and b as well as the boundary data $\hat{g}$ that are supposed to hold throughout this chapter.

Assumption 1.1. Let $a \in H_{pw}^{m+1}(\mathcal{E})$ with $0 < \underline{a} \le a_e(x) \le \overline{a}$ as well as $|\partial_x^j a_e(x)| \le \overline{a}$ for all $x \in (0,\ell_e)$, $e \in \mathcal{E}$, and $j \le 2m$ for some $m \ge 0$. Further, let $b_e \ge \underline{b} > 0$ be constant and positive for all edges $e \in \mathcal{E}$, i.e., the flow direction corresponds to the direction of the edges, and it holds that

$$\sum\nolimits_{e\in\mathcal{E}(v)} b_e n_e(v) = 0 \tag{B}$$

at all interior vertices $v \in \mathcal{V}_0$, which ensures the conservation of the background flow at junctions. Moreover, the boundary data satisfies $\hat{g} \in C^{m+1}([0,t_{max}];\ell_2(\mathcal{V}_\partial))$ up to some time point $t_{max} > 0$, and $\partial_t^n \hat{g}(0) = 0$ for $0 \le n \le m$.

Remark 1.2. Together with the conservation condition (B) for the background flow the coupling conditions (1.11)–(1.12) guarantee conservation of mass at junctions. The restriction on b being positive could easily be relaxed to b being bounded away from zero, because otherwise (1.9) degenerates to an ordinary differential equation. The assumption on the boundary data $\hat{g}$ ensures consistency with trivial initial data $u(0) = 0$ which in turn avoids the occurrence of initial layers.

Example 1.3 (Contaminant transport in water supply networks)**.**
The transport of a solved contaminant in a water supply network can be modeled by (1.9)–(1.12). The concentration of the contaminant is then given by u and we assume that the contaminant is injected into the network at inflow boundary vertices $v \in \mathcal{V}_\partial^{in}$. Since water is an incompressible fluid with a constant density, the conservation of mass principle implies that the averaged flow velocity modeled by b_e is constant in each pipe $e \in \mathcal{E}$ and that condition (B) is satisfied at junctions. The parameter a equals 1 in this example. Hence, Assumption 1.1 is fulfilled. A possible scenario is investigated in Section 1.4.1.

As a first step of our analysis, we now establish the well-posedness of the pure transport problem on networks (1.9)–(1.12).

Theorem 1.4. *Let Assumption 1.1 hold. Then,* (1.9)–(1.12) *has a unique solution*

$$u \in C^{m+1}([0,t_{max}];L^2(\mathcal{E})) \cap C^0([0,t_{max}];H^{m+1}_{pw}(\mathcal{E})), \quad \hat{u} \in C^m([0,t_{max}];\ell_2(\mathcal{V}_0))$$

with initial condition being chosen as $u(0)=0$*. Moreover, "mass" is conserved up to flux over the network boundary, i.e.,*

$$\frac{d}{dt}(au(t),1)_{L^2(\mathcal{E})} = \sum\nolimits_{v\in\mathcal{V}_\partial^{in}} b_e\hat{g}_v(t) - \sum\nolimits_{v\in\mathcal{V}_\partial^{out}} b_e u_e(v,t), \tag{1.13}$$

and "energy" is dissipated due to mixing at junctions, i.e.,

$$\begin{aligned}\frac{d}{dt}\|a^{1/2}u(t)\|^2_{L^2(\mathcal{E})} = &\sum\nolimits_{v\in\mathcal{V}_\partial^{in}} b_e|\hat{g}_v(t)|^2 - \sum\nolimits_{v\in\mathcal{V}_\partial^{out}} b_e|u_e(v,t)|^2 \\ &- \sum\nolimits_{v\in\mathcal{V}_0}\sum\nolimits_{e\in\mathcal{E}^{in}(v)} b_e|u_e(v,t)-\hat{u}_v(t)|^2.\end{aligned} \tag{1.14}$$

Proof. In order to show well-posedness, we transform (1.9)–(1.12) into an inhomogeneous abstract Cauchy problem of the form

$$z'(t) = \mathcal{A}z(t) + f(t), \quad t>0, \qquad z(0)=z_0 \tag{iACP}$$

with operator $(\mathcal{A},\mathcal{D}(\mathcal{A}))$ on a reflexive Banach space $\mathcal{X}$. For $f \in C^1([0,t_{max};\mathcal{X})$ and $z_0\in\mathcal{X}$, existence of a unique solution $z\in C^1([0,t_{max};\mathcal{X})\cap C^0([0,t_{max};\mathcal{D}(\mathcal{A}))$ is guaranteed if $(\mathcal{A},\mathcal{D}(\mathcal{A}))$ is the generator of a strongly continuous semigroup; see [46, Ch. VI, Cor. 7.6]. This in turn can be verified using a variant of the Lumer-Phillips theorem for reflexive Banach spaces that can be found in [46, Ch. II, Cor. 3.20].

Step 1 (Transformation into (iACP)**).** As a first step, we transform (1.9)–(1.12) into a problem with homogeneous inflow boundary data. For this let us introduce a function $w(t)\in H^1(\mathcal{E})\cap H^2_{pw}(\mathcal{E})$ for $0\le t\le t_{max}$, which is affine linear on every edge and satisfies $w(v,t)=\hat{g}_v(t)$ at $v\in\mathcal{V}_\partial^{in}$ and $w(v,t)=0$ at $v\in\mathcal{V}\backslash\mathcal{V}_\partial^{in}$. Then, any solution of (1.9)–(1.12) can be split into $u=z-w$ with z satisfying

$$a_e(x)\partial_t z_e(x,t) + b_e\partial_x z_e(x,t) = f_e(x,t) \tag{1.15}$$

for all $x\in(0,\ell_e)$, $e\in\mathcal{E}$ with $f_e(x,t)=a_e(x)\partial_t w_e(x,t)+b_e\partial_x w_e(x,t)$. Moreover, z vanishes at the network inflow boundary due to the construction of w, i.e.,

$$z_e(v,t)=0, \qquad v\in\mathcal{V}_\partial^{in},\ e\in\mathcal{E}(v). \tag{1.16}$$

Since w vanishes at junctions, z satisfies the same coupling conditions (1.11)–(1.12) as the original solution u, i.e.,

$$z_e(v,t)=\hat{z}_v(t), \qquad v\in\mathcal{V}_0,\ e\in\mathcal{E}^{out}(v) \tag{1.17}$$

with mixing value

$$\hat{z}_v(t) = \frac{\sum_{e\in\mathcal{E}^{in}(v)} b_e z_e(v,t)}{\sum_{e\in\mathcal{E}^{in}(v)} b_e}. \tag{1.18}$$

At the initial time, we have $z(0) = 0$. Then, z solves (iACP) with $z(0) = 0$ on the Hilbert space $\mathcal{X} := L^2(\mathcal{E})$ with norm and scalar product defined by

$$\|z\|_{\mathcal{X}} := \|a^{1/2} z\|_{L^2(\mathcal{E})} \qquad \text{and} \qquad (z, w)_{\mathcal{X}} := (az, w)_{L^2(\mathcal{E})}, \tag{1.19}$$

which are well-defined since a is strictly positive and uniformly bounded from below and above by Assumption 1.1. Note that each Hilbert space is a reflexive Banach space. The operator $(\mathcal{A}, \mathcal{D}(\mathcal{A}))$ is given by

$$\mathcal{D}(\mathcal{A}) := \{z \in H^1_{pw}(\mathcal{E}) : z \text{ satisfies (1.16)–(1.18) for some } \hat{z} \in \ell_2(\mathcal{V}_0)\}, \tag{1.20}$$

which is a dense subspace of $\mathcal{X}$, and

$$\mathcal{A} : \mathcal{D}(\mathcal{A}) \subset \mathcal{X} \to \mathcal{X}, \qquad \mathcal{A}z|_e := -\frac{b_e}{a_e} \partial_x z_e. \tag{1.21}$$

On each edge $e \in \mathcal{E}$ the source term satisfies $f \in C^1([0, t_{max}]; \mathcal{X})$ by construction of w.

Step 2 (Application of the Lumer-Phillips theorem). In order to establish the existence of a unique solution to (iACP), we have to verify that $(\mathcal{A}, \mathcal{D}(\mathcal{A}))$ is the generator of a strongly continuous semigroup. According to [46, Ch. II, Cor. 3.20] $(\mathcal{A}, \mathcal{D}(\mathcal{A}))$ even generates a contraction semigroup if $(\mathcal{A}, \mathcal{D}(\mathcal{A}))$ is dissipative, i.e.,

$$\|(\lambda - \mathcal{A})z\|_{\mathcal{X}} \geq \lambda \|z\|_{\mathcal{X}} \qquad \text{for all } \lambda > 0,\ z \in \mathcal{D}(\mathcal{A}) \tag{1.22}$$

and $\lambda - \mathcal{A}$ is surjective for some $\lambda > 0$. For each $z \in \mathcal{D}(\mathcal{A})$ it holds that

$$(\mathcal{A}z, z)_{\mathcal{X}} = -(b\partial_x z, z)_{L^2(\mathcal{E})} = -\sum\nolimits_{v \in \mathcal{V}} \sum\nolimits_{e \in \mathcal{E}(v)} \tfrac{1}{2} b_e |z_e(v)|^2 n_e(v) = \sum\nolimits_{v \in \mathcal{V}} (*).$$

Using the coupling conditions (1.17)–(1.18) we find that at interior vertices $v \in \mathcal{V}_0$ the right-hand side equals

$$(*) = \sum\nolimits_{e \in \mathcal{E}^{out}(v)} \tfrac{1}{2} b_e |z_e(v)|^2 - \sum\nolimits_{e \in \mathcal{E}^{in}(v)} \tfrac{1}{2} b_e |z_e(v)|^2 \leq 0,$$

where we used that by definition of $\hat{z}$ as mixing value (1.18), the flow conservation condition (B), and Jensen's inequality, the first term can be estimated by

$$\begin{aligned} \sum\nolimits_{e \in \mathcal{E}^{out}(v)} b_e |\hat{z}_v|^2 &= \sum\nolimits_{e \in \mathcal{E}^{out}(v)} b_e \left| \frac{\sum_{e \in \mathcal{E}^{in}(v)} b_e z_e(v)}{\sum_{e \in \mathcal{E}^{in}(v)} b_e} \right|^2 \\ &\leq \sum\nolimits_{e \in \mathcal{E}^{out}(v)} b_e \frac{\sum_{e \in \mathcal{E}^{in}(v)} b_e |z_e(v)|^2}{\sum_{e \in \mathcal{E}^{in}(v)} b_e} \leq \sum\nolimits_{e \in \mathcal{E}^{in}(v)} b_e |z_e(v)|^2. \end{aligned}$$

Since z vanishes at inflow boundary vertices by (1.16) and $b_e > 0$, we find that

$$(\mathcal{A}z, z)_{\mathcal{X}} \leq \sum\nolimits_{v \in \mathcal{V}_\partial^{in}} \tfrac{1}{2} b_e |\hat{z}_v|^2 - \sum\nolimits_{v \in \mathcal{V}_\partial^{out}} \tfrac{1}{2} b_e |z_e(v)|^2 \leq 0.$$

This immediately implies that (1.22) is satisfied for all $\lambda > 0$, since

$$\|(\lambda - \mathcal{A})z\|_{\mathcal{X}} \|z\|_{\mathcal{X}} \geq ((\lambda - \mathcal{A})z, z)_{\mathcal{X}} = (\lambda z, z)_{\mathcal{X}} - (\mathcal{A}z, z)_{\mathcal{X}} \geq \lambda \|z\|^2_{\mathcal{X}}. \tag{1.23}$$

It remains to show that $\lambda - \mathcal{A}$ is surjective for some $\lambda > 0$. On each edge $e \in \mathcal{E}$ and for every $y \in \mathcal{X}$ we can solve $(\lambda - \mathcal{A})|_e z_e = \lambda z_e + \frac{b_e}{a_e}\partial_x z_e = y_e$ analytically, and obtain

$$z_e(x) = z_e(0)e^{-\lambda \int_0^x a_e(s)\,ds/b_e} + \int_0^x \frac{a_e(s)}{b_e} y_e(s) e^{-\lambda \int_s^x a_e(\sigma)\,d\sigma/b_e}\,ds. \tag{1.24}$$

Using the fact that $z_e(0) = z_e(v) = 0$ for $v \in \mathcal{V}_\partial^{in}$ by (1.16) as well as $z_e(0) = z_e(v) = \hat{z}_v$ for $v \in \mathcal{V}_0,\ e \in \mathcal{E}^{out}(v)$ by (1.17) with $\hat{z}_v$ specified as mixing value (1.18), finding $\hat{z}_v$ reduces to solving the following linear system of equations

$$\sum_{e\in\mathcal{E}^{out}(v)} b_e \hat{z}_v - \sum_{e=(v_e^i,\,v)\in\mathcal{E}^{in}(v)} b_e \hat{z}_{v_e^i} e^{-\lambda a_e(\ell_e)/b_e} = \sum_{e\in\mathcal{E}^{in}(v)} \int_0^{\ell_e} \frac{a_e(s)}{b_e} y_e(s) e^{-\lambda \int_s^x a_e(\sigma)\,d\sigma/b_e}\,ds.$$

The system matrix can be seen to be strictly diagonally dominant due to the flow conservation condition (B) and the bounds on the parameters in Assumption 1.1. Consequently, the system is uniquely solvable and the nodal values $(\hat{z}_v)_{v\in\mathcal{V}_0}$ are uniquely determined. It holds that $z \in \mathcal{D}(\mathcal{A})$ by its construction in (1.24), so we proved that $\lambda - \mathcal{A}$ is surjective for $\lambda > 0$. Consequently, [46, Ch. II, Cor. 3.20] implies that $(\mathcal{A}, \mathcal{D}(\mathcal{A}))$ generates a contraction semigroup. This in turn guarantees well-posedness of (iACP), i.e., the existence of a unique solution $z \in C^1([0, t_{max}]; \mathcal{X}) \cap C^0([0, t_{max}]; \mathcal{D}(\mathcal{A}))$.

Step 3 (Well-posedness and regularity). By the construction and regularity of w we obtain the existence of a solution $u = w - z$ of (1.9)–(1.12) with

$$u \in C^1([0, t_{max}]; L^2(\mathcal{E})) \cap C^0([0, t_{max}]; H^1_{pw}(\mathcal{E})).$$

Uniqueness can be deduced from the fact that the difference of two solutions $z = u_1 - u_2$ of (1.9)–(1.12) satisfies (iACP) with $f \equiv 0$ and $z_0 \equiv 0$. Since (iACP) is well-posed as shown above, this implies $z \equiv 0$.

Higher regularity of the solution in turn follows from the fact that by differentiating (1.9)–(1.12) with respect to time we find that $\partial_t^n u$ is also a solution with boundary data $\partial_t^n \hat{g}$ and initial data $\partial_t^n u(0) = 0$. Due to the regularity and compatibility conditions on $\hat{g}$ in Assumption 1.1, we obtain

$$\partial_t^n u \in C^1([0, t_{max}]; L^2(\mathcal{E})) \cap C^0([0, t_{max}]; H^1_{pw}(\mathcal{E})) \quad \text{for all } 0 \le n \le m,$$

i.e., $u \in C^{m+1}([0, t_{max}]; L^2(\mathcal{E}))$. Using the fact that $\partial_x u_e = \frac{a_e}{b_e}\partial_t u_e$ and the regularity assumption on a, we find that $u \in C^0([0, t_{max}]; H^{m+1}_{pw}(\mathcal{E}))$. From the definition of the mixing values $\hat{u}_v$ in (1.12) we then deduce that $\hat{u} \in C^m([0, t_{max}]; \ell_2(\mathcal{V}_0))$ by the trace theorem, which eventually yields the desired regularity of the solution.

Step 4 (Conservation of mass and energy identity). Conservation of mass (1.13) follows by integrating (1.9) over each edge $e \in \mathcal{E}$, summing up, and using the boundary and coupling conditions (1.10)–(1.12), i.e.,

$$\begin{aligned}\frac{d}{dt}(au(t), 1)_{L^2(\mathcal{E})} &= -(b\partial_x u(t), 1)_{L^2(\mathcal{E})} = -\sum\nolimits_{v\in\mathcal{V}} \sum\nolimits_{e\in\mathcal{E}(v)} b_e u_e(v,t) \\ &= \sum\nolimits_{v\in\mathcal{V}_\partial^{in}} b_e \hat{g}_v(t) - \sum\nolimits_{v\in\mathcal{V}_\partial^{out}} b_e u_e(v,t).\end{aligned}$$

In a similar manner, multiplying (1.9) with u and integrating over the network yields

$$\begin{aligned}\frac{d}{dt}\|a^{1/2}u(t)\|^2_{L^2(\mathcal{E})} &= 2(a\partial_t u(t), u(t))_{L^2(\mathcal{E})} = -2(b\partial_x u(t), u(t))_{L^2(\mathcal{E})} \\ &= -\sum\nolimits_{v\in\mathcal{V}} b_e|u_e(v,t)|^2 n_e(v) \\ &= \sum\nolimits_{v\in\mathcal{V}_\partial^{in}} b_e|\hat{g}_v(t)|^2 - \sum\nolimits_{v\in\mathcal{V}_\partial^{out}} b_e|u_e(v,t)|^2 - \sum\nolimits_{v\in\mathcal{V}_0}(**)\end{aligned}$$

using the boundary condition (1.10). The latter term equals

$$\begin{aligned}(**) &= \sum\nolimits_{e\in\mathcal{E}^{in}(v)} b_e|u_e(v,t)|^2 - \sum\nolimits_{e\in\mathcal{E}^{out}(v)} b_e|u_e(v,t)|^2 \\ &= \sum\nolimits_{e\in\mathcal{E}^{in}(v)} b_e(|u_e(v,t)|^2 - |\hat{u}_v(t)|^2) \\ &= \sum\nolimits_{e\in\mathcal{E}^{in}(v)} b_e|u_e(v,t)-\hat{u}_v(t)|^2 + 2\sum\nolimits_{e\in\mathcal{E}^{in}(v)} \big(b_e u_e(v,t)\hat{u}_v(t) - b_e|\hat{u}_v(t)|^2\big),\end{aligned}$$

where we used (1.11) as well as the flow conservation condition (B). The last term in the last line vanishes due to the fact that $\hat{u}_v$ does not depend on $e \in \mathcal{E}(v)$ and that $\sum_{e\in\mathcal{E}^{in}(v)} b_e u_e(v,t) = \sum_{e\in\mathcal{E}^{in}(v)} b_e\hat{u}_v(t)$ by (1.12), which then leads to (1.14). This concludes the proof of Theorem 1.4. □

1.1.3. Convection-diffusion problem

The pure transport problem does not account for diffusive effects and might thus not capture all features of the process. As a next step, we therefore consider the incorporation of diffusion. On each edge $e \in \mathcal{E}$ we assume that

$$a_e(x)\partial_t u_e^\varepsilon(x,t) + b_e\partial_x u_e^\varepsilon(x,t) = \varepsilon\partial_{xx}u_e^\varepsilon(x,t) \tag{1.25}$$

holds for all $x \in (0,\ell_e)$ and $t > 0$ with small diffusion coefficient $\varepsilon > 0$ being constant. Note that with minor changes in the arguments, it is also possible to choose ε to be space-dependent. Dirichlet conditions are prescribed at the whole network boundary, i.e.,

$$u_e^\varepsilon(v,t) = \hat{g}_v(t), \quad v \in \mathcal{V}_\partial,\ e \in \mathcal{E}(v),\ t > 0. \tag{1.26}$$

At interior vertices we now enforce continuity by

$$u_e^\varepsilon(v,t) = \hat{u}_v^\varepsilon(t), \quad v \in \mathcal{V}_0,\ e \in \mathcal{E}(v),\ t > 0, \tag{1.27}$$

which is caused by the infinite spread of diffusion, as well as conservation of the total flux

$$\sum\nolimits_{e\in\mathcal{E}(v)} \big(b_e u_e^\varepsilon(v,t) - \varepsilon\partial_x u_e^\varepsilon(v,t)\big)n_e(v) = 0, \quad v \in \mathcal{V}_0,\ e \in \mathcal{E}(v),\ t > 0, \tag{1.28}$$

ensuring conservation of mass at junctions. When complemented with suitable initial data, the convection-diffusion problem on networks is fully described by (1.25)–(1.28).

Remark 1.5. At each junction $v \in \mathcal{V}_0$ the number of coupling conditions (1.27)–(1.28) equals $|\mathcal{E}(v)| + 1$, which suffices to enforce continuity of the solution and to guarantee

conservation of mass at junctions. In contrast to the coupling conditions (1.11)–(1.12) for the transport problem, which account for $|\mathcal{E}^{out}(v)|+1$ conditions and only ensure outflow continuity and conservation of mass. We thus observe a change not only in the type but also in the number of coupling conditions in the limit of vanishing diffusion $\varepsilon \to 0$. This eventually leads to boundary layers at the outflow boundary of each pipe. A closer investigation will be given in Section 1.2, and an illustration can be found in Figure 1.2.

With similar arguments as for the transport problem, we can show well-posedness of the convection-diffusion problem (1.25)–(1.28) via semigroup theory.

Theorem 1.6. *Let Assumption 1.1 hold. Then, for any $\varepsilon > 0$ there exists a unique solution*

$$\begin{aligned} &u^\varepsilon \in C^{m+1}([0,t_{max}]; L^2(\mathcal{E})) \cap C^0([0,t_{max}]; H^{2m+2}_{pw}(\mathcal{E}) \cap H^1(\mathcal{E})), \\ &\hat{u}^\varepsilon \in C^m([0,t_{max}]; \ell_2(\mathcal{V}_0)) \end{aligned}$$

of (1.25)–(1.28) *with initial condition $u^\varepsilon(0) = 0$. Moreover, "mass" is conserved up to flux over the network boundary, i.e.,*

$$\frac{d}{dt}(au^\varepsilon(t),1)_{L^2(\mathcal{E})} = \sum\nolimits_{v\in\mathcal{V}_\partial} \big(-b_e\hat{g}_v(t) + \varepsilon\partial_x u^\varepsilon_e(v,t)\big)n_e(v), \tag{1.29}$$

and "energy" is dissipated due to diffusion, i.e.,

$$\begin{aligned} \frac{1}{2}\frac{d}{dt}\|a^{1/2}u(t)\|^2_{L^2(\mathcal{E})} = &-\varepsilon\|\partial_x u^\varepsilon(t)\|^2_{L^2(\mathcal{E})} \\ &- \sum\nolimits_{v\in\mathcal{V}_\partial} \Big(\tfrac{1}{2}b_e\hat{g}_v(t) - \varepsilon\partial_x u^\varepsilon_e(v,t)\Big)\hat{g}_v(t)n_e(v). \end{aligned} \tag{1.30}$$

Proof. Similar to the transport problem on networks, we can prove the well-posedness of (1.25)–(1.28) by transforming it into an abstract Cauchy problem (iACP).

Step 1 (Transformation into (iACP)**).** Let us first transform (1.25)–(1.28) into a problem with homogeneous boundary data by introducing a function $w(t) \in H^1(\mathcal{E})$ which is constructed as follows: On a network that has at least one interior vertex, we define w_e as quadratic polynomial for all $v \in \mathcal{V}_\partial,\ e \in \mathcal{E}(v)$ with $w_e(v,t) = \hat{g}_v(t)$ for $v \in \mathcal{V}_\partial$ and $w_e(v_0,t) = 0,\ \partial_x w_e(v_0,t) = 0$ for $v_0 = e \cap \mathcal{V}_0$. On the remaining edges, we set $w_e \equiv 0$. If the network consists of only one edge then w is affine linear with $w(v,t) = \hat{g}(t)$ for $v \in \mathcal{V}_\partial$. We can then split any solution u^ε to (1.25)–(1.28) into $u^\varepsilon = w - z$ with z solving

$$a_e(x)\partial_t z_e(x,t) + b_e\partial_x z_e(x,t) - \varepsilon\partial_{xx} z_e(x,t) = f_e(x,t), \quad x \in (0,\ell_e),\ e \in \mathcal{E}. \tag{1.31}$$

The right hand side is given by $f_e(x,t) := a_e(x)\partial_t w_e(x,t) + b_e\partial_x w_e(x,t) - \varepsilon\partial_{xx} w_e(x,t)$ for each $e \in \mathcal{E}$, and satisfies $f \in C^1([0,t_{max}]; L^2(\mathcal{E}))$ due to the construction of w and the regularity of $\hat{g}$. At the network boundary z vanishes, i.e.,

$$z_e(v,t) = 0, \qquad v \in \mathcal{V}_\partial,\ e \in \mathcal{E}(v), \tag{1.32}$$

and at interior vertices z satisfies the same coupling conditions (1.27)–(1.28) as the original solution u^ε due to the construction of w. Moreover, $z(0) = 0$. The problem for z can then

be rewritten as (iACP) with spaces $\mathcal{X} := L^2(\mathcal{E})$ equipped with norm and scalar product introduced in (1.19), operator $(\mathcal{A}, \mathcal{D}(A))$ defined by

$$\mathcal{D}(\mathcal{A}) := \{z \in H^2_{pw}(\mathcal{E}) : z \text{ satisfies (1.32) and (1.27)–(1.28) for some } \hat{z} \in \ell_2(\mathcal{V}_0)\},$$

which is a dense subspace of $\mathcal{X}$, and

$$\mathcal{A} : \mathcal{D}(\mathcal{A}) \subset \mathcal{X} \to \mathcal{X}, \quad \mathcal{A}z|_e := -\tfrac{1}{a_e}(b_e \partial_x z_e - \varepsilon \partial_{xx} z_e).$$

The source term and initial condition in (iACP) are given by f above and $z_0 = 0$.

Step 2 (Application of the Lumer-Phillips theorem). As a next step, we will verify that $(\mathcal{A}, \mathcal{D}(\mathcal{A}))$ generates a contraction semigroup. First, we show that $(\mathcal{A}, \mathcal{D}(\mathcal{A}))$ is dissipative, i.e., satisfies (1.22). For $z \in \mathcal{D}(\mathcal{A})$ it holds that

$$\begin{aligned}(\mathcal{A}z, z)_{\mathcal{X}} &= -(b\partial_x z - \varepsilon \partial_{xx} z, z)_{L^2(\mathcal{E})} \\ &= -\varepsilon \|\partial_x z\|^2_{L^2(\mathcal{E})} - \sum\nolimits_{v \in \mathcal{V}} \sum\nolimits_{e \in \mathcal{E}(v)} \big(\tfrac{1}{2} b_e |z_e(v)|^2 - \varepsilon \partial_x z_e(v) z_e(v)\big) n_e(v).\end{aligned}$$

The first term is negative, and since z vanishes at the network boundary $v \in \mathcal{V}_\partial$ due to (1.32) it remains to estimate the second term at interior vertices $v \in \mathcal{V}_0$. Using the coupling conditions (1.27)–(1.28) and the flow conservation condition (B) we find that

$$\begin{aligned}&-\sum\nolimits_{v \in \mathcal{V}_0} \sum\nolimits_{e \in \mathcal{E}(v)} \big(\tfrac{1}{2} b_e |z_e(v)|^2 - \varepsilon \partial_x z_e(v) z_e(v)\big) n_e(v) \\ &\quad = -\sum\nolimits_{v \in \mathcal{V}_0} \tfrac{1}{2} |\hat{z}_v|^2 \sum\nolimits_{e \in \mathcal{E}(v)} b_e n_e(v) + \sum\nolimits_{v \in \mathcal{V}_0} \hat{z}_v \sum\nolimits_{e \in \mathcal{E}(v)} \varepsilon \partial_x z_e(v) n_e(v) = 0,\end{aligned}$$

which ultimately yields

$$(\mathcal{A}z, z)_{\mathcal{X}} = -\varepsilon \|\partial_x z\|^2_{L^2(\mathcal{E})} \le 0.$$

This in turn implies that (1.22) holds for all $\lambda > 0$ due to (1.23). It remains to verify that $\lambda - \mathcal{A}$ is surjective for some $\lambda > 0$. By (1.23) and the Lax-Milgram Lemma, the problem $\lambda z - \mathcal{A}z = f$ can be shown to have a unique weak solution

$$z \in H^1_0(\mathcal{E}) := \{w \in H^1(\mathcal{E}) : w(v) = 0 \text{ for all } v \in \mathcal{V}_\partial\}$$

for all $f \in \mathcal{X}$, i.e., z solves

$$(a\lambda z, w)_{L^2(\mathcal{E})} - (bz, \partial_x w)_{L^2(\mathcal{E})} + (\varepsilon \partial_x z, \partial_x w)_{L^2(\mathcal{E})} = (af, w)_{L^2(\mathcal{E})} \tag{1.33}$$

for all $w \in H^1_0(\mathcal{E})$. Note that the coupling condition (1.27) is strongly enforced in the space $H^1_0(\mathcal{E})$, whereas the coupling condition (1.28) appears naturally in (1.33). The nodal values $(\hat{z}_v)_{v \in \mathcal{V}_0}$ are well-defined for $H^1(\mathcal{E})$-functions due to the trace theorem. We further see that $z \in H^2_{pw}(\mathcal{E})$ by integrating (1.31) over each edge $e \in \mathcal{E}$ since $f \in \mathcal{X} = L^2(\mathcal{E})$. This shows that $z \in \mathcal{D}(\mathcal{A})$, which then implies surjectivity of $\lambda - \mathcal{A}$ for $\lambda > 0$. Hence, all conditions of [46, Ch. II, Cor. 3.20] are satisfied, and $(\mathcal{A}, \mathcal{D}(\mathcal{A}))$ generates a contraction semigroup, which in turn guarantees well-posedness of (iACP).

Step 3 (Well-posedness and regularity). Well-posedness and higher regularity of the solution are obtained with the same arguments as in Step 3 of the proof of Theorem 1.4.

Again, the regularity and construction of w yields the existence of a solution $u^\varepsilon = w - z$ to (1.25)–(1.28) with $u^\varepsilon \in C^1([0,t_{max}]; L^2(\mathcal{E})) \cap C^0([0,t_{max}]; H^1(\mathcal{E}) \cap H^2_{pw}(\mathcal{E}))$. Uniqueness follows from the fact that the difference of two solutions $z = u_1^\varepsilon - u_2^\varepsilon$ of (1.25)–(1.28) satisfies (iACP) with $z_0 \equiv 0$ and $f \equiv 0$, whose unique solution is $z \equiv 0$.

By differentiating (1.25)–(1.28) with respect to time, we find that $\partial_t^n u^\varepsilon$ is also a solution for boundary data $\partial_t^n \hat{g}$ and initial data $\partial_t^n u^\varepsilon(0) = 0$. Due to the regularity and compatibility conditions on $\hat{g}$ in Assumption 1.1, semigroup theory yields the existence of a unique solution $\partial_t^n u^\varepsilon \in C^1([0,t_{max}]; L^2(\mathcal{E})) \cap C^0([0,t_{max}]; H^2_{pw}(\mathcal{E}) \cap H^1(\mathcal{E}))$ for all $0 \le n \le m$, which immediately implies $u^\varepsilon \in C^{m+1}([0,t_{max}]; L^2(\mathcal{E}))$. By the trace theorem we deduce that $\hat{u}^\varepsilon \in C^m([0,t_{max}]; \ell_2(\mathcal{V}_0))$. Using the fact that $\varepsilon \partial_{xx} u_e^\varepsilon = a_e \partial_t u_e^\varepsilon + b_e \partial_x u_e^\varepsilon$ and the bounds on a and its derivatives in Assumption 1.1, we find that $u \in C^0([0,t_{max}]; H^{2m+2}_{pw}(\mathcal{E}))$.

Step 4 (Conservation of mass and energy equality). Conservation of mass (1.29) follows from integrating (1.25) over each edge, summing up and use the boundary and coupling conditions (1.26)–(1.28), more precisely

$$\begin{aligned}
\frac{d}{dt}(au^\varepsilon(t), 1)_{L^2(\mathcal{E})} &= -(b\partial_x u^\varepsilon(t) - \varepsilon \partial_{xx} u^\varepsilon(t), 1)_{L^2(\mathcal{E})} \\
&= -\sum_{v \in \mathcal{V}} \sum_{e \in \mathcal{E}(v)} \big(b_e u_e^\varepsilon(v,t) - \varepsilon \partial_x u_e^\varepsilon(v,t)\big) n_e(v) \\
&= -\sum_{v \in \mathcal{V}_\partial} \big(b_e \hat{g}_v(t) - \varepsilon \partial_x u_e^\varepsilon(v,t)\big) n_e(v).
\end{aligned}$$

In the same spirit, multiplying (1.25) with u^ε and integrating over the network yields

$$\begin{aligned}
\frac{1}{2}\frac{d}{dt}\|a^{1/2} u^\varepsilon(t)\|^2_{L^2(\mathcal{E})} &= (a\partial_t u^\varepsilon(t), u^\varepsilon(t))_{L^2(\mathcal{E})} \\
&= -(b\partial_x u^\varepsilon(t), u^\varepsilon(t))_{L^2(\mathcal{E})} + (\varepsilon \partial_{xx} u^\varepsilon(t), u^\varepsilon(t))_{L^2(\mathcal{E})} \\
&= -\varepsilon \|\partial_x u^\varepsilon(t)\|^2_{L^2(\mathcal{E})} - \sum_{v \in \mathcal{V}} \sum_{e \in \mathcal{E}(v)} \big(\tfrac{1}{2} b_e |u_e^\varepsilon(v,t)|^2 - \varepsilon \partial_x u_e^\varepsilon(v,t) u_e^\varepsilon(v,t)\big) n_e(v) \\
&= -\varepsilon \|\partial_x u^\varepsilon(t)\|^2_{L^2(\mathcal{E})} - \sum_{v \in \mathcal{V}_\partial} \sum_{e \in \mathcal{E}(v)} \big(\tfrac{1}{2} b_e \hat{g}_v(t) - \varepsilon \partial_x u_e^\varepsilon(v,t)\big) \hat{g}_v(t) n_e(v),
\end{aligned}$$

where we applied integration-by-parts onto the last term in the second line and used the fact that $\partial_x u^\varepsilon u^\varepsilon = \frac{1}{2}\partial_x |u^\varepsilon|^2$. The contributions at interior vertices cancel due to the coupling conditions (1.27)–(1.28). This concludes the proof of Theorem 1.6. □

1.2. Asymptotic analysis

This section is devoted to the analysis of the asymptotic behavior of solutions u^ε to the convection-diffusion problem on networks (1.25)–(1.28) for vanishing diffusion $\varepsilon \to 0$ and is based on our publication [40]. The main result is the extension of the well-known asymptotic estimate (1.6) for singularly perturbed convection-diffusion problems on a single interval to networks.

Theorem 1.7. *Let Assumption 1.1 hold, and let u^ε be the solution to* (1.25)–(1.28) *with $\varepsilon > 0$ and u the solution to* (1.9)–(1.12) *with initial conditions $u^\varepsilon(0) = u(0) = 0$. Then,*

$$\|u^\varepsilon - u\|_{L^\infty(0,t_{max}; L^2(\mathcal{E}))} \le C\sqrt{\varepsilon} \tag{1.34}$$

with a constant C that only depends on t_{max} and the bounds on the parameters in Assumption 1.1 but is independent of ε.

Before we prove this theorem, we state some auxiliary results that are needed for the proof as well as for later investigations.

1.2.1. Auxiliary results

In the following, we will derive bounds on the solution to the convection-diffusion problem on networks and its derivatives, which will then be needed for the proof of the main result and later on for the analysis of the numerical approximation. A key step for this is the derivation of a weak maximum principle on networks.

Lemma 1.8 (Maximum principle)**.** *Let Assumption 1.1 hold, and let*

$$u \in C^1([0,t_{max}]; L^2(\mathcal{E})) \cap C^0([0,t_{max}]; H^2_{pw}(\mathcal{E}) \cap H^1(\mathcal{E}))$$

be a given function that satisfies

$$a_e(x)\partial_t u_e(x,t) + b_e \partial_x u_e(x,t) - \varepsilon \partial_{xx} u_e(x,t) \geq 0, \qquad x \in (0,\ell_e),\ e \in \mathcal{E}, \tag{1.35}$$

$$u_e(v,t) \geq 0, \qquad v \in \mathcal{V}_\partial,\ e \in \mathcal{E}(v), \tag{1.36}$$

$$\sum\nolimits_{e\in\mathcal{E}(v)} \varepsilon \partial_x u_e(v,t) n_e(v) = 0, \qquad v \in \mathcal{V}_0 \tag{1.37}$$

for all $0 < t < t_{max}$ with initial value $u(0) \geq 0$. Then, $u_e(x,t) \geq 0$ for all $0 \leq x \leq \ell_e,\ e \in \mathcal{E}$ and $0 \leq t \leq t_{max}$.

Proof. Following standard procedure [49], we multiply (1.35) with $w = \min(u,0)$ and integrate over the network to find that

$$\begin{aligned} 0 &\geq (a\partial_t u, w)_{L^2(\mathcal{E})} + (b\partial_x u, w)_{L^2(\mathcal{E})} - (\varepsilon \partial_{xx} u, w)_{L^2(\mathcal{E})} \\ &= (a\partial_t u, w)_{L^2(\mathcal{E})} - (bu, \partial_x w)_{L^2(\mathcal{E})} + (\varepsilon \partial_x u, \partial_x w)_{L^2(\mathcal{E})}, \end{aligned} \tag{1.38}$$

where we applied integration-by-parts to the second and third terms in the first line. Contributions at interior vertices $v \in \mathcal{V}_0$ vanish due to the continuity of u and w across junctions, condition (B), and (1.37), whereas contributions at boundary vertices $v \in \mathcal{V}_\partial$ vanish due to $w(v) = 0$ which holds by (1.36). Let us now define the set

$$\mathcal{E}_-(t) = \{x \in [0,\ell_{e_1}] : u_{e_1}(x,t) < 0\} \times \cdots \times \{x \in [0,\ell_{e_l}] : u_{e_l}(x,t) < 0\}$$

of the spatial domain where u is negative at time t. Then, $w(t) \equiv u(t)$ on $\mathcal{E}_-(t)$ and $w(t) \equiv 0$ and $\partial_x w(t) \equiv 0$ on its complement due to the definition of w. From this and the inequality (1.38) we deduce that

$$\begin{aligned} 0 &\geq (a\partial_t u(t), u(t))_{L^2(\mathcal{E}_-(t))} - (bu(t), \partial_x u(t))_{L^2(\mathcal{E}_-(t))} + (\varepsilon \partial_x u(t), \partial_x u(t))_{L^2(\mathcal{E}_-(t))} \\ &\geq (a\partial_t u(t), u(t))_{L^2(\mathcal{E}_-(t))} \end{aligned}$$

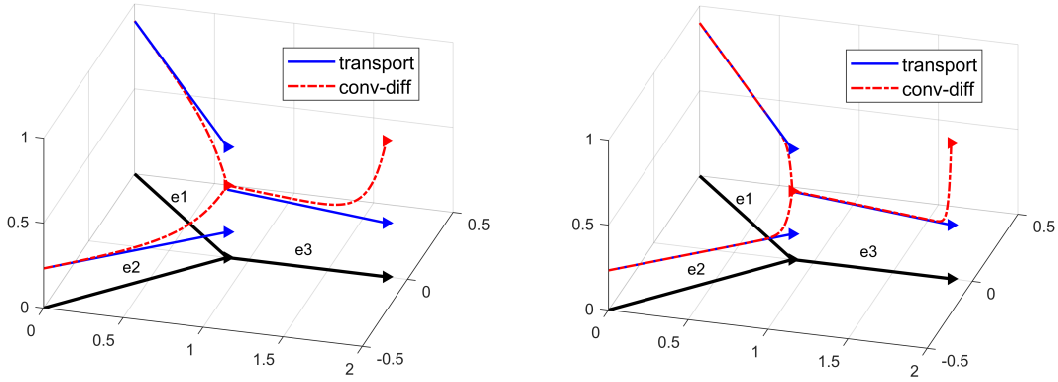

Figure 1.2.: Snapshots of solutions u and u^ε to the transport (blue, solid) and the convection-diffusion problem (red, dashed) on a tripod network with edges e_1, e_2 carrying flow into and edge e_3 carrying flow out of the interior vertex for a larger (left) and a smaller (right) value of ε. The change in coupling conditions and the occurrence of boundary layers are clearly visible.

at time t, where we used that the third term in the first line is positive, and the second term vanishes. This holds since $bu\partial_x u = \frac{1}{2}b\partial_x|u|^2$ and by integrating this expression the vertex contributions cancel out due to continuity of u at junctions, flow condition (B), and the fact that $u \equiv 0$ on the boundary of $\mathcal{E}_-(t)$ by definition and (1.36). Integrating with respect to time then leads to

$$0 \geq \int_0^t (a\partial_t u(s), u(s))_{L^2(\mathcal{E}_-(s))}\, ds = \int_0^t \frac{1}{2}\frac{d}{dt}\int_{\mathcal{E}_-(s)} a(x)|u(x,s)|^2\, dx\, ds$$
$$= \int_{\mathcal{E}_-(t)} \frac{1}{2}a(x)|u(x,t)|^2\, dx.$$

Note that the first equality holds due to the fundamental theorem of calculus, the fact that u vanishes on the boundary of $\mathcal{E}_-(s)$ for all $0 < s < t$, and $\mathcal{E}_-(0) = \{\,\}$ since $u(0) \geq 0$. From $a(x) \geq \underline{a} > 0$ we can then conclude that $u \equiv 0$ on $\mathcal{E}_-(t)$ for all $0 \leq t \leq t_{max}$ and thus $u \geq 0$. □

We are now in the position to derive bounds on the solution of (1.25)–(1.28) and its derivatives using similar arguments as in [77, 104], where the stationary and the time-dependent convection-diffusion problem on an interval were investigated; also see [115]. An illustration of the behavior of the convection-diffusion solution is given in Figure 1.2.

Lemma 1.9. *Let Assumption 1.1 hold, and let u^ε be the solution to* (1.25)–(1.28) *with initial condition $u^\varepsilon(0) = 0$. Then,*

$$|\partial_t^n \partial_x^j u_e^\varepsilon(x,t)| \leq C(1 + \varepsilon^{-j} e^{-b_e(\ell_e - x)/\varepsilon}) \tag{1.39}$$

holds for all $n \leq m$, $j \leq 2(m-n)+1$, and $0 \leq x \leq \ell_e$, $e \in \mathcal{E}$, $0 < t < t_{max}$ with a constant C that is independent of ε.

Proof. We divide the proof into two steps, where we first show (1.39) for $j = 0$ and $n \geq 0$. Bounds on higher derivatives can then in a second step be derived via induction over j.

Step 1 (Boundedness of u^ε and its time derivatives). We first show that u^ε and $\partial_t^n u^\varepsilon$ are uniformly bounded independently of ε, which follows from the weak maximum principle with standard arguments. We define a function w with

$$w_e(x,t) := \max_{v\in\mathcal{V}_\partial,\, 0\leq s\leq t_{max}} |\hat{g}_v(s)| \pm u^\varepsilon(x,t)$$

for $e \in \mathcal{E}$, which by construction satisfies the conditions from Lemma 1.8. It immediately follows that $w \geq 0$ and we conclude that u^ε can be bounded by the maximum of its boundary data. By differentiating (1.25) n-times with respect to time, we see that $\partial_t^n u^\varepsilon$ also solves (1.25)–(1.28) with boundary data $\partial_t^n \hat{g}$ and initial data $\partial_t^n u^\varepsilon(0) = 0$. The same argument applies again and it turns out that $\partial_t^n u^\varepsilon$ can be bounded by the maximum norm of $\partial_t^n \hat{g}$. The bounds for higher spatial derivatives are then established via induction over j in the next step.

Step 2 (Induction over j). Let us now assume that (1.39) holds for all $n \leq m$ and $0 \leq i \leq j-1$. We show that it then also holds for j and all $n \leq m$. As a first step we prove that $|\partial_t^n \partial_x^j u_e^\varepsilon(\ell_e,t)| \leq c\varepsilon^{-j}$. By the mean value theorem, we know that there exists $y \in (\ell_e - \varepsilon, \ell_e)$, so that

$$\partial_t^n \partial_x^j u_e^\varepsilon(y,t) = \frac{1}{\varepsilon}\big(\partial_t^n \partial_x^{j-1} u_e^\varepsilon(\ell_e,t) - \partial_t^n \partial_x^{j-1} u_e^\varepsilon(\ell_e-\varepsilon,t)\big) \leq c\varepsilon^{-j},$$

which holds due to the induction hypothesis. By differentiating (1.25) with respect to space and time we find that

$$a_e(x)\partial_t \partial_t^n \partial_x^{j-1} u_e^\varepsilon(x,t) + b_e \partial_x \partial_t^n \partial_x^{j-1} u_e^\varepsilon(x,t) - \varepsilon \partial_{xx} \partial_t^n \partial_x^{j-1} u_e^\varepsilon(x,t) = f_e^\varepsilon(x,t) \tag{1.40}$$

with right-hand side given by

$$f_e^\varepsilon(x,t) = -\sum_{i=1}^{j-1} \binom{j-1}{i} \partial_x^i a_e(x) \partial_x^{j-i-1} \partial_t^n u_e^\varepsilon(x,t).$$

Using (1.40) and the fundamental theorem of calculus we deduce that

$$\begin{aligned}
\partial_t^n \partial_x^j u_e^\varepsilon(\ell_e,t) &= \partial_t^n \partial_x^j u_e^\varepsilon(y,t) + \int_y^{\ell_e} \partial_{xx} \partial_t^n \partial_x^{j-1} u_e^\varepsilon(x,t)\, dx \qquad (1.41)\\
&= \partial_t^n \partial_x^j u_e^\varepsilon(y,t) + \varepsilon^{-1} \int_y^{\ell_e} a_e(x) \partial_t^{n+1} \partial_x^{j-1} u_e^\varepsilon(x,t) + b_e \partial_t^n \partial_x^j u_e^\varepsilon(x,t) - f_e^\varepsilon(x,t)\, dx\\
&\leq c\varepsilon^{-j} + \max_{x\in(y,\ell_e)} \big(|a_e(x)\partial_t^{n+1}\partial_x^{j-1} u_e^\varepsilon(x,t)| + |f_e^\varepsilon(x,t)|\big) + \max_{x\in(y,\ell_e)} 2\varepsilon^{-1} b_e |\partial_t^n \partial_x^{j-1} u_e^\varepsilon(x,t)|\\
&\leq c'\varepsilon^{-j}.
\end{aligned}$$

Note that the last three terms in the third line are bounded by $c''\varepsilon^{-j}$ due to the induction hypotheses and the bounds in Assumption 1.1. We now fix a time point $0 \leq t \leq t_{max}$ and define on each edge $e \in \mathcal{E}$ a function $w_e(x) := \partial_t^n \partial_x^j u_e^\varepsilon(x,t)$, which by (1.40) is a solution to the ordinary differential equation

$$b_e w_e(x) - \varepsilon w_e'(x) = \eta_e^\varepsilon(x) := -a_e(x)\partial_t^{n+1}\partial_x^{j-1} u_e^\varepsilon(x,t) + f_e^\varepsilon(x,t) \tag{1.42}$$

with value at the endpoint of the edge given by $w_e(\ell_e) = \partial_t^n \partial_x^j u_e^\varepsilon(\ell_e, t)$. The right-hand side can be estimated by

$$|\eta_e^\varepsilon(x)| \leq c(1 + \varepsilon^{-(j-1)} e^{-b_e(\ell_e - x)/\varepsilon}), \tag{1.43}$$

using the induction hypothesis and the bounds in Assumption 1.1. Solving (1.42) by means of the variation-of-constants-formula, we find that

$$\begin{aligned} w_e(x) &= w_e(\ell_e) e^{-b_e(\ell_e - x)/\varepsilon} + \varepsilon^{-1} \int_x^{\ell_e} e^{-b_e(\sigma - x)/\varepsilon} \eta_e(\sigma)\, d\sigma \\ &\leq c'\, \varepsilon^{-j} e^{-b_e(\ell_e - x)/\varepsilon} + \varepsilon^{-1} \int_x^{\ell_e} e^{-b_e(\sigma - x)/\varepsilon} c(1 + \varepsilon^{-(j-1)} e^{-b_e(\ell_e - \sigma)/\varepsilon})\, d\sigma \\ &\leq c'\, \varepsilon^{-j} e^{-b_e(\ell_e - x)/\varepsilon} + c\varepsilon^{-j} e^{-b_e(\ell_e - x)/\varepsilon} (\ell - x) + \tfrac{c}{b_e}(1 - e^{-b_e(\ell - x)/\varepsilon}) \\ &\leq c''(1 + \varepsilon^{-j} e^{-b_e(\ell_e - x)/\varepsilon}), \end{aligned}$$

where we used (1.41) and (1.43) throughout the estimations. This shows that (1.39) holds for j and all $n \leq m$. By induction, the proof of Lemma 1.9 is completed. □

1.2.2. Proof of Theorem 1.7

The proof of Theorem 1.7 for a single pipe is given in [109, p.159-166]; see [8] for the original reference. The main idea is to introduce a boundary layer function w^ε which approximates the difference between the convection-diffusion and the transport solution with accuracy $\mathcal{O}(\sqrt{\varepsilon})$, i.e., we split the error into

$$\|u^\varepsilon - u\|_{L^\infty(0,t_{max};L^2(\mathcal{E}))} \leq \|u^\varepsilon - u - w^\varepsilon\|_{L^\infty(0,t_{max};L^2(\mathcal{E}))} + \|w^\varepsilon\|_{L^\infty(0,t_{max};L^2(\mathcal{E}))} \tag{1.44}$$

and want to show that both terms on the right-hand side can be estimated by $C\sqrt{\varepsilon}$ with a constant that is independent of ε. We proceed similarly as on a single pipe, but since the construction of the boundary layer function is more involved on networks, we present the complete proof.

Step 1 (Construction of boundary layer function). Let us define the boundary layer function w^ε on $e = (v_e^i, v_e^o) \in \mathcal{E}$ by

$$w_e^\varepsilon(x,t) := (\hat{u}_{v_e^o}(t) - u_e(v_e^o, t)) e^{-b_e(\ell_e - x)/\varepsilon}. \tag{1.45}$$

Note that at boundary vertices $\mathcal{V}_\partial$ the nodal value $\hat{u}_v$ does formally not exist, but for ease of notation we set $\hat{u}_v = \hat{g}_v$ at $v \in \mathcal{V}_\partial$. The particular construction of the boundary layer function is motivated in Figure 1.2. We immediately see that w^ε solves

$$b_e \partial_x w_e^\varepsilon - \varepsilon \partial_{xx} w_e^\varepsilon = 0 \tag{1.46}$$

and further satisfies

$$\|w^\varepsilon\|_{L^\infty(0,t_{max};L^2(\mathcal{E}))} \leq c\sqrt{\varepsilon}. \tag{1.47}$$

By the error splitting (1.44) it remains to estimate the norm of the remainder $\eta^\varepsilon := u^\varepsilon - u - w^\varepsilon$ for which we find by inserting η^ε into the convection-diffusion equation, testing with η^ε, and integrating over the network that

$$\begin{aligned}\frac{1}{2}\frac{d}{dt}\|a^{1/2}\eta^\varepsilon\|^2_{L^2(\mathcal{E})} &= (a\partial_t\eta^\varepsilon,\eta^\varepsilon)_{L^2(\mathcal{E})} \\ &= -(b\partial_x\eta^\varepsilon,\eta^\varepsilon)_{L^2(\mathcal{E})} + (\varepsilon\partial_{xx}\eta^\varepsilon,\eta^\varepsilon)_{L^2(\mathcal{E})} + (\varepsilon\partial_{xx}u,\eta^\varepsilon)_{L^2(\mathcal{E})} - (a\partial_t w^\varepsilon,\eta^\varepsilon)_{L^2(\mathcal{E})} \\ &= (i)+(ii)+(iii)+(iv).\end{aligned} \tag{1.48}$$

Here, we used that u, u^ε and w^ε satisfy (1.9), (1.25) and (1.46), respectively. Before we estimate the terms $(i)-(iv)$, we investigate the remainder η^ε in more detail.

Step 2 (Investigation of η^ε). In the following, we compute the values of η^ε at initial time $t=0$ and at all vertices $v\in\mathcal{V}$ of the network. At $t=0$ it holds that $\eta^\varepsilon(0)=0$ since $u^\varepsilon(0)=u(0)=0$. Let us note that this also holds true as long as u^ε and u have the same initial condition. At inflow boundary vertices $v\in\mathcal{V}_\partial^{in}$ and corresponding edges $e=(v,v_e^o)$ we find that

$$\eta^\varepsilon(v,t) = \hat{g}_v(t) - \hat{g}_v(t) - (\hat{g}_v(t) - u_e(v,t))e^{-b_e\ell_e/\varepsilon} \le c\varepsilon, \tag{1.49}$$

since the transport solution does not depend on ε and $e^{-b_e\ell_e/\varepsilon}$ can be estimated by $c'\varepsilon$. At outflow boundary vertices $v\in\mathcal{V}_\partial^{out}$ with corresponding edges $e=(v_e^i,v)$, however, $\eta^\varepsilon(v,t)$ vanishes, more precisely

$$\eta^\varepsilon(v,t) = \hat{g}_v(t) - u_e(v,t) - (\hat{g}_v(t) - u_e(v,t)) = 0. \tag{1.50}$$

It remains to investigate the values of η^ε at interior vertices $v\in\mathcal{V}_0$ for which we find that

$$\eta_e^\varepsilon(v,t) = \hat{u}_v^\varepsilon(t) - \hat{u}_v(t), \qquad e=(v_e^i,v)\in\mathcal{E}^{in}(v), \tag{1.51}$$

$$\eta_e^\varepsilon(v,t) = \hat{u}_v^\varepsilon(t) - \hat{u}_v(t) - (\hat{u}_{v_e^o}(t) - u_e(v_e^o,t))e^{-b_e\ell_e/\varepsilon}, \qquad e=(v,v_e^o)\in\mathcal{E}^{out}(v). \tag{1.52}$$

Step 3 (Estimation of $(i)-(iv)$). We are now in the position to estimate the terms in (1.48) by exploiting the properties of η^ε derived in the previous step.

Estimation of (i). Using the fact that $\partial_x\eta^\varepsilon\eta^\varepsilon = \frac{1}{2}\partial_x|\eta^\varepsilon|^2$ the first term equals

$$(i) = -(b\partial_x\eta^\varepsilon,\eta^\varepsilon)_{L^2(\mathcal{E})} = -\sum_{v\in\mathcal{V}}\sum_{e\in\mathcal{E}(v)}\tfrac{1}{2}b_e|\eta_e^\varepsilon(v)|^2 n_e(v) = \sum_{v\in\mathcal{V}}(*).$$

At inflow boundary vertices $v\in\mathcal{V}_\partial^{in}$ we conclude from (1.49) that $(*)\le c\varepsilon$, whereas at outflow boundary vertices it holds that $(*)=0$ by (1.50). At interior vertices $v\in\mathcal{V}_0$ using (1.51)–(1.52) and the flow conservation condition (B) we find that

$$\begin{aligned}(*) &= \sum_{\mathcal{E}^{out}(v)}\tfrac{1}{2}b_e\big(\hat{u}_v^\varepsilon - \hat{u}_v - (\hat{u}_{v_e^o} - u_e(v_e^o))e^{-b_e\ell_e/\varepsilon}\big)^2 - \sum_{\mathcal{E}^{in}(v)}\tfrac{1}{2}b_e\big(\hat{u}_v^\varepsilon - \hat{u}_v\big)^2 \\ &= \sum_{\mathcal{E}^{out}(v)}\tfrac{1}{2}b_e(\hat{u}_v^\varepsilon - \hat{u}_v)^2 + \tfrac{1}{2}b_e(\hat{u}_v^\varepsilon - \hat{u}_v)(\hat{u}_{v_e^o} - u_e(v_e^o))e^{-b_e\ell_e/\varepsilon} \\ &\qquad + \tfrac{1}{2}b_e(\hat{u}_{v_e^o} - u_e(v_e^o))^2 e^{-2b_e\ell_e/\varepsilon} - \sum_{\mathcal{E}^{in}(v)}\tfrac{1}{2}b_e\big(\hat{u}_v^\varepsilon - \hat{u}_v\big)^2 \le c\varepsilon.\end{aligned}$$

The first term in the second line and the last term in the third line cancel because of the flow conservation condition (B). Additionally, we used the uniform boundedness of u^ε shown in Lemma 1.9. Overall, we obtain $(i) \leq c\varepsilon$.

Estimation of (ii). Applying integration-by-parts, the second term in (1.48) can be transformed into

$$\begin{aligned}(ii) = (\varepsilon\partial_{xx}\eta^\varepsilon, \eta^\varepsilon)_{L^2(\mathcal{E})} &= -(\varepsilon\partial_x\eta^\varepsilon, \partial_x\eta^\varepsilon)_{L^2(\mathcal{E})} + \sum\nolimits_{v\in\mathcal{V}} \sum\nolimits_{e\in\mathcal{E}(v)} \varepsilon\partial_x\eta^\varepsilon(v)\eta^\varepsilon(v)n_e(v) \\ &= -\varepsilon\|\partial_x\eta^\varepsilon\|^2_{L^2(\mathcal{E})} + \sum\nolimits_{v\in\mathcal{V}}(**).\end{aligned}$$

The first term is negative and will be needed later on for stability. Before we estimate $(**)$ at boundary and interior vertices, let us evaluate the spatial derivative of the boundary layer function w^ε, i.e.,

$$\partial_x w_e^\varepsilon(v) = \frac{b_e}{\varepsilon}(\hat{u}_v - u_e(v)) \leq c\varepsilon^{-1}, \qquad e \in \mathcal{E}^{in}(v), \tag{1.53}$$

$$\partial_x w_e^\varepsilon(v) = \frac{b_e}{\varepsilon}(\hat{u}_{v_e^o} - u_e(v_e^o))e^{-b_e\ell_e/\varepsilon} \leq c', \qquad e = (v, v_e^o) \in \mathcal{E}^{out}(v). \tag{1.54}$$

For $e \in \mathcal{E}^{out}(v)$ we can deduce from Lemma 1.9 that $\partial_x u_e^\varepsilon(v)$ is uniformly bounded independently of ε. Together with (1.54) this yields uniform bounds for $\eta_e^\varepsilon(v)$. At boundary vertices, using (1.49)–(1.50), we can therefore conclude that

$$\sum\nolimits_{v\in\mathcal{V}_\partial}(**) = \sum\nolimits_{v\in\mathcal{V}_\partial^{in}} \varepsilon\partial_x\eta_e^\varepsilon(v)\eta_e^\varepsilon(v)n_e(v) \leq c\varepsilon.$$

At interior vertices, (1.51)–(1.52) leads to

$$(**) = \sum_{e\in\mathcal{E}(v)} \varepsilon\partial_x\eta_e^\varepsilon(v)(\hat{u}_e^\varepsilon(v) - \hat{u}_e(v))n_e(v) + \sum_{e\in\mathcal{E}^{out}(v)} \varepsilon\partial_x\eta_e^\varepsilon(v)(\hat{u}_{v_e^o} - u_e(v_e^o))e^{-b_e\ell_e/\varepsilon}.$$

The fact that $\partial_x\eta_e^\varepsilon(v)$ is bounded independently of ε for $e \in \mathcal{E}^{out}(v)$ allows us to bound the second term by $c\varepsilon^2$. The first term can be split into the following three terms

$$\begin{aligned}&\sum\nolimits_{e\in\mathcal{E}(v)} \varepsilon\partial_x u_e^\varepsilon(v)(\hat{u}_e^\varepsilon(v) - \hat{u}_e(v))n_e(v) - \sum\nolimits_{e\in\mathcal{E}(v)} \varepsilon\partial_x u_e(v)(\hat{u}_e^\varepsilon(v) - \hat{u}_e(v))n_e(v) \\ &\quad - \sum\nolimits_{e\in\mathcal{E}(v)} \varepsilon\partial_x w_e^\varepsilon(v)(\hat{u}_e^\varepsilon(v) - \hat{u}_e(v))n_e(v) = (a) + (b) + (c).\end{aligned}$$

The first term (a) vanishes due to the coupling conditions (1.27)–(1.28) and the flow conservation condition (B), which together imply that $\sum_{e\in\mathcal{E}(v)} \varepsilon\partial_x u_e^\varepsilon(v)n_e(v) = 0$. By the boundedness of $u, \partial_x u$ and u^ε independent of ε, the second term (b) can be bounded by $c\varepsilon$. Using (1.53)–(1.54) the last term can be rewritten as

$$\begin{aligned}(c) = &- \sum\nolimits_{e\in\mathcal{E}^{in}(v)} b_e(\hat{u}_v - u_e(v))(\hat{u}_e^\varepsilon(v) - \hat{u}_e(v)) \\ &+ \sum\nolimits_{e\in\mathcal{E}^{out}(v)} b_e(\hat{u}_{v_e^o} - u_e(v_e^o))e^{-b_e\ell_e/\varepsilon}(\hat{u}_e^\varepsilon(v) - \hat{u}_e(v)).\end{aligned}$$

The first term on the right-hand side vanishes due to the coupling conditions (1.11)–(1.12) and the flow conservation (B). The fact that u and u^ε are bounded independently of ε allows us to estimate the second term by $c\varepsilon$. In total, we obtain $(ii) \leq c\varepsilon$.

Estimation of (iii). The third term in (1.48) can be estimated by

$$\begin{aligned}(iii) &= (\varepsilon\partial_{xx}u, \eta^\varepsilon)_{L^2(\mathcal{E})} = -(\varepsilon\partial_x u, \partial_x\eta^\varepsilon)_{L^2(\mathcal{E})} + \sum\nolimits_{v\in\mathcal{V}}\sum\nolimits_{e\in\mathcal{E}(v)} \varepsilon\partial_x u_e(v)\eta_e^\varepsilon(v)n_e(v)\\ &\le \tfrac{\varepsilon}{2}\|\partial_x u\|^2_{L^2(\mathcal{E})} + \tfrac{\varepsilon}{2}\|\partial_x\eta^\varepsilon\|_{L^2(\mathcal{E})} + \sum\nolimits_{v\in\mathcal{V}}\sum\nolimits_{e\in\mathcal{E}(v)} \varepsilon\partial_x u_e(v)\eta_e^\varepsilon(v)n_e(v),\end{aligned}$$

where we applied integration-by-parts and used Young's inequality. The first term can be bounded by $c\varepsilon$, the second term absorbed into (ii) and the contributions at the junctions can also be estimated by $c\varepsilon$ due to the uniform boundedness of $\partial_x u$ and η^ε. Overall, we find that $(iii) \le c\varepsilon$.

Estimation of (iv). Applying Young's inequality to the last term in (1.48) yields

$$(iv) = -(a\partial_x w^\varepsilon, \eta^\varepsilon)_{L^2(\mathcal{E})} \le \tfrac{1}{2}\|a^{1/2}\partial_t w^\varepsilon\|^2_{L^2(\mathcal{E})} + \tfrac{1}{2}\|a^{1/2}\eta^\varepsilon\|^2_{L^2(\mathcal{E})}.$$

On each edge $e \in \mathcal{E}$ the first term can further be estimated by

$$\|a^{1/2}\partial_t w^\varepsilon\|^2_{L^2(e)} = \int_0^{\ell_e} a_e(\partial_t\hat{u}_{v_e^o} - \partial_t u_e(v_e^o))^2 e^{-2b_e(\ell_e - x)/\varepsilon} \le c\varepsilon,$$

because $\partial_t u$, $\partial_t\hat{u}$ are uniformly bounded independently of ε by Lemma 1.9. Since the graph is finite, this estimate extends to the whole network.

Step 4 (Application of Grönwall's Lemma). By (1.48) and the estimates for the appearing terms $(i) - (iv)$, we obtain

$$\frac{1}{2}\frac{d}{dt}\|a^{1/2}\eta^\varepsilon\|^2_{L^2(\mathcal{E})} \le c\varepsilon + \frac{1}{2}\|a^{1/2}\eta^\varepsilon\|^2_{L^2(\mathcal{E})}.$$

Integrating over $(0,t)$ and applying Grönwall's Lemma, see e.g. [116, Lemma 2.7], immediately leads to

$$\|\eta^\varepsilon(t)\|^2_{L^2(\mathcal{E})} \le 2\underline{a}ce^t\varepsilon \le 2\underline{a}ce^{t_{max}}\varepsilon \tag{1.55}$$

for all $0 < t < t_{max}$, since $\eta^\varepsilon(0) = 0$. The error splitting (1.44) and the estimate for w^ε in (1.47) then yield (1.34) with a constant C that depends on t_{max} and the bounds in Assumption 1.1 but which is independent of ε. □

The proof of Theorem 1.7 concludes our analytical considerations. In the next section, we focus on a suitable numerical approximation with special emphasis on asymptotic stability for vanishing diffusion $\varepsilon \to 0$.

1.3. Numerical approximation

In the following, we investigate the numerical approximation of the pure transport and the convection-diffusion problem on networks described by (1.9)–(1.12) and (1.25)–(1.28), respectively. We first propose and analyze the spatial semi-discretization by a hybrid discontinuous Galerkin approach that turns out to be particularly well-suited for handling

the convection-dominated regime and the coupling conditions at network junctions. After that, we present the fully discrete scheme, where we apply the discontinuous Galerkin method also for the time discretization. In order to overcome convergence issues due to boundary and interior layers and degenerate derivatives of the convection-diffusion solution u^ε, see Section 1.2, we investigate the numerical treatment for vanishing diffusion $\varepsilon \to 0$ by layer-adapted meshes. This section is based on our publications [39, 41].

1.3.1. Mesh and approximation spaces

We split each edge $e \simeq (0, \ell_e) \in \mathcal{E}$ into sub-intervals $0 = x_e^1 < x_e^2 < \cdots < x_e^{M_e} = \ell_e$ and collect them in the spatial mesh

$$\mathcal{T}_h = \{T_e^i = (x_e^{i-1}, x_e^i) : i = 1, .., M_e,\ e \in \mathcal{E}\}.$$

The local and global mesh sizes are denoted by $h_e^i = x_e^i - x_e^{i-1}$ and $h = \max_{e,i} h_e^i$. We also write h_T for the size of $T \in \mathcal{T}_h$ and define $h_{loc}|_T = h_T$. For each $T = (x^{in}, x^{out}) \in \mathcal{T}_h$ we call x^{in} the inflow and x^{out} the outflow boundary of T, since by Assumption 1.1 the direction of the edges coincides with the flow direction. We collect the inflow and outflow boundaries of all elements $T \in \mathcal{T}_h$ in the sets $\partial\mathcal{T}_h^{in}$ and $\partial\mathcal{T}_h^{out}$, respectively. Let us further introduce the outward normal on the mesh by $n|_T(x^{in}) = -1$ and $n|_T(x^{out}) = 1$. The set of interior grid points is given by

$$\mathcal{X}_h = \{x_e^i : i = 1, \ldots, M_e - 1,\ e \in \mathcal{E}\}.$$

Note that $\mathcal{G}_h = (\mathcal{V} \cup \mathcal{X}_h, \mathcal{T}_h)$ can be understood as a refinement of the original graph $\mathcal{G} = (\mathcal{V}, \mathcal{E})$. We will thus treat all grid points in $\mathcal{V} \cup \mathcal{X}_h$ in the same manner. On the spatial mesh $\mathcal{T}_h$, let us now define the following discrete space

$$W_h = \{w_h \in L^2(\mathcal{E}) : w_h|_T \in \mathcal{P}_k(T) \text{ for all } T \in \mathcal{T}_h\}$$

with $\mathcal{P}_k$ being the space of polynomials of degree $\leq k$. We now seek to approximate the solutions $u^\varepsilon(t)$ and $u(t)$ at $0 \leq t \leq t_{max}$ by a discrete function in W_h that can be discontinuous at grid points. In order to approximate the corresponding nodal values at $\mathcal{V}_0 \cup \mathcal{X}_h$, we further introduce the space of *hybrid variables*

$$\hat{W}_h = \{\hat{w}_h \in \ell_2(\mathcal{V} \cup \mathcal{X}_h) : \hat{w}_h(v) = 0 \text{ for all } v \in \mathcal{V}_\partial\}.$$

Note that the hybrid variables at all boundary vertices are set to zero and have only been introduced for ease of notation. In comparison to the continuous problems where hybrid variables only existed at network junctions $v \in \mathcal{V}_0$, we now additionally introduced them at all interior mesh points $x_e^i \in \mathcal{X}_h$. An illustration of their placement is given in Figure 1.3. Let us further introduce the mesh-dependent scalar products

$$(u, w)_{\mathcal{T}_h} = \sum\nolimits_{T \in \mathcal{T}_h} (u, w)_{L^2(T)}, \quad \langle u, w\rangle_{\partial\mathcal{T}_h} = \sum\nolimits_{T_e^i \in \mathcal{T}_h} u(x_e^{i-1})w(x_e^{i-1}) + u(x_e^i)w(x_e^i)$$

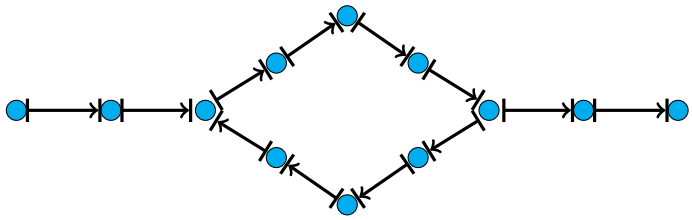

Figure 1.3.: Placement of hybrid variables indicated in (cyan, circles) in a simple spatial mesh with two sub-intervals per edge for the network depicted in Figure 1.1.

with corresponding norms $\|w\|^2_{\mathcal{T}_h} = (w,w)_{\mathcal{T}_h}$ and $|w|^2_{\partial\mathcal{T}_h} = \langle w,w\rangle_{\partial\mathcal{T}_h}$. The latter scalar product and norm can also be defined on the sets $\partial\mathcal{T}_h^{in}$ and $\partial\mathcal{T}_h^{out}$. We will also make use of the broken Sobolev spaces on $\mathcal{T}_h$ that are given by

$$H^k_{pw}(\mathcal{T}_h) = \{w \in L^2(\mathcal{E}) : w|_T \in H^k(T) \text{ for all } T \in \mathcal{T}_h\}$$

with corresponding norms $\|w\|^2_{H^k_{pw}(\mathcal{T}_h)} = \sum_{T\in\mathcal{T}_h} \|w\|^2_{H^k(T)}$.

1.3.2. Semi-discrete hybrid-dG method

Let us first introduce and analyze the spatial semi-discretization using a hybrid discontinuous Galerkin approach.

Problem 1.10. Find $u_h^\varepsilon \in C^1([0,t_{max}];W_h)$, $\hat{u}_h^\varepsilon \in C^0([0,t_{max}];\hat{W}_h)$ with $u_h^\varepsilon(0) = 0$ and

$$(a\partial_t u_h^\varepsilon(t), w_h)_{\mathcal{T}_h} + b_h(u_h^\varepsilon(t), \hat{u}_h^\varepsilon(t); w_h, \hat{w}_h) + \varepsilon d_h(u_h^\varepsilon(t), \hat{u}_h^\varepsilon(t); w_h, \hat{w}_h) = l_h^\varepsilon(t; w_h) \quad (1.56)$$

for all $w_h \in W_h$, $\hat{w}_h \in \hat{W}_h$ and $0 < t < t_{max}$ with bilinear and linear forms defined by

$$b_h(v_h, \hat{v}_h; w_h, \hat{w}_h) := -(bv_h, \partial_x w_h)_{\mathcal{T}_h} + \langle nbv_h^{up}, w_h - \hat{w}_h\rangle_{\partial\mathcal{T}_h}, \quad (1.57)$$

$$\begin{aligned} d_h(v_h, \hat{v}_h; w_h, \hat{w}_h) := {} & (\partial_x v_h, \partial_x w_h)_{\mathcal{T}_h} - \langle n\partial_x v_h, w_h - \hat{w}_h\rangle_{\partial\mathcal{T}_h} \\ & + \langle n(v_h - \hat{v}_h), \partial_x w_h\rangle_{\partial\mathcal{T}_h} + \langle \tfrac{\alpha}{h_{loc}}(v_h - \hat{v}_h), w_h - \hat{w}_h\rangle_{\partial\mathcal{T}_h}, \end{aligned} \quad (1.58)$$

$$l_h^\varepsilon(t; w_h) := -\langle nb\hat{g}(t), w_h\rangle_{\mathcal{V}_\partial^{in}} + \varepsilon\langle n\hat{g}(t), \partial_x w_h\rangle_{\mathcal{V}_\partial} + \varepsilon\langle \tfrac{\alpha}{h_{loc}}\hat{g}(t), w_h\rangle_{\mathcal{V}_\partial}. \quad (1.59)$$

Furthermore, we denote by $nbv_h^{up} = \max(nb,0)v_h + \min(nb,0)\hat{v}_h$ the convective upwind flux, by $h_{loc}|_T = h_T$ the local mesh size for $T \in \mathcal{T}_h$, and by $\alpha > 0$ a stabilization parameter.

Remark 1.11. By formally setting $\varepsilon = 0$, Problem 1.10 yields a viable approximation for the pure transport problem on networks described by (1.9)–(1.12). In particular, the method is able to handle the change in the number and type of coupling conditions in the transition from the convection-diffusion to the pure transport problem. One may thus call the scheme formally *asymptotic preserving*.

Basic properties

Let us collect some basic properties of the method described in Problem 1.10.

Lemma 1.12. *The bilinear forms defined in* (1.57) *and* (1.58) *satisfy*

$$\begin{aligned} b_h(w_h, \hat{w}_h; w_h, \hat{w}_h) &= \tfrac{1}{2}|b^{1/2}(w_h - \hat{w}_h)|^2_{\partial\mathcal{T}_h}, \\ d_h(w_h, \hat{w}_h; w_h, \hat{w}_h) &= \|\partial_x w_h\|^2_{\mathcal{T}_h} + |\tfrac{\alpha}{h_{loc}}(w_h - \hat{w}_h)|^2_{\partial\mathcal{T}_h} \end{aligned}$$

for all discrete functions $w_h \in W_h,\ \hat{w}_h \in \hat{W}_h$.

Proof. For the bilinear form b_h we find that

$$\begin{aligned} b_h(w_h, \hat{w}_h; w_h, \hat{w}_h) &= -(bw_h, \partial_x w_h)_{\mathcal{T}_h} + \langle nbw_h^{up}, w_h - \hat{w}_h\rangle_{\partial\mathcal{T}_h} \\ &= -\tfrac{1}{2}\langle nbw_h, w_h\rangle_{\partial\mathcal{T}_h} + \langle nbw_h, w_h - \hat{w}_h\rangle_{\partial\mathcal{T}_h^{out}} + \langle nb\hat{w}_h, w_h - \hat{w}_h\rangle_{\partial\mathcal{T}_h^{in}} \\ &= \tfrac{1}{2}|b^{1/2}w_h|^2_{\partial\mathcal{T}_h} - \langle bw_h, \hat{w}_h\rangle_{\partial\mathcal{T}_h} + \tfrac{1}{2}|b^{1/2}\hat{w}_h|^2_{\partial\mathcal{T}_h} \\ &= \tfrac{1}{2}|b^{1/2}(w_h - \hat{w}_h)|^2_{\partial\mathcal{T}_h}, \end{aligned}$$

where we used that $|b^{1/2}\hat{w}_h|_{\partial\mathcal{T}_h^{in}} = |b^{1/2}\hat{w}_h|_{\partial\mathcal{T}_h^{out}}$ due to the flow conservation condition (B) and the fact that $\hat{w}_h(v) = 0$ for all $v \in \mathcal{V}_\partial$. The equation for d_h immediately follows from its definition, since for $v_h = w_h,\ \hat{v}_h = \hat{w}_h$ the second and third terms in (1.58) cancel. □

As a next step, we investigate the well-posedness of the semi-discrete method as well as the uniform boundedness of its solution.

Lemma 1.13. *Let Assumption 1.1 hold. Then, Problem 1.10 has a unique solution*

$$u_h^\varepsilon \in C^{m+1}([0, t_{max}]; W_h), \quad \hat{u}_h^\varepsilon \in C^m([0, t_{max}]; \hat{W}_h)$$

for all $\varepsilon \geq 0$. *Moreover,* $\|\partial_t^n u_h^\varepsilon(t)\|_{\mathcal{T}_h} \leq C$ *for all* $0 \leq n \leq m$ *and* $0 \leq t \leq t_{max}$ *with a constant* C *only depending on* $\hat{g}$ *and the bounds in Assumption 1.1, but not on* ε *and* $\mathcal{T}_h$.

Proof. By testing (1.56) with $w_h = 0,\ \hat{w}_h = \chi_x$ for $x \in \mathcal{X}_h \cup \mathcal{V}_0$ we find a unique representation of $\hat{u}_h^\varepsilon$ in terms of u_h^ε. From Lemma 1.12 we deduce that $b_h + \varepsilon d_h$ is elliptic on $W_h \times \hat{W}_h$. The hybrid variables can thus be eliminated from the semi-discrete problem on the algebraic level. Now, choosing a suitable basis of the finite-dimensional space W_h, we can transform (1.56) into an ordinary differential equation for u_h^ε. The existence of a unique solution $u_h^\varepsilon \in C^1([0, t_{max}]; W_h),\ \hat{u}_h^\varepsilon \in C^0([0, t_{max}]; \hat{W}_h)$ then follows from the Picard-Lindelöf theorem; see e.g. [116, Theorem 2.2]. By differentiating (1.56) with respect to time we obtain higher regularity of the solution with the same arguments.

It remains to verify the uniform boundedness of the solution u_h^ε and its time derivatives. For this let us define a function $g_h(t) \in H^1(\mathcal{E})$ for all $0 \leq t \leq t_{max}$, so that $g_h(t)|_e \in \mathcal{P}_1(e)$ for all $e \in \mathcal{E}$, $g_h(v, t) = \hat{g}_v(t)$ at $v \in \mathcal{V}_\partial$, and $g_h(v, t) = 0$ at $v \in \mathcal{V}_0$. Note that $g_h \in C^{m+1}([0, t_{max}]; W_h)$ due to the regularity of $\hat{g}$. We further set $\hat{g}_h(x, t) = g_h(x, t)$ at $x \in \mathcal{X}_h \cup \mathcal{V}_0$ and $\hat{g}_h(v, t) = 0$ at $v \in \mathcal{V}_\partial$, i.e., $\hat{g}_h \in C^{m+1}([0, t_{max}]; \hat{W}_h)$. We can then write the solution to Problem 1.10 as $u_h^\varepsilon = g_h - z_h^\varepsilon,\ \hat{u}_h^\varepsilon = \hat{g}_h - \hat{z}_h^\varepsilon$ with $(z_h^\varepsilon, \hat{z}_h^\varepsilon)$ satisfying

$$\begin{aligned} (a\partial_t z_h^\varepsilon(t), w_h)_{\mathcal{T}_h} + b_h(z_h^\varepsilon(t), \hat{z}_h^\varepsilon(t); w_h, \hat{w}_h) + \varepsilon d_h(z_h^\varepsilon(t), \hat{z}_h^\varepsilon(t); w_h, \hat{w}_h) \\ = (a\partial_t g_h(t), w_h)_{\mathcal{T}_h} + (b\partial_x g_h(t), w_h)_{\mathcal{T}_h} \\ + \varepsilon(\partial_x g_h(t), \partial_x w_h)_{\mathcal{T}_h} - \varepsilon\langle n\partial_x g_h(t), w_h - \hat{w}_h\rangle_{\partial\mathcal{T}_h} \end{aligned} \tag{1.60}$$

for all $w_h \in W_h,\ \hat{w}_h \in \hat{W}_h$, where we used the continuity of g_h within edges and across junctions as well as the fact that $g_h = \hat{g}$ at the network boundary. Now, by testing (1.60) with $(z_h^\varepsilon, \hat{z}_h^\varepsilon)$ and multiplying by 2 we find that

$$\begin{aligned}\frac{d}{dt}\|a^{1/2}z_h^\varepsilon(t)\|_{\mathcal{T}_h}^2 + |b^{1/2}(z_h^\varepsilon - \hat{z}_h^\varepsilon)|_{\partial\mathcal{T}_h}^2 + \varepsilon\|\partial_x z_h^\varepsilon\|_{\mathcal{T}_h}^2 + \varepsilon|(\tfrac{\alpha}{h_{loc}})^{1/2}(z_h^\varepsilon - \hat{z}_h^\varepsilon)|_{\partial\mathcal{T}_h}^2 \\ \leq \|a^{1/2}\partial_t g_h(t)\|_{\mathcal{T}_h}^2 + |\tfrac{b}{a^{1/2}}\partial_x g_h(t)|_{\mathcal{T}_h}^2 + \|a^{1/2}z_h^\varepsilon(t)\|_{\mathcal{T}_h}^2 + \varepsilon\|\partial_x g_h(t)\|_{\mathcal{T}_h}^2 \\ + \varepsilon\|\partial_x z_h^\varepsilon(t)\|_{\mathcal{T}_h}^2 + \varepsilon|(\tfrac{h_{loc}}{\alpha})^{1/2}\partial_x g_h(t)|_{\partial\mathcal{T}_h}^2 + \varepsilon|(\tfrac{\alpha}{h_{loc}})^{1/2}(z_h^\varepsilon(t) - \hat{z}_h^\varepsilon(t))|_{\partial\mathcal{T}_h}^2,\end{aligned}$$

where we used the discrete stability of the bilinear forms in Lemma 1.12 to estimate the left-hand side of (1.60), and Cauchy-Schwarz and Young's inequality for the right-hand side. Note that the first and the last term in the last line can be absorbed into the first line. Integrating over $(0,t)$ and applying Grönwall's lemma, see e.g. in [116, Lemma 2.7], then yields

$$\begin{aligned}\|a^{1/2}z_h^\varepsilon(t)\|_{\mathcal{T}_h}^2 \leq e^t\|a^{1/2}z_h^\varepsilon(0)\|_{\mathcal{T}_h}^2 + e^t\int_0^t \big(\|a^{1/2}\partial_t g_h(s)\|_{\mathcal{T}_h}^2 + |\tfrac{b}{a^{1/2}}\partial_x g_h(s)|_{\mathcal{T}_h}^2 \\ +\varepsilon\|\partial_x g_h(s)\|_{\mathcal{T}_h}^2 + \varepsilon|(\tfrac{h_{loc}}{\alpha})^{1/2}\partial_x g_h(s)|_{\partial\mathcal{T}_h}^2\big)\ ds\end{aligned}$$

with $z_h^\varepsilon(0) = g_h(0)$. Due to the definition of g_h, the bounds on the parameters in Assumption 1.1 and the fact that ε and h_{loc} are supposed to be small, we can bound the right-hand side by a constant that depends on $\hat{g}$ and $\partial_t\hat{g}$ but not on ε and $\mathcal{T}_h$. Since $u_h^\varepsilon = g_h - z_h^\varepsilon$, this already yields boundedness of u_h^ε. Observing that $\partial_t^n u_h^\varepsilon$ solves (1.56) with boundary data $\partial_t^n\hat{g}$, we can show boundedness of $\partial_t^n u_h^\varepsilon$ independent of ε and $\mathcal{T}_h$ in the same way. □

Finally, we verify the consistency of the proposed method, which means that the exact solution of the transport problem (1.9)–(1.12) and convection-diffusion problem (1.25)–(1.28) also solve Problem 1.10 for $\varepsilon = 0$ and $\varepsilon > 0$, respectively.

Lemma 1.14. *Let $(u,\hat{u})$ and $(u^\varepsilon,\hat{u}^\varepsilon)$ be the solutions to (1.9)–(1.12) and (1.25)–(1.28) with initial values $u(0) = 0$ and $u^\varepsilon(0) = 0$, respectively. We set $\hat{u}(x) = u(x)$ and $\hat{u}^\varepsilon(x) = u^\varepsilon(x)$ for $x \in \mathcal{X}_h$ and $\hat{u}^\varepsilon(v) = \hat{u}(v) = 0$ for $v \in \mathcal{V}_\partial$. Then, $(u,\hat{u})$ and $(u^\varepsilon,\hat{u}^\varepsilon)$ solve (1.56) for all $w_h \in W_h,\ \hat{w}_h \in \hat{W}_h$ for $\varepsilon = 0$ and $\varepsilon > 0$, respectively.*

Proof. We test the bilinear form b_h with w_h and $\hat{w}_h \equiv 0$ and observe that

$$b_h(u^\varepsilon,\hat{u}^\varepsilon;w_h,0) = -(bu^\varepsilon,\partial_x w_h)_{\mathcal{T}_h} + \langle nbu^{\varepsilon,up},w_h\rangle_{\partial\mathcal{T}_h} = (b\partial_x u^\varepsilon,w_h)_{\mathcal{T}_h} - \langle nb\hat{g},w_h\rangle_{\mathcal{V}_\partial^{in}},$$

since u^ε is continuous within edges and across junctions by (1.27) and therefore $nbu^{\varepsilon,up} = nbu^\varepsilon$ at $\mathcal{X}_h \cup \mathcal{V}_0 \cup \mathcal{V}_\partial^{out}$ and $u^\varepsilon = \hat{g}$ at $\mathcal{V}_\partial^{in}$. This identity also holds for $(u,\hat{u})$, since u is continuous within edges and outflow continuous across junctions, see (1.11), which suffices to ensure $nbu^{up} = nbu$. Consequently, $(u,\hat{u})$ solves (1.56) for all $w_h \in W_h$ and $\hat{w}_h \equiv 0$ and $\varepsilon = 0$. In the same manner, testing the bilinear form d_h with w_h and $\hat{w}_h \equiv 0$ we find that

$$\begin{aligned}d_h(u^\varepsilon,\hat{u}^\varepsilon;w_h,0) &= (\partial_x u^\varepsilon,\partial_x w_h)_{\mathcal{T}_h} - \langle n\partial_x u^\varepsilon,w_h\rangle_{\partial\mathcal{T}_h} \\ &\quad + \langle n(u^\varepsilon - \hat{u}^\varepsilon),\partial_x w_h\rangle_{\partial\mathcal{T}_h} + \langle \tfrac{\alpha}{h_{loc}}(u^\varepsilon - \hat{u}^\varepsilon),w_h\rangle_{\partial\mathcal{T}_h} \\ &= -(\partial_{xx}u^\varepsilon,\partial_x w_h)_{\mathcal{T}_h} + \langle nu^\varepsilon,\partial_x w_h\rangle_{\mathcal{V}_\partial} + \langle \tfrac{\alpha}{h_{loc}}u^\varepsilon,w_h\rangle_{\mathcal{V}_\partial},\end{aligned}$$

where we applied integration-by-parts to the first term in the first line. Note that element boundary contributions cancel with the second term in the first line. Due to the continuity of u^ε at interior mesh points and across vertices, the first and second terms in the second line vanish except at the network boundary. Comparing with $l_h^\varepsilon(t; w_h)$ in (1.59), we find that $(u^\varepsilon, \hat{u}^\varepsilon)$ solves (1.56) for all $w_h \in W_h$ and $\hat{w}_h \equiv 0$ and $\varepsilon > 0$. It remains to verify the variational identities for $\hat{w}_h \in \hat{W}_h$ when testing (1.56) with $w_h \equiv 0$, $\hat{w}_h = \chi_x$ for $x \in \mathcal{V}_0 \cup \mathcal{X}_h$. They readily follow from the coupling conditions (1.11)–(1.12) as well as (1.27)–(1.28). This concludes the proof. □

Preliminary error estimate

We are now in the position to derive a first localized error estimate for the semi-discrete scheme given in Problem 1.10.

Lemma 1.15. *Let Assumption 1.1 hold and $t_{max} > 0$. Further, let $(u^0, \hat{u}^0)$ and $(u^\varepsilon, \hat{u}^\varepsilon)$ be the solutions to (1.9)–(1.12) and (1.25)–(1.28) with initial condition $u^0(0) = u^\varepsilon(0) = 0$, and let $(u_h^\varepsilon, \hat{u}_h^\varepsilon)$ be the corresponding solution to Problem 1.10 for $\varepsilon \geq 0$. Then,*

$$\|u^\varepsilon(t) - u_h^\varepsilon(t)\|^2_{L^2(\mathcal{E})} \leq C \sum\nolimits_{T \in \mathcal{T}_h} (\varepsilon h_T^{2k} + h_T^{2k+2}) \|u^\varepsilon\|^2_{H^1(0,t;\, H^{k+1}(T))} \tag{1.61}$$

for all $0 \leq t \leq t_{max}$, $\varepsilon \geq 0$ and $k \leq m$ with constant C being independent of ε and $\mathcal{T}_h$.

Proof. Following [117, Ch. 12] we introduce the upwind projection $\pi_h : H^1_{pw}(\mathcal{E}) \to W_h$ by

$$\pi_h w(x_{e\,-}^i) = w(x_e^i) \qquad \text{for all } i = 1, \ldots, M_e,\ e \in \mathcal{E}, \tag{1.62}$$

$$\int_T (w - \pi_h w)\, p\, dx = 0 \qquad \text{for all } p \in \mathcal{P}_{k-1}(T),\ T \in \mathcal{T}_h, \tag{1.63}$$

where $\pi_h w(x_{e\,-}^i) = \lim_{s \to 0,\, s > 0} \pi_h w(x_e^i - s)$ denotes the upwind value of $\pi_h w$. The projection error can be estimated by standard estimates; see [72, App. C]. More precisely, for any element $T = (x^{in}, x^{out}) \in \mathcal{T}_h$ and function $w \in H^{k+1}(T)$ we have $\pi_h w(x^{out}) = w(x^{out})$ and

$$\begin{aligned} \|w - \pi_h w\|_{L^2(T)} &\leq C h_T^{k+1} \|w\|_{H^{k+1}(T)}, \\ \|\partial_x w - \pi_h \partial_x w\|_{L^2(T)} &\leq C h_T^{k} \|w\|_{H^{k+1}(T)}, \\ |w(x^{in}) - \pi_h w(x^{in})| &\leq C h_T^{k+1/2} \|w\|_{H^{k+1}(T)}, \\ |\partial_x w - \partial_x \pi_h w|_{\partial T} &\leq C h_T^{k-1/2} \|w\|_{H^{k+1}(T)}. \end{aligned} \tag{1.64}$$

We can then split the error $u^\varepsilon - u_h^\varepsilon$ into a projection and a discrete component, i.e.,

$$\|u^\varepsilon(t) - u_h^\varepsilon(t)\|_{L^2(\mathcal{E})} \leq \|\underbrace{u^\varepsilon(t) - \pi_h u^\varepsilon(t)}_{=:\eta_h(t)}\|_{L^2(\mathcal{E})} + \|\underbrace{u_h^\varepsilon(t) - \pi_h u^\varepsilon(t)}_{=:e_h(t)}\|_{L^2(\mathcal{E})}.$$

Note that we understand $\pi_h u^\varepsilon$ pointwise in time. The projection error η_h can be estimated by (1.64) and summing over all elements $T \in \mathcal{T}_h$. It remains to investigate the discrete error component. We set $\hat{u}_v^\varepsilon = 0$ at $v \in \mathcal{V}_\partial$ and $\hat{u}_x^\varepsilon = u^\varepsilon(x)$ at $x \in \mathcal{X}_h$, as well as $\hat{\pi}_h u^\varepsilon = \hat{u}^\varepsilon$.

By testing (1.56) with $w_h = e_h$ and $\hat{w}_h = \hat{e}_h$ and using consistency of the method, see Lemma 1.14, we find that

$$\begin{aligned}\frac{1}{2}\frac{d}{dt}\|a^{1/2}e_h(t)\|^2_{\mathcal{T}_h} &= (a\partial_t e_h(t), e_h(t))_{\mathcal{T}_h} = -b_h(e_h(t), \hat{e}_h(t); e_h(t), \hat{e}_h(t)) \\ &\quad - \varepsilon d_h(e_h(t), \hat{e}_h(t); e_h(t), \hat{e}_h(t)) + (a\partial_t \eta_h(t), e_h(t))_{\mathcal{T}_h} \\ &\quad + b_h(\eta_h(t), \hat{\eta}_h(t); e_h(t), \hat{e}_h(t)) + \varepsilon d_h(\eta_h(t), \hat{\eta}_h(t); e_h(t), \hat{e}_h(t)) \\ &= (i) + \cdots + (v).\end{aligned}$$

By the discrete stability of the bilinear forms given in Lemma 1.12, it holds that

$$(i) + (ii) = -\tfrac{1}{2}|b^{1/2}(e_h(t) - \hat{e}_h(t))|^2_{\partial\mathcal{T}_h} - \varepsilon\|\partial_x e_h(t)\|^2_{\mathcal{T}_h} - \varepsilon|(\tfrac{\alpha}{h_{loc}})^{1/2}(e_h(t) - \hat{e}_h(t))|^2_{\partial\mathcal{T}_h}.$$

Using Cauchy-Schwarz and Young's inequality, the projection error estimates (1.64), as well as the fact that $\partial_t \pi_h u^\varepsilon = \pi_h \partial_t u^\varepsilon$, we can estimate the third term by

$$\begin{aligned}(iii) &\le \tfrac{1}{2}\|a^{1/2}\partial_t \eta(t)\|^2_{\mathcal{T}_h} + \tfrac{1}{2}\|a^{1/2}e_h(t)\|^2_{\mathcal{T}_h} \\ &\le \tfrac{1}{2}C\sum\nolimits_{T\in\mathcal{T}_h} h_T^{2k+2}\|\partial_t u^\varepsilon(t)\|^2_{H^{k+1}(T)} + \tfrac{1}{2}\|a^{1/2}e_h(t)\|^2_{\mathcal{T}_h}.\end{aligned}$$

By the properties of the upwind projection π_h we find that

$$(iv) = -(\eta_h(t), \partial_x e_h(t))_{\mathcal{T}_h} + \langle nb\eta_h^{up}(t), e_h(t) - \hat{e}_h(t)\rangle_{\partial\mathcal{T}_h} = 0,$$

where the first term vanishes due to (1.63) and the second term since $\eta_h^{up} = 0$ which follows from (1.62). Using Cauchy-Schwarz and Young's inequality as well as the discrete trace inequality, see e.g. [120], we can estimate the last term by

$$\begin{aligned}(v) &= \varepsilon(\partial_x \eta_h(t), \partial_x e_h(t))_{\mathcal{T}_h} - \varepsilon\langle\partial_x \eta_h(t), e_h(t) - \hat{e}_h(t)\rangle_{\partial\mathcal{T}_h} \\ &\quad + \varepsilon\langle\eta_h(t) - \hat{\eta}_h(t), \partial_x e_h(t)\rangle_{\partial\mathcal{T}_h} + \varepsilon\langle\tfrac{\alpha}{h_{loc}}(\eta_h(t) - \hat{\eta}_h(t), e_h(t) - \hat{e}_h(t))\rangle_{\partial\mathcal{T}_h} \\ &\le \varepsilon\|\partial_x e_h(t)\|^2_{\mathcal{T}_h} + \varepsilon|(\tfrac{\alpha}{h_{loc}})^{1/2}(e_h(t) - \hat{e}_h(t))|^2_{\partial\mathcal{T}_h} + \tfrac{\varepsilon}{2}\|\partial_x \eta_h(t)\|^2_{\mathcal{T}_h} \\ &\quad + \tfrac{\varepsilon}{2}(C_{tr}^2 + \alpha)|h_{loc}^{-1/2}(\eta_h(t) - \hat{\eta}_h(t))|^2_{\partial\mathcal{T}_h} + \tfrac{\varepsilon}{2}|(\tfrac{h_{loc}}{\alpha})^{1/2}\partial_x \eta_h(t)|^2_{\partial\mathcal{T}_h}.\end{aligned}$$

The first two terms cancel with $(i) + (ii)$, whereas the remaining terms can be estimated using the error estimates (1.64) for the upwind projection. In summary, we obtain

$$\frac{d}{dt}\|a^{1/2}e_h(t)\|^2_{\mathcal{T}_h} \le \|a^{1/2}e_h(t)\|^2_{\mathcal{T}_h} + \sum_{T\in\mathcal{T}_h}\Big(Ch_T^{2k+2}\|\partial_t u^\varepsilon(t)\|^2_{H^{k+1}(T)} + C'\varepsilon h_T^{2k}\|u^\varepsilon(t)\|^2_{H^{k+1}(T)}\Big).$$

Intergrating over $(0, t)$ and applying Grönwall's lemma, see e.g. [116, Lemma 2.7], yields

$$\|a^{1/2}e_h(t)\|^2_{\mathcal{T}_h} \le e^t\|a^{1/2}e_h(0)\|^2_{\mathcal{T}_h} + C''e^t\sum\nolimits_{T\in\mathcal{T}_h}(\varepsilon h_T^{2k} + h_T^{2k+2})\|u^\varepsilon\|^2_{H^1(0,t;H^{k+1}(T))}.$$

Note that $e_h(0) = 0$ since $u_h^\varepsilon(0) = \pi_h u^\varepsilon(0)$ and $a \ge \underline{a}$ by Assumption 1.1. This concludes the proof of Lemma 1.15. □

Remark 1.16. On uniform meshes $h_T \approx h$ the localized error estimate (1.61) in Lemma 1.15 yields order optimal convergence for the pure transport problem, i.e.,

$$\|u^0 - u_h^0\|_{L^\infty(0,t_{max};L^2(\mathcal{E}))} \leq Ch^{k+1}.$$

For small $\varepsilon > 0$, however, the derivatives of u^ε degenerate as shown in Lemma 1.9, and (1.61) leads to

$$\|u^\varepsilon - u_h^\varepsilon\|_{L^\infty(0,t_{max};L^2(\mathcal{E}))} \leq C_\varepsilon(\varepsilon h^k + h^{k+1})$$

with a constant C_ε that depends on ε and, in particular, blows up for $\varepsilon \to 0$. Consequently, (1.61) does not provide ε-uniform convergence estimates on uniform meshes. We can overcome this issue by using suitably adapted meshes; see Section 1.3.4.

1.3.3. Fully discrete hybrid-dG method

For the time discretization, we apply the discontinuous Galerkin time-stepping method as presented in [117, Ch. 12]. We consider discrete time points $0 = t^0 < t^1 < \cdots < t^N = t_{max}$ with local and global time step sizes $\tau^n = t^n - t^{n-1}$ and $\tau = \max_n \tau^n$, and denote by $\mathcal{S}^\tau = \{(t^{n-1}, t^n] : n = 1, \ldots, N\}$ the corresponding temporal mesh. We search for piecewise polynomials in time of degree $\leq k$ and define for $w \in \mathcal{P}_k(\mathcal{S}^\tau)$, i.e., $w|_{(t^{n-1},t^n]} \in \mathcal{P}_k((t^{n-1}, t^n])$ for all $n = 1, \ldots, N$, the following expressions

$$w(t_+^n) = \lim_{s\to 0, s>0} w(t^n + s) \qquad \text{and} \qquad [w]^n = w(t_+^n) - w(t^n),$$

denoting the downwind limit value and the jump over the time interface at t^n. We now propose the following fully discretized scheme.

Problem 1.17. Find $u_h^{\varepsilon,\tau} \in \mathcal{P}_k(\mathcal{S}^\tau; W_h)$ and $\hat{u}_h^{\varepsilon,\tau} \in \mathcal{P}_k(\mathcal{S}^\tau; \hat{W}_h)$ with $u_h^{\varepsilon,\tau}(0) = 0$, so that

$$\begin{aligned}\int_{t^{n-1}}^{t^n} \Big(&(a\partial_t u_h^{\varepsilon,\tau}(t), w_h^\tau(t))_{\mathcal{T}_h} + b_h(u_h^{\varepsilon,\tau}(t), u_h^{\varepsilon,\tau}(t); w_h^\tau(t), \hat{w}_h^\tau(t)) \\ &+ \varepsilon d_h(u_h^{\varepsilon,\tau}(t), u_h^{\varepsilon,\tau}(t); w_h^\tau(t), \hat{w}_h^\tau(t))\Big)\, dt + (a[u_h^{\varepsilon,\tau}]^{n-1}, w_h^\tau(t_+^{n-1}))_{\mathcal{T}_h} \\ = &\int_{t^{n-1}}^{t^n} l_h^\varepsilon(t; w_h^\tau(t))\, dt\end{aligned} \tag{1.65}$$

holds for all $w_h^\tau \in \mathcal{P}_k((t^{n-1}, t^n]; W_h)$, $\hat{w}_h^\tau \in \mathcal{P}_k((t^{n-1}, t^n]; \hat{W}_h)$ and $n = 1, \ldots, N$ with bilinear and linear forms b_h, d_h, l_h^ε defined in (1.57)–(1.59).

Remark 1.18. Just like the semi-discrete method, the fully discrete scheme is formally *asymptotic preserving*, i.e., by setting $\varepsilon = 0$ in (1.65) the solution of Problem 1.17 yields a viable approximation for the pure transport problem on networks (1.9)–(1.12).

Basic properties

Let us first investigate the well-posedness and consistency of the fully discrete method.

Lemma 1.19. *Let Assumption 1.1 hold. Then, Problem 1.17 is well-posed for all $\varepsilon \geq 0$.*

Proof. By choosing a basis of the trial spaces $\mathcal{P}_k((t^{n-1}, t^n]; W_h)$ and $\mathcal{P}_k((t^{n-1}, t^n]; \hat{W}_h)$, equation (1.65) can be transformed into a linear system of equations for which solvability is equivalent to the uniqueness of solutions to the homogeneous system. We thus have to show that for fixed $n = 1, \dots, N$ and $u_h^{\varepsilon,\tau}(t^{n-1}) = 0$ equation (1.65) with zero right-hand side has a unique solution. Testing with $w_h = u_h^{\varepsilon,\tau}$, $\hat{w}_h = \hat{u}_h^{\varepsilon,\tau}$ and using the discrete stability of the bilinear forms in Lemma 1.12, we find that

$$\int_{t^{n-1}}^{t^n} \Big((a\partial_t u_h^{\varepsilon,\tau}, u_h^{\varepsilon,\tau})_{\mathcal{T}_h} + \tfrac{1}{2}|b^{1/2}(u_h^{\varepsilon,\tau} - \hat{u}_h^{\varepsilon,\tau})|^2_{\partial\mathcal{T}_h} + \varepsilon|(\tfrac{\alpha}{h_{loc}})^{1/2}(u_h^{\varepsilon,\tau} - \hat{u}_h^{\varepsilon,\tau})|^2_{\partial\mathcal{T}_h} \tag{1.66}$$
$$+ \varepsilon\|\partial_x u_h^{\varepsilon,\tau}\|_{\mathcal{T}_h}\Big)\, dt + (a[u_h^{\varepsilon,\tau}]^{n-1}, u_h^{\varepsilon,\tau}(t_+^{n-1}))_{\mathcal{T}_h} \leq \int_{t^{n-1}}^{t^n} l_h(t; u_h^{\varepsilon,\tau})\, dt = 0.$$

We further observe that

$$\int_{t^{n-1}}^{t^n} (a\partial_t u_h^{\varepsilon,\tau}, u_h^{\varepsilon,\tau})_{\mathcal{T}_h}\, dt + (a[u_h^{\varepsilon,\tau}]^{n-1}, u_h^{\varepsilon,\tau}(t_+^{n-1}))_{\mathcal{T}_h} \tag{1.67}$$
$$= \tfrac{1}{2}\|a^{1/2}u_h^{\varepsilon,\tau}(t^n)\|^2_{\mathcal{T}_h} + \tfrac{1}{2}\|a^{1/2}u_h^{\varepsilon,\tau}(t_+^{n-1})\|^2_{\mathcal{T}_h} - (au_h^{\varepsilon,\tau}(t^{n-1}), u_h^{\varepsilon,\tau}(t_+^{n-1})).$$

The last term vanishes for $u_h^{\varepsilon,\tau}(t^{n-1}) = 0$, and the solution $u_h^{\varepsilon,\tau}$ of the homogeneous system thus satisfies

$$\tfrac{1}{2}\|a^{1/2}u_h^{\varepsilon,\tau}(t^n)\|^2_{\mathcal{T}_h} + \tfrac{1}{2}\|a^{1/2}u_h^{\varepsilon,\tau}(t_+^{n-1})\|^2_{\mathcal{T}_h} + \int_{t^{n-1}}^{t^n} \Big(\tfrac{1}{2}|b^{1/2}(u_h^{\varepsilon,\tau} - u_h^{\hat{\varepsilon},\tau})|^2_{\partial\mathcal{T}_h} \tag{1.68}$$
$$+\varepsilon|(\tfrac{\alpha}{h_{loc}})^{1/2}(u_h^{\varepsilon,\tau} - \hat{u}^{\varepsilon,n})|^2_{\partial\mathcal{T}_h} + \varepsilon\|\partial_x u_h^{\varepsilon,\tau}\|_{\mathcal{T}_h}\Big)\, dt = 0.$$

This yields uniqueness for $\varepsilon > 0$. In the case $\varepsilon = 0$, i.e., for the pure transport problem, we can only conclude that $u_h^{0,\tau}(t^n) = u_h^{0,\tau}(t_+^{n-1}) = 0$ as well as $\frac{1}{2}|b^{1/2}(u_h^{0,\tau}(t) - \hat{u}_h^{0,\tau}(t))|^2_{\partial\mathcal{T}_h} = 0$. In order to obtain uniqueness, we test (1.65) with $w_h = \pi^\tau(e^{-t}u_h^{0,\tau})$, $\hat{w}_h = \pi^\tau(e^{-t}\hat{u}_h^{0,\tau})$ with π^τ being the L^2-projection in time. The first and the fourth term on the left-hand side of (1.65) then equal

$$\int_{t^{n-1}}^{t^n} (a\partial_t u_h^{0,\tau}, w_h)\, dt + (a[u_h^{0,\tau}]^{n-1}, w_h(t_+^{n-1}))_{\mathcal{T}_h} = \int_{t^{n-1}}^{t^n} (a\partial_t u_h^{0,\tau}, e^{-t}u_h)\, dt$$
$$= \int_{t^{n-1}}^{t^n} \tfrac{1}{2}e^{-t}\|u_h^{0,\tau}\|^2_{\mathcal{T}_h}\, dt + \tfrac{1}{2}e^{-t}\|u_h^{0,\tau}(t)\|^2_{\mathcal{T}_h}\Big|_{t^{n-1}}^{t^n} = \int_{t^{n-1}}^{t^n} \tfrac{1}{2}e^{-t}\|u_h^{0,\tau}\|^2_{\mathcal{T}_h}\, dt,$$

where we used that the second term in the first line and the second term in the second line both vanish due to (1.68). Again, using the property of the L^2-projection as well as Lemma 1.12, we find that the second term on the left-hand side of (1.65) equals

$$\int_{t^{n-1}}^{t^n} b_h(u_h^{0,\tau}, \hat{u}_h^{0,\tau}; w_h, \hat{w}_h)\, dt = \int_{t^{n-1}}^{t^n} \tfrac{1}{2}e^{-t}|b^{1/2}(u_h^{0,\tau} - \hat{u}_h^{0,\tau})|^2_{\partial\mathcal{T}_h}\, dt = 0,$$

which holds due to (1.68). In summary, we obtain

$$\int_{t^{n-1}}^{t^n} \tfrac{1}{2}e^{-t}\|u_h^{0,\tau}\|^2_{\mathcal{T}_h}\, dt = 0,$$

from which we conclude that $u_h^{0,\tau} = 0$, i.e., uniqueness of the solution for $\varepsilon = 0$. □

A key ingredient for our analysis is the consistency of the fully discrete scheme, which almost readily follows from the consistency of the semi-discrete method.

Lemma 1.20. *Let* $(u^0, \hat{u}^0)$ *and* $(u^\varepsilon, \hat{u}^\varepsilon)$ *be the solutions to* (1.9)–(1.12) *and* (1.25)–(1.28) *with initial values* $u^0(0) = u^\varepsilon(0) = 0$*, respectively. We set* $\hat{u}^0(x) = u^0(x)$ *and* $\hat{u}^\varepsilon(x) = u^\varepsilon(x)$ *for* $x \in \mathcal{X}_h$ *and* $\hat{u}^0(v) = \hat{u}^\varepsilon(v) = 0$ *for* $v \in \mathcal{V}_\partial$*. Then,* $(u^0, \hat{u}^0)$ *and* $(u^\varepsilon, \hat{u}^\varepsilon)$ *solve* (1.65) *for* $\varepsilon = 0$ *and* $\varepsilon > 0$*, respectively. Moreover, the corresponding semi-discrete solution* $(u_h^\varepsilon, \hat{u}_h^\varepsilon)$ *to Problem 1.10 also satisfies* (1.65) *for all* $\varepsilon \geq 0$*.*

Proof. We observe that

$$\int_{t^{n-1}}^{t^n} (a\partial_t u^\varepsilon, w_h)_{\mathcal{T}_h}\, dt + ([u^\varepsilon]^{n-1}, w_h(t_+^{n-1}))_{\mathcal{T}_h} = \int_{t^{n-1}}^{t^n} (a\partial_t u^\varepsilon, w_h)_{\mathcal{T}_h}\, dt,$$

since u^ε is continuous in time for $\varepsilon \geq 0$. The same holds for the semi-discrete solution u_h^ε. Since u^0 and u^ε are consistent with the semi-discrete scheme, see Lemma 1.14, consistency of the fully discrete scheme then immediately follows by integrating (1.56) over time. □

Preliminary error estimate

By splitting the error into a spatial and a temporal component, and using Lemma 1.15 for the former, we can prove the following localized error estimate.

Lemma 1.21. *Let* $(u^0, \hat{u}^0)$ *and* $(u^\varepsilon, \hat{u}^\varepsilon)$ *be the solutions to* (1.9)–(1.12) *and* (1.25)–(1.28)*, respectively, and let* $(u_h^{\varepsilon,\tau}, \hat{u}_h^{\varepsilon,\tau})$ *be the corresponding solution to Problem 1.17. Then,*

$$\|u^\varepsilon(t^n) - u_h^{\varepsilon,\tau}(t^n)\|_{L^2(\mathcal{E})}^2 \leq C \sum_{T \in \mathcal{T}_h} (\varepsilon h_T^{2k} + h_T^{2k+2}) \|u^\varepsilon\|_{H^1(0,t^n;H^{k+1}(T))}^2 + C'\tau^{2k+1} \tag{1.69}$$

for all $n = 1, \ldots, N$ *and* $\varepsilon \geq 0$*. The constants* C, C' *are independent of* ε*,* $\mathcal{T}_h$*, and* τ*.*

Proof. We split the error into a spatial and a temporal error component, i.e.,

$$\|u^\varepsilon(t^n) - u_h^{\varepsilon,\tau}(t^n)\|_{L^2(\mathcal{E})} \leq \|u^\varepsilon(t^n) - u_h^\varepsilon(t^n)\|_{L^2(\mathcal{E})} + \|u_h^\varepsilon(t^n) - u_h^{\varepsilon,\tau}(t^n)\|_{L^2(\mathcal{E})}$$

with $(u_h^\varepsilon, \hat{u}_h^\varepsilon)$ being the corresponding semi-discrete solution to Problem 1.10. Then, Lemma 1.15 yields an estimate for the first term. For the second term, we will show

$$\|u_h^\varepsilon(t^n) - u_h^{\varepsilon,\tau}(t^n)\|_{L^2(\mathcal{E})} \leq C\tau^{k+1/2} \|u_h^\varepsilon\|_{H^{k+1}(0,t^n;L^2(\mathcal{E}))} \leq C'\tau^{k+1/2}, \tag{1.70}$$

where the second inequality already follows from the bounds on the semi-discrete solution in Lemma 1.13. In order to prove the first inequality, we introduce the L^2-projection in time by $\pi^\tau : L^2(0, t_{max}) \to \mathcal{P}_k(S^\tau)$ such that

$$\int_{t^{n-1}}^{t^n} (w - \pi^\tau w) p\, dt = 0 \qquad \text{for all } p \in \mathcal{P}_k((t^{n-1}, t^n]),\ n = 1, \ldots, N,$$

and we understand $\pi^\tau u_h^\varepsilon$ and $\pi^\tau \hat{u}_h^\varepsilon$ pointwise in space. We split the error into a projection and a discrete component, i.e.,

$$\|u_h^\varepsilon(t^n) - u_h^{\varepsilon,\tau}(t^n)\|_{L^2(\mathcal{E})} \leq \|\underbrace{u_h^\varepsilon(t^n) - \pi^\tau u_h^\varepsilon(t^n)}_{=:\eta_h^\tau(t^n)}\|_{L^2(\mathcal{E})} + \|\underbrace{u_h^{\varepsilon,\tau}(t^n) - \pi^\tau u_h^\varepsilon(t^n)}_{=:e_h^\tau(t^n)}\|_{L^2(\mathcal{E})}.$$

The projection error η_h^τ can be estimated by standard estimates leading to

$$\|\eta_h^\tau(t^n)\|_{L^2(\mathcal{E})} \leq C\tau^{k+1/2}\|u_h^\varepsilon\|_{H^{k+1}(0,t^n;L^2(\mathcal{E}))} \leq C'\tau^{k+1/2},$$

see [72, App. C], where the second inequality again follows from the bounds in Lemma 1.13. It remains to investigate the discrete error. Testing (1.65) with $w_h^\tau = e_h^\tau,\ \hat{w}_h^\tau = \hat{e}_h^\tau$ yields

$$\begin{aligned}
&\int_{t^{n-1}}^{t^n} (a\partial_t e_h^\tau, e_h^\tau)_{\mathcal{T}_h}\ dt + (a[e_h^\tau]^{n-1}, e_h^\tau(t_+^{n-1}))_{\mathcal{T}_h} \qquad (1.71)\\
&\quad = -\int_{t^{n-1}}^{t^n} \Big(b_h(e_h^\tau, \hat{e}_h^\tau; e_h^\tau, e_h^\tau) + \varepsilon d_h(e_h^\tau, \hat{e}_h^\tau; e_h^\tau, e_h^\tau)\Big)\ dt + \int_{t^{n-1}}^{t^n} l_h^\varepsilon(t; e_h^\tau)\ dt\\
&\quad\quad - \int_{t^{n-1}}^{t^n} (a\partial_t \pi^\tau u_h^\varepsilon, e_h^\tau)_{\mathcal{T}_h}\ dt - (a[\pi^\tau u_h^\varepsilon]^{n-1}, e_h^\tau(t_+^{n-1}))_{\mathcal{T}_h}\\
&\quad\quad - \int_{t^{n-1}}^{t^n} \Big(b_h(\pi^\tau u_h^\varepsilon, \pi^\tau \hat{u}_h^\varepsilon; e_h^\tau, e_h^\tau) + \varepsilon d_h(\pi^\tau u_h^\varepsilon, \pi^\tau \hat{u}_h^\varepsilon; e_h^\tau, e_h^\tau)\Big)\ dt\\
&\quad = (i) + \cdots + (vii).
\end{aligned}$$

By Lemma 1.12 the first two terms equal

$$(i) + (ii) = -\int_{t^{n-1}}^{t^n} \big(\tfrac{1}{2}|b^{1/2}(e_h^\tau - \hat{e}_h^\tau)|_{\partial\mathcal{T}_h}^2 + \varepsilon\|\partial_x e_h^\tau\|_{\mathcal{T}_h}^2 + \varepsilon|\tfrac{\alpha}{h_{loc}}(e_h^\tau - \hat{e}_h^\tau)|_{\partial\mathcal{T}_h}^2\big)\ dt \leq 0.$$

The definition of the L^2-projection then leads to

$$\begin{aligned}
(vi) + (vii) &= -\int_{t^{n-1}}^{t^n} \big(b_h(u_h^\varepsilon, \hat{u}_h^\varepsilon; e_h^\tau, e_h^\tau) + \varepsilon d_h(u_h^\varepsilon, \hat{u}_h^\varepsilon; e_h^\tau, e_h^\tau)\big)\ dt\\
&= \int_{t^{n-1}}^{t^n} (a\partial_t u_h^\varepsilon, e_h^\tau)_{\mathcal{T}_h}\ dt + (a[u_h^\varepsilon]^{n-1}, e_h^\tau(t_+^{n-1}))_{\mathcal{T}_h} - \int_{t^{n-1}}^{t^n} l_h^\varepsilon(t; e_h^\tau)\ dt,
\end{aligned}$$

where we used consistency of the method, which was established in Lemma 1.20. The last term cancels with (iii). The first two terms together with $(iv) + (v)$ then equal

$$\begin{aligned}
&\int_{t^{n-1}}^{t^n} (a\partial_t \eta_h^\tau, e_h^\tau)_{\mathcal{T}_h}\ dt + (a[\eta_h^\tau]^{n-1}, e_h^\tau(t_+^{n-1}))_{\mathcal{T}_h}\\
&\quad = -\int_{t^{n-1}}^{t^n} (a\eta_h^\tau, \partial_t e_h^\tau)_{\mathcal{T}_h}\ dt + (a\eta_h^\tau(t^n), e_h^\tau(t^n))_{\mathcal{T}_h}\\
&\quad\quad - (a\eta_h^\tau(t_+^{n-1}), e_h^\tau(t_+^{n-1}))_{\mathcal{T}_h} + (a[\eta_h^\tau]^{n-1}, e_h^\tau(t_+^{n-1}))_{\mathcal{T}_h}\\
&\quad = (a\eta_h^\tau(t^n), e_h^\tau(t^n))_{\mathcal{T}_h} - (a\eta_h^\tau(t^{n-1}), e_h^\tau(t_+^{n-1}))_{\mathcal{T}_h}.
\end{aligned}$$

Note that the first term in the second line vanishes due to the definition of the projection and the fact that a does not depend on the time. Summing (1.71) over n leads to

$$\begin{aligned}
&\sum\nolimits_{i=1}^n \int_{t^{i-1}}^{t^i} (a\partial_t e_h^\tau, e_h^\tau)_{\mathcal{T}_h}\ dt + (a[e_h^\tau]^{i-1}, e_h^\tau(t_+^{i-1}))_{\mathcal{T}_h} \qquad (1.72)\\
&\quad\quad \leq \sum\nolimits_{i=1}^n (a\eta_h^\tau(t^i), e_h^\tau(t^i))_{\mathcal{T}_h} - (a\eta_h^\tau(t^{i-1}), e_h^\tau(t_+^{i-1}))_{\mathcal{T}_h}.
\end{aligned}$$

The left-hand side of (1.72) equals

$$\begin{aligned}(lhs) &= \tfrac{1}{2}\|a^{1/2}e_h^\tau(t^n)\|_{\mathcal{T}_h}^2 + \sum_{i=1}^{n-1}\Big(\tfrac{1}{2}\|a^{1/2}e_h^\tau(t^i)\|_{\mathcal{T}_h}^2 - \tfrac{1}{2}\|a^{1/2}e_h^\tau(t_+^i)\|_{\mathcal{T}_h}^2 + (a[e_h^\tau]^i, e_h^\tau(t_+^i))_{\mathcal{T}_h}\Big) \\ &\quad - \tfrac{1}{2}\|a^{1/2}e_h^\tau(t_+^0)\|_{\mathcal{T}_h}^2 + (a[e_h^\tau]^0, e_h^\tau(t_+^0))_{\mathcal{T}_h} \\ &= \tfrac{1}{2}\|a^{1/2}e_h^\tau(t^n)\|_{\mathcal{T}_h}^2 + \sum_{i=1}^{n-1}\tfrac{1}{2}\|a^{1/2}[e_h^\tau]^i\|_{\mathcal{T}_h}^2 + \tfrac{1}{2}\|a^{1/2}e_h^\tau(t_+^0)\|_{\mathcal{T}_h}^2 - (ae_h^\tau(t^0), e_h^\tau(t_+^0))_{\mathcal{T}_h}.\end{aligned}$$

For the right-hand side of (1.72) we find by using Young's inequality that

$$\begin{aligned}(rhs) &= (a\eta_h^\tau(t^n), e_h^\tau(t^n))_{\mathcal{T}_h} - \sum_{i=1}^{n-1}(a\eta(t^i), [e_h^\tau]^i)_{\mathcal{T}_h} - (a\eta_h^\tau(t^0), e_h^\tau(t_+^0))_{\mathcal{T}_h} \\ &\le \|a^{1/2}\eta_h^\tau(t^n)\|_{\mathcal{T}_h}^2 + \tfrac{1}{4}\|a^{1/2}e_h^\tau(t^n)\|_{\mathcal{T}_h}^2 + \sum_{i=1}^{n-1}\Big(\|a^{1/2}\eta(t^i)\|_{\mathcal{T}_h}^2 + \tfrac{1}{4}\|a[e_h^\tau]^i\|_{\mathcal{T}_h}^2\Big) \\ &\quad + \|a^{1/2}\eta_h^\tau(t^0)\|_{\mathcal{T}_h}^2 + \tfrac{1}{4}\|a^{1/2}e_h^\tau(t_+^0)\|_{\mathcal{T}_h}^2.\end{aligned}$$

Together, this yields

$$\begin{aligned}\tfrac{1}{4}\|a^{1/2}e_h^\tau(t^n)\|_{\mathcal{T}_h}^2 + \tfrac{1}{4}\sum_{i=1}^{n-1}\|a^{1/2}[e_h^\tau]^i\|_{\mathcal{T}_h}^2 &\le \|a^{1/2}e_h^\tau(t^0)\|_{\mathcal{T}_h}^2 + \|a^{1/2}\eta_h^\tau(t^n)\|_{\mathcal{T}_h}^2 \\ &\quad + \sum_{i=1}^{n-1}\|a^{1/2}\eta(t^i)\|_{\mathcal{T}_h}^2 + \|a^{1/2}\eta_h^\tau(t^0)\|_{\mathcal{T}_h}^2.\end{aligned}$$

From standard projection error estimates, see [72, App. C], and the bounds on a in Assumption 1.1 we deduce

$$\|a^{1/2}e_h^\tau(t^n)\|_{\mathcal{T}_h}^2 \le \|a^{1/2}e_h^\tau(t^n)\|_{\mathcal{T}_h}^2 + \sum_{i=1}^{n-1}\|a^{1/2}[e_h^\tau]^i\|_{\mathcal{T}_h}^2 \le C\tau^{2k+1}\|u_h^\varepsilon\|_{H^{k+1}(0,t^n;L^2(\mathcal{E}))}^2,$$

where we used the fact that $\|a^{1/2}e_h^\tau(t_-^0)\|_{\mathcal{T}_h} = 0$, since $u_h^{\varepsilon,\tau}(0) = \pi^\tau u_h^\varepsilon(0)$. Since $a \ge \bar{a} > 0$, this proves (1.70). □

Remark 1.22. The convergence rate in time stated in Lemma 1.21 is sub-optimal by a factor of 1/2. In [48, Ch. 69, Thm. 69.18] and [117, Ch. 12, Thm. 12.1] the authors showed an optimal order error estimate for the dG time-stepping applied to the parabolic problem $\partial_t u + \mathcal{A}u = f$, where the spatial operator $\mathcal{A}$ is supposed to be elliptic and continuous with respect to a certain norm. For the proof, they used an upwind projection in time similar to the one that was utilized for the proof of the preliminary error estimate for the semi-discrete scheme in Lemma 1.15. Since our problem degenerates to a hyperbolic one for $\varepsilon \to 0$, the assumptions on $\mathcal{A}$ do not hold uniformly in ε. Applying the upwind projection is thus not leading to optimal order convergence rates uniformly in ε. In particular, we do not obtain reasonable error estimates in the limit $\varepsilon = 0$. However, this does not happen in the lowest order case of $k = 0$ in time, which corresponds to the implicit Euler time-stepping, since the upwind projection in time equals the pointwise interpolation at the endpoint of each time interval. For higher order $k \ge 1$, we ensure ε-uniform convergence estimates by using the L^2-projection in time, but ultimately lose 1/2 order. Moreover, in [117, Ch. 12, Thm. 12.2] error estimates in the L^2-norm in time could be derived from the error estimates at the time grid points. A key assumption is that the spatial operator $\mathcal{A}$ is symmetric, which is not the case here. So far, we were not able to transfer these results to our problem. It might be possible to analyze our method in the framework of Runge-Kutta methods and derive order

optimal error estimates as well as superconvergence results at the time grid points since the dG time-stepping using the Radau quadrature to approximate the time intervals can be shown to be equivalent to the Radau IIA Runge-Kutta method; see [1, 119]. We refer to [63, Ch. IV.5] for the analysis of implicit Runge-Kutta methods.

1.3.4. ε-Uniform error estimates

As outlined in Remark 1.16, the localized error estimate (1.69) in Lemma 1.21 for the fully discrete hybrid-dG method does not yield ε-uniform error estimates on uniform meshes $h_T \approx h$, since derivatives of the exact solution blow up at the outflow boundary of the edges; see Lemma 1.9. To overcome this issue we will set up a suitably adapted mesh on which we can derive ε-uniform convergence under reasonable regularity assumptions on the solution.

Construction of the layer-adapted mesh

The starting point for the construction of the adapted spatial mesh is a quasi-uniform mesh $\mathcal{T}_h^0$ with step size $h_T \approx h$ for all $T \in \mathcal{T}_h^0$. We now distinguish between two cases. If $\varepsilon < h^{2k}$, i.e., ε is very small compared to h, then we keep the uniform mesh and set $\mathcal{T}_h = \mathcal{T}_h^0$. If $\varepsilon \geq h^{2k}$ we construct a layer-adapted mesh similar to the one proposed by Gartland in [56], which is fine close to the outflow boundary of each pipe and coarse away from it. More precisely, for every $e \in \mathcal{E}$ we introduce a transition point

$$x_e^* = \ell_e - \frac{k+1}{b_e}\varepsilon \log(1/\varepsilon). \tag{1.73}$$

In $[0, x_e^*]$ we take the corresponding grid points from the uniform coarse mesh $\mathcal{T}_h^0$ and add the transition point $x_e^{M_e^*} = x_e^*$, where M_e^* indicates the number of grid points in $[0, x_e^*]$. Note that $M_e^* \leq \ell_e h^{-1}$. All points in the coarse part are collected in $\mathcal{T}_h^{\varepsilon,1}$. In the boundary layer region $(x_e^*, \ell_e]$ the grid points are defined recursively by

$$h_e^i = \varepsilon h e^{b_e(\ell_e - x_e^i)/\varepsilon(k+1)}, \quad x_e^{i-1} = x_e^i - h_e^i,\ i \leq M_e \quad \text{with} \quad x_e^{M_e} = \ell_e. \tag{1.74}$$

The index M_e is chosen so that $x_e^{M_e^*+1}$ is the last point that is strictly larger x_e^*. We collect these points in $\mathcal{T}_h^{\varepsilon,2}$. The full mesh is then given by $\mathcal{T}_h^{\varepsilon} = \mathcal{T}_h^{\varepsilon,1} \cup \mathcal{T}_h^{\varepsilon,2}$ and we set $\mathcal{T}_h = \mathcal{T}_h^{\varepsilon}$. An illustration of the layer-adapted mesh is given in Figure 1.4. Note that we will use a uniform temporal mesh $\mathcal{S}^\tau$ with $\tau^n \approx \tau$ in both cases.

ε-Uniform error estimate

Let us now set up a suitable approximation strategy exploiting the previously introduced layer-adapted mesh, which leads to the following ε-uniform error estimates.

Theorem 1.23. *Let Assumption 1.1 hold, and let* $(u^0, \hat{u}^0)$ *be the solution to* (1.9)–(1.12)

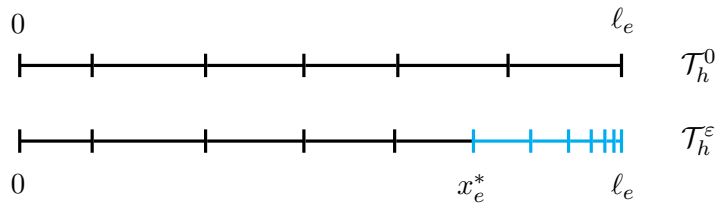

Figure 1.4.: Quasi-uniform mesh $\mathcal{T}_h^0$ for a single interval (top) and corresponding layer-adapted mesh $\mathcal{T}_h^\varepsilon = \mathcal{T}_h^{\varepsilon,1} \cup \mathcal{T}_h^{\varepsilon,2}$ (bottom) with layer region (x_e^*, ℓ^e) in cyan.

and $(u^\varepsilon, \hat{u}^\varepsilon)$ *be the solution to* (1.25)–(1.28) *with* $u^0(0) = u^\varepsilon(0) = 0$. *We define*

$$\tilde{u}_h^{\varepsilon,\tau} := \begin{cases} u_h^{0,\tau}, & \varepsilon < h^{2k}, \\ u_h^{\varepsilon,\tau}, & \varepsilon \geq h^{2k} \end{cases} \tag{1.75}$$

with $(u_h^{0,\tau}, \hat{u}_h^{0,\tau})$ *being the solution to Problem 1.17 for* $\varepsilon = 0$ *on* $\mathcal{T}_h^0 \times \mathcal{S}^\tau$ *and* $(u_h^{\varepsilon,\tau}, \hat{u}_h^{\varepsilon,\tau})$ *being the solution to Problem 1.17 for* $\varepsilon > 0$ *on* $\mathcal{T}_h^\varepsilon \times \mathcal{S}^\tau$. *Then,*

$$\|u^\varepsilon(t^n) - \tilde{u}_h^{\varepsilon,\tau}(t^n)\|_{L^2(\mathcal{E})} \leq C \max(h^{k+1}, \min(\sqrt{\varepsilon}, h^k)) + C'\tau^{k+1/2} \tag{1.76}$$

holds for all $n = 1, \ldots, N$. *Moreover, the number of elements in* $\mathcal{T}_h^\varepsilon$ *is bounded by* $C''h^{-1}$ *for all* $\varepsilon > 0$. *The constants* C, C', C'' *are independent of* ε, $\mathcal{T}_h$ *and* τ.

Proof. We consider both cases $\varepsilon < h^{2k}$ and $\varepsilon \geq h^{2k}$ separately and exploit the construction of the layer-adapted mesh and of the approximation $\tilde{u}_h^{\varepsilon,\tau}$ in the investigations.

Case 1 ($\varepsilon < h^{2k}$). By the triangle inequality, we can split the error into

$$\|u^\varepsilon(t^n) - \tilde{u}_h^{\varepsilon,\tau}(t^n)\|_{L^2(\mathcal{E})} \leq \|u^\varepsilon(t^n) - u^0(t^n)\|_{L^2(\mathcal{E})} + \|u^0(t^n) - u_h^{0,\tau}(t^n)\|_{L^2(\mathcal{E})},$$

where we inserted the definition of $\tilde{u}_h^{\varepsilon,\tau}$ given in (1.75). For the first term, we use the asymptotic estimate in Theorem 1.7, i.e.,

$$\|u^\varepsilon(t^n) - u^0(t^n)\|_{L^2(\mathcal{E})} \leq c\sqrt{\varepsilon},$$

whereas the second term can be estimated by the localized error estimate (1.69) in Lemma 1.21 which yields in the case $\varepsilon = 0$ on the uniform mesh $\mathcal{T}_h^0$ that

$$\|u^0(t^n) - u_h^{0,\tau}(t^n)\|_{L^2(\mathcal{E})} \leq c' h^{k+1} + C'\tau^{k+1/2}.$$

Overall, by combining the two estimates, we obtain (1.76) for the case $\varepsilon = 0$.

Case 2 ($\varepsilon \geq h^{2k}$). By the localized error estimate given in Lemma 1.21 it holds that

$$\|u^\varepsilon(t^n) - u_h^{\varepsilon,\tau}(t^n)\|_{L^2(\mathcal{E})}^2 \leq c' \sum\nolimits_{T \in \mathcal{T}_h} (\varepsilon h_T^{2k} + h_T^{2k+2}) \|u^\varepsilon\|_{H^1(0,t^n;H^{k+1}(T))}^2 + C'\tau^{2k+1}$$

with constants c', C' that are independent of $\varepsilon, \mathcal{T}_h$ and τ. Moreover, by Lemma 1.9 we know that for $T_e^i = (x_e^{i-1}, x_e^i)$ it holds that

$$\begin{aligned} \int_0^{t^n} \int_{T_e^i} |\partial_t^s \partial_x^j u_e^\varepsilon(x,t)|^2 \, dx \, dt &\leq \int_0^{t^n} \int_{T_e^i} c^2 (1 + \varepsilon^{-j} e^{-b_e(\ell_e - x)/\varepsilon}) \, dx \, dt \\ &\leq c^2 t^n h_{T_e^i} (1 + \varepsilon^{-j} e^{-b_e(\ell_e - x_e^i)/\varepsilon}) \end{aligned}$$

for $s = 0, 1$ and $j \leq k+1$. For $T_e^i \in \mathcal{T}_h^{\varepsilon,1}$, i.e., $x_e^i \leq x_e^*$ as defined in (1.73), we can immediately deduce that

$$\int_0^{t^n} \int_{T_e^i} |\partial_t^n \partial_x^j u_e^\varepsilon(x,t)|^2 \, dx \, dt \leq 2c^2 t^n h_e^i.$$

Hence, by summing over $T \in \mathcal{T}_h^{\varepsilon,1}$ it follows that

$$\sum\nolimits_{T \in \mathcal{T}_h^{\varepsilon,1}} (\varepsilon h_T^{2k} + h_T^{2k+2}) \|u^\varepsilon\|^2_{H^1(0,t^n;H^{k+1}(T))} \leq c''(t^n)(\varepsilon h^{2k} + h^{2k+2}).$$

For $T_e^i = (x_e^{i-1}, x_e^i) \in \mathcal{T}_h^{\varepsilon,2}$, i.e., $x_e^{i-1} \geq x_e^*$, the spatial mesh is defined recursively by (1.74). Similarly as above, the bounds (1.39) yield for small ε that

$$\begin{aligned}
&\sum\nolimits_{T_e^i \in \mathcal{T}_h^{\varepsilon,2}} (\varepsilon (h_e^i)^{2k} + (h_e^i)^{2k+2}) \|u^\varepsilon\|^2_{H^1(0,t^n;H^{k+1}(T_e^i))} \\
&\quad \leq \sum\nolimits_{T_e^i \in \mathcal{T}_h^{\varepsilon,2}} c''(t^n)(\varepsilon (h_e^i)^{2k} + (h_e^i)^{2k+2}) \int_{x_e^{i-1}}^{x_e^i} \varepsilon^{-2(k+1)} e^{2b_e(\ell_e - x)/\varepsilon} \, dx = (i) + (ii).
\end{aligned}$$

Inserting the definition of $h_e^i = \varepsilon h e^{b_e(\ell_e - x_e^i)/\varepsilon(k+1)}$ then yields for the first term

$$\begin{aligned}
(i) &= \sum\nolimits_{T_e^i \in \mathcal{T}_h^{\varepsilon,2}} \varepsilon^{-1} h^{2k} e^{2kb_e(\ell_e - x_e^i)/\varepsilon(k+1)} \int_{x_e^{i-1}}^{x_e^i} e^{2b_e(\ell_e - x)/\varepsilon} \, dx \\
&\leq \sum\nolimits_{e \in \mathcal{E}} \varepsilon^{-1} h^{2k} \int_{x_e^*}^{\ell_e} e^{2b_e(\ell_e - x)/\varepsilon(k+1)} \, dx \leq \sum\nolimits_{e \in \mathcal{E}} h^{2k \frac{k+1}{b_e}} \leq c''' h^{2k}.
\end{aligned}$$

The second term can be estimated in a similar way, i.e.,

$$\begin{aligned}
(ii) &= \sum\nolimits_{T_e^i \in \mathcal{T}_h^{\varepsilon,2}} h^{2k+2} e^{2kb_e(\ell_e - x_e^i)/\varepsilon(k+1)} \int_{x_e^{i-1}}^{x_e^i} e^{2b_e(\ell_e - x)/\varepsilon} \, dx \\
&\leq \sum\nolimits_{e \in \mathcal{E}} h^{2k+2} (\ell_e - x_e^*) \leq c'''' h^{2k+2}.
\end{aligned}$$

Finally, combining the estimates for $\mathcal{T}_h^{\varepsilon,1}$ and $\mathcal{T}_h^{\varepsilon,2}$ yields (1.76) in the case $\varepsilon \geq h^{2k}$.

Bound on number of elements in $\mathcal{T}_h^\varepsilon$. It remains to derive a bound on the number of elements in $\mathcal{T}_h^{\varepsilon,2}$. Following the arguments in [56, p.645] and [110, p.8], we first show that the number of elements M^S in $\bigcup_{e \in \mathcal{E}} (x_e^S, \ell_e) \cap \mathcal{T}_h^{\varepsilon,2}$ with Shishkin transition point $x_e^S = \ell_e - \frac{k+1}{b_e} \varepsilon \log(1/h)$ can be bounded by ch^{-1}. It holds that

$$M^S = \sum\nolimits_{e \in \mathcal{E}} \sum\nolimits_{i:\, x_e^S < x_e^i \leq \ell_e} \frac{h_e^{i-1}}{h_e^i} \frac{h_e^i}{h_e^{i-1}}. \tag{1.77}$$

By the definition of the mesh sizes in (1.74) and of the Shishkin transition point, we find

$$h_e^i \leq \varepsilon h e^{b_e(\ell_e - x_e^S)/\varepsilon(k+1)} = \varepsilon$$

and the first fraction can thus be estimated by

$$\frac{h_e^{i-1}}{h_e^i} = e^{b_e h_e^i / \varepsilon(k+1)} \leq e^{b_e/(k+1)}.$$

Inserting this into (1.77) and using the construction of the mesh (1.74) yields

$$\begin{aligned} M^S &= \sum\nolimits_{e\in\mathcal{E}} \sum\nolimits_{i:\, x_e^S < x_e^i \le \ell_e} e^{b_e/(k+1)} h_e^i (\varepsilon h)^{-1} e^{-b_e(\ell_e - x_e^{i-1})/\varepsilon(k+1)} \\ &\le \sum\nolimits_{e\in\mathcal{E}} e^{b_e/(k+1)} (\varepsilon h)^{-1} \int_{x_e^S}^{\ell_e} e^{-b_e(\ell_e - x)/\varepsilon(k+1)}\, dx \\ &\le \sum\nolimits_{e\in\mathcal{E}} e^{b_e/(k+1)} \tfrac{k+1}{b_e} h^{-1} \le c h^{-1}. \end{aligned}$$

The last estimate holds since the network is finite. It remains to investigate the number of elements M^* in $\bigcup_{e\in\mathcal{E}} (x_e^*, x_e^S) \cap \mathcal{T}_h^{\varepsilon,2}$. By construction of the mesh in (1.74) we conclude that $h_T \ge \varepsilon$ for $T \subset (x_e^*, x_e^S)$. Consequently, the number of elements is larger than

$$\sum\nolimits_{e\in\mathcal{E}} (x_e^S - x_e^*)/\varepsilon \le \sum\nolimits_{e\in\mathcal{E}} \tfrac{k+1}{b_e} (\log(1/\varepsilon) - \log(1/h)) \le |\mathcal{E}|(2k-1)\tfrac{k+1}{\underline{b}} \log(1/h),$$

where we used that $\varepsilon \ge h^{2k}$, which is crucial in order to get a bound that is independent of ε. In summary, the number of elements in $\mathcal{T}_h^{\varepsilon,2}$ can be bounded by

$$c(h^{-1} + \log(1/h)) \le c' h^{-1},$$

and since the number of elements in the coarse part $\mathcal{T}_h^{\varepsilon,1}$ is bounded by $c'' h^{-1}$ by construction, we obtain the desired bound for $\mathcal{T}_h^{\varepsilon}$. □

1.4. Numerical illustration

In order to illustrate our theoretical findings, we conclude this chapter with some numerical experiments. We first consider the contaminant transport in water described in Example 1.3, before we have a look at the transport of gas mixtures. We both verify the asymptotic estimate from Theorem 1.7 as well as the uniform error estimate for the fully discrete hybrid-dG approximation presented in Theorem 1.23.

1.4.1. Contaminant transport in water supply networks

As a test instance, we consider the GasLib-11 network that consists of 11 pipes and vertices with 3 entries, 2 exits, and one loop. The topology is depicted in Figure 1.5. We assume that each edge has length $\ell_e = 1$. From Example 1.3 we know that $a_e = 1$ in all edges $e \in \mathcal{E}$, since water is an incompressible fluid with a constant density. Moreover, the flow velocities are constant in each pipe and given by

$$b_{e_1} = b_{e_2} = b_{e_5} = b_{e_6} = b_{e_9} = 2, \quad b_{e_3} = b_{e_8} = b_{e_{10}} = b_{e_{11}} = 1, \quad b_{e_4} = b_{e_7} = 3,$$

so that the flow conservation condition (B) at junctions is satisfied. We choose

$$\hat{g}_{v_1}(t) = \frac{2}{t_{max}^3} t^3, \quad \hat{g}_{v_4}(t) = \hat{g}_{v_7}(t) = 0, \quad \hat{g}_{v_{10}}(t) = \frac{3}{2t_{max}^4} t^4, \quad \hat{g}_{v_{11}}(t) = \frac{5}{2t_{max}^3} t^3$$

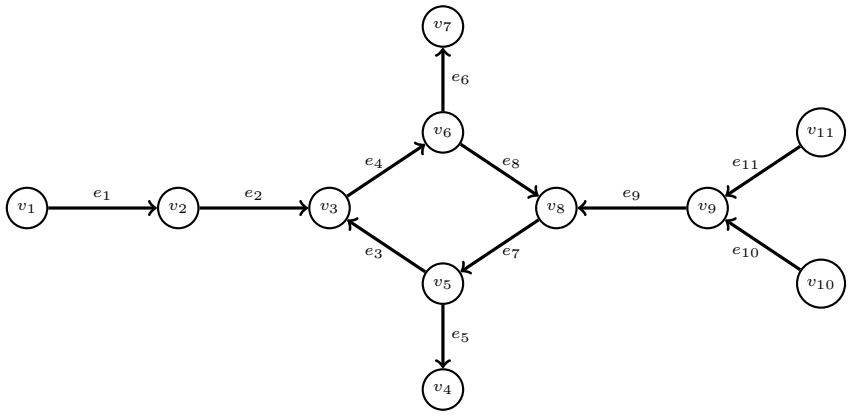

Figure 1.5.: GasLib-11 network from [112].

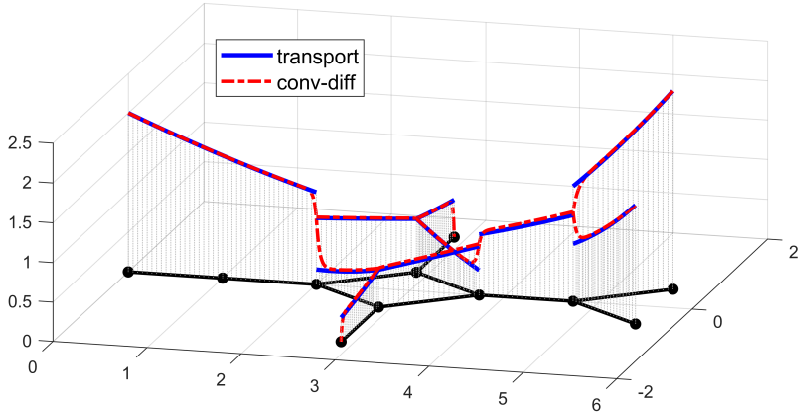

Figure 1.6.: Solution to the convection-diffusion problem for $\varepsilon = 0.05$ (red, dashed) and the limiting transport problem for $\varepsilon = 0$ (blue, solid). Discontinuities at junctions in the transport limit are clearly visible. They are smoothed out for small $\varepsilon > 0$ by diffusion, leading to the expected boundary layers at the network outflow boundaries and interior vertices. Outside of the layer regions, both solutions more or less coincide.

as boundary data, which are compatible with trivial initial conditions $u^\varepsilon(0) = u^0(0) = 0$ and fulfill Assumption 1.1 for $m = 2$. As time horizon we pick $t_{\max} = 6$. For the numerical approximation, we set $k = 2$, i.e., piecewise quadratic polynomials in space and time. The stabilization parameter in (1.65) is chosen as $\alpha = 1$.

Asymptotic estimate. At all network junctions having more than one ingoing pipe, i.e., at v_3, v_8 and v_9, we expect the solution of the pure transport problem to be discontinuous and the solution to the convection-diffusion problem to have interior layers for small ε. Moreover, at all outflow boundary vertices, we predict boundary layers. An illustration of this behavior for the chosen data is given in Figure 1.6. We now compare the solutions to Problem 1.17 for $\varepsilon > 0$ and $\varepsilon = 0$ on a fine grid with $h = \tau = 10^{-2}$. For solving the convection-diffusion problem we use the corresponding layer-adapted mesh in order to

ε	1	10^{-1}	10^{-2}	10^{-3}	10^{-4}	10^{-5}	10^{-6}	10^{-7}
err	8.608e-1	2.538e-1	7.155e-2	2.229e-2	7.039e-3	2.225e-3	7.037e-4	2.225e-4
rate	-	0.530	0.550	0.506	0.501	0.500	0.500	0.500

Table 1.1.: Error and convergence rates between solutions to Problem 1.17 for different values of $\varepsilon > 0$ and the pure transport limit $\varepsilon = 0$ on a grid with $h = \tau = 10^{-2}$.

resolve the boundary layers. The error is computed by

$$\text{err} = \max_{n=0,\dots,N} \|u_h^\varepsilon(t^n) - u_h^0(t^n)\|_{L^2(\mathcal{E})}.$$

Our observations are displayed in Table 1.1, and we clearly see the asymptotic convergence of order $\mathcal{O}(\sqrt{\varepsilon})$ that was shown in Theorem 1.7 on the continuous level.

Discretization error. Let us now investigate the convergence behavior of the hybrid-dG method for various choices of $\varepsilon \geq 0$ as well as mesh sizes. For our choice of parameters and data, the error estimates from Theorem 1.23 are valid with $k = 2$. The dG time-stepping method with quadratic polynomials was implemented as Radau IIA Runge-Kutta method with 3 steps. Both methods are equivalent when approximating all integrals in the dG method using the corresponding Radau quadrature rule. For details, we refer to [1, 119]. In order to give an estimate on the error, we generate a reference solution on a finer mesh $\mathcal{T}_h^{ref}$ with N_{ref} uniform time steps, where $\mathcal{T}_h^{ref}$ is given by the layer-adapted mesh $\mathcal{T}_h^\varepsilon$ for $\varepsilon > 0$ and the uniform mesh $\mathcal{T}_h^0$ for $\varepsilon = 0$, both obtained by two uniform refinements of the finest mesh considered in our tests. The number of reference time steps N_{ref} equals two times the number of time steps applied in the finest mesh. The error is then approximated by

$$\|u^\varepsilon - \tilde{u}_h^\varepsilon\|_{ref} = \max_{n=0,\dots,N_{ref}} \|u_{ref}^\varepsilon(t^n) - I_{ref}\tilde{u}_h^\varepsilon(t^n)\|_{L^2(\mathcal{E})}$$

with I_{ref} being the interpolation operator onto the reference mesh. In the tests depicted in Figure 1.7 we choose $h = \tau$, i.e., the uniform spatial and the time step size coincide.

The left plot in Figure 1.7 shows the error for $\tilde{u}_h^\varepsilon = u_h^\varepsilon$ on the layer-adapted mesh $\mathcal{T}_h^\varepsilon$, which is relevant in the regime $\varepsilon \geq h^{2k}$. We observe second-order convergence as indicated by the uniform error estimate (1.76) in Theorem 1.23. Only for $\varepsilon = 10^{-5}$ on a coarse mesh, we have a slight increase in the convergence, which can be justified by the fact that the diffusion term can be considered as a perturbation for small ε and large h. The number of elements in the Shishkin part (x_e^S, ℓ_e) of the layer-adapted mesh $\mathcal{T}_h^\varepsilon$ is at most $4h^{-1}$ with not more than 5 extra elements per edge in the transition region (x_e^*, x_e^S).

In the right plot in Figure 1.7 we see the error for the transport approximation $\tilde{u}_h^\varepsilon = u_h^0$ on the uniform mesh $\mathcal{T}_h^0$. This case is relevant in the regime $\varepsilon < h^{2k}$. Theorem 1.23 yields $\|u^\varepsilon - u_h^0\|_{ref} \leq C \max(h^{k+1}, \sqrt{\varepsilon}) + C'\tau^{k+1/2}$. If ε is small compared to h, we see a convergence of order $k + 1 = 3$. When $\sqrt{\varepsilon}$ becomes the dominating term in the error estimate, i.e., when h becomes smaller and smaller compared to ε, we observe a saturation that culminates in a constant error. There is no suboptimality in convergence for the time discretization visible indicating that our estimates are not sharp. In the limit

$\varepsilon = 0$ we observe a slight increase in the convergence rate, which might be caused by the superconvergence properties of the Radau IIA Runge-Kutta method; see [63, Ch. IV.5].

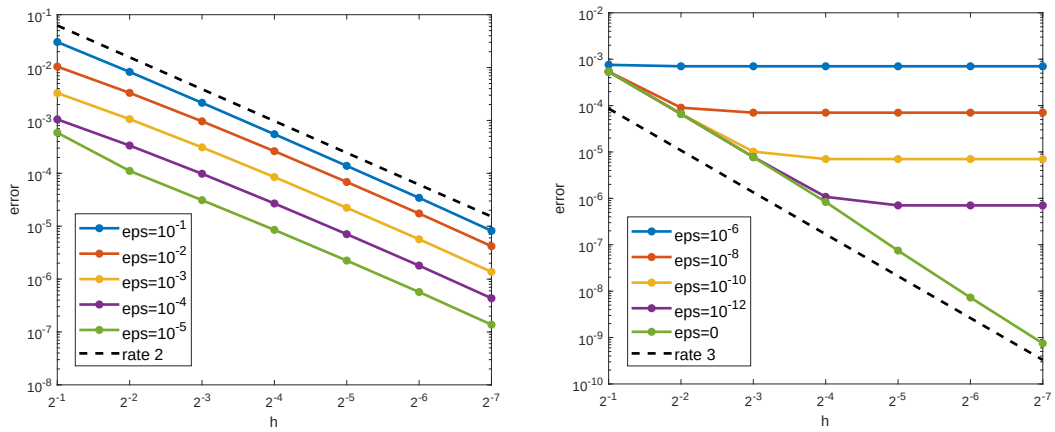

Figure 1.7.: (Left) Error for $\tilde{u}_h^\varepsilon = u_h^\varepsilon$ on layer-adapted mesh $\mathcal{T}_h^\varepsilon$ with $\tau = h$. (Right) Error for $\tilde{u}_h^\varepsilon = u_h^0$ on uniform mesh $\mathcal{T}_h^0$ with $h = \tau$.

1.4.2. Transport of gas mixtures in pipe networks

Let us present a second numerical test that is motivated by the transport of gas mixtures in pipe networks. In comparison to the previous experiment, the parameter a_e in the model equations (1.9) and (1.25) will now depend on the spatial position in the network. The steady flow of gas in a pipe network can be modeled by the following system

$$\partial_x m_e(x) = 0, \tag{1.78}$$

$$A_e(x)\partial_x p_e(x) = -\frac{\lambda}{2D_e(x)}|m_e(x)|v_e(x) \tag{1.79}$$

for $x \in (0, \ell_e)$, $e \in \mathcal{E}$ with m_e, p_e, v_e denoting mass flow rate, pressure, and flow velocity of the gas, A_e, D_e being cross-sectional area and diameter of the pipe, and λ is a friction parameter. The gas density ρ is a function of the pressure and vice versa, i.e., $p = p(\rho)$, and $m_e = A_e \rho_e v_e$. At pipe junctions $v \in \mathcal{V}_0$, conservation of mass and energy is ensured by the following coupling conditions

$$\sum\nolimits_{e \in \mathcal{E}(v)} m_e n_e(v) = 0 \qquad \text{and} \qquad p_{e_i}(v) = p_{e_j}(v) \quad \text{for all } v \in \mathcal{V}_0,\ e_i, e_j \in \mathcal{E}(v). \tag{1.80}$$

At network boundary vertices $\mathcal{V}_\partial$ either the mass flow rate or the density has to be prescribed. Note that in order to get a unique solution, the density has to be fixed at least at one vertex $v \in \mathcal{V}_\partial$. This model, which is also known as the Weymouth equations, is widely used for simulation and optimization of gas flow in pipe networks; see e.g. [78]. Note that a solution can be computed explicitly. We now assume that the gas is a mixture of j components that have the averaged density ρ and are transported within the total gas flow. Then, (1.9)–(1.12) models the transport of the gas mixture with u^i being the fraction of

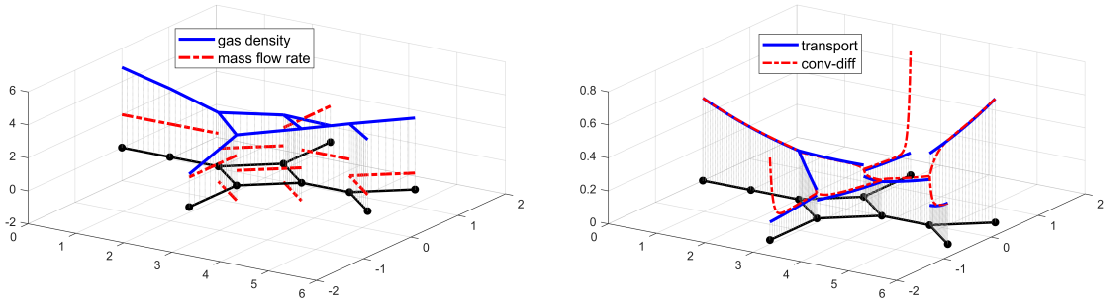

Figure 1.8.: (Left) Solution to the Weymouth equations (1.78)–(1.80) on the network topology depicted in Figure 1.5. (Right) The corresponding solution to the transport problem for $\varepsilon = 0$ (blue, solid) and the convection-diffusion problem for $\varepsilon = 0.1$ (red, dashed) on the same network with reversed direction of edges e_3 and e_8. The expected discontinuities and boundary layers at network junctions v_5, v_6, and v_9 as well as at the outflow boundary vertices v_4 and v_7 are clearly visible.

the i-th component for $i = 1, .., j-1$ and $1-\sum_{i=1}^{j-1} u^i$ being the fraction of j-th component. The corresponding densities of the gas components are given by ρu^i, $i = 1, .., j-1$ and $\rho(1-\sum_{i=1}^{j-1} u^i)$. The parameters a and b in (1.9)–(1.12) and (1.25)–(1.28) equal

$$a_e = A_e \rho_e \qquad \text{and} \qquad b_e = m_e \qquad \text{for all } e \in \mathcal{E}.$$

Assumption 1.1 is satisfied since $b_e = m_e$ is constant in each pipe $e \in \mathcal{E}$ due to (1.78) and conserved at junctions due to (1.80), i.e., condition (B) is fulfilled. Moreover, $a_e = A_e \rho_e$ is supposed to be uniformly bounded from below and above and sufficiently smooth. Let us now again consider the network structure from Figure 1.5 and assume that each edge has length $\ell_e = 1$, diameter $D_e = 1$ and cross-sectional area $A_e = \pi(D_e/2)^2$. As boundary data for the gas flow we prescribe the mass flow at the inflow boundary vertices $v \in \mathcal{V}_\partial^{in}$ and the gas density at the outflow boundary vertices $v \in \mathcal{V}_\partial^{out}$, more precisely

$$m(v_1) = 2, \quad \rho(v_4) = 2, \quad \rho(v_7) = 1, \quad m(v_{10}) = 1, \quad m(v_{11}) = 1$$

with the density to pressure relation $p(\rho) = c^2\rho$, where c is the speed of sound that is rescaled to 1. The solution to (1.78)–(1.80) that corresponds to this choice of boundary data is shown in Figure 1.8 (left). The flow rate in the edges e_3 and e_8 is negative, i.e., the direction of the flow and the edge do not coincide. For simplicity, we thus change the direction of the edges e_3 und e_8, so that Assumption 1.1 holds. Let us now assume that the gas is a mixture of two components with fractions u^1 and $u^2 = 1 - u^1$. The boundary data for u^1 is chosen as

$$\hat{g}_{v_1}(t) = \frac{1}{2t_{max}^3} t^3, \quad \hat{g}_{v_4}(t) = \frac{1}{2}, \quad \hat{g}_{v_7}(t) = \frac{3}{4}, \quad \hat{g}_{v_{10}}(t) = \frac{1}{4t_{max}^4} t^4, \quad \hat{g}_{v_{11}}(t) = \frac{3}{4t_{max}^3} t^3.$$

An illustration of the corresponding solution on the network, where the direction of the edges e_3 und e_8 is changed, is given in Figure 1.8 (right). We performed the same experiments for the asymptotic and the discretization error as in the previous section and obtained similar results. We thus omit their presentation here.

1.5. Discussion and outlook

Let us conclude this chapter with a short discussion on open problems and possible future research directions.

Asymptotic analysis. The consideration of more general coupling conditions as proposed in [60] and, in particular, a corresponding asymptotic analysis might be of interest. We expect that all results transfer with no major difficulties. Moreover, nonlinear problems and their asymptotic convergence in different metrics could be considered. We think of models appearing in the context of traffic flow [55] or cross-diffusion systems [75]. A possible tool for the analysis is given by entropy methods; see [75] for an introduction. Similar techniques will also be exploited for the analysis of a numerical scheme for gas flow in pipe networks in Chapter 3.

Numerical approximation. Some open problems appeared in the investigation of the numerical approximation. The error analysis of the fully discrete method given by Problem 1.17 in the spirit of [48, 117], which was presented in Section 1.3.3, only yielded a suboptimal convergence rate in time. A thorough analysis via techniques for Runge-Kutta methods might restore order optimal estimates and even lead to superconvergence results; we refer to [63, Ch. IV.5] for a comprehensive overview of implicit Runge-Kutta methods. Moreover, for some numerical tests not presented here, we observed superconvergence in space for the lowest-order approximation with piecewise linear polynomials in the diffusion-dominated regime. This behavior could be worth investigating. Furthermore, our way of handling transport problems on networks by introducing additional hybrid variables at junctions could in principle be applied to other discretization approaches like standard discontinuous Galerkin, upwind finite differences, or streamline upwind Petrov-Galerkin (SUPG) methods. Possible other research directions include the application of our numerical method to problems with more general coupling conditions or nonlinear problems.

2

Kinetic chemotaxis and diffusion limits on networks

The movement of bacteria and microorganisms, or more generally cells, is influenced by external stimuli. If they react to the presence of a chemical substance, the process is called *chemotaxis*. If the chemical substance acts as an attractor, we speak of *positive chemotaxis* and call the substance *chemoattractant*. Chemotactic phenomena are widely studied, in particular for *Escherichia coli* [2] and various slime mold species [32], but they also appear in other biological phenomena like embryological development, where cells migrate to form complex organisms [32], and in the immune system, where leukocytes react to substances present at the center of inflammation, e.g., bacterial toxins [121]. We are particularly interested in chemotactic processes on one-dimensional networks. These problems find application, e.g., in dermal wound healing and the growth of slime molds.

Dermal wound healing. The structural component of the skin is the so-called *extracellular matrix (ECM)* which is a 3D network of fibrous proteins such as collagen. If the skin is injured, the *fibroblasts* create a new provisional ECM and, driven by chemotaxis, migrate on the ECM to fill the wound. Certain diseases, such as diabetes, can cause wounds to heal extremely slowly or not at all. The use of artificial scaffolds that consist of networks of crossed polymeric threads can accelerate wound healing. These scaffolds are inserted into the wound supporting the fibroblasts to migrate. Chemotaxis on networks allows us to model this process. Here, the network represents the artificial scaffold and the evolution equations approximate the propagation of the fibroblasts on this scaffold; for details we refer to [14] and the references therein.

Slime molds. Driven by chemotaxis, the slime mold *Physarum polycephalum* grows in a network structure. Thickened irregular nodes are connected by thin tubes that are used for the transport of nutrients and the transfer of chemical signals through the organism. The interesting characteristic is that it grows in the shortest path manner toward food or other attractors. A possible way to model this growth process is to consider a fixed network that connects attractors with each other and to approximate the evolution by chemotaxis on this predefined network; see [9] and the references therein.

Problem setting

On the microscopic level, we model chemotaxis by kinetic equations; see e.g. [19, 99, 102]. We assume that the evolution of the bacteria or cell density $u(x, w, t)$ at the point $x \in X = (0, \ell)$ and time $t \geq 0$ having velocity $w \in \mathcal{W} = (-1, 1)$ is described by

$$\partial_t u(x, w, t) + w\partial_x u(x, w, t) = \sigma(x)\big(\bar{u}(x, t) - u(x, w, t)\big) + \alpha w \partial_x \bar{c}(x, t)\bar{u}(x, t) \tag{2.1}$$

with $\bar{u} = \frac{1}{2}\int_{\mathcal{W}} u(w)\, dw$ being the velocity average of the bacteria density. The transport part on the left-hand side describes the movement in a straight line with velocity $w \in \mathcal{W}$, whereas the right-hand side models a spontaneous reorientation called tumbling. We distinguish between aimless reorientation and chemotactically oriented tumbling, which is driven by the presence of a chemoattractant with concentration $\bar{c}$. Here, the bar symbol is misused to indicate that $\bar{c}$ does not depend on the velocity. The chemoattractant itself is produced by the bacteria and we assume that

$$\partial_t \bar{c}(x, t) - D\partial_{xx}\bar{c}(x, t) + \delta\bar{c}(x, t) = \gamma\bar{u}(x, t) \tag{2.2}$$

for $x \in X$ and $t \geq 0$. Here, D is the diffusion coefficient, and δ and γ are the decay and production rate, respectively. The equations (2.1)–(2.2) have to be complemented with suitable boundary conditions. We assume that the chemoattractant and the bacteria are confined to X, which is modeled by no-flux boundary conditions for $\bar{c}$, i.e.,

$$\partial_x \bar{c}(x, t) = 0 \qquad \text{for } x \in \{0, \ell\},\ t > 0. \tag{2.3}$$

For the kinetic transport equation (2.1) we need one boundary condition at the inflow boundary of the phase space $\mathcal{Q} = X \times \mathcal{W}$ which depends on the moving direction; see Figure 2.2 for an illustration. We prescribe the following reflection condition

$$u(x, w, t) = u(x, -w, t) \qquad \text{for } (x, w) \in \{0\} \times (0, 1] \cup \{\ell\} \times [-1, 0),\ t > 0, \tag{2.4}$$

which ensures that bacteria do not leave the domain X. Local existence of solutions to (2.1)–(2.4) can be shown by standard arguments for nonlinear evolution equations; see e.g. [49]. For the kinetic chemotaxis model in dimension $d = 3$, no global existence results are available if the tumbling depends on $\nabla\bar{c}$; see [19, 70]. In dimension $d = 1$, however, there are more promising results. In [67, 68, 71] a general class of kinetic models for chemotaxis on the full state space $X = \mathbb{R}$ is studied with $\mathcal{W} = \{-1, 1\}$. The tumbling has a general structure depending on $\bar{c}$ and $\partial_x\bar{c}$. The local existence of solutions is proven via the method of characteristics or the vanishing viscosity method and fixed point arguments. Furthermore, suitable conditions for the tumbling are derived in order to guarantee the global existence of solutions. Let us note that these conditions are, however, not satisfied for the choice in (2.1). In this work, we only consider the local in time existence of solutions.

Asymptotic analysis and diffusion limit

We introduce a small parameter $\varepsilon > 0$ and make the following assumptions:

- The aimless tumbling occurs more frequently than the chemotactically oriented tumbling, i.e., we set $\sigma^\varepsilon = \sigma/\varepsilon$.
- The mean free path between tumbling events goes to zero, i.e., we rescale the bacteria density by $u^\varepsilon(x, w, t) = u(x, w, t/\varepsilon)$.

This leads to the rescaled kinetic transport equation

$$\varepsilon^2 \partial_t u^\varepsilon + \varepsilon w \partial_x u^\varepsilon = \sigma(\bar{u}^\varepsilon - u^\varepsilon) + \varepsilon \alpha w \partial_x \bar{c}^\varepsilon \bar{u}^\varepsilon. \tag{2.5}$$

The dynamics of the chemoattractant $\bar{c}^\varepsilon = \bar{c}$ is not affected by the scaling, i.e.,

$$\partial_t \bar{c}^\varepsilon - D\partial_{xx}\bar{c}^\varepsilon + \delta \bar{c}^\varepsilon = \gamma \bar{u}^\varepsilon. \tag{2.6}$$

We refer to [19, 27] for details. By formal asymptotic expansions, the classical Keller-Segel equations, which are given by

$$\partial_t \bar{u}^0 - \partial_x(\bar{a}\partial_x \bar{u}^0 - \bar{\chi}\partial_x \bar{c}^0 \bar{u}^0) = 0, \tag{2.7}$$

$$\partial_t \bar{c}^0 - D\partial_{xx}\bar{c}^0 + \delta \bar{c}^0 = \gamma \bar{u}^0 \tag{2.8}$$

with coefficients $\bar{a} = \int_{\mathcal{W}} \sigma^{-1} w^2 \, dw$ and $\bar{\chi} = \int_{\mathcal{W}} \alpha \sigma^{-1} w^2 \, dw$, can be obtained in the diffusion limit $\varepsilon \to 0$. Note that the bacterial density $\bar{u}^0 = \bar{u}^0(x, t)$ does not depend on the velocity anymore. This model was first introduced by Keller and Segel [76] and has been widely investigated in the literature; a good overview can be found in [66, 69]. Let us note that in dimension $d = 1$ solutions to (2.7)–(2.8) can be shown to exist globally in time [97], whereas in $d = 2, 3$ a finite time blow-up can occur; see [69] and the references therein. A purely formal derivation of the limit problem in $d = 1$ for $\mathcal{W} = \{-1, 1\}$ given by a Keller-Segel type equation is provided in [68], whereas the rigorous convergence of solutions u^ε to the limit $\bar{u}^0$ is investigated in [71]. The proof is based on the derivation of ε-independent a-priori bounds and asymptotic expansions. For similar results in the multidimensional case let us refer to [19, 71]. The asymptotic analysis and the derivation of quantitative convergence rates by asymptotic expansions are based on arguments from [5, 27] where the neutron transport was investigated. Here, we closely follow the approach of [43] for stationary monokinetic linear transport problems in dimension $d = 3$, which is based on variational arguments and energy estimates. This will turn out to be particularly well-suited for the extension to networks.

Extension to networks

We consider networks described by finite, directed, and connected graphs. Edges are identified as intervals and (2.5)–(2.6) are assumed to hold on each edge. In order to connect the solutions across network junctions, additional coupling conditions are required that ensure the conservation of mass for u^ε and $\bar{c}^\varepsilon$. For a proper choice of these conditions, the local existence of solutions can be established by semigroup theory [46, 100], Galerkin approximations [49], and fixed point arguments [49]. Recently, a kinetic model for chemotaxis on networks with flux-limited chemotactically oriented tumbling was considered in

[10] leading to the corresponding flux-limited Keller-Segel model in the diffusion limit [103]. The authors proposed a set of coupling conditions at network junctions and formally derived the corresponding ones for the limiting Keller-Segel problem proposed in [9]. However, no rigorous asymptotic analysis was given. The Keller-Segel model on networks was then further investigated in [44] and local and global in time existence of solutions were proven. A hyperbolic-parabolic model for chemotaxis was studied in [14, 59, 61, 89]. By writing the system in Riemann variants, one recovers the kinetic model considered by [68] with velocity $w \in \mathcal{W} = \{-1, 1\}$. This model was extended to networks and suitable coupling conditions were proposed that ensured conservation of mass. The coupling for the chemoattractant, however, differed from the corresponding coupling conditions proposed in [9, 10, 44]. The local existence of solutions was proven via semigroup theory and fixed point arguments. Moreover, conditions that guarantee global existence were derived, e.g., the smallness of initial data [59] or positivity of solutions [61]. So far a rigorous asymptotic analysis for the kinetic chemotaxis model on networks to its diffusion limit seems to be missing to the best of our knowledge and we attempt to close this gap with our work.

Main contributions

Let us now summarize the main contributions of this chapter, which are not yet published and are first presented here. This is joint work with *Herbert Egger, Kathrin Hellmuth* and *Matthias Schlottbom*, a publication is in preparation.

- We extend the rescaled kinetic model for chemotaxis (2.5)–(2.6) to networks and propose suitable coupling conditions at network junctions that ensure the conservation of mass. We then establish the existence of solutions up to a time point $T > 0$ uniformly for all $\varepsilon > 0$ via Banach's fixed point theorem and standard arguments. Moreover, based on energy estimates we derive a-priori estimates for the local solutions that are uniform in ε and play a crucial role in the asymptotic analysis.

- Based on the a-priori estimates we then prove that solutions converge to corresponding weak solutions of the Keller-Segel system on networks in the diffusion limit $\varepsilon \to 0$. Moreover, for suitably regular parameters and data we show the following quantitative convergence estimate

$$\|u^\varepsilon - \bar{u}^0\|_{L^\infty(0,T;L^2)} + \|\bar{c}^\varepsilon - \bar{c}^0\|_{L^\infty(0,T;H^1)} \leq C\varepsilon^{1/2}. \tag{2.9}$$

  The proof is based on energy estimates and asymptotic expansions. We closely follow [27, 43] where the Neutron transport in dimension $d = 3$ and its diffusion limit were investigated. In [27], however, no energy estimates are used, whereas in [43] only the stationary problem was considered.

Outline

In Section 2.1 we introduce the kinetic model for chemotaxis on networks and propose suitable coupling conditions at junctions. The local existence of solutions is then established

in Section 2.2 and a-priori estimates are derived that will be crucial for the asymptotic analysis presented in Section 2.3. Therein, we first present the Keller-Segel model on networks, before we rigorously show the convergence of solutions. Finally, we prove the quantitative asymptotic estimate (2.9), and close this chapter with a discussion of open problems and an outlook on further research directions.

2.1. Model problem

In the first section, we present the rescaled kinetic model for chemotaxis on networks and propose suitable coupling conditions at network junctions. We start by introducing the basic notation that will be used throughout this chapter.

2.1.1. Notation and function spaces

Following the notation from Chapter 1, a network is described by a finite, connected, and directed graph $\mathcal{G} = (\mathcal{V}, \mathcal{E})$ with vertices $\mathcal{V} = \{v_1, \dots, v_m\}$ and edges $\mathcal{E} = \{e_1, \dots, e_l\} \subset \mathcal{V} \times \mathcal{V}$. We allow for a rather general topology that can include circles. The set of incident edges to a vertex $v \in \mathcal{V}$ is given by $\mathcal{E}(v) = \{e \in \mathcal{E} : e = (v, \cdot) \text{ or } e = (\cdot, v)\}$. If a vertex has only one incident edge, it belongs to the set of boundary vertices $\mathcal{V}_\partial = \{v \in \mathcal{V} : |\mathcal{E}(v)| = 1\}$ with $|\mathcal{E}(v)|$ denoting the cardinality of $\mathcal{E}(v)$. Otherwise, the vertex is contained in the set of interior vertices $\mathcal{V}_0 = \mathcal{V} \backslash \mathcal{V}_\partial$. In order to indicate the start and the end of an edge $e \in \mathcal{E}$, we define the outward normal n with $n|_e = n_e$ that for $e = (v_i, v_j) \in \mathcal{E}$ takes the values

$$n_e(v_i) = -1, \qquad n_e(v_j) = 1, \qquad \text{and} \qquad n_e(v) = 0 \quad \text{for } v \in \mathcal{V} \backslash \{v_i, v_j\}.$$

Moreover, we introduce the sets of edges pointing into or out of each vertex $v \in \mathcal{V}$ by

$$\mathcal{E}^{in}(v) = \{e \in \mathcal{E} : n_e(v) = 1\} \qquad \text{and} \qquad \mathcal{E}^{out}(v) = \{e \in \mathcal{E} : n_e(v) = -1\},$$

and the sets of ingoing and outgoing boundary vertices by

$$\mathcal{V}_\partial^{in} = \{v \in \mathcal{V}_\partial : n_e(v) = -1\} \qquad \text{and} \qquad \mathcal{V}_\partial^{out} = \{v \in \mathcal{V}_\partial : n_e(v) = 1\}.$$

An illustration is given in Figure 2.1. Every edge $e \in \mathcal{E}$ is identified by an interval $e = (0, \ell_e)$ with $\ell_e > 0$ being the length of the edge. We abuse the notation $\mathcal{E} = \prod_{e \in \mathcal{E}} (0, \ell_e)$ for the state space and further introduce the velocity space $\mathcal{W} = (-1, 1)$ and the phase space $\mathcal{Q} = \mathcal{E} \times \mathcal{W}$ on the network. The inflow and outflow boundaries of the phase space depend on the velocity and are given by

$$\mathcal{Q}_\partial^{in} = \mathcal{V}_\partial^{in} \times (0, 1] \cup \mathcal{V}_\partial^{out} \times [-1, 0) \quad \text{and} \quad \mathcal{Q}_\partial^{out} = \mathcal{V}_\partial^{in} \times [-1, 0) \cup \mathcal{V}_\partial^{out} \times (0, 1].$$

For each interior vertex $v \in \mathcal{V}_0$ the sets of edges carrying flow into or out of the vertex also depend on the velocity and we introduce

$$\begin{aligned} \mathcal{Q}^{in}(v) &= \mathcal{E}^{in}(v) \times (0, 1] \cup \mathcal{E}^{out}(v) \times [-1, 0), \\ \mathcal{Q}^{out}(v) &= \mathcal{E}^{in}(v) \times [-1, 0) \cup \mathcal{E}^{out}(v) \times (0, 1]. \end{aligned}$$

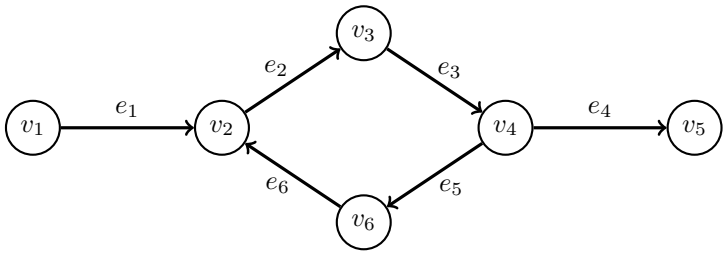

Figure 2.1.: A network with edges $e_1 = (v_1, v_2)$, $e_2 = (v_2, v_3)$, $e_3 = (v_3, v_4)$, $e_4 = (v_4, v_5)$, $e_5 = (v_4, v_6)$, and $e_6 = (v_6, v_2)$, boundary vertices $\mathcal{V}_\partial = \{v_1, v_5\}$, and interior vertices $\mathcal{V}_0 = \{v_2, v_3, v_4, v_6\}$. The incident edges to the vertex v_2 are collected in the set $\mathcal{E}(v_2) = \{e_1, e_2, e_6\}$, which can be split into the sets $\mathcal{E}^{in}(v_2) = \{e_1, e_6\}$ and $\mathcal{E}^{out}(v_2) = \{e_2\}$ of edges pointing into or out of the vertex v_2. The ingoing and outgoing boundary vertices of the network are given by $\mathcal{V}_\partial^{in} = \{v_1\}$ and $\mathcal{V}_\partial^{out} = \{v_5\}$.

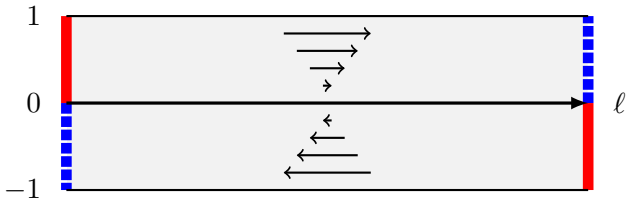

Figure 2.2.: Inflow and outflow boundary for a single pipe $e = (0, \ell)$ and velocity space $\mathcal{W} = (-1, 1)$ depicted in (red, solid) and (blue, dotted), respectively.

An illustration of the in- and outflow boundary for a single edge is provided in Figure 2.2.

Let us further introduce function spaces on the network. The spaces of square-integrable functions on the state and the phase space are given by

$$L^2(\mathcal{E}) = \{\bar{c} : \bar{c}_e \in L^2(0, \ell_e) \text{ for all } e \in \mathcal{E}\},$$
$$L^2(\mathcal{Q}) = \{u : u_e \in L^2((0, \ell_e) \times (-1, 1)) \text{ for all } e \in \mathcal{E}\},$$

respectively, where $\bar{c}_e = \bar{c}|_e$ denotes the restriction onto the edge $e \in \mathcal{E}$ and the bar symbol indicates that the function $\bar{c}$ does not depend on the velocity w. We also use the bar symbol to denote the velocity average of a function $u \in L^2(\mathcal{Q})$ by

$$\bar{u} = \frac{1}{2} \int_{\mathcal{W}} u(w)\, dw.$$

The L^2-scalar products and norms are given by

$$(\bar{c}, \bar{\phi})_{L^2(\mathcal{E})} = \int_{\mathcal{E}} \bar{c}(x)\bar{z}(x)\, dx \qquad \text{and} \qquad \|\bar{c}\|^2_{L^2(\mathcal{E})} = (\bar{c}, \bar{c})_{L^2(\mathcal{E})},$$
$$(u, z)_{L^2(\mathcal{Q})} = \int_{\mathcal{Q}} u(x, w) z(x, w)\, d(x, w) \qquad \text{and} \qquad \|u\|^2_{L^2(\mathcal{Q})} = (u, u)_{L^2(\mathcal{Q})},$$

where we abbreviate

$$\int_{\mathcal{E}} \bar{c}(x)\, dx = \sum\nolimits_{e \in \mathcal{E}} \int_0^{\ell_e} \bar{c}_e(x)\, dx \quad \text{and} \quad \int_{\mathcal{Q}} u(x, w)\, d(x, w) = \int_{\mathcal{E}} \int_{\mathcal{W}} u(x, w)\, dw\, dx.$$

Other L^p-spaces can be defined in the same manner. We will further make use of the following abbreviations

$$\int_{\mathcal{Q}_\partial^{in}} u(w,t)\ dw = \sum\nolimits_{v\in\mathcal{V}_\partial^{in}} \int_0^1 u_e(v,w,t)\ dw + \sum\nolimits_{v\in\mathcal{V}_\partial^{out}} \int_{-1}^0 u_e(v,w,t)\ dw,$$

$$\int_{\mathcal{Q}^{in}(v_0)} u(v_0,w,t)\ dw = \sum\nolimits_{e\in\mathcal{E}^{in}(v_0)} \int_0^1 u_e(v_0,w,t)\ dw + \sum\nolimits_{e\in\mathcal{E}^{out}(v_0)} \int_{-1}^0 u_e(v_0,w,t)\ dw$$

with $v_0 \in \mathcal{V}_0$ that can similarly be defined for $\mathcal{Q}_\partial^{out}$ and $\mathcal{Q}^{out}(v_0)$. The broken Sobolev spaces on the state space of the network are given by

$$H^k_{pw}(\mathcal{E}) = \{\bar{c} \in L^2(\mathcal{E}) : \bar{c}_e \in H^k(0,\ell_e) \text{ for all } e \in \mathcal{E}\}$$

with associated norm and scalar product

$$(\bar{c},\bar{\phi})_{H^k_{pw}(\mathcal{E})} = \sum\nolimits_{e\in\mathcal{E}} (\bar{c}_e,\bar{\phi}_e)_{H^k(0,\ell_e)} \quad \text{and} \quad \|\bar{c}\|^2_{H^k_{pw}(\mathcal{E})} = (\bar{c},\bar{c})_{H^k_{pw}(\mathcal{E})}.$$

Note that functions in $H^k_{pw}(\mathcal{E})$ are continuous within edges for $k > 1/2$, but might be discontinuous at network junctions. We thus denote by

$$H^1(\mathcal{E}) = \{\bar{c} \in H^1_{pw}(\mathcal{E}) : \bar{c}_{e_i}(v) = \bar{c}_{e_j}(v) \text{ for all } v \in \mathcal{V}_0,\ e_i, e_j \in \mathcal{E}(v)\}$$

the space of $H^1_{pw}(\mathcal{E})$-functions that are additionally continuous at network junctions. Each $\bar{c} \in H^1(\mathcal{E})$ then takes a unique value $\bar{c}(v)$ at $v \in \mathcal{V}_0$.

For $t \geq 0$ and some Banach space X with norm $\|\cdot\|_X$, the corresponding Bochner spaces are defined in the usual manner, i.e., the space of measurable functions with values in X is given by $L^p(0,t;X)$ and equipped with the norm

$$\|u\|^p_{L^p(0,t;X)} = \int_0^t \|u(s)\|^p_X\ ds,\ 1 \leq p < \infty, \quad \text{and} \quad \|u\|_{L^\infty(0,t;X)} = \operatorname{ess}\sup_{0\leq s\leq t} \|u(s)\|_X.$$

In the same spirit, the spaces of weakly differentiable functions in time with values in X are given by $W^{k,p}(0,t;X)$, and $H^k(0,t;X)$ for $p = 2$, equipped with their natural norms. Furthermore, we introduce the spaces $C^k([0,t];X)$ equipped with the norms

$$\|u\|_{C^k([0,t];X)} = \max_{i\leq k,\, 0\leq s\leq t} \|u^{(i)}(s)\|_X$$

that include all k-times continuously differentiable functions in time with values in X.

2.1.2. Kinetic model for chemotaxis on networks

We are now in the position to introduce the kinetic model for chemotaxis on networks. Let $\mathcal{G} = (\mathcal{V},\mathcal{E})$ be as above. On each edge $e \in \mathcal{E}$ and for some $T > 0$ we assume that the bacteria density u^ε and concentration of the chemoattractant $\bar{c}^\varepsilon$ satisfy

$$\varepsilon^2\partial_t u^\varepsilon_e + \varepsilon w\partial_x u^\varepsilon_e + \sigma_e(u^\varepsilon_e - \bar{u}^\varepsilon_e) = \varepsilon\alpha_e w\partial_x \bar{c}^\varepsilon_e \bar{u}^\varepsilon_e \quad \text{in } (0,\ell_e)\times(-1,1)\times(0,T), \tag{2.10}$$

$$\partial_t \bar{c}^\varepsilon_e - D_e\partial_{xx}\bar{c}^\varepsilon_e + \delta_e\bar{c}^\varepsilon_e = \gamma_e\bar{u}^\varepsilon_e \quad \text{in } (0,\ell_e)\times(0,T). \tag{2.11}$$

For the bacteria density u^ε we further require that

$$u_e^\varepsilon(v,w,t) = u_e^\varepsilon(v,-w,t) \qquad \text{for } (v,w) \in \mathcal{Q}_\partial^{in},\ e \in \mathcal{E}(v),\ t \in (0,T) \tag{2.12}$$

at the network inflow boundary, and

$$u_e^\varepsilon(v,w,t) = \hat{u}_v^\varepsilon(|w|,t) \qquad \text{for } v \in \mathcal{V}_0,\ (e,w) \in \mathcal{Q}^{out}(v),\ t \in (0,T) \tag{2.13}$$

at network junctions with mixing value defined by

$$\hat{u}_v^\varepsilon(|w|,t) = \frac{1}{|\mathcal{E}(v)|}\Big(\sum\nolimits_{e\in\mathcal{E}^{in}(v)} u_e^\varepsilon(v,|w|,t) + \sum\nolimits_{e\in\mathcal{E}^{out}(v)} u_e^\varepsilon(v,-|w|,t)\Big). \tag{2.14}$$

The initial condition is chosen as

$$u^\varepsilon(0) = \bar{u}_I \qquad \text{on } \mathcal{Q}. \tag{2.15}$$

The concentration $\bar{c}^\varepsilon$ is assumed to satisfy

$$\partial_x \bar{c}_e^\varepsilon(v,t) = 0 \qquad \text{for } v \in \mathcal{V}_\partial,\ e \in \mathcal{E}(v),\ t \in (0,T) \tag{2.16}$$

at the network boundary. Additionally, we impose coupling conditions at junctions by

$$\bar{c}_{e_i}^\varepsilon(v,t) = \bar{c}_{e_j}^\varepsilon(v,t) \qquad \text{for } v \in \mathcal{V}_0,\ e_i,e_j \in \mathcal{E}(v),\ t \in (0,T), \tag{2.17}$$

$$\sum\nolimits_{e\in\mathcal{E}(v)} D_e \partial_x \bar{c}_e^\varepsilon(v,t) n_e(v) = 0 \qquad \text{for } v \in \mathcal{V}_0,\ t \in (0,T). \tag{2.18}$$

Finally, at the initial time we set

$$\bar{c}^\varepsilon(0) = \bar{c}_I \qquad \text{on } \mathcal{E}. \tag{2.19}$$

Remark 2.1. As for a single interval, we need to prescribe one boundary condition at each end of every edge for the chemoattractant $\bar{c}^\varepsilon$ and one boundary condition at the inflow boundary of each edge for the bacteria density u^ε. Moreover, we assume that the network is closed, which is guaranteed by no-flux boundary condition (2.16). The coupling conditions (2.17)–(2.18) for $\bar{c}^\varepsilon$ ensure the continuity of the solution and the conservation of mass at network junctions. Furthermore, we assume that bacteria entering a vertex $v \in \mathcal{V}$ do not change their speed and leave the vertex through one of the incident edges $e \in \mathcal{E}(v)$ with the same probability. At the network boundary, this is modeled by the reflection boundary condition (2.12), and at the junctions by the mixing conditions (2.13)–(2.14) that also guarantee the conservation of mass.

For the rest of this chapter, we make the following assumptions on the parameters and data that could, however, be relaxed to some extent.

Assumption 2.2. Let $\sigma \in L^\infty(\mathcal{E})$ with $0 < \sigma_{min} \le \sigma_e(x) \le \sigma_{max}$ for all $0 \le x \le \ell_e,\ e \in \mathcal{E}$ and further let $\alpha_e, D_e, \delta_e, \gamma_e \ge 0$ be constant on each edge $e \in \mathcal{E}$ and bounded from above by $\alpha_{max}, D_{max}, \delta_{max}, \gamma_{max} > 0$. Additionally, let $0 < D_{min} \le D_e$. Moreover, let $0 < \varepsilon \le 1$ be constant. Further, let $\bar{u}_I, \bar{c}_I \in H^1(\mathcal{E})$ be independent of ε and let the compatibility condition $D\partial_{xx}\bar{c}_I - \delta\bar{c}_I + \gamma\bar{u}_I \in H^1(\mathcal{E})$ hold.

2.2. Existence of solutions

As a first step of our analysis, we state and prove the existence of a unique solution $(u^\varepsilon, \bar{c}^\varepsilon)$ to (2.10)–(2.19) up to a certain time point $T > 0$ independent of ε and establish corresponding a-priori estimates.

Theorem 2.3. *Let Assumption 2.2 hold. Then, there exists a time point $T > 0$ so that for all $\varepsilon > 0$ the system* (2.10)–(2.19) *has a unique solution*

$$\begin{aligned} &u^\varepsilon \in C^1([0,T]; L^2(\mathcal{Q})) \cap C^0([0,T]; Z), \\ &\bar{c}^\varepsilon \in W^{1,\infty}(0,T; H^1(\mathcal{E})) \cap H^2(0,T; L^2(\mathcal{E})) \cap H^1(0,T; H^2_{pw}(\mathcal{E})). \end{aligned}$$

The solution space Z for the bacteria density u^ε is defined by

$$Z := \{z \in L^2(\mathcal{Q}) : w\partial_x z \in L^2(\mathcal{Q}),\ z \text{ satisfies } (2.12) - (2.14)\}. \tag{2.20}$$

Moreover, the following a-priori bounds hold

(a) $\|u^\varepsilon\|_{C^0([0,T];L^2(\mathcal{Q}))} \le C$,

(b) $\|u^\varepsilon - \bar{u}^\varepsilon\|_{L^2(0,T;L^2(\mathcal{Q}))} \le C\varepsilon$,

(c) $\sum_{v\in\mathcal{V}_0} \int_0^T \int_{\mathcal{Q}^{in}(v)} |w| \left|u^\varepsilon(v,w,t) - \hat{u}^\varepsilon_v(|w|,t)\right|^2 \, dw\, dt \le C\varepsilon$,

(d) $\|\bar{c}^\varepsilon\|_{L^\infty(0,T;H^1(\mathcal{E}))} + \|\bar{c}^\varepsilon\|_{H^1(0,T;L^2(\mathcal{E}))} + \|\bar{c}^\varepsilon\|_{L^2(0,T;H^2_{pw}(\mathcal{E}))} \le C$,

(e) $\|\varepsilon\partial_t u^\varepsilon\|_{C^0([0,T];L^2(\mathcal{Q}))} \le C$,

(f) $\|w\partial_x u^\varepsilon\|_{L^2(0,T;L^2(\mathcal{Q}))} \le C$

with a generic constant C that only depends on T and the bounds in Assumption 2.2, but not on ε. Finally, the global balance laws

$$\int_{\mathcal{Q}} u^\varepsilon(x,w,t)\ d(x,w) = \int_{\mathcal{E}} \bar{u}_I(x)\ dx, \tag{2.21}$$

$$\int_{\mathcal{E}} \bar{c}^\varepsilon(x,t)\ dx = \int_{\mathcal{E}} \bar{c}_I(x)\ dx + \int_0^t \int_{\mathcal{E}} \gamma\bar{u}^\varepsilon(x,s) - \delta\bar{c}^\varepsilon(x,s)\ dx\ ds \tag{2.22}$$

are valid for all $0 \le t \le T$.

Outline of the proof. In order to prove the local existence of solutions, we follow standard procedure: We linearize the nonlinear system (2.10)–(2.19) and replace u^ε on the right-hand sides of (2.10) and (2.11) by a function $z^\varepsilon \in C^1([0,T]; L^2(\mathcal{Q}))$. Then, the kinetic transport and the parabolic problem for the chemoattractant decouple. The well-posedness of both linearized systems and suitable a-priori bounds are established separately in Section 2.2.1 and 2.2.2. Via a fixed point argument, we then show the existence of solutions to (2.10)–(2.19) that satisfy the a-priori bounds (a)–(f) in Section 2.2.3. For ease of presentation, let us in the following choose a-priori $T \le 1$.

2.2.1. Linearized problem for the chemoattractant

Let z^ε be given. On each edge $e \in \mathcal{E}$ we consider

$$\partial_t \bar{c}_e^\varepsilon - D_e \partial_{xx} \bar{c}_e^\varepsilon + \delta_e \bar{c}_e^\varepsilon = \gamma_e \bar{z}_e^\varepsilon \qquad \text{in } (0, \ell_e) \times (0, T) \tag{2.23}$$

complemented by the network boundary and coupling conditions (2.16)–(2.18) and initial condition (2.19). Note that this system does not depend on u^ε anymore. Well-posedness is guaranteed by the following result.

Lemma 2.4. *Let Assumption 2.2 hold and let $z^\varepsilon \in C^1([0,T]; L^2(\mathcal{Q}))$ with $z^\varepsilon(0) = \bar{u}_I$. Then, there exists a unique solution*

$$\bar{c}^\varepsilon \in W^{1,\infty}(0,T; H^1(\mathcal{E})) \cap H^2(0;T; L^2(\mathcal{E})) \cap H^1(0,T; H^2_{pw}(\mathcal{E}))$$

to (2.23) *with boundary and coupling conditions* (2.16)–(2.18) *and initial condition* (2.19) *that satisfies*

$$\begin{aligned} &\|\partial_t \bar{c}^\varepsilon\|^2_{L^2(0,T;L^2(\mathcal{E}))} + \|\partial_{xx} \bar{c}^\varepsilon\|^2_{L^2(0,T;L^2(\mathcal{E}))} + \|\bar{c}^\varepsilon\|^2_{L^\infty(0,T;H^1(\mathcal{E}))} + \|\partial_x \bar{c}^\varepsilon\|^2_{L^4(0,T;L^\infty(\mathcal{E}))} \\ &\qquad \le C\big(\|\bar{c}_I\|^2_{H^1(\mathcal{E})} + T\|\bar{z}^\varepsilon\|^2_{C^0([0,T];L^2(\mathcal{E}))}\big), \end{aligned} \tag{2.24}$$

$$\begin{aligned} &\|\partial_{tt} \bar{c}^\varepsilon\|^2_{L^2(0,T;L^2(\mathcal{E}))} + \|\partial_{txx} \bar{c}^\varepsilon\|^2_{L^2(0,T;L^2(\mathcal{E}))} + \|\partial_t \bar{c}^\varepsilon\|^2_{L^\infty(0,T;H^1(\mathcal{E}))} + \|\partial_{tx} \bar{c}^\varepsilon\|^2_{L^4(0,T;L^\infty(\mathcal{E}))} \\ &\qquad \le C'\big(\|D\partial_{xx}\bar{c}_I - \delta \bar{c}_I + \gamma \bar{u}_I\|^2_{H^1(\mathcal{E})} + T\|\partial_t \bar{z}^\varepsilon\|^2_{C^0([0,T];L^2(\mathcal{E}))}\big) \end{aligned} \tag{2.25}$$

with constants C, C' that are independent of ε and $T \le 1$.

Proof. The existence of a unique solution

$$\bar{c}^\varepsilon \in L^\infty(0,T; H^1(\mathcal{E})) \cap H^1(0,T; L^2(\mathcal{E})) \cap L^2(0,T; H^2_{pw}(\mathcal{E}))$$

to (2.23), (2.16)–(2.19) can be proven by Galerkin approximations and energy estimates; see [44, Lemma B.1]. Moreover,

$$\|\partial_t \bar{c}^\varepsilon\|^2_{L^2(0,T;L^2(\mathcal{E}))} + \|\bar{c}^\varepsilon\|^2_{L^\infty(0,T;H^1(\mathcal{E}))} \le C\big(\|\bar{c}_I\|^2_{H^1(\mathcal{E})} + T\|\bar{z}^\varepsilon\|^2_{C^0([0,T];L^2(\mathcal{E}))}\big) \tag{2.26}$$

with a constant C that only depends on the bounds on D, δ, and γ in Assumption 2.2. The estimate for $\partial_{xx}\bar{c}^\varepsilon$ in (2.24) can be derived from (2.23) and the bounds on $\partial_t \bar{c}^\varepsilon$ and $\bar{c}^\varepsilon$ in (2.26). By interpolation theory [6, Thm. 5.1.2, Thm. 6.4.5] and embedding results in dimension $d = 1$ [28] one can see that

$$L^\infty(0,T; L^2(\mathcal{E})) \cap L^2(0,T; H^1_{pw}(\mathcal{E})) \hookrightarrow L^4(0,T; H^{3/4}_{pw}(\mathcal{E})) \hookrightarrow L^4(0,T; L^\infty(\mathcal{E}))$$

are continuous. From (2.26) we can thus deduce that

$$\|\partial_x \bar{c}^\varepsilon\|^2_{L^4(0,T;L^\infty(\mathcal{E}))} \le C'\big(\|\bar{c}_I\|^2_{H^1(\mathcal{E})} + T\|\bar{z}^\varepsilon\|^2_{C^0([0,T];L^2(\mathcal{E}))}\big)$$

with C' being independent of ε and T since $T \le 1$ is assumed a-priori. In summary, this yields the estimate (2.24). The higher regularity of the solution and the estimate (2.25) for $\partial_t \bar{c}^\varepsilon$ then follow by the same arguments, since $\partial_t \bar{c}^\varepsilon$ solves (2.23) with right-hand side $\partial_t \bar{z}^\varepsilon \in C^0([0,T]; L^2(\mathcal{E}))$, network boundary and coupling conditions (2.16)–(2.18) and initial condition $\partial_t \bar{c}^\varepsilon(0) = D\partial_{xx}\bar{c}_I - \delta \bar{c}_I + \gamma \bar{u}_I \in H^1(\mathcal{E})$ due to (2.23) and (2.19), the fact that $z^\varepsilon(0) = \bar{u}_I$, and Assumption 2.2. □

2.2.2. Linearized kinetic problem

Let z^ε as above and $\bar{c}^\varepsilon$ be the corresponding solution to (2.23), (2.16)–(2.19). We assume

$$\varepsilon^2 \partial_t u_e^\varepsilon + \varepsilon w \partial_x u_e^\varepsilon + \sigma_e (u_e^\varepsilon - \bar{u}_e^\varepsilon) = \varepsilon \alpha_e w \partial_x \bar{c}_e^\varepsilon \bar{z}_e^\varepsilon \qquad \text{in } (0, \ell_e) \times (-1, 1) \times (0, T) \tag{2.27}$$

on each edge $e \in \mathcal{E}$ with network boundary and coupling conditions (2.12)–(2.14) and initial condition (2.15). The existence of a unique solution and corresponding a-priori estimates are provided by the following lemma.

Lemma 2.5. *Let Assumption 2.2 hold and let $z^\varepsilon \in C^1([0,T]; L^2(\mathcal{E}))$ with $z^\varepsilon(0) = \bar{u}_I$ be given, and $\bar{c}^\varepsilon$ be the corresponding solution to* (2.23), (2.16)–(2.19)*. Then, there exists a unique solution*

$$u^\varepsilon \in C^1([0,T]; L^2(\mathcal{Q})) \cap C^0([0,T]; Z)$$

to (2.27), (2.12)–(2.15) *with Z defined in* (2.20) *that satisfies for all $0 \le t \le T$*

$$\begin{aligned} &\|u^\varepsilon(t)\|_{L^2(\mathcal{Q})}^2 + \sum\nolimits_{v \in \mathcal{V}_0} \int_0^t \int_{\mathcal{Q}^{in}(v)} \varepsilon^{-1} |w| |u^\varepsilon(v,w,s) - \hat{u}_v^\varepsilon(|w|,s)|^2 \, dw \, ds \\ &\quad + \varepsilon^{-2} \|\sigma^{1/2}(u^\varepsilon - \bar{u}^\varepsilon)\|_{L^2(0,t;L^2(\mathcal{Q}))}^2 \le \|\bar{u}_I\|_{L^2(\mathcal{E})}^2 + \|\sigma^{-1/2} \alpha w \partial_x \bar{c}^\varepsilon \bar{z}^\varepsilon\|_{L^2(0,t;L^2(\mathcal{Q}))}^2, \end{aligned} \tag{2.28}$$

$$\begin{aligned} \|\varepsilon \partial_t u^\varepsilon(t)\|_{L^2(\mathcal{Q})}^2 &\le \|w \partial_x \bar{u}_I - \alpha w \partial_x \bar{c}_I \bar{u}_I\|_{L^2(\mathcal{Q})}^2 \\ &\quad + \|\varepsilon \alpha \sigma^{-1/2} w (\partial_{tx} \bar{c}^\varepsilon \bar{z}^\varepsilon + \partial_x \bar{c}^\varepsilon \partial_t \bar{z}^\varepsilon)\|_{L^2(0,t;L^2(\mathcal{Q}))}^2. \end{aligned} \tag{2.29}$$

Proof. **Step 1 (Existence of a unique solution).** We rewrite (2.27), (2.12)–(2.15) as an abstract inhomogeneous Cauchy problem of the form

$$\frac{d}{dt} u^\varepsilon(t) = (\mathcal{A}^\varepsilon + \mathcal{B}^\varepsilon) u^\varepsilon(t) + f^\varepsilon(t) \quad \text{for } 0 \le t \le T, \qquad u^\varepsilon(0) = \bar{u}_I \tag{iACP}$$

with operators $(\mathcal{A}^\varepsilon, \mathcal{D}(\mathcal{A}^\varepsilon))$ and $(\mathcal{B}^\varepsilon, \mathcal{X})$ given by

$$\begin{aligned} &\mathcal{A}^\varepsilon : \mathcal{D}(\mathcal{A}^\varepsilon) \subset \mathcal{X} \to \mathcal{X}, \quad \mathcal{A}^\varepsilon u^\varepsilon := -\frac{1}{\varepsilon} w \partial_x u^\varepsilon, \\ &\mathcal{B}^\varepsilon : \mathcal{X} \to \mathcal{X}, \quad \mathcal{B}^\varepsilon u^\varepsilon := -\frac{\sigma}{\varepsilon^2} (u^\varepsilon - \bar{u}^\varepsilon), \end{aligned}$$

spaces $\mathcal{X} := L^2(\mathcal{Q})$ and $\mathcal{D}(\mathcal{A}^\varepsilon) := Z$ with Z defined in (2.20), and right-hand side

$$f^\varepsilon(t) := \varepsilon^{-1} \alpha w \partial_x \bar{c}^\varepsilon(t) \bar{z}^\varepsilon(t).$$

Note that $\mathcal{D}(\mathcal{A}^\varepsilon)$ is dense in $\mathcal{X}$, i.e., $\mathcal{A}^\varepsilon$ is densely defined. Since $\bar{u}_I \in H^1(\mathcal{E})$ is independent of $w \in \mathcal{W}$ by Assumption 2.2 and thus in $\mathcal{D}(\mathcal{A}^\varepsilon)$ and $f^\varepsilon \in H^1(0,T;\mathcal{X})$ due to Lemma 2.4 and the regularity of z^ε, the existence of a unique solution

$$u^\varepsilon \in C^1([0,T]; \mathcal{X}) \cap C^0([0,T]; \mathcal{D}(\mathcal{A}^\varepsilon))$$

to (iACP) is guaranteed by [46, Ch. VI, Cor. 7.6] if $(\mathcal{A}^\varepsilon + \mathcal{B}^\varepsilon, \mathcal{D}(\mathcal{A}^\varepsilon))$ generates a strongly continuous semigroup $(S(t))_{0 \le t \le T}$ on $\mathcal{X}$, which will be verified in the sequel.

Step 1.1 ($\mathcal{A}^\varepsilon$ and $(\mathcal{A}^\varepsilon)^*$ are dissipative). By definition of $\mathcal{A}^\varepsilon$ it holds that

$$(\mathcal{A}^\varepsilon z, z)_{\mathcal{X}} = -\frac{1}{\varepsilon}(w\partial_x z, z)_{\mathcal{X}} = -\int_{\mathcal{Q}} \frac{1}{2\varepsilon} w \frac{d}{dx}|z(x,w)|^2 \, d(x,w) \tag{2.30}$$
$$= -\sum\nolimits_{v\in\mathcal{V}} \sum\nolimits_{e\in\mathcal{E}(v)} \int_{\mathcal{W}} \frac{1}{2\varepsilon} w |z_e(v,w)|^2 \, n_e(v) \, dw.$$

Since $z \in \mathcal{D}(\mathcal{A}^\varepsilon)$ satisfies the reflection boundary condition (2.12) at the network inflow boundary $\mathcal{Q}^{in}_\partial$ we observe that

$$-\sum\nolimits_{v\in\mathcal{V}_\partial} \int_{\mathcal{W}} \frac{1}{2\varepsilon} w |z_e(v,w)|^2 n_e(v) \, dw \tag{2.31}$$
$$= -\int_{\mathcal{Q}^{in}_\partial} \frac{1}{2\varepsilon} w |z(-w)|^2 \, n \, dw - \int_{\mathcal{Q}^{out}_\partial} \frac{1}{2\varepsilon} w |z(w)|^2 \, n \, dw = 0$$

by definition of the inflow and outflow boundary of the phase space $\mathcal{Q}$. At network junctions $v \in \mathcal{V}_0$ we deduce from the coupling condition (2.13) that

$$-\sum\nolimits_{e\in\mathcal{E}(v)} \int_{\mathcal{W}} \frac{1}{2\varepsilon} w |z_e(v,w)|^2 \, n_e(v) \, dw = -\int_{\mathcal{Q}^{in}(v)} \frac{1}{2\varepsilon} w |z(v,w)|^2 \, n(v) \, dw \tag{2.32}$$
$$-\int_{\mathcal{Q}^{out}(v)} \frac{1}{2\varepsilon} w |\hat{z}_v(|w|)|^2 \, n(v) \, dw = (a1) + (a2).$$

By definition of $\mathcal{Q}^{out}(v)$ and the mixing value in (2.14) the second term equals

$$\begin{aligned}
(a2) &= -\sum\nolimits_{e\in\mathcal{E}^{in}(v)} \int_{-1}^{0} \frac{1}{2\varepsilon} w |\hat{z}_v(|w|)|^2 \, dw + \sum\nolimits_{e\in\mathcal{E}^{out}(v)} \int_{0}^{1} \frac{1}{2\varepsilon} w |\hat{z}_v(|w|)|^2 \, dw \\
&= \int_0^1 \frac{1}{2\varepsilon} w \hat{z}_v(|w|) \big(\sum\nolimits_{e\in\mathcal{E}(v)} \hat{z}_v(|w|) \big) \, dw \\
&= \sum\nolimits_{e\in\mathcal{E}^{in}(v)} \int_0^1 \frac{1}{2\varepsilon} w \hat{z}_v(|w|) z_e(v,w) \, dw - \sum\nolimits_{e\in\mathcal{E}^{out}(v)} \int_{-1}^{0} \frac{1}{2\varepsilon} w \hat{z}_v(|w|) z_e(v,w) \, dw \\
&= \int_{\mathcal{Q}^{in}(v)} \frac{1}{2\varepsilon} w \hat{z}_v(|w|) z(v,w) n(v) \, dw,
\end{aligned}$$

where we used that $\hat{z}_v$ does not depend on $e \in \mathcal{E}(v)$ and that $\sum_{e\in\mathcal{E}(v)} 1/|\mathcal{E}(v)| = 1$. In summary, we obtain

$$\begin{aligned}
(a1) + (a2) &= -\int_{\mathcal{Q}^{in}(v)} \frac{1}{2\varepsilon} w |z(v,w)|^2 \, n(v) \, dw + \int_{\mathcal{Q}^{in}(v)} \frac{1}{\varepsilon} w \hat{z}_v(|w|) z(v,w) \, n(v) \, dw \\
&\quad + \int_{\mathcal{Q}^{out}(v)} \frac{1}{2\varepsilon} w |\hat{z}_v(|w|)|^2 \, n(v) \, dw \\
&= -\int_{\mathcal{Q}^{in}(v)} \frac{1}{2\varepsilon} w |z(v,w) - \hat{z}_v(|w|)|^2 \, n(v) \, dw \\
&= -\int_{\mathcal{Q}^{in}(v)} \frac{1}{2\varepsilon} |w| |z(v,w) - \hat{z}_v(|w|)|^2 \, dw,
\end{aligned} \tag{2.33}$$

where we used that

$$\int_{\mathcal{Q}^{out}(v)} \frac{1}{2\varepsilon} w |\hat{z}_v(|w|)|^2 n(v) \, dw = -\int_{\mathcal{Q}^{in}(v)} \frac{1}{2\varepsilon} w |\hat{z}_v(|w|)|^2 n(v) \, dw.$$

From (2.30)–(2.33) we can then conclude that for $z \in \mathcal{D}(\mathcal{A}^\varepsilon)$ it holds

$$(\mathcal{A}^\varepsilon z, z)_{\mathcal{X}} = -\sum_{v\in\mathcal{V}_0} \int_{\mathcal{Q}^{in}(v)} \frac{1}{2\varepsilon}|w||z(v,w) - \hat{z}_v(|w|)|^2 \, dw \leq 0. \tag{2.34}$$

Since $\mathcal{X}$ is a Hilbert space, this implies that $(z, (\mathcal{A}^\varepsilon)^*)_{\mathcal{X}} \leq 0$ holds as well. Moreover, from

$$\|(\lambda - \mathcal{A}^\varepsilon)z\|_{\mathcal{X}}\|z\|_{\mathcal{X}} \geq ((\lambda - \mathcal{A}^\varepsilon)z, z)_{\mathcal{X}} = (\lambda z, z)_{\mathcal{X}} - (\mathcal{A}^\varepsilon z, z)_{\mathcal{X}} \geq \lambda\|z\|^2_{\mathcal{X}}$$

then immediately follows that $\mathcal{A}^\varepsilon$ and $(\mathcal{A}^\varepsilon)^*$ are dissipative; see [46, Ch. II, Def. 3.13].

Step 1.2 ($\mathcal{A}^\varepsilon$ is closed). Let $(y_n)_n \subset \mathrm{rg}(\lambda - \mathcal{A}^\varepsilon)$ be a sequence in the range of the operator $\lambda - \mathcal{A}^\varepsilon : \mathcal{D}(\mathcal{A}^\varepsilon) \to \mathcal{X}$ for some $\lambda > 0$ with $y_n = (\lambda - \mathcal{A}^\varepsilon)z_n$ and $y_n \to y \in \mathcal{X}$. We then have

$$\begin{aligned}
\|y_m - y_n\|^2_{\mathcal{X}} &= \|(\lambda - \mathcal{A}^\varepsilon)(z_m - z_n)\|^2_{\mathcal{X}} \\
&= \|\lambda(z_m - z_n)\|^2_{\mathcal{X}} - 2\lambda(\mathcal{A}^\varepsilon(z_m - z_n), z_m - z_n)_{\mathcal{X}} + \|\mathcal{A}^\varepsilon(z_m - z_n)\|^2_{\mathcal{X}} \\
&\geq \|\lambda(z_m - z_n)\|^2_{\mathcal{X}} + \varepsilon^{-2}\|w\partial_x(z_m - z_n)\|^2_{\mathcal{X}},
\end{aligned}$$

where we used that $(\mathcal{A}^\varepsilon z, z)_{\mathcal{X}} \leq 0$ for all $z \in \mathcal{D}(\mathcal{A}^\varepsilon)$. Consequently, (z_n) is a Cauchy sequence in the space $\mathcal{D}(\mathcal{A}^\varepsilon)$ that is a Hilbert space equipped with the scalar product $(u, z)_{\mathcal{D}(\mathcal{A}^\varepsilon)} = (u, z)_{L^2(\mathcal{Q})} + (w\partial_x u, w\partial_x z)_{L^2(\mathcal{Q})}$ and the corresponding norm. Hence, (z_n) converges in $\mathcal{D}(\mathcal{A}^\varepsilon)$ with limit $z \in \mathcal{D}(\mathcal{A}^\varepsilon)$ and $(\lambda - \mathcal{A}^\varepsilon)z = y$. We have thus shown that the range $\mathrm{rg}(\lambda - \mathcal{A}^\varepsilon)$ is closed in $\mathcal{X}$ for some $\lambda > 0$, which by [46, Ch. II, Prop. 3.14] implies that the dissipative operator $(\mathcal{A}^\varepsilon, \mathcal{D}(\mathcal{A}^\varepsilon))$ is closed.

Step 1.3 ($\mathcal{A}^\varepsilon + \mathcal{B}^\varepsilon$ generates a strongly continuous semigroup). From Step 1.1 and Step 1.2 we can conclude that $(\mathcal{A}^\varepsilon, \mathcal{D}(\mathcal{A}^\varepsilon))$ is the generator of a contraction semigroup; see [46, Ch. II, Cor. 3.17]. Since $\mathcal{B}^\varepsilon$ is linear and bounded by $\|\mathcal{B}^\varepsilon\| \leq 2\sigma_{max}/\varepsilon^2$, the bounded perturbation theorem [46, Ch. III, Thm. 1.3] yields that $(\mathcal{A}^\varepsilon + \mathcal{B}^\varepsilon, \mathcal{D}(\mathcal{A}^\varepsilon))$ then generates a strongly continuous semigroup.

Step 2 (A-priori estimates). Let us now derive a-priori estimates for the solution u^ε to (2.27), (2.12)–(2.15) respectively (iACP) via energy estimates. Multiplying (iACP) with u^ε and integrating over $\mathcal{Q} \times (0, t)$ with $0 \leq t \leq T$ yields

$$\begin{aligned}
\frac{1}{2}\int_0^t \frac{d}{dt}\|u^\varepsilon(s)\|^2_{L^2(\mathcal{Q})} \, ds &= (\mathcal{A}^\varepsilon u^\varepsilon, u^\varepsilon)_{L^2(0,t;L^2(\mathcal{Q}))} + (\mathcal{B}^\varepsilon u^\varepsilon, u^\varepsilon)_{L^2(0,t;L^2(\mathcal{Q}))} \\
&\quad + (f^\varepsilon, u^\varepsilon)_{L^2(0,t;L^2(\mathcal{Q}))} = (i) + (ii) + (iii).
\end{aligned}$$

We know from (2.34) that

$$(i) = -\sum_{v\in\mathcal{V}_0} \int_0^t \int_{\mathcal{Q}^{in}(v)} \frac{1}{2\varepsilon}|w|\big|u^\varepsilon(v,w,s) - \hat{u}^\varepsilon_v(|w|,s)\big|^2 \, dw \, ds,$$

since $u^\varepsilon(t) \in \mathcal{D}(\mathcal{A}^\varepsilon)$ for all $0 \leq t \leq T$. Moreover,

$$(ii) = -(\frac{\sigma}{\varepsilon^2}(u^\varepsilon - \bar{u}^\varepsilon), u^\varepsilon)_{L^2(0,t;L^2(\mathcal{Q}))} = -\varepsilon^{-2}\|\sigma^{1/2}(u^\varepsilon - \bar{u}^\varepsilon)\|^2_{L^2(0,t;L^2(\mathcal{Q}))},$$

where we used that the velocity average of $u^\varepsilon - \bar{u}^\varepsilon$ is zero. Since $\bar{f}^\varepsilon = \overline{\varepsilon^{-1}\alpha w \partial_x \bar{c}^\varepsilon \bar{z}^\varepsilon} = 0$, the third term can be estimated by Hölder's and Young's inequality, more precisely

$$\begin{aligned}(iii) &= (f^\varepsilon - \bar{f}^\varepsilon, u^\varepsilon - \bar{u}^\varepsilon)_{L^2(0,t;L^2(\mathcal{Q}))} = (f^\varepsilon, u^\varepsilon - \bar{u}^\varepsilon)_{L^2(0,t;L^2(\mathcal{Q}))} \\ &\leq \frac{\varepsilon^2}{2}\|\sigma^{-1/2} f^\varepsilon\|^2_{L^2(0,t;L^2(\mathcal{Q}))} + \frac{1}{2\varepsilon^2}\|\sigma^{1/2}(u^\varepsilon - \bar{u}^\varepsilon)\|^2_{L^2(0,t;L^2(\mathcal{Q}))},\end{aligned}$$

where the last term can be absorbed into (ii). In summary, this yields (2.28).

In order to derive the estimate (2.29) we observe that $\partial_t u^\varepsilon$ is mild solution to (iACP) with right-hand side $\partial_t f^\varepsilon \in L^2(0,T;\mathcal{X})$ and initial condition

$$\partial_t u^\varepsilon(0) = \partial_t u^\varepsilon_I := -\varepsilon^{-1} w \partial_x \bar{u}_I - \varepsilon^{-1}\alpha w \partial_x \bar{c}_I \bar{u}_I \in L^2(\mathcal{Q}),$$

which holds due to (2.27), (2.19), (2.15), and the fact that $z^\varepsilon(0) = \bar{u}_I$, which is independent of $w \in \mathcal{W}$ by Assumption (2.2). To be able to apply the energy estimates, we approximate the right-hand side $\partial_t f^\varepsilon$ by a sequence of functions $(\partial_t f^\varepsilon_n)_n \subset H^1(0,T;\mathcal{X})$ with $\bar{f}^\varepsilon_n(t) = 0$ and the initial condition by $(\partial_t u^\varepsilon_{I,n})_n \subset \mathcal{D}(\mathcal{A}^\varepsilon)$ so that

$$\|f^\varepsilon_n - f^\varepsilon\|_{L^2(0,T;\mathcal{X})} \to 0 \qquad \text{and} \qquad \|\partial_t u^\varepsilon_{I,n} - \partial_t u^\varepsilon_I\|_{\mathcal{X}} \to 0 \qquad \text{for } n \to \infty. \tag{2.35}$$

We denote the corresponding classical solution to (iACP) for $\partial_t f^\varepsilon_n$ and $\partial_t u^\varepsilon_{I,n}$ by $\partial_t u^\varepsilon_n$, which satisfies $\partial_t u^\varepsilon_n \in C^1([0,T];\mathcal{X}) \cap C^0([0,T];\mathcal{D}(\mathcal{A}^\varepsilon))$ by the same arguments as in Step 1. Moreover, since the mapping $(\partial_t f^\varepsilon, \partial_t u^\varepsilon_I) \mapsto \partial_t u^\varepsilon$ is linear and $\big(S(t)\big)_{0\leq t\leq T}$ is strongly continuous, we have

$$\max_{t\in[0,T]} \|\partial_t u^\varepsilon_n(t) - \partial_t u^\varepsilon(t)\|_{\mathcal{X}} \to 0 \qquad \text{for } n \to \infty. \tag{2.36}$$

By similar energy estimate as for u^ε derived above, testing with $\partial_t u^\varepsilon_n$ now leads to

$$\|\partial_t u^\varepsilon_n(t)\|^2_{L^2(\mathcal{Q})} \leq \|\partial_t u^\varepsilon_I\|^2_{L^2(\mathcal{Q})} + \varepsilon^2 \|\sigma^{-1/2}\partial_t f^\varepsilon_n\|^2_{L^2(0,t;L^2(\mathcal{Q}))}.$$

Via (2.35)–(2.36) and the triangle inequality, we finally deduce that

$$\|\partial_t u^\varepsilon(t)\|^2_{L^2(\mathcal{Q})} \leq \|\partial_t u^\varepsilon_I\|^2_{L^2(\mathcal{Q})} + \varepsilon^2 \|\sigma^{-1/2}\partial_t f^\varepsilon\|^2_{L^2(0,t;L^2(\mathcal{Q}))},$$

which shows (2.29) and concludes the proof of Lemma 2.5. □

2.2.3. Proof of Theorem 2.3

By using the results for the linearized problems derived in Lemma 2.4 and 2.5, we are now in the position to establish the existence of a unique solution to (2.10)–(2.19) via a fixed point argument and show the corresponding a-priori bounds (a)–(f).

Step 1 (Existence of solutions). Let us define the mapping

$$\Phi : \mathcal{S}_T \to C^1([0,T];L^2(\mathcal{Q})), \qquad z^\varepsilon \mapsto u^\varepsilon$$

with u^ε solving (2.27), (2.12)–(2.15) for $\bar{c}^\varepsilon$ solution to (2.23), (2.16)–(2.19) on the space

$$\mathcal{S}_T := \{z^\varepsilon \in C^1([0,T];L^2(\mathcal{Q})) : z^\varepsilon(0) = \bar{u}_I,\ \|z^\varepsilon\|^2_{\varepsilon,T} \leq C_{\mathcal{S}}\}$$

for some constant $C_{\mathcal{S}}$ and with ε-weighted norm defined by

$$\|z^\varepsilon\|^2_{\varepsilon,T} := \|z^\varepsilon\|^2_{C^0([0,T];L^2(\mathcal{Q}))} + \varepsilon^2\|\partial_t z^\varepsilon\|^2_{C^0([0,T];L^2(\mathcal{Q}))}.$$

By Lemma 2.4 and 2.5, Φ is well-defined.

Step 1.1 ($\Phi(\mathcal{S}_T) \subset \mathcal{S}_T$). Let $u^\varepsilon = \Phi(z^\varepsilon)$ for $z^\varepsilon \in \mathcal{S}_T$. Then, by (2.15) it holds that $u^\varepsilon(0) = \bar{u}_I$. Moreover, by (2.28)–(2.29) we obtain

$$\begin{aligned}
\|u^\varepsilon\|^2_{\varepsilon,T} &\le \|\bar{u}_I\|^2_{L^2(\mathcal{E})} + \|\alpha\sigma^{-1/2} w\partial_x\bar{c}^\varepsilon\bar{z}^\varepsilon\|^2_{L^2(0,T;L^2(\mathcal{Q}))} + \|w\partial_x\bar{u}_I - \alpha w\partial_x\bar{c}_I\bar{u}_I\|^2_{L^2(\mathcal{Q})} \\
&\quad + \|\varepsilon\alpha\sigma^{-1/2} w(\partial_{tx}\bar{c}^\varepsilon\bar{z}^\varepsilon + \partial_x\bar{c}^\varepsilon\partial_t\bar{z}^\varepsilon)\|^2_{L^2(0,T;L^2(\mathcal{Q}))} \\
&\le \|\bar{u}_I\|^2_{L^2(\mathcal{E})} + \tfrac{\alpha^2_{max}}{\sigma_{min}}\|\partial_x\bar{c}^\varepsilon\|^2_{L^4(0,T;L^\infty(\mathcal{E}))}\|z^\varepsilon\|^2_{L^4(0,T;L^2(\mathcal{Q}))} \\
&\quad + \|w\partial_x\bar{u}_I - \alpha w\partial_x\bar{c}_I\bar{u}_I\|^2_{L^2(\mathcal{Q})} + 2\tfrac{\alpha^2_{max}}{\sigma_{min}}\Big(\|\varepsilon\partial_{tx}\bar{c}^\varepsilon\|^2_{L^4(0,T;L^\infty(\mathcal{E}))}\|z^\varepsilon\|^2_{L^4(0,T;L^2(\mathcal{Q}))} \\
&\quad + \|\partial_x\bar{c}^\varepsilon\|^2_{L^4(0,T;L^\infty(\mathcal{E}))}\|\varepsilon\partial_t z^\varepsilon\|^2_{L^4(0,T;L^2(\mathcal{Q}))}\Big),
\end{aligned}$$

where we applied the triangle and Hölder's inequality. By (2.24)–(2.25) we have

$$\begin{aligned}
\|\partial_x\bar{c}^\varepsilon\|^2_{L^4(0,T;L^\infty(\mathcal{E}))} &\le C\Big(\|\bar{c}_I\|^2_{H^1(\mathcal{E})} + T\|\bar{z}^\varepsilon\|^2_{C^0([0,T];L^2(\mathcal{E}))}\Big), \\
\|\varepsilon\partial_{tx}\bar{c}^\varepsilon\|^2_{L^4(0,T;L^\infty(\mathcal{E}))} &\le C'\Big(\|\varepsilon(D\partial_{xx}\bar{c}_I - \delta\bar{c}_I + \gamma\bar{u}_I)\|^2_{H^1(\mathcal{E})} + T\|\varepsilon\partial_t\bar{z}^\varepsilon\|^2_{C^0([0,T];L^2(\mathcal{E}))}\Big).
\end{aligned}$$

This enables us to estimate

$$\begin{aligned}
\|u^\varepsilon\|^2_{\varepsilon,T} &\le \|\bar{u}_I\|^2_{L^2(\mathcal{E})} + \|w\partial_x\bar{u}_I - \alpha w\partial_x\bar{c}_I\bar{u}_I\|^2_{L^2(\mathcal{Q})} \\
&\quad + C''T^{1/2}\|z^\varepsilon\|^2_{C^0([0,T];L^2(\mathcal{Q}))} + C'''T^{1/2}\|\varepsilon\partial_t z^\varepsilon\|^2_{C^0([0,T];L^2(\mathcal{Q}))}
\end{aligned}$$

with constants C'', C''' that only depend on $\|z^\varepsilon\|_{C^0([0,T];L^2(\mathcal{Q}))}$ and $\|\varepsilon\partial_t z^\varepsilon\|_{C^0([0,T];L^2(\mathcal{Q}))}$, the initial data, and the bounds on the parameters, that are all bounded independently of ε by Assumption 2.2 and since $z^\varepsilon \in \mathcal{S}_T$. Consequently, for $C_{\mathcal{S}}$ large enough but independent of ε, more precisely $C_{\mathcal{S}} > \|\bar{u}_I\|^2_{L^2(\mathcal{E})} + \|w\partial_x\bar{u}_I - \alpha w\partial_x\bar{c}_I\bar{u}_I\|^2_{L^2(\mathcal{Q})}$, and T sufficiently small, but also independent of ε, it holds that $\|u^\varepsilon\|^2_{\varepsilon,T} \le C_{\mathcal{S}}$, i.e., $u^\varepsilon \in \mathcal{S}_T$.

Step 1.2 (Φ is a contraction). Let $(u^\varepsilon_1, \bar{c}^\varepsilon_1)$ and $(u^\varepsilon_2, \bar{c}^\varepsilon_2)$ be the solutions for z^ε_1 and $z^\varepsilon_2 \in \mathcal{S}_T$, respectively. Then, $u^\varepsilon_1 - u^\varepsilon_2$ solves (2.27), (2.12)–(2.15) with zero initial condition and right-hand side $f^\varepsilon = \varepsilon\alpha w(\partial_x\bar{c}^\varepsilon_1\bar{z}^\varepsilon_1 - \partial_x\bar{c}^\varepsilon_2\bar{z}^\varepsilon_2)$ in (2.27). Proceeding similarly as above, (2.28)–(2.29) yield

$$\begin{aligned}
\|u^\varepsilon_1 - u^\varepsilon_2\|^2_{\varepsilon,T} &\le \|\sigma^{-1/2}\alpha w(\partial_x\bar{c}^\varepsilon_1\bar{z}^\varepsilon_1 - \partial_x\bar{c}^\varepsilon_2\bar{z}^\varepsilon_2)\|^2_{L^2(0,T;L^2(\mathcal{Q}))} \\
&\quad + \varepsilon^2\|\sigma^{-1/2}\alpha w(\partial_{tx}\bar{c}^\varepsilon_1\bar{z}^\varepsilon_1 + \partial_x\bar{c}^\varepsilon_1\partial_t\bar{z}^\varepsilon_1 - \partial_{tx}\bar{c}^\varepsilon_2\bar{z}^\varepsilon_2 - \partial_x\bar{c}^\varepsilon_2\partial_t\bar{z}^\varepsilon_2)\|^2_{L^2(0,T;L^2(\mathcal{Q}))} = (i) + (ii).
\end{aligned}$$

Applying the triangle and Hölder's inequality, the first term can be estimated by

$$\begin{aligned}
(i) \le 2\alpha^2_{max}\sigma^{-1}_{min}\Big(&\|\partial_x\bar{c}^\varepsilon_1\|^2_{L^4(0,T;L^\infty(\mathcal{E}))}\|z^\varepsilon_1 - z^\varepsilon_2\|^2_{L^4(0,T;L^2(\mathcal{Q}))} \\
&+ \|\partial_x\bar{c}^\varepsilon_1 - \partial_x\bar{c}^\varepsilon_2\|^2_{L^4(0,T;L^\infty(\mathcal{E}))}\|z^\varepsilon_2\|^2_{L^4(0,T;L^2(\mathcal{Q}))}\Big).
\end{aligned}$$

From (2.24) we further conclude that

$$\|\partial_x \bar{c}_1^\varepsilon\|^2_{L^4(0,T;L^\infty(\mathcal{E}))}\|z_1^\varepsilon - z_2^\varepsilon\|^2_{L^4(0,T;L^2(\mathcal{Q}))} \leq C_1 T^{1/2}\|z_1^\varepsilon - z_2^\varepsilon\|^2_{C^0([0,T];L^2(\mathcal{Q}))},$$
$$\|\partial_x \bar{c}_1^\varepsilon - \partial_x \bar{c}_2^\varepsilon\|^2_{L^4(0,T;L^\infty(\mathcal{E}))}\|z_2^\varepsilon\|^2_{L^4(0,T;L^2(\mathcal{Q}))} \leq C_2 T^{3/2}\|z_1^\varepsilon - z_2^\varepsilon\|^2_{C^0([0,T];L^2(\mathcal{Q}))}.$$

In the same way, we estimate

$$(ii) \leq \frac{2\varepsilon^2\alpha_{max}^2}{\sigma_{min}}\Big(\|\partial_{tx}\bar{c}_1^\varepsilon\bar{z}_1^\varepsilon - \partial_{tx}\bar{c}_2^\varepsilon\bar{z}_2^\varepsilon\|^2_{L^2(0,T;L^2(\mathcal{E}))} + \|\partial_x\bar{c}_1^\varepsilon\partial_t\bar{z}_1^\varepsilon - \partial_x\bar{c}_2^\varepsilon\partial_t\bar{z}_2^\varepsilon)\|^2_{L^2(0,T;L^2(\mathcal{E}))}\Big),$$

where we applied the triangle inequality. Hölder's inequality and (2.25) then allows us to estimate the first term by

$$\begin{aligned}\varepsilon^2\|\partial_{tx}\bar{c}_1^\varepsilon\bar{z}_1^\varepsilon - \partial_{tx}\bar{c}_2^\varepsilon\bar{z}_2^\varepsilon\|^2_{L^2(0,T;L^2(\mathcal{E}))} &\leq 2\|\varepsilon(\partial_{tx}\bar{c}_1^\varepsilon - \partial_{tx}\bar{c}_2^\varepsilon)\|^2_{L^4(0,T;L^\infty(\mathcal{E}))}\|z_1^\varepsilon\|^2_{L^4(0,T;L^2(\mathcal{Q}))}\\ &\quad + 2\|\varepsilon\partial_{tx}\bar{c}_2^\varepsilon\|^2_{L^4(0,T;L^\infty(\mathcal{E}))}\|z_1^\varepsilon - z_2^\varepsilon\|^2_{L^4(0,T;L^2(\mathcal{Q}))}\\ &\leq C_3T^{3/2}\|\varepsilon(\partial_t z_1^\varepsilon - \partial_t z_2^\varepsilon)\|^2_{C^0([0,T];L^2(\mathcal{Q}))} + C_4T^{1/2}\|z_1^\varepsilon - z_2^\varepsilon\|^2_{C^0([0,T];L^2(\mathcal{Q}))}.\end{aligned}$$

In a similar manner, (2.24) yields for the second term

$$\begin{aligned}\varepsilon^2\|\partial_x\bar{c}_1^\varepsilon\partial_t\bar{z}_1^\varepsilon - \partial_x\bar{c}_2^\varepsilon\partial_t\bar{z}_2^\varepsilon)\|^2_{L^2(0,T;L^2(\mathcal{E}))} &\leq 2\|\partial_x\bar{c}_1^\varepsilon - \partial_x\bar{c}_2^\varepsilon\|^2_{L^4(0,T;L^\infty(\mathcal{E}))}\|\varepsilon\partial_t z_1^\varepsilon\|^2_{L^4(0,T;L^2(\mathcal{Q}))}\\ &\quad +2\|\partial_x\bar{c}_2^\varepsilon\|^2_{L^4(0,T;L^\infty(\mathcal{E}))}\|\varepsilon(\partial_t z_1^\varepsilon - \partial_t z_2^\varepsilon)\|^2_{L^4(0,T;L^2(\mathcal{Q}))}\\ &\leq C_5T^{3/2}\|z_1^\varepsilon - z_2^\varepsilon\|^2_{C^0([0,T];L^2(\mathcal{Q}))} + C_6T^{1/2}\|\varepsilon(\partial_t z_1^\varepsilon - \partial_t z_2^\varepsilon)\|^2_{C^0([0,T];L^2(\mathcal{Q}))}.\end{aligned}$$

By carefully tracking the constants, we see that $C_1 - C_6$ only depend on $\|z_i^\varepsilon\|_{C^0([0,T];L^2(\mathcal{Q}))}$ and $\|\varepsilon\partial_t z_i^\varepsilon\|_{C^0([0,T];L^2(\mathcal{Q}))}$, $i = 1, 2$, which are bounded independently of ε since $z_1^\varepsilon,\ z_2^\varepsilon \in \mathcal{S}_T$, as well as the bounds on the initial data and parameters that are independent of ε by Assumption 2.2. In summary, we can thus estimate

$$\|u_1^\varepsilon - u_2^\varepsilon\|^2_{\varepsilon,T} \leq CT^{1/2}\|z_1^\varepsilon - z_2^\varepsilon\|^2_{\varepsilon,T}.$$

Consequently, there exists a time point T sufficiently small but independent of ε so that Φ is a contraction.

Step 1.3 (Φ has a fixed point). For T sufficiently small but independent of ε and all $\varepsilon > 0$ the mapping Φ has a fixed point in $\mathcal{S}_T$ by Banach's fixed point theorem, i.e., (2.10)–(2.19) has a solution

$$\begin{aligned}&u^\varepsilon \in C^1([0,T];L^2(\mathcal{Q})) \cap C^0([0,T];Z),\\ &\bar{c}^\varepsilon \in W^{1,\infty}(0,T;H^1(\mathcal{E})) \cap H^2(0,T;L^2(\mathcal{E})) \cap H^1(0,T;H^2_{pw}(\mathcal{E}))\end{aligned}$$

up to T that satisfies

$$\|u^\varepsilon\|^2_{\varepsilon,T} = \|u^\varepsilon\|^2_{C^0([0,T];L^2(\mathcal{Q}))} + \varepsilon^2\|\partial_t u^\varepsilon\|^2_{C^0([0,T];L^2(\mathcal{Q}))} \leq C_{\mathcal{S}},$$

where $C_{\mathcal{S}}$ does not depend on ε. This already proves the a-priori bounds (a) and (e).

Step 2 (A-priori bounds). Let us now verify the remaining a-priori bounds. The bound (d) on $\bar{c}^\varepsilon$ directly follows from (2.24), (a), and Assumption 2.2. The bounds (b)

and (c) are a direct consequence of (2.28), since the right-hand side can be bounded independently of ε due to (a), (d), and Assumption 2.2, more precisely

$$\|\sigma^{-1/2}\alpha w\partial_x\bar{c}^\varepsilon\bar{u}^\varepsilon\|_{L^2(0,T;L^2(\mathcal{Q}))} \leq \sigma_{min}^{-1}\alpha_{max}^2\|\partial_x\bar{c}^\varepsilon\|_{L^2(0,T;L^\infty(\mathcal{Q}))}\|\bar{u}^\varepsilon\|_{L^\infty(0,T;L^2(\mathcal{Q}))} \leq C,$$

where we applied Hölder's inequality and used the embedding $H^1_{pw}(\mathcal{E}) \hookrightarrow L^\infty(\mathcal{E})$ in dimension $d = 1$. In order to verify (f), we deduce from (2.10) that

$$\begin{aligned}\|w\partial_x u^\varepsilon\|_{L^2(0,T;L^2(\mathcal{Q}))} \leq \|\varepsilon\partial_t u^\varepsilon\|_{L^2(0,T;L^2(\mathcal{Q}))} + \|\frac{\sigma}{\varepsilon}(u^\varepsilon - \bar{u}^\varepsilon)\|_{L^2(0,T;L^2(\mathcal{Q}))} \\ + \|\alpha w\partial_x\bar{c}^\varepsilon\bar{u}^\varepsilon\|_{L^2(0,T;L^2(\mathcal{Q}))} \leq C,\end{aligned}$$

where we used that the first term on the right-hand side is bounded by (e), the second term by (b), and the last term can be bounded as above.

Step 3 (Proof of the mass balances). We integrate (2.10) over $\mathcal{Q}$ and obtain

$$\begin{aligned}\frac{d}{dt}\int_{\mathcal{Q}} \varepsilon^2 u^\varepsilon(x,w,t)\ d(x,w) &= -\int_{\mathcal{Q}} \varepsilon w\partial_x u^\varepsilon(x,w,t)\ d(x,w) + \int_{\mathcal{Q}} \varepsilon\alpha w\partial_x\bar{c}^\varepsilon\bar{u}^\varepsilon\ d(x,w) \\ &\quad - \int_{\mathcal{Q}} \sigma(x)(u^\varepsilon(x,w,t) - \bar{u}^\varepsilon(x,w,t))\ d(x,w) \\ &= -\sum\nolimits_{v\in\mathcal{V}}\sum\nolimits_{e\in\mathcal{E}(v)}\int_{\mathcal{W}} \varepsilon w u_e^\varepsilon(v,w,t)n_e(v)\ dw = 0,\end{aligned}$$

where we used that the velocity average of $u^\varepsilon - \bar{u}^\varepsilon$ and $w\partial_x\bar{c}^\varepsilon\bar{u}^\varepsilon$ is zero, and that the sum over the vertices vanishes due to the reflection boundary condition (2.12) at the network inflow boundary and the mixing condition (2.13)–(2.14) at network junctions. Integrating over $(0,t)$ then yields (2.21). Similarly, integrating (2.11) over $\mathcal{E}$ leads to

$$\begin{aligned}\frac{d}{dt}\int_{\mathcal{E}} \bar{c}^\varepsilon(x,t)\ dx &= \int_{\mathcal{E}} D\partial_{xx}\bar{c}^\varepsilon(x,t) - \delta\bar{c}^\varepsilon(x,t) + \gamma\bar{u}^\varepsilon(x,t)\ dx \\ &= \sum\nolimits_{v\in\mathcal{V}}\sum\nolimits_{e\in\mathcal{E}(v)} D_e\partial_x\bar{c}^\varepsilon(v,t)n_e(v) + \int_{\mathcal{E}} \gamma\bar{u}^\varepsilon(x,t) - \delta\bar{c}^\varepsilon(x,t)\ dx.\end{aligned}$$

The sum over the vertices vanishes due to the no-flux boundary conditions (2.16) at the network boundary and the coupling condition (2.18) at the network junctions. Integrating over $(0,t)$ proves the mass balance (2.22) for $\bar{c}^\varepsilon$. □

Remark 2.6. Local solutions to (2.10)–(2.19) can be extended in time with initial conditions $u^\varepsilon(T) \in Z$ and $\bar{c}^\varepsilon(T) \in H^1(\mathcal{E})$. However, the time of existence T that we obtain in the fixed point argument of the proof can go to zero. Theorem 2.3 thus only guarantees the local existence of solutions uniformly in ε up to a time point T that is independent of ε. However, by replacing (2.10) with

$$\varepsilon^2\partial_t u_e^\varepsilon + \varepsilon w\partial_x u_e^\varepsilon + \sigma(u_e^\varepsilon - \bar{u}_e^\varepsilon) = \varepsilon\alpha_e w b(\partial_x\bar{c}_e^\varepsilon)\bar{u}_e^\varepsilon, \qquad \text{in } (0,\ell_e)\times(-1,1)\times(0,T)$$

on each edge $e \in \mathcal{E}$ with cut-off function b that can be chosen, e.g., as

$$b(u) = \max(B, \min(-B, u))$$

for some constant $B > 0$, one can show via energy estimates that the bounds (a) and (e) hold for all time points $T > 0$, which implies the existence of global solutions.

2.3. Asymptotic analysis

This section is dedicated to the analysis of the asymptotic behavior of solutions $(u^\varepsilon, \bar{c}^\varepsilon)$ to (2.10)–(2.19) for $\varepsilon \to 0$. We first introduce the limiting problem for $\varepsilon = 0$, whose solution is denoted by $(\bar{u}^0, \bar{c}^0)$. In a second step, we show that $(u^\varepsilon, \bar{c}^\varepsilon) \to (\bar{u}^0, \bar{c}^0)$ and then derive quantitative convergence rates.

2.3.1. The limit problem

The limit problem of (2.10)–(2.19) for $\varepsilon \to 0$ is given by the classical Keller-Segel system on networks [9, 44]. On each edge $e \in \mathcal{E}$ it holds that

$$\partial_t \bar{u}_e^0 - \partial_x(\bar{a}_e \partial_x \bar{u}_e^0 - \bar{\chi}_e \partial_x \bar{c}_e^0 \bar{u}_e^0) = 0 \qquad \text{in } (0, \ell_e) \times (0, T), \tag{2.37}$$

$$\partial_t \bar{c}_e^0 - D_e \partial_{xx} \bar{c}_e^0 + \delta_e \bar{c}_e^0 = \gamma_e \bar{u}_e^0 \qquad \text{in } (0, \ell_e) \times (0, T) \tag{2.38}$$

with network boundary conditions

$$\bar{a}_e(v) \partial_x \bar{u}_e^0(v,t) - \bar{\chi}_e(v) \partial_x \bar{c}_e^0(v,t) \bar{u}_e^0(v,t) = 0 \quad \text{for } v \in \mathcal{V}_\partial,\ e \in \mathcal{E}(v),\ t \in (0,T), \tag{2.39}$$

$$\partial_x \bar{c}_e^0(v,t) = 0 \quad \text{for } v \in \mathcal{V}_\partial,\ e \in \mathcal{E}(v),\ t \in (0,T), \tag{2.40}$$

and coupling conditions at network junctions $v \in \mathcal{V}_0$ given by

$$\bar{u}_{e_i}^0(v,t) = \bar{u}_{e_j}^0(v,t) \qquad \text{for } e_i, e_j \in \mathcal{E}(v),\ t \in (0,T), \tag{2.41}$$

$$\bar{c}_{e_i}^0(v,t) = \bar{c}_{e_j}^0(v,t) \qquad \text{for } e_i, e_j \in \mathcal{E}(v),\ t \in (0,T), \tag{2.42}$$

as well as

$$\sum\nolimits_{e \in \mathcal{E}(v)} \big(\bar{a}_e(v) \partial_x \bar{u}_e^0(v,t) - \bar{\chi}_e(v) \partial_x \bar{c}_e^0(v,t) \bar{u}_e^0(v,t)\big) n_e(v) = 0 \quad \text{for } t \in (0,T), \tag{2.43}$$

$$\sum\nolimits_{e \in \mathcal{E}(v)} D_e \partial_x \bar{c}_e^0(v,t) n_e(v) = 0 \quad \text{for } t \in (0,T). \tag{2.44}$$

At the initial time, we have

$$\bar{u}^0(0) = \bar{u}_I \qquad \text{on } \mathcal{E}, \tag{2.45}$$

$$\bar{c}^0(0) = \bar{c}_I \qquad \text{on } \mathcal{E}. \tag{2.46}$$

The coefficients $\bar{a}$ and $\bar{\chi}$ are defined by

$$\bar{a}_e(x) := \sigma_e(x)^{-1} \int_{\mathcal{W}} w^2 \, dw \qquad \text{and} \qquad \bar{\chi}_e(x) := \alpha_e \sigma_e(x)^{-1} \int_{\mathcal{W}} w^2 \, dw \tag{2.47}$$

for $x \in (0, \ell_e)$ and $e \in \mathcal{E}$.

Sufficiently regular solutions $(\bar{u}^0, \bar{c}^0)$ that satisfy (2.37)–(2.46) in a pointwise sense, e.g., continuously differentiable in time and twice continuously differentiable in space, can be characterized by the following weak formulation.

Lemma 2.7. *Let* $(\bar{u}^0, \bar{c}^0)$ *be a sufficiently regular solution to* (2.37)–(2.46)*. Then,*

$$\langle \partial_t \bar{u}^0, \bar{\psi} \rangle + (\bar{a}\partial_x \bar{u}^0 - \bar{\chi}\partial_x \bar{c}^0 \bar{u}^0, \partial_x \bar{\psi})_{L^2(0,T;L^2(\mathcal{E}))} = 0, \tag{2.48}$$

$$(\partial_t \bar{c}^0, \bar{\phi})_{L^2(0,T;L^2(\mathcal{E}))} + (D\partial_x \bar{c}^0, \partial_x \bar{\phi})_{L^2(0,T;L^2(\mathcal{E}))} + (\delta \bar{c}^0, \bar{\phi})_{L^2(0,T;L^2(\mathcal{E}))} = (\gamma \bar{u}^0, \bar{\phi})_{L^2(0,T;L^2(\mathcal{E}))} \tag{2.49}$$

holds for all test functions $\bar{\psi}$, $\bar{\phi} \in L^2(0,T;H^1(\mathcal{E}))$ *with* $\langle \cdot, \cdot \rangle$ *denoting the duality bracket in* $L^2(0,T;H(\mathcal{E})^*) \times L^2(0,T;H^1(\mathcal{E}))$.

Proof. Multiplying (2.37) by $\bar{\psi} \in L^2(0,T;H^1(\mathcal{E}))$ and integrating over $\mathcal{E} \times (0,T)$ yields

$$\begin{aligned} 0 &= (\partial_t \bar{u}^0, \bar{\psi})_{L^2(0,T;L^2(\mathcal{E}))} - (\partial_x(\bar{a}\partial_x \bar{u}^0 - \bar{\chi}\partial_x \bar{c}^0 \bar{u}^0), \bar{\psi})_{L^2(0,T;L^2(\mathcal{E}))} \\ &= (\partial_t \bar{u}^0, \bar{\psi})_{L^2(0,T;L^2(\mathcal{E}))} + (\bar{a}\partial_x \bar{u}^0 - \bar{\chi}\partial_x \bar{c}^0 \bar{u}^0, \partial_x \bar{\psi})_{L^2(0,T;L^2(\mathcal{E}))} \\ &\quad - \sum_{v \in \mathcal{V}} \sum_{e \in \mathcal{E}(v)} \int_0^T \big(\bar{a}_e(v)\partial_x \bar{u}_e^0(v,t) - \bar{\chi}_e(v)\partial_x \bar{c}_e^0(v,t)\bar{u}_e^0(v,t)\big)\bar{\psi}_e(v,t)n_e(v)\ dt, \end{aligned}$$

where we applied integration-by-parts in space to the second term in the first line. The contributions at network boundary vertices $v \in \mathcal{V}_\partial$ vanish due to the boundary condition (2.39) and at interior vertices $v \in \mathcal{V}_0$ due to the coupling condition (2.43) and the fact that $\bar{\psi}$ is continuous over junctions. Consequently, $(\bar{u}^0, \bar{c}^0)$ satisfies (2.48) since $L^2(\mathcal{E}) \subset H^1(\mathcal{E})^*$. Testing (2.38) with $\bar{\phi} \in L^2(0,T;H^1(\mathcal{E}))$ and integrating over $\mathcal{E} \times (0,T)$ leads to

$$0 = (\partial_t \bar{c}^0, \bar{\phi})_{L^2(0,T;L^2(\mathcal{E}))} - (D\partial_{xx} \bar{c}^0, \bar{\phi})_{L^2(0,T;L^2(\mathcal{E}))} + (\delta \bar{c}^0 - \gamma \bar{u}^0, \bar{\phi})_{L^2(0,T;L^2(\mathcal{E}))}.$$

Applying integration-by-parts in space to the second term yields

$$\begin{aligned} -(D\partial_{xx} \bar{c}^0, \bar{\phi})_{L^2(0,T;L^2(\mathcal{E}))} &= (D\partial_x \bar{c}^0, \partial_x \bar{\phi})_{L^2(0,T;L^2(\mathcal{E}))} \\ &\quad - \sum_{v \in \mathcal{V}} \sum_{e \in \mathcal{E}(v)} \int_0^T D_e \partial_x \bar{c}_e^0(v,t)\bar{\phi}_e(v,t)n_e(v)\ dt. \end{aligned}$$

The contributions at the boundary vertices $v \in \mathcal{V}_\partial$ vanish due to the no-flux boundary condition (2.40) and at the interior vertices $v \in \mathcal{V}_0$ due to the coupling condition (2.44) and the fact that $\bar{\phi}$ is continuous over junctions. This shows that $(\bar{u}^0, \bar{c}^0)$ satisfies (2.49), and concludes the proof. □

The equations (2.48)–(2.49) are also well-defined for less regular functions. We call a pair of functions

$$\begin{aligned} \bar{u}^0 &\in L^2(0,T;H^1(\mathcal{E})) \cap H^1(0,T;H^1(\mathcal{E})^*), \\ \bar{c}^0 &\in L^\infty(0,T;H^1(\mathcal{E})) \cap H^1(0,T;L^2(\mathcal{E})), \end{aligned}$$

that satisfies (2.48)–(2.49) for all $\bar{\psi}$, $\bar{\phi} \in L^2(0,T;H^1(\mathcal{E}))$ and $\bar{u}^0(0) = \bar{u}_I$, $\bar{c}^0(0) = \bar{c}_I$, a *weak solution* to (2.37)–(2.46).

Theorem 2.8. *Let Assumption 2.2 hold. Then, there exists a unique local weak solution* $(\bar{u}^0, \bar{c}^0)$ *to* (2.37)–(2.46)*. Under the additional reasonable assumption of positive initial data, one can even guarantee the global existence of a unique weak solution.*

Proof. One can show the local existence of weak solutions by Galerkin approximation, energy estimates, and fixed point arguments. Global existence can then be verified by deriving sharper estimates for solutions exploiting positivity and mass conservation. For details we refer to [44, Thm. 3.1 and Thm. 3.2]. □

2.3.2. Convergence to the limit problem

Let us now investigate the asymptotic behavior of $(u^\varepsilon, \bar{c}^\varepsilon)$ for $\varepsilon \to 0$.

Theorem 2.9. *Let Assumption 2.2 hold and let $(u^\varepsilon, \bar{c}^\varepsilon)$ be the unique solution to* (2.10)–(2.19) *in the sense of Theorem 2.3. Then, there exists a weakly convergent subsequence with limit $(\bar{u}^0, \bar{c}^0)$ that is the (unique) weak solution to* (2.37)–(2.46).

Proof. **Step 1 (Convergent subsequences).** From the bounds (a), (d), and (f), and the Banach-Alaoglu Theorem, see e.g. [25], we conclude that $(u^\varepsilon, \bar{c}^\varepsilon)$ has a weakly convergent subsequence with limit

$$(u^0, \bar{c}^0) \in L^2(0,T;L^2(\mathcal{Q})) \times H^1(0,T;L^2(\mathcal{E})) \cap L^2(0,T;H^1(\mathcal{E}) \cap H^2_{pw}(\mathcal{E})),$$

so that $w\partial_x u^0 \in L^2(0,T;L^2(\mathcal{Q}))$ and

$$u^\varepsilon \rightharpoonup u^0 \qquad \text{weakly in } L^2(0,T;L^2(\mathcal{Q})), \tag{2.50}$$

$$w\partial_x u^\varepsilon \rightharpoonup w\partial_x u^0 \qquad \text{weakly in } L^2(0,T;L^2(\mathcal{Q})), \tag{2.51}$$

$$\bar{c}^\varepsilon \rightharpoonup \bar{c}^0 \qquad \text{weakly in } H^1(0,T;L^2(\mathcal{E})) \cap L^2(0,T;H^1(\mathcal{E}) \cap H^2_{pw}(\mathcal{E})). \tag{2.52}$$

It further holds that $H^1(0,T;L^2(\mathcal{E})) \cap L^2(0,T;H^1(\mathcal{E}) \cap H^2_{pw}(\mathcal{E}))$ is compactly embedded in $L^2(0,T;H^1(\mathcal{E}))$ by the Aubin-Lions lemma; see e.g. [111, Lemma 7.7]. Hence,

$$\bar{c}^\varepsilon \to \bar{c}^0 \qquad \text{strongly in } L^2(0,T;H^1(\mathcal{E})), \tag{2.53}$$

which immediately follows from (2.52). From (b) and the weakly lower semicontinuity of norms, we can further deduce that u^0 is independent of w, since

$$\|u^0 - \bar{u}^0\|_{L^2(0,T;L^2(\mathcal{Q}))} \le \liminf_\varepsilon \|u^\varepsilon - \bar{u}^\varepsilon\|_{L^2(0,T;L^2(\mathcal{Q}))} = 0.$$

In the following, we thus write $u^0 = \bar{u}^0$. From (2.51) we further deduce that $\partial_x u^0 = \partial_x \bar{u}^0 \in L^2(0,T;L^2(\mathcal{E}))$. On each edge $e = (0, \ell_e) \in \mathcal{E}$ let us now define the trace operator that evaluates a function at the start or end of e by

$$\gamma_v : Z_e \to L^2(\mathcal{W} \times (0,T)), \quad u_e \mapsto u_e(v)$$

for $v \in \{0, \ell_e\}$ with $Z_e = \{u_e \in L^2(e \times \mathcal{W} \times (0,T)) : w\partial_x u_e \in L^2(e \times \mathcal{W} \times (0,T))\}$ and w-weighted norms associated to the spaces given by

$$\|u_e\|^2_{Z_e} = \|u_e\|^2_{L^2(e\times\mathcal{W}\times(0,T))} + \|w\partial_x u_e\|^2_{L^2(e\times\mathcal{W}\times(0,T))} \quad \text{and} \quad \||w|^{1/2}u\|_{L^2(\mathcal{W}\times(0,T))}.$$

By the fundamental theorem of calculus we then see that at the start of the edge it holds

$$|w|u_e(0)^2 = |w|u_e(x)^2 - \int_0^x |w|\partial_x\big(u_e(s)^2\big)\, ds = |w|u_e(x)^2 - 2\int_0^x |w|u_e(s)\partial_x u_e(s)\, ds.$$

Integrating over $e \times \mathcal{W} \times (0,T)$ and applying Hölder's and Young's inequality to the last term yields

$$\||w|^{1/2}u_e(0)\|^2_{L^2(\mathcal{W}\times(0,T))} \le (1 + \ell_e^{-1})\|u_e\|^2_{L^2(e\times\mathcal{W}\times(0,T))} + \|w\partial_x u_e\|^2_{L^2(e\times\mathcal{W}\times(0,T))}.$$

The same holds at the end ℓ_e of the edge. Consequently, γ_v is continuous. From the fact that u^ε and $w\partial_x u^\varepsilon$ are bounded by (a) and (f) we can then conclude

$$u_e^\varepsilon(v) \rightharpoonup \bar{u}_e^0(v) \qquad\qquad \text{weakly in } L^2(\mathcal{W}\times(0,T))$$

associated with the norm $\||w|^{1/2}u\|_{L^2(\mathcal{W}\times(0,T))}$ for all $v\in\mathcal{V},\ e\in\mathcal{E}(v)$. This also allows us to introduce the value $\hat{u}_v^0$ as the weak limit of $\hat{u}_v^\varepsilon$ which was defined as the mixing value in (2.14) for $v\in\mathcal{V}_0$. Note that $\hat{u}_v^0$ does not depend on w anymore. Then, the coupling condition (2.13) and (c) yield

$$\begin{aligned}\|\bar{u}_e^0(v)-\hat{u}_v^0\|^2_{L^2(0,T)} &= \||w|^{1/2}(\bar{u}_e^0(v)-\hat{u}_v^0)\|^2_{L^2(\mathcal{W}\times(0,T))}\\ &\le \liminf_\varepsilon \||w|^{1/2}(u_e^\varepsilon(v)-\hat{u}_v^\varepsilon)\|^2_{L^2(\mathcal{W}\times(0,T))}\to 0\end{aligned}$$

for $\varepsilon\to 0$ and all $v\in\mathcal{V}_0,\ e\in\mathcal{E}(v)$, i.e., $\bar{u}_0$ is continuous across network junctions.

Step 2 (Convergence to the limit). Let us now show that the limit $(\bar{u}^0,\bar{c}^0)$ is the weak solution to the limit problem (2.37)–(2.46), i.e., $(\bar{u}^0,\bar{c}^0)$ solves the weak formulation (2.48)–(2.49) and satisfies $\bar{u}^0(0)=\bar{u}_I$ and $\bar{c}^0(0)=\bar{c}_I$.

Step 2.1 ($(\bar{u}^0,\bar{c}^0)$ solves (2.49)*).* Let $\bar{\phi}\in L^2(0,T;H^1(\mathcal{E}))$. It then holds that

$$\begin{aligned}&(\partial_t\bar{c}^0,\bar{\phi})_{L^2(0,T;L^2(\mathcal{E}))}+(D\partial_x\bar{c}^0,\partial_x\bar{\phi})_{L^2(0,T;L^2(\mathcal{E}))}+(\delta\bar{c}^0-\gamma\bar{u}^0,\bar{\phi})_{L^2(0,T;L^2(\mathcal{E}))}\\ &\quad=\lim_\varepsilon\Big((\partial_t\bar{c}^\varepsilon,\bar{\phi})_{L^2(0,T;L^2(\mathcal{E}))}+(D\partial_x\bar{c}^\varepsilon,\partial_x\bar{\phi})_{L^2(0,T;L^2(\mathcal{E}))}+(\delta\bar{c}^\varepsilon-\gamma\bar{u}^\varepsilon,\bar{\phi})_{L^2(0,T;L^2(\mathcal{E}))}\Big)\\ &\quad=0\end{aligned}$$

by (2.50) and (2.52), i.e., $(\bar{u}^0,\bar{c}^0)$ solves (2.49). The last equation holds by testing (2.11) with $\bar{\phi}$ and integrating over $\mathcal{E}\times(0,T)$, which leads to

$$0=(\partial_t\bar{c}^\varepsilon,\bar{\phi})_{L^2(0,T;L^2(\mathcal{E}))}-(D\partial_{xx}\bar{c}^\varepsilon,\partial_x\bar{\phi})_{L^2(0,T;L^2(\mathcal{E}))}+(\delta\bar{c}^\varepsilon-\gamma\bar{u}^0,\bar{\phi})_{L^2(0,T;L^2(\mathcal{E}))}.$$

Applying integration-by-parts in space to the second term then yields

$$\begin{aligned}-(D\partial_{xx}\bar{c}^\varepsilon,\partial_x\bar{\phi})_{L^2(0,T;L^2(\mathcal{E}))} &= (D\partial_x\bar{c}^\varepsilon,\bar{\phi})_{L^2(0,T;L^2(\mathcal{E}))}\\ &\quad-\sum\nolimits_{v\in\mathcal{V}}\sum\nolimits_{e\in\mathcal{E}(v)}\int_0^T D_e\partial_x\bar{c}_e^\varepsilon(v,t)\bar{\phi}_e(v,t)n_e(v)\,dt.\end{aligned}$$

The contributions at the boundary vertices $v\in\mathcal{V}_\partial$ vanish due to the no-flux boundary condition (2.16) and at the interior vertices $v\in\mathcal{V}_0$ due to the coupling condition (2.18) and the fact that $\bar{\psi}$ is continuous over junctions.

Step 2.2 ($\bar{c}^0(0)=\bar{c}_I$). Testing with $\bar{\phi}_0\in C^1([0,T];H^1(\mathcal{E}))$ so that $\bar{\phi}_0(T)=0$ and applying integration-by-parts in time, we can conclude from (2.49) that

$$\begin{aligned}0&=(\partial_t\bar{c}^0,\bar{\phi}_0)_{L^2(0,T;L^2(\mathcal{E}))}+(D\partial_x\bar{c}^0,\partial_x\bar{\phi}_0)_{L^2(0,T;L^2(\mathcal{E}))}+(\delta\bar{c}^0-\gamma\bar{u}^0,\bar{\phi}_0)_{L^2(0,T;L^2(\mathcal{E}))}\\ &=-(\bar{c}^0,\partial_t\bar{\phi}_0)_{L^2(0,T;L^2(\mathcal{E}))}-(\bar{c}^0(0),\bar{\phi}_0(0))_{L^2(\mathcal{E})}+(D\partial_x\bar{c}^0,\partial_x\bar{\phi}_0)_{L^2(0,T;L^2(\mathcal{E}))}\\ &\quad+(\delta\bar{c}^0-\gamma\bar{u}^0,\bar{\phi}_0)_{L^2(0,T;L^2(\mathcal{E}))}.\end{aligned}$$

With similar arguments as above and by applying integration-by-parts in time we have

$$\begin{aligned}0 = &\lim_\varepsilon \Big(-(\bar{c}^\varepsilon, \partial_t \bar{\phi}_0)_{L^2(0,T;L^2(\mathcal{E}))} - (\bar{c}_I, \bar{\phi}_0(0))_{L^2(\mathcal{E})} + (D\partial_x \bar{c}^\varepsilon, \partial_x \bar{\phi}_0)_{L^2(0,T;L^2(\mathcal{E}))} \\ &\qquad + (\delta \bar{c}^\varepsilon - \gamma \bar{u}^\varepsilon, \bar{\phi}_0)_{L^2(0,T;L^2(\mathcal{E}))}\Big) \\ = &- (\bar{c}^0, \partial_t \bar{\phi}_0)_{L^2(0,T;L^2(\mathcal{E}))} - (\bar{c}_I, \bar{\phi}_0(0))_{L^2(\mathcal{E})} + (D\partial_x \bar{c}^0, \partial_x \bar{\phi}_0)_{L^2(0,T;L^2(\mathcal{E}))} \\ &\qquad + (\delta \bar{c}^0 - \gamma \bar{u}^0, \bar{\phi}_0)_{L^2(0,T;L^2(\mathcal{E}))},\end{aligned}$$

where we used that $\bar{c}^\varepsilon(0) = \bar{c}_I$ by (2.19). As $\phi_0(0)$ is arbitrary, comparing the terms yields $\bar{c}^0(0) = \bar{c}_I$. Since $\bar{c}_I \in H^1(\mathcal{E})$ by Assumption 2.2 and $\bar{u}^0 \in L^2(0,T;L^2(\mathcal{Q}))$, by standard existence and regularity theory [49] we find that, additionally, $\bar{c}^0 \in L^\infty(0,T;H^1(\mathcal{E}))$.

Step 2.3 ($(\bar{u}^0, \bar{c}^0)$ solves (2.48)). Let $\bar{\psi} \in C_0^\infty([0,T]; C_{pw}^\infty(\mathcal{E}) \cap H^1(\mathcal{E}))$ with $C_{pw}^\infty(\mathcal{E})$ denoting the set of edgewise smooth functions on the network. It then holds that

$$\begin{aligned}&(w\partial_x \bar{u}^0, \sigma^{-1} w \partial_x \bar{\psi})_{L^2(0,T;L^2(\mathcal{E}))} = \lim_\varepsilon (w\partial_x u^\varepsilon, \sigma^{-1} w \partial_x \bar{\psi})_{L^2(0,T;L^2(\mathcal{Q}))} \\ &\quad = \lim_\varepsilon \Big(-(\varepsilon \partial_t u^\varepsilon, \sigma^{-1} w \partial_x \bar{\psi})_{L^2(0,T;L^2(\mathcal{Q}))} - (\varepsilon^{-1}(u^\varepsilon - \bar{u}^\varepsilon), w\partial_x \bar{\psi})_{L^2(0,T;L^2(\mathcal{Q}))} \\ &\qquad\qquad + (\alpha w \partial_x \bar{c}^\varepsilon \bar{u}^\varepsilon, \sigma^{-1} w \partial_x \bar{\psi})_{L^2(0,T;L^2(\mathcal{Q}))}\Big) \\ &\quad = \lim_\varepsilon \Big((i)^\varepsilon + (ii)^\varepsilon + (iii)^\varepsilon \Big) \qquad (2.54)\end{aligned}$$

by (2.51) and (2.10). Let us consider the terms separately. Applying integration-by-parts in time and using the fact that $\bar{\psi}$ and its derivatives vanish at $t = 0, T$ yields

$$(i)^\varepsilon = (\varepsilon u^\varepsilon, \sigma^{-1} w \partial_{tx} \bar{\psi})_{L^2(0,T;L^2(\mathcal{Q}))} \le \varepsilon \sigma_{min}^{-1} \|u^\varepsilon\|_{L^2(0,T;L^2(\mathcal{Q}))} \|\partial_{tx}\bar{\psi}\|_{L^2(0,T;L^2(\mathcal{Q}))} \to 0$$

for $\varepsilon \to 0$ due to (a). Since the velocity average of $w\bar{u}^\varepsilon \partial_x \bar{\psi}$ is zero, it holds that

$$\begin{aligned}(ii)^\varepsilon &= (\varepsilon^{-1} w \partial_x u^\varepsilon, \bar{\psi})_{L^2(0,T;L^2(\mathcal{Q}))} - \sum_{v\in\mathcal{V}} \sum_{e\in\mathcal{E}(v)} \int_0^T \int_{\mathcal{W}} \varepsilon^{-1} w u_e^\varepsilon(v,w,t) \bar{\psi}_e(v,t) n_e(v)\, dw\, dt \\ &= (ii.1)^\varepsilon + \sum\nolimits_{v\in\mathcal{V}} (ii.2)_v^\varepsilon, \qquad (2.55)\end{aligned}$$

where we applied integration-by-parts in space. By (2.10) the first term equals

$$\begin{aligned}(ii.1)^\varepsilon = &- (\partial_t u^\varepsilon, \bar{\psi})_{L^2(0,T;L^2(\mathcal{Q}))} - (\varepsilon^{-2}\sigma(u^\varepsilon - \bar{u}^\varepsilon), \bar{\psi})_{L^2(0,T;L^2(\mathcal{Q}))} \\ &+ (\varepsilon^{-1}\alpha w \partial_x \bar{c}^\varepsilon \bar{u}^\varepsilon, \bar{\psi})_{L^2(0,T;L^2(\mathcal{Q}))} = -(\partial_t u^\varepsilon, \bar{\psi})_{L^2(0,T;L^2(\mathcal{Q}))}.\end{aligned}$$

Note that the last term in the first line and the first term in the second line vanish since their velocity average is zero. In order to estimate the second term in (2.55), we distinguish between network boundary and interior vertices. For the former, we find by the reflection boundary condition (2.12) at $\mathcal{Q}_\partial^{in}$ that

$$\sum_{v\in\mathcal{V}_\partial} (ii.2)_v^\varepsilon = -\int_0^T \Big(\int_{\mathcal{Q}_\partial^{in}} \varepsilon^{-1} w u^\varepsilon(-w,t) \bar{\psi}(t) n\, dw + \int_{\mathcal{Q}_\partial^{out}} \varepsilon^{-1} w u^\varepsilon(w,t) \bar{\psi}(t) n\, dw \Big)\, dt = 0.$$

Here, we used that $\bar{\psi}$ is independent of the velocity w. At network junctions $v \in \mathcal{V}_0$, the coupling conditions (2.13)–(2.14) and the fact that $\bar{\psi}$ is continuous over the junctions yield

$$(ii.2)_v^\varepsilon = -\int_0^T \varepsilon^{-1}\bar{\psi}(v,t)\Big(\int_{Q^{in}(v)} wu^\varepsilon(v,w,t)n(v)\ dw + \int_{Q^{out}(v)} w\hat{u}_v^\varepsilon(w,t)n(v)\ dw\Big)\ dt = 0,$$

since by definition of the mixing value in (2.14) it holds that

$$\begin{aligned}
\int_{Q^{out}(v)} w\hat{u}_v^\varepsilon(|w|,t)n(v)\ dw &= -\sum\nolimits_{e\in\mathcal{E}(v)} \int_0^1 w\hat{u}_v^\varepsilon(|w|,t)\ dw \\
&= -\sum\nolimits_{e\in\mathcal{E}(v)} \int_0^1 w\frac{1}{|\mathcal{E}(v)|}\big(\sum\nolimits_{e\in\mathcal{E}^{in}(v)} u_e^\varepsilon(v,|w|,t) + \sum\nolimits_{e\in\mathcal{E}^{out}(v)} u_e^\varepsilon(v,-|w|,t)\big)\ dw \\
&= -\sum\nolimits_{e\in\mathcal{E}^{in}(v)} \int_0^1 wu_e^\varepsilon(v,w,t)\ dw + \sum\nolimits_{e\in\mathcal{E}^{out}(v)} \int_{-1}^0 wu_e^\varepsilon(v,w,t)\ dw \\
&= -\int_{Q^{in}(v)} wu^\varepsilon(v,w,t)n(v)\ dw,
\end{aligned}$$

where we used that $\sum_{e\in\mathcal{E}(v)} 1/|\mathcal{E}(v)| = 1$. From (2.55) we can then conclude that

$$(ii)^\varepsilon = -(\partial_t u^\varepsilon, \bar{\psi})_{L^2(0,T;L^2(\mathcal{Q}))} = (u^\varepsilon, \partial_t\bar{\psi})_{L^2(0,T;L^2(\mathcal{Q}))} \to (\bar{u}^0, \partial_t\bar{\psi})_{L^2(0,T;L^2(\mathcal{Q}))} \tag{2.56}$$

for $\varepsilon \to 0$, where we applied integration-by-parts in time and used (2.50). For the third term in (2.54) we exploit (2.50) and the fact that $\partial_x\bar{c}^0 \in L^2(0,T;L^2(\mathcal{Q}))$ in order to obtain

$$\begin{aligned}
(iii)^\varepsilon &= (\alpha w\partial_x\bar{c}^0\bar{u}^\varepsilon, \sigma^{-1}w\partial_x\bar{\psi})_{L^2(0,T;L^2(\mathcal{Q}))} + (\alpha w(\partial_x\bar{c}^\varepsilon - \partial_x\bar{c}^0)\bar{u}^\varepsilon, \sigma^{-1}w\partial_x\bar{\psi})_{L^2(0,T;L^2(\mathcal{Q}))} \\
&\to (\alpha\sigma^{-1}w^2\partial_x\bar{c}^0\bar{u}^0, \partial_x\bar{\psi})_{L^2(0,T;L^2(\mathcal{Q}))}
\end{aligned}$$

for $\varepsilon \to 0$, where we used that the second term vanishes since

$$\begin{aligned}
&(\alpha w(\partial_x\bar{c}^\varepsilon - \partial_x\bar{c}^0)\bar{u}^\varepsilon, \sigma^{-1}w\partial_x\bar{\psi})_{L^2(0,T;L^2(\mathcal{Q}))} \\
&\qquad \le \alpha\sigma_{min}^{-1}\|\partial_x\bar{c}^\varepsilon - \partial_x\bar{c}^0\|_{L^2(0,T;L^2(\mathcal{Q}))}\|\bar{u}^\varepsilon\|_{L^2(0,T;L^2(\mathcal{Q}))}\|\partial_x\bar{\psi}\|_{L^\infty(0,T;L^\infty(\mathcal{E}))} \to 0
\end{aligned}$$

for $\varepsilon \to 0$ which holds due to (2.53) and (a). In summary, we find that

$$(w\partial_x\bar{u}^0, \sigma^{-1}w\partial_x\bar{\psi})_{L^2(0,T;L^2(\mathcal{Q}))} = (\bar{u}^0, \partial_t\bar{\psi})_{L^2(0,T;L^2(\mathcal{Q}))} + (\alpha\sigma^{-1}w^2\partial_x\bar{c}^0\bar{u}^0, \partial_x\bar{\psi})_{L^2(0,T;L^2(\mathcal{Q}))}.$$

Since $\partial_x\bar{c}^0 \in L^\infty(0,T;L^2(\mathcal{E}))$ and $\bar{u}_0 \in L^2(0,T;H^1(\mathcal{E})) \subset L^2(0,T;L^\infty(\mathcal{E}))$, the term on the left-hand side and the second term on the right-hand side are well-defined and bounded for $\bar{\psi} \in L^2(0,T;H^1(\mathcal{E}))$, i.e., $\bar{u}^0$ has a weak time derivative $\partial_t\bar{u}^0 \in L^2(0,T;H^1(\mathcal{E})^*)$. Replacing $\bar{\psi}$ by its representative in $L^2(0,T;H^1(\mathcal{E}))$ and due to the definition of the coefficients in (2.47) we see that $(\bar{u}^0, \bar{c}^0)$ solves (2.48).

Step 2.4 ($\bar{u}^0(0) = \bar{u}_I$). From the above considerations, we know that

$$\bar{u}^0 \in L^2(0,T;H^1(\mathcal{E})) \cap H^1(0,T;H^1(\mathcal{E})^*),$$

which yields $\bar{u}^0 \in C^0([0,T];L^2(\mathcal{E}))$; see e.g. [11, Thm. II.5.12]. Consequently, evaluations at $t = 0$ are well-defined. Testing (2.48) with $\bar{\psi}_0 \in C^\infty([0,T];C^\infty(\mathcal{E}))$ so that $\partial_t^k\bar{\psi}_0(T) = 0$ for all $k \ge 0$ and applying integration-by-parts in time yields

$$\begin{aligned}
-(\bar{u}^0, \partial_t\bar{\psi}_0)_{L^2(0,T;L^2(\mathcal{E}))} &- (\bar{u}^0(0), \bar{\psi}_0(0))_{L^2(\mathcal{E})} \\
&+ (\bar{a}\partial_x\bar{u}^0 - \bar{\chi}\partial_x\bar{c}^0\bar{u}^0, \partial_x\bar{\psi}_0)_{L^2(0,T;L^2(\mathcal{E}))} = 0.
\end{aligned} \tag{2.57}$$

Let us now revisit the computations from above with test function $\bar{\psi}_0$. Starting from (2.54), we consider the terms $(i)^\varepsilon$–$(iii)^\varepsilon$ separately. For the first term, we obtain

$$\begin{aligned}(i)^\varepsilon &= -(\varepsilon\partial_t u^\varepsilon, \sigma^{-1} w\partial_x\bar{\psi}_0)_{L^2(0,T;L^2(\mathcal{Q}))}\\ &= (\varepsilon u^\varepsilon, \sigma^{-1} w\partial_{tx}\bar{\psi}_0)_{L^2(0,T;L^2(\mathcal{Q}))} + (\varepsilon\bar{u}_I, \sigma^{-1} w\partial_x\bar{\psi}_0(0))_{L^2(\mathcal{Q})}\\ &\leq \varepsilon\sigma_{min}^{-1}\|u^\varepsilon\|_{L^2(0,T;L^2(\mathcal{Q}))}\|\partial_{tx}\bar{\psi}_0\|_{L^2(0,T;L^2(\mathcal{E}))} + \varepsilon\sigma_{min}^{-1}\|\bar{u}_I\|_{L^2(\mathcal{E})}\|\partial_x\bar{\psi}_0(0)\|_{L^2(\mathcal{E})} \to 0\end{aligned}$$

for $\varepsilon \to 0$ by (a), where we used the initial condition (2.15) for u^ε. All computations for $(ii)^\varepsilon$ remain valid. Starting from (2.56) it now holds that

$$\begin{aligned}(ii)^\varepsilon = (ii.1)^\varepsilon = -(\partial_t u^\varepsilon, \bar{\psi}_0)_{L^2(0,T;L^2(\mathcal{Q}))} &= (u^\varepsilon, \partial_t\bar{\psi}_0)_{L^2(0,T;L^2(\mathcal{Q}))} + (\bar{u}_I, \bar{\psi}_0(0))_{L^2(\mathcal{E})}\\ &\to (\bar{u}^0, \partial_t\bar{\psi}_0)_{L^2(0,T;L^2(\mathcal{Q}))} + (\bar{u}_I, \bar{\psi}_0(0))_{L^2(\mathcal{E})}\end{aligned}$$

for $\varepsilon \to 0$ by (2.50) and (2.15). The computations for $(iii)^\varepsilon$ are also still valid. In summary, we obtain

$$\begin{aligned}(w\partial_x\bar{u}^0, \sigma^{-1} w\partial_x\bar{\psi}_0)_{L^2(0,T;L^2(\mathcal{Q}))} &= (\bar{u}^0, \partial_t\bar{\psi}_0)_{L^2(0,T;L^2(\mathcal{Q}))} + (\bar{u}_I, \bar{\psi}_0(0))_{L^2(\mathcal{E})}\\ &\quad + (\alpha\sigma^{-1} w^2\partial_x\bar{c}^0\bar{u}^0, \partial_x\bar{\psi}_0)_{L^2(0,T;L^2(\mathcal{Q}))},\end{aligned}$$

which is by definition of the coefficients in (2.47) equivalent to

$$-(\bar{u}^0, \partial_t\bar{\psi}_0)_{L^2(0,T;L^2(\mathcal{E}))} - (\bar{u}_I, \bar{\psi}_0(0))_{L^2(\mathcal{E})} + (\bar{a}\partial_x\bar{u}^0 - \bar{\chi}\partial_x\bar{c}^0\bar{u}^0, \partial_x\bar{\psi}_0)_{L^2(0,T;L^2(\mathcal{E}))} = 0.$$

Since $\bar{\psi}(0)$ is arbitrary, comparing with (2.57) shows that $\bar{u}^0(0) = \bar{u}_I$. This concludes the proof of Theorem 2.9. □

2.3.3. Quantitative convergence estimates

We will now establish quantitative convergence rates for $(u^\varepsilon, \bar{c}^\varepsilon) \to (\bar{u}^0, \bar{c}^0)$ under the following additional assumptions:

(A1) $\quad \sigma \in W^{1,\infty}(\mathcal{E}) \quad$ with $\quad |\sigma_e'(x)| \leq \sigma_{max}$ for all $0 \leq x \leq \ell_e,\ e \in \mathcal{E}$,

(A2) $\quad \bar{a}\partial_x\bar{u}_I - \bar{\chi}\partial_x\bar{c}_I\bar{u}_I \in H_0(\mathrm{div};\mathcal{E})$

with $H_0(\mathrm{div};\mathcal{E}) = \{\bar{c} \in H^1_{pw}(\mathcal{E}) : \sum_{e\in\mathcal{E}(v)} \bar{c}_e(v)n_e(v) = 0 \text{ for all } v \in \mathcal{V}\}$. One can then show that the weak solution to the limit problem (2.37)–(2.46) enjoys higher regularity; see [44, Theorem 3.4].

Lemma 2.10. *Let Assumption 2.2 and (A1)–(A2) hold. Then, the solution* $(\bar{u}^0, \bar{c}^0)$ *to the limit problem* (2.37)–(2.46) *from Theorem 2.8 additionally satisfies*

$$\begin{aligned}\bar{u}^0 &\in H^1(0,T;H^1(\mathcal{E})) \cap L^2(0,T;H^2_{pw}(\mathcal{E})),\\ \bar{c}^0 &\in W^{1,\infty}(0,T;H^1(\mathcal{E})) \cap L^\infty(0,T;H^2_{pw}(\mathcal{E})).\end{aligned}$$

Let us now state the second main result of this section.

Theorem 2.11. *Let Assumption 2.2 and (A1)–(A2) hold and let* $(u^\varepsilon, \bar{c}^\varepsilon)$ *be the solution to* (2.10)–(2.19) *in the sense of Theorem 2.3 satisfying the bounds (a)–(f) uniformly in* ε *up to the time point* T *and let* $(\bar{u}^0, \bar{c}^0)$ *be the corresponding solution to the limit problem* (2.37)–(2.46)*. Then,*

$$\|u^\varepsilon - \bar{u}^0\|_{L^\infty(0,T;L^2(\mathcal{Q}))} + \|\bar{c}^\varepsilon - \bar{c}^0\|_{L^\infty(0,T;H^1(\mathcal{E}))} \leq C\varepsilon^{1/2}$$

holds with a constant C *that is independent of* ε*.*

Proof. The proof follows the arguments in [43]. We make use of the asymptotic expansions

$$\begin{aligned} u^\varepsilon &= \bar{u}^0 + \varepsilon u^1 + \phi^\varepsilon \qquad \text{with} \quad u^1 := -\sigma^{-1} w \partial_x \bar{u}^0 + \alpha\sigma^{-1} w \partial_x \bar{c}^0 \bar{u}^0, \\ \bar{c}^\varepsilon &= \bar{c}^0 + \bar{\eta}^\varepsilon. \end{aligned}$$

These equations in fact define the remainder terms ϕ^ε and $\bar{\eta}^\varepsilon$. Since $\bar{u}^0$ and $\bar{c}^0$ do not depend on ε, u^1 is bounded independently of ε. By (A1) and the regularity of the limit solution, we see that $u^1 \in H^1(0,T;L^2(\mathcal{Q})) \cap L^2(0,T;H^1_{pw}(\mathcal{Q}))$. Due to the continuous embedding $H^1 \hookrightarrow C^0$ in dimension $d = 1$, pointwise evaluations in space or in time are well-defined. It remains to show that ϕ^ε and $\bar{\eta}^\varepsilon$ tend to zero as $\varepsilon \to 0$ with appropriate rates.

Step 1 (Investigation of $\bar{\eta}^\varepsilon$). Inserting the expansion of $\bar{c}^\varepsilon$ into (2.11) and using the fact that $\bar{c}^\varepsilon$ solves (2.10)–(2.19) and $\bar{c}^0$ solves (2.37)–(2.46), we find that $\bar{\eta}^\varepsilon$ is solution to

$$\begin{aligned} \partial_t \bar{\eta}^\varepsilon_e - D_e \partial_{xx} \bar{\eta}^\varepsilon_e + \delta_e \bar{\eta}^\varepsilon_e &= \gamma_e \bar{\phi}^\varepsilon_e && \text{in } (0,\ell_e) \times (0,T), \\ \partial_x \bar{\eta}^\varepsilon_e(v,t) &= 0 && \text{for } v \in \mathcal{V}_\partial,\ e \in \mathcal{E}(v),\ t \in (0,T), \\ \bar{\eta}^\varepsilon_{e_i}(v,t) &= \bar{\eta}^\varepsilon_{e_j}(v,t) && \text{for } v \in \mathcal{V}_0,\ e_i, e_j \in \mathcal{E}(v),\ t \in (0,T), \\ \sum\nolimits_{e \in \mathcal{E}(v)} D_e \partial_x \eta^\varepsilon_e(v,t) n_e(v) &= 0, && \text{for } v \in \mathcal{V}_0,\ t \in (0,T), \\ \bar{\eta}^\varepsilon(0) &= 0 && \text{on } \mathcal{E}. \end{aligned}$$

Here, we used that $\bar{u}^1 = 0$ and hence $\bar{\phi}^\varepsilon = \bar{u}^\varepsilon - \bar{u}^0$. With similar arguments as in Lemma 2.4 one can see that

$$\|\bar{\eta}^\varepsilon\|_{L^\infty(0,T;H^1(\mathcal{E}))} + \|\partial_t \bar{\eta}^\varepsilon\|_{L^2(0,T;L^2(\mathcal{E}))} + \|\partial_{xx} \bar{\eta}^\varepsilon\|_{L^2(0,T;L^2(\mathcal{E}))} \leq C\|\bar{\phi}^\varepsilon\|_{L^2(0,T;L^2(\mathcal{E}))}, \tag{2.58}$$

which can be shown by appropriate energy estimates; see [44, Lemma B.1]. By the continuous embedding $H^1 \hookrightarrow L^\infty$ in dimension $d = 1$ we further have

$$\|\partial_x \bar{\eta}^\varepsilon\|_{L^2(0,T;L^\infty(\mathcal{E}))} \leq C\|\bar{\eta}^\varepsilon\|_{L^2(0,T;H^2_{pw}(\mathcal{E}))} \leq C'\|\bar{\phi}^\varepsilon\|_{L^2(0,T;L^2(\mathcal{E}))}. \tag{2.59}$$

Note that all constants are independent of ε.

Step 2 (Investigation of ϕ^ε). Since u^ε solves (2.10) and $\bar{u}^0$ solves (2.37), we have

$$\begin{aligned} \varepsilon^2 \partial_t \phi^\varepsilon_e + \varepsilon w \partial_x \phi^\varepsilon_e + \sigma(\phi^\varepsilon_e - \bar{\phi}^\varepsilon_e) = \varepsilon \alpha_e w \partial_x \bar{c}^\varepsilon_e \bar{u}^\varepsilon_e - \varepsilon^2 \partial_t \bar{u}^0_e - \varepsilon w \partial_x \bar{u}^0_e \\ - \varepsilon^3 \partial_t u^1_e - \varepsilon^2 w \partial_x u^1_e - \varepsilon\sigma(u^1_e - \bar{u}^1_e) = f^\varepsilon_e \end{aligned}$$

with right-hand side defined by

$$f_e^\varepsilon := \varepsilon\alpha_e w(\partial_x \bar{c}_e^\varepsilon \bar{u}_e^\varepsilon - \partial_x \bar{c}_e^0 \bar{u}_e^0) - \varepsilon^2\big(\partial_x(\bar{a}_e \partial_x \bar{u}_e^0 - \bar{\chi}_e \bar{u}_e^0 \partial_x \bar{c}_e^0) + w\partial_x u_e^1\big) - \varepsilon^3 \partial_t u_e^1.$$

Here, we used the fact that $\bar{u}^1 = 0$ and $\varepsilon\sigma u^1 = -\varepsilon w \partial_x \bar{u}^0 + \varepsilon\alpha w \bar{u}^0 \partial_x \bar{c}^0$. Note that by regularity of $(u^\varepsilon, \bar{c}^\varepsilon)$ and $(\bar{u}^0, \bar{c}^0)$ it holds that $f^\varepsilon \in L^2(\mathcal{Q})$. At the network inflow boundary $(v, w) \in \mathcal{Q}_\partial^{in}$ we deduce from the reflection boundary condition (2.12) for u^ε that

$$\phi_e^\varepsilon(v, w) = u_e^\varepsilon(v, w) - \bar{u}_e^0(v) - \varepsilon u_e^1(v, w) = u_e^\varepsilon(v, -w) - \bar{u}_e^0(v) = \phi_e^\varepsilon(v, -w).$$

Here, we used that $u^1(v, w) = u^1(v, -w) = 0$ due to the boundary condition (2.39) for $(\bar{u}^0, \bar{c}^0)$ and the definition of $\bar{a}$ and $\bar{\chi}$ in (2.47). At the junctions $v \in \mathcal{V}_0$ of the network, the coupling conditions (2.13)–(2.14) and (2.41) for u^ε and $\bar{u}^0$ yield

$$\begin{aligned}\phi_e^\varepsilon(v, w) &= \hat{u}_v^\varepsilon(|w|) - \bar{u}_e^0(v) - \varepsilon u_e^1(v, w)\\ &= \frac{1}{|\mathcal{E}(v)|}\Big(\sum\nolimits_{e' \in \mathcal{E}^{in}(v)} \phi_{e'}^\varepsilon(v, |w|) + \sum\nolimits_{e' \in \mathcal{E}^{out}(v)} \phi_{e'}^\varepsilon(v, -|w|)\Big) - \varepsilon u_e^1(v, w)\end{aligned}$$

for $(e, w) \in \mathcal{Q}^{out}(v)$. We additionally used that by (2.43) and (2.47) we have

$$\begin{aligned}&\sum\nolimits_{e \in \mathcal{E}^{in}(v)} u_e^1(v, |w|) + \sum\nolimits_{e \in \mathcal{E}^{out}(v)} u_e^1(v, -|w|, t)\\ &\quad = |w| \sum\nolimits_{e \in \mathcal{E}(v)} \big(- \sigma_e^{-1}(v)\partial_x \bar{u}_e^0(v, t) + \alpha_e \sigma_e^{-1}(v) \bar{u}_e^0(v, t) \partial_x \bar{c}_e^0(v, t)\big) n_e(v) = 0.\end{aligned}$$

Consequently, the remainder ϕ^ε solves the following system: On each edge $e \in \mathcal{E}$ it holds

$$\varepsilon^2 \partial_t \phi_e^\varepsilon + \varepsilon w \partial_x \phi_e^\varepsilon + \sigma_e(\phi_e^\varepsilon - \bar{\phi}_e^\varepsilon) = f_e^\varepsilon \qquad \text{in } (0, \ell_e) \times (-1, 1) \times (0, T) \tag{2.60}$$

with inflow boundary conditions

$$\phi_e^\varepsilon(v, w, t) = \phi_e^\varepsilon(v, -w, t) \qquad \text{for } (v, w) \in \mathcal{Q}_\partial^{in},\ e \in \mathcal{E}(v),\ t \in (0, T), \tag{2.61}$$

coupling conditions at $v \in \mathcal{V}_0$

$$\phi_e^\varepsilon(v, w, t) = \hat{\phi}_v^\varepsilon(|w|, t) - \varepsilon u_e^1(v, w, t) \qquad \text{for } (e, w) \in \mathcal{Q}^{out}(v),\ t \in (0, T) \tag{2.62}$$

with mixing value

$$\hat{\phi}_v^\varepsilon(|w|, t) = \frac{1}{|\mathcal{E}(v)|}\big(\sum\nolimits_{e \in \mathcal{E}^{in}(v)} \phi_e^\varepsilon(v, |w|, t) + \sum\nolimits_{e \in \mathcal{E}^{out}(v)} \phi_e^\varepsilon(v, -|w|, t)\big), \tag{2.63}$$

and initial condition

$$\phi^\varepsilon(0) = -\varepsilon u^1(0) \qquad \text{on } \mathcal{Q}. \tag{2.64}$$

Step 3 (Energy estimates for ϕ^ε). By multiplying (2.60) with ϕ_e^ε, integrating over $(0, \ell_e) \times (-1, 1) \times (0, t)$ with $0 \le t \le T$ and summing over all edges $e \in \mathcal{E}$, we obtain

$$\begin{aligned}&\frac{\varepsilon^2}{2}\|\phi^\varepsilon(t)\|_{L^2(\mathcal{Q})}^2 - \frac{\varepsilon^2}{2}\|\phi^\varepsilon(0)\|_{L^2(\mathcal{Q})}^2 + \|\sigma^{1/2}(\phi^\varepsilon - \bar{\phi}^\varepsilon)\|_{L^2(0,t;L^2(\mathcal{Q}))}^2 \qquad (2.65)\\ &\quad = -\sum\nolimits_{v \in \mathcal{V}} \sum\nolimits_{e \in \mathcal{E}(v)} \int_0^t \int_{\mathcal{W}} \frac{\varepsilon}{2} w |\phi_e^\varepsilon(v, w, s)|^2 n_e(v)\ dw\ ds + (f^\varepsilon, \phi^\varepsilon)_{L^2(0,t;L^2(\mathcal{Q}))}\\ &\quad = (i) + (ii).\end{aligned}$$

We proceed by estimating the two terms on the right-hand side.

Estimation of (i). At the network inflow boundary $\mathcal{Q}_\partial^{in}$ condition (2.61) yields

$$-\sum\nolimits_{v\in\mathcal{V}_\partial}\int_0^t\int_{\mathcal{W}}\frac{\varepsilon}{2}w|\phi_e^\varepsilon(v,w,s)|^2 n_e(v)\ dw\ dt$$
$$=-\int_0^t\Big(\int_{\mathcal{Q}_\partial^{in}}\frac{\varepsilon}{2}w|\phi_e^\varepsilon(-w,s)|^2\,n\ dw+\int_{\mathcal{Q}_\partial^{out}}\frac{\varepsilon}{2}w|\phi_e^\varepsilon(w,s)|^2\,n\ dw\Big)\ ds=0.$$

At junctions $v\in\mathcal{V}_0$, however, by using the coupling condition (2.62) we find that

$$-\sum\nolimits_{e\in\mathcal{E}(v)}\int_0^t\int_{\mathcal{W}}\frac{\varepsilon}{2}w|\phi_e^\varepsilon(v,w,s)|^2 n_e(v)\ dw\ ds=-\int_0^t\Big(\int_{\mathcal{Q}^{in}(v)}\frac{\varepsilon}{2}w|\phi_e^\varepsilon(v,w,s)|^2 n(v)\ dw$$
$$+\int_{\mathcal{Q}^{out}(v)}\frac{\varepsilon}{2}w\big|\hat\phi_v^\varepsilon(|w|,s)-\varepsilon u_e^1(v,w,s)\big|^2 n(v)\ dw\Big)\ ds=(a)+(b)$$

The term (b) can be further split into

$$(b)=-\int_0^t\int_{\mathcal{Q}^{out}(v)}\frac{\varepsilon}{2}w\Big(|\hat\phi_v^\varepsilon(|w|,s)|^2-2\varepsilon u_e^1(v,w,s)\hat\phi_v^\varepsilon(|w|,s)+|\varepsilon u_e^1(v,w,s)|^2\Big)n(v)\ dw\ ds$$
$$=(b1)+(b2)+(b3).$$

The definition of the mixing value in (2.63) and Jensen's inequality enable us to estimate

$$(b1)=\sum\nolimits_{e\in\mathcal{E}(v)}\int_0^t\int_0^1\frac{\varepsilon}{2}w|\hat\phi_v^\varepsilon(|w|,s)|^2\ dw\ ds$$
$$\le\int_0^t\Big(\sum_{e\in\mathcal{E}^{in}(v)}\int_0^1\frac{\varepsilon}{2}w|\phi_v^\varepsilon(v,w,s)|^2\ dw+\sum_{e\in\mathcal{E}^{out}(v)}\int_0^1\frac{\varepsilon}{2}w|\phi_v^\varepsilon(v,-w,s)|^2\ dw\Big)\ ds$$
$$=\int_0^t\int_{\mathcal{Q}^{in}(v)}\frac{\varepsilon}{2}w|\phi_v^\varepsilon(v,w,s)|^2\,n(v)\ dw,$$

where we used that $\hat\phi_v^\varepsilon$ does not depend on $e\in\mathcal{E}(v)$. Consequently, $(a)+(b1)\le 0$. Since $u^1=-\sigma^{-1}w\partial_x\bar u^0+\alpha\sigma^{-1}w\bar u^0\partial_x\bar c^0$, we have

$$(b2)=\int_0^t\Big(\int_0^1\varepsilon^2w^2\hat\phi_v^\varepsilon(|w|,s)\ dw\cdot\sum\nolimits_{e\in\mathcal{E}(v)}\big(-\sigma_e^{-1}(v)\partial_x\bar u_e^0(v,s)$$
$$+\alpha_e\sigma_e^{-1}(v)\bar u_e^0(v,s)\partial_x\bar c_e^0(v,s)\big)n_e(v)\Big)\ ds=0.$$

The sum vanishes due to the coupling condition (2.43) for $(\bar u^0,\bar c^0)$ and the definition of the coefficients $\bar a$ and $\bar\chi$ in (2.47). Since u^1 is bounded independently of ε by Lemma 2.10, the remaining term can be estimated by $(b3)\le C\varepsilon^3$ with a constant C that does not depend on ε. In summary, we conclude that $(i)\le C\varepsilon^3$.

Estimation of (ii). Using the fact that $\bar f^\varepsilon=0$ since $\overline{w\partial_x u_1}=-\partial_x(\bar a\partial_x\bar u^0-\bar\chi\bar u^0\partial_x\bar c^0)$ and $\bar u_1=0$, the second term can be expanded by

$$(f^\varepsilon,\phi^\varepsilon)_{L^2(0,t;L^2(\mathcal{Q}))}=(f^\varepsilon,\phi^\varepsilon-\bar\phi^\varepsilon)_{L^2(0,t;L^2(\mathcal{Q}))}$$
$$\le\tfrac12\|\sigma^{-1/2}f^\varepsilon\|^2_{L^2(0,t;L^2(\mathcal{Q}))}+\tfrac12\|\sigma^{1/2}(\phi^\varepsilon-\bar\phi^\varepsilon)\|^2_{L^2(0,t;L^2(\mathcal{Q}))},$$

where we applied Hölder's and Young's inequality. The last term can be absorbed into the right-hand side of (2.65). Now, dividing (2.65) by ε^2, and using our findings for (i) and (ii) we obtain

$$\|\phi^\varepsilon(t)\|^2_{L^2(\mathcal{Q})} \leq \|\phi^\varepsilon(0)\|^2_{L^2(\mathcal{Q})} + C\varepsilon + \varepsilon^{-2}\|\sigma^{-1/2} f^\varepsilon\|^2_{L^2(0,t;L^2(\mathcal{Q}))}.$$

It remains to estimate the norm of f^ε for which the triangle inequality yields

$$\begin{aligned}\varepsilon^{-2}\|\sigma^{-1/2} f^\varepsilon\|^2_{L^2(0,t;L^2(\mathcal{Q}))} &\leq \|\sigma^{-1/2}\alpha w(\partial_x \bar{c}^\varepsilon \bar{u}^\varepsilon - \partial_x \bar{c}^0 \bar{u}^0)\|^2_{L^2(0,t;L^2(\mathcal{Q}))} \\ &\quad + \varepsilon^2\|\sigma^{-1/2}\partial_x(\bar{a}\partial_x \bar{u}^0 - \bar{\chi}\bar{u}^0\partial_x \bar{c}^0) + \sigma^{-1/2} w\partial_x u_1\|^2_{L^2(0,t;L^2(\mathcal{Q}))} \\ &\quad + \varepsilon^4\|\sigma^{-1/2}\partial_t u_1\|^2_{L^2(0,t;L^2(\mathcal{Q}))} \\ &= (c1) + (c2) + (c3).\end{aligned}$$

The third term can be estimated by $(c3) \leq \mathcal{O}(\varepsilon^4)$ since $\partial_t u_1$ is bounded independently of ε by construction and Lemma 2.10. Similarly, the second term can be estimated by $(c2) \leq \mathcal{O}(\varepsilon^2)$ since $\bar{u}^0$ and $\bar{c}^0$ as well as their derivatives are bounded independently of ε. It remains to investigate the first term for which we find that

$$\begin{aligned}(c1) \leq \alpha^2_{max}\sigma^{-1}_{min}\Big(&\|\partial_x \bar{c}^\varepsilon - \partial_x \bar{c}^0\|^2_{L^2(0,t;L^\infty(\mathcal{E}))}\|u^\varepsilon\|^2_{L^\infty(0,t;L^2(\mathcal{Q}))} \\ &+ \|\partial_x \bar{c}^0\|^2_{L^\infty(0,t;L^\infty(\mathcal{E}))}\|\bar{u}^\varepsilon - \bar{u}^0\|^2_{L^2(0,t;L^2(\mathcal{E}))}\Big).\end{aligned}$$

Note that $\partial_x \bar{c}^0 \in L^\infty(0,t;L^\infty(\mathcal{E}))$ due to the regularity of $\bar{c}^0$ in Lemma 2.10 and the continuous embedding $H^1 \hookrightarrow L^\infty$ in dimension $d = 1$. Moreover, $\|u^\varepsilon\|^2_{L^\infty(0,t;L^2(\mathcal{Q}))} \leq C$ by the a-priori bound (a). By the definition of the remainder $\bar{\eta}^\varepsilon$ we have

$$\|\partial_x \bar{c}^\varepsilon - \partial_x \bar{c}^0\|^2_{L^2(0,t;L^\infty(\mathcal{E}))} = \|\partial_x \bar{\eta}^\varepsilon\|^2_{L^2(0,t;L^\infty(\mathcal{E}))} \leq C\|\bar{\phi}^\varepsilon\|^2_{L^2(0,t;L^2(\mathcal{E}))} \leq C\|\phi^\varepsilon\|^2_{L^2(0,t;L^2(\mathcal{Q}))},$$

where we additionally used (2.59). Moreover, using that $\bar{\phi}^\varepsilon = \bar{u}^\varepsilon - \bar{u}^0$ due to the definition of ϕ^ε and the fact that $\bar{u}^1 = 0$, we can estimate

$$\|\bar{u}^\varepsilon - \bar{u}^0\|^2_{L^2(0,t;L^2(\mathcal{E}))} = \|\bar{\phi}^\varepsilon\|^2_{L^2(0,t;L^2(\mathcal{E}))} \leq \|\phi^\varepsilon\|^2_{L^2(0,t;L^2(\mathcal{Q}))}.$$

In summary, we thus obtain

$$\|\phi^\varepsilon(t)\|^2_{L^2(\mathcal{Q})} \leq \|\phi^\varepsilon(0)\|^2_{L^2(\mathcal{Q})} + C\varepsilon + C'\int_0^t \|\phi^\varepsilon(s)\|^2_{L^2(\mathcal{Q})}\, ds.$$

By (2.64) and the definition of u^1 we have $\|\phi^\varepsilon(0)\|^2_{L^2(\mathcal{Q})} = \|\varepsilon u^1(0)\|^2_{L^2(\mathcal{Q})} \leq C\varepsilon^2$. Note that pointwise evaluations of u^1 in time are well-defined due to the regularity of the limit solution; see Lemma 2.10. Applying Grönwall's Lemma [116, Lemma 2.7] then yields

$$\|\phi^\varepsilon(t)\|^2_{L^2(\mathcal{Q})} \leq C''\varepsilon$$

with a constant C'' that is independent of ε. From (2.58) we can then deduce that

$$\|\bar{c}^\varepsilon - \bar{c}^0\|_{L^\infty(0,T;H^1(\mathcal{E}))} = \|\bar{\eta}^\varepsilon\|_{L^\infty(0,T;H^1(\mathcal{E}))} \leq C\|\bar{\phi}^\varepsilon\|_{L^2(0,T;L^2(\mathcal{E}))} \leq C''\varepsilon^{1/2}.$$

This concludes the proof of Theorem 2.11. □

We are now at the end of our investigations for the kinetic chemotaxis on networks. Some open problems arose in the course of this chapter, which will be discussed in the following.

2.4. Discussion and outlook

Let us end this chapter with a short discussion of open problems and possible future research directions.

Existence of global solutions. In Theorem 2.3 we only proved the local existence of solutions up to a time point T that is, however, independent of ε. The proof was based on energy estimates and fixed point arguments. We expect the need for other techniques in order to verify global existence of solutions. In [44], the Keller-Segel model on networks was investigated and global solutions were derived by highly exploiting the positivity and mass conservation property that led to sharper bounds on solutions, which were crucial for the proof. In [71], the global existence of solutions for a general class of kinetic models for chemotaxis on the real line with velocity space $\mathcal{W} = \{-1, 1\}$ was proven by deriving sharper estimates via the fundamental solution to the heat equation and the Fourier transform. However, the assumptions on the tumbling kernel therein are not satisfied by our model. Let us also refer to [59, 61] where a hyperbolic-parabolic model for chemotaxis on networks was studied and global existence of solutions was derived for small initial data or positive solutions. The possible extension of these results leaves room for future research.

Optimal asymptotic convergence. In the asymptotic convergence result in Theorem 2.11 we lose a factor $\mathcal{O}(\varepsilon^{1/2})$ at the network junctions in the estimation of (i) in Step 3 of the proof. A similar phenomenon also appeared in [43], where the stationary monokinetic linear transport problem on a domain in dimension $d = 3$ with Dirichlet boundary data and its asymptotic convergence to the diffusion limit were investigated. With L^2-energy estimates, the same convergence reduction appeared at the domain boundary but could be overcome by an alternative L^∞-analysis. It seems not surprising that our analysis also leads to a convergence reduction, but it might be possible to apply similar techniques to restore the full order.

General coupling conditions. Our coupling conditions for the kinetic model (2.10)–(2.19) are a special case of the more general ones proposed in [10]. More precisely, the coupling for the chemoattractant $\bar{c}^\varepsilon$ is identical, whereas a more general mixing condition is prescribed for the bacteria density u^ε, i.e., at $v \in \mathcal{V}_0$ it is assumed that

$$u_e^\varepsilon(v, w, t) = \sum\nolimits_{e' \in \mathcal{E}^{in}(v)} \xi_{e,e'}^v u_{e'}^\varepsilon(v, |w|, t) + \sum\nolimits_{e' \in \mathcal{E}^{out}(v)} \xi_{e,e'}^v u_{e'}^\varepsilon(v, -|w|, t)$$

holds for $(e, w) \in \mathcal{Q}^{out}(v)$ and $t > 0$ with $\xi_{e,e'}^v \geq 0$ and $\sum_{e \in \mathcal{E}(v)} \xi_{e,e'}^v = 1$ ensuring the conservation of mass at junctions. Our coupling conditions correspond to the choice $\xi_{e,e'}^v = 1/|\mathcal{E}(v)|$. Similar general mixing conditions were considered in [14, 61]. The extension of our results to these more general coupling conditions could be of interest.

Numerical approximation. So far, we have not considered a proper numerical approximation of the kinetic chemotaxis model on networks. In particular, the asymptotic behavior of discrete solutions toward the diffusion limit is of interest. Galerkin methods based on P_N-like approximations could be investigated; we refer to [42] where the stationary radiative transfer equation on a domain in dimension $d = 2, 3$ was considered.

The transfer to networks where coupling conditions play a crucial role and the asymptotic behavior for $\varepsilon \to 0$ needs to be studied. In [10] the numerical approximation of a kinetic model for chemotaxis on networks via relaxation methods was considered and a suitable incorporation of the coupling at network junctions was proposed. The diffusion limit, i.e., the Keller-Segel model on networks, was investigated in [9, 44], where the numerical treatment by a finite volume and a finite element approach was considered, respectively.

Finally, the consideration of other kinetic equations (on networks) and corresponding asymptotic investigations leave room for further research; let us refer to the survey [101].

3

Gas transport in pipe networks

The modeling, simulation, and optimization of gas transport in pipe networks are of high practical and scientific interest. In the course of the energy transition, new challenges arise which make fundamental research in this field even more important. This chapter contributes to the analysis and numerical approximation of transient gas flow models and their simplifications, which then in turn can be useful for the operation and optimal control of gas networks [15, 78, 98].

Problem setting

We consider the non-isothermal Euler system with friction and heat exchange with the surroundings on a single pipe of length ℓ. The balance equations for mass, momentum, and energy are given by

$$a\partial_t \rho + \partial_x m = 0, \tag{3.1}$$

$$\partial_t m + \partial_x (a\rho v^2 + ap) = -\frac{\lambda}{2d}|m|v, \tag{3.2}$$

$$\partial_t E + \partial_x (v(E + ap)) = -\frac{\alpha a}{d}(\theta - \theta^0) - \frac{\lambda}{2d}|m|v^2, \tag{3.3}$$

see [15]. The space- and time-dependent variables of interest are the gas density ρ, the gas velocity v and mass flux $m = a\rho v$, the gas pressure p, its temperature θ, and the total energy density $E = \frac{1}{2}a\rho v^2 + a\rho e$ with e being the specific internal energy. The parameters a and d denote the cross-sectional area and diameter of the pipe, whereas λ and α are the friction and heat transfer coefficients. The ambient temperature is given by θ^0 and is assumed to be constant. To close the system, we prescribe e, p, and θ as functions of density ρ and specific entropy s via

$$e = e(\rho, s) \qquad \text{with} \qquad p = \partial_\rho e(\rho, s)\rho^2 \qquad \text{and} \qquad \theta = \partial_s e(\rho, s). \tag{3.4}$$

We refer to [17, 58] for further details on the thermodynamic modeling.

The typical situation in networks is long pipes and time scales motivating the rescaling $x \to x/\varepsilon^2$ and $t \to t/\varepsilon^2$ with a scaling parameter $\varepsilon > 0$ that is assumed to be small. After

the division by ε^2 in (3.1)–(3.3) we see that $\lambda/\varepsilon^2 \to \lambda = \mathcal{O}(1/\varepsilon^2)$ and $\alpha/\varepsilon^2 \to \alpha = \mathcal{O}(1/\varepsilon^2)$, i.e., friction and heat exchange with the ambient medium are large. Let us now introduce the following rescaled quantities

$$\tau = \varepsilon t, \qquad w = \frac{1}{\varepsilon} v, \qquad \gamma = \varepsilon^2 \frac{\lambda}{2d}, \qquad \beta = \varepsilon^2 \alpha \frac{a}{d},$$

which correspond to a long time, low Mach, as well as the large friction and heat transfer regime. This leads to the following rescaled non-isothermal gas transport model

$$a\partial_\tau \rho + \partial_x m = 0, \tag{3.5}$$

$$\varepsilon^2 \partial_\tau m + \partial_x(\varepsilon^2 a\rho w^2 + ap) = -\gamma |m| w, \tag{3.6}$$

$$\varepsilon^3 \partial_\tau E^\varepsilon + \varepsilon^3 \partial_x(w(E^\varepsilon + ap)) = -\beta(\theta - \theta^0) - \varepsilon^3 \gamma |m| w^2 \tag{3.7}$$

with rescaled total energy density $E^\varepsilon = \frac{1}{2}\varepsilon^2 a\rho w^2 + a\rho e(\rho, s)$. Details on the rescaling can be found in [15]. In the limit $\varepsilon \to 0$ the third equation (3.7) reduces to $\theta = \theta^0$, i.e., an isothermal regime. In this case, the specific entropy s can be expressed as a function of the density ρ by (3.4) and so can the internal energy e and the pressure p. The two remaining equations (3.5)–(3.6) then yield the following parabolic system

$$a\partial_\tau \rho + \partial_x m = 0, \tag{3.8}$$

$$a\partial_x p = -\gamma |m| w, \tag{3.9}$$

that is closed via the state relation $p = p(\rho)$. This model is widely used in the community to model gas transport in long pipes and pipe networks [3]. Existence results are established both on a single pipe [30, 105] and on networks [113] based on a reformulation of (3.8)–(3.9) into a single doubly degenerate parabolic equation of second-order. The uniqueness of solutions is a more delicate issue and seems to be not completely settled yet; see [113] and the discussion therein. Since ε^3 converges faster to zero than ε^2, an intermediate simplification is given by the rescaled isothermal Euler system with friction

$$a\partial_\tau \rho + \partial_x m = 0, \tag{3.10}$$

$$\varepsilon^2 \partial_\tau m + \partial_x(\varepsilon^2 a\rho w^2 + ap) = -\gamma |m| w. \tag{3.11}$$

The formal rescaling in the isothermal regime for gas pipelines and networks has also been investigated in [98]. Local existence of smooth solutions for appropriate data and constitutive relations can be guaranteed for both the non-isothermal and the isothermal model; see [95] and the references therein. An investigation for the isothermal gas transport in pipe networks is given in [62]. Due to the stabilizing effect of large friction and heat transfer, solutions in gas pipelines and networks are expected to remain smooth for all time. A rigorous justification of this observation seems to be missing up to date.

Isothermal gas transport

In the first part of this chapter, we consider the isothermal gas transport in pipe networks. We assume that (3.10)–(3.11) are satisfied on each pipe. In order to prescribe

the behavior at entries, exits, and junctions of the network, appropriate boundary and coupling conditions are required; see e.g. [35, 106]. As a basis for the analysis and numerical approximation of our model problem, we use a suitable weak characterization of solutions that turns out to have the structure of a dissipative Hamiltonian system. This particular structure allows for a simple proof of global balance laws. We refer to [92, 118] for similar structures that arise in the context of port-Hamiltonian modeling. The stability of solutions with respect to perturbations in parameters and data, in particular the asymptotic behavior of solutions for $\varepsilon \to 0$, has been studied in [37]. The key for the investigations therein was the underlying energy structure of the problem which allowed the use of so-called relative energy estimates to measure the distances between (perturbed) solutions and by that derive stability. Relative energy estimates are a well-known tool for the analysis of quasi-linear evolution problems. A summary of results concerning parabolic equations can be found in [75] and an introduction to the application for hyperbolic balance laws in [26]. An example for the investigation of asymptotic limits via relative energy estimates is given in [52], where low Mach limits of Euler and Navier-Stokes equations are considered. The parabolic limit to the isothermal Euler equations with linear damping was also studied in [74, 87, 91].

Main contributions

Let us now give an overview of the main contributions presented in this chapter. The focus lies on a suitable numerical approximation of the isothermal gas transport that preserves the underlying structure of the problem. This in turn yields the foundation for a convergence analysis. In the second part, we investigate the non-isothermal gas transport and extend some results from the isothermal case.

Structure-preserving discretization of the isothermal gas transport

The first main contribution of this chapter is the proposition and rigorous analysis of a suitable numerical method for the isothermal gas transport model (3.10)–(3.11) on pipe networks. The results have been published in

> H. Egger, J. Giesselmann, T. Kunkel, and N. Philippi. An asymptotic-preserving discretization scheme for gas transport in pipe networks. *IMA J. Numer. Anal.*, 2022.

The variational formulation of model equations allows for a structure-preserving discretization via Galerkin projection [36]. For the spatial discretization, we use a mixed finite element approach and approximate the density ρ with a piecewise constant function ρ_h and the mass flux m with a piecewise linear function m_h. The method is then complemented by the implicit Euler time-stepping leading to a fully discrete scheme that resembles the standard approximation for related wave propagation problems [57, 73]. A closely related scheme for isothermal flow problems on networks has been proposed in [35, 36]; also see [18, 90] for similar approaches. Our method is formally asymptotic preserving, i.e., by

setting $\varepsilon = 0$ we obtain a viable approximation of the parabolic limit problem (3.8)–(3.9) on networks. A rigorous convergence analysis leads to the following error estimate

$$\|\rho(\tau^n) - \rho_h^n\|_{L^2}^2 + \varepsilon^2 \|m(\tau^n) - m_h^n\|_{L^2}^2 + \sum_{k=1}^{n} \Delta\tau \|m(\tau^k) - m_h^k\|_{L^3}^3 \leq C(h^2 + \Delta\tau^2) \quad (3.12)$$

with h and $\Delta\tau$ being the spatial and temporal mesh size, respectively, and ρ_h^n, m_h^n the discrete solutions at the time point τ^n. This result holds under the assumption of subsonic flow and sufficiently smooth solutions, which are in particular bounded away from the vacuum. Moreover, no shocks or discontinuities are allowed, which is reasonable for gas flow in pipe networks where typical flow velocities are around $10 - 20\, m/s$ [98]. Let us stress that the error estimate (3.12) holds uniformly for all $\varepsilon \geq 0$ sufficiently small, in particular also for the limit $\varepsilon = 0$. The key for the proof is the preserved energy structure of the method that allows us to derive discrete stability of the scheme via relative energy estimates, where we closely follow the continuous stability analysis derived in [37]. Relative energy techniques have been successfully used for the analysis of numerical schemes in the literature, we refer to [50, 54, 84] and [7] for the application to the compressible Navier-Stokes equations and to the Euler equations in the large friction limit, respectively. Numerical tests demonstrate the validity of the error estimate (3.12).

Extension to the non-isothermal gas transport

The second part of this chapter is dedicated to the extension of some ideas and results for the isothermal gas transport in pipe networks to the non-isothermal regime. The content is first presented in this thesis. On each pipe, we assume that (3.5)–(3.7) hold and complement the equations by suitable boundary conditions at the network boundary and coupling conditions at interior junctions that ensure basic physical principles, i.e., conservation of mass, no energy production, and no entropy dissipation. The choice of the correct set of coupling conditions, however, seems to be not fully settled. We refer to [22, 23, 65, 86] for different proposals and corresponding investigations. The system (3.5)–(3.7) can be reformulated and a corresponding variational characterization of smooth solutions turns out to have a similar "energy structure" as the isothermal model, which allows for a simple proof of global balance laws. A rigorous stability and asymptotic analysis, however, is not yet available and left for future research.

We then focus on a suitable numerical approximation. We propose a structure-preserving discretization via a Galerkin method based on the variational formulation, which extends the mixed finite element scheme for the isothermal gas transport. For the approximation of the additional entropy transport we use a hybrid discontinuous Galerkin approach that is particularly well-suited for handling coupling conditions at network junctions; see Chapter 1 and [39]. By setting $\varepsilon = 0$ we obtain a viable scheme for the parabolic limit problem. Moreover, discrete global balance laws are valid and the method can be shown to dissipate energy under the assumption of subsonic flow bounded away from vacuum. Numerical tests on a simple network are presented for illustration. An error analysis in the spirit of the isothermal gas approximation might be possible but remains to be investigated. Our

approach is not standard for the numerical approximation of inviscid compressible flow problems, which has been studied intensively in the literature. Finite volume methods are most commonly used and a rather complete theory has been developed for scalar conservation laws. Only partial results are however available for systems; we refer to [81, 88] and the references therein. A higher-order generalization of finite volume schemes is provided by discontinuous Galerkin methods [31]. For the approximation of gas flow in pipe networks, finite volume methods based on local Riemann solvers are a common approach. We refer to [93] for the application to the isothermal Euler system. The extension to the non-isothermal regime, however, seems not fully settled; some approaches in this direction can be found in [13, 65].

Outline

In Section 3.1 we introduce the isothermal gas transport model on pipe networks and investigate its basic properties. Moreover, we revisit some results from [37] and present the main assumptions that will be made throughout the first part of this chapter. Section 3.2 is dedicated to the numerical approximation of the isothermal gas transport. The main result is the rigorous error estimate (3.12) of our proposed mixed finite element method. We then focus on the extension of ideas and results to the non-isothermal gas transport. The model problem on pipe networks and its basic properties are presented in Section 3.3, whereas a suitable structure-preserving discretization is proposed in Section 3.4 and the proof of discrete global balance laws is given therein. We conclude this chapter with some numerical tests illustrating our theoretical findings, which are presented in Section 3.5.

3.1. Isothermal gas transport

In this section, we consider the isothermal gas transport in pipe networks. We present the model problem and introduce suitable coupling conditions at network junctions. Then, basic properties as well as the asymptotic behavior of solutions are investigated under suitable assumptions that are reasonable for gas flow in pipe networks.

3.1.1. Preliminaries

Let us first introduce the notation which will be used throughout this chapter and present a transformation of the model equations.

Notation and function spaces

Following the notation from previous publications [39] and Chapter 1.1.1, we represent the gas network by a finite, directed, and connected graph $\mathcal{G} = (\mathcal{V}, \mathcal{E})$ with vertices $\mathcal{V} = \{v_1, \dots, v_m\}$ and edges or pipes $\mathcal{E} = \{e_1, \dots, e_l\} \subset \mathcal{V} \times \mathcal{V}$. We allow for a rather

general topology that, in particular, can include cycles. Every pipe is identified by an interval $(0, \ell_e)$ with ℓ_e depicting its length. For each vertex $v \in \mathcal{V}$ we collect all incident edges in the set $\mathcal{E}(v) = \{e \in \mathcal{E} : e = (v, \cdot) \text{ or } e = (\cdot, v)\}$. Moreover, the set of vertices is split into the sets of boundary vertices $\mathcal{V}_\partial = \{v \in \mathcal{V} : |\mathcal{E}(v)| = 1\}$ and interior vertices $\mathcal{V}_0 = \mathcal{V} \backslash \mathcal{V}_\partial$ with $|\mathcal{E}(v)|$ denoting the cardinality of $\mathcal{E}(v)$. To each edge $e = (v_i, v_j)$ we associate two numbers $n_e(v_i) = -1$ and $n_e(v_j) = 1$ to indicate its start and end vertex, and we set $n_e(v) = 0$ for all $v \in \mathcal{V} \backslash \{v_i, v_j\}$. An illustration of a network is given in Figure 3.1. Let us further introduce the space of square-integrable functions on the network

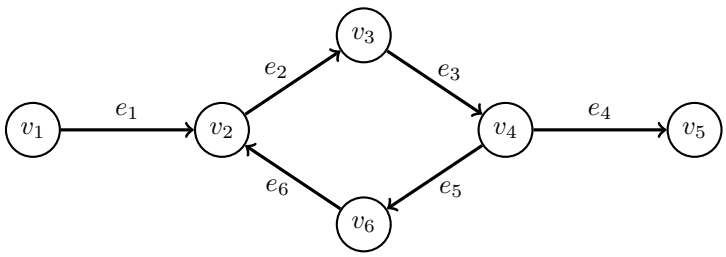

Figure 3.1.: A network with edges $e_1 = (v_1, v_2)$, $e_2 = (v_2, v_3)$, $e_3 = (v_3, v_4)$, $e_4 = (v_4, v_5)$, $e_5 = (v_4, v_6)$, and $e_6 = (v_6, v_2)$, boundary vertices $\mathcal{V}_\partial = \{v_1, v_5\}$, and interior vertices $\mathcal{V}_0 = \{v_2, v_3, v_4, v_6\}$. The set $\mathcal{E}(v_2) = \{e_1, e_2, e_6\}$ contains all incident edges to the vertex v_2.

by $L^2(\mathcal{E}) = \{u : u_e \in L^2(0, \ell_e) \text{ for all } e \in \mathcal{E}\}$ with $u_e = u|_e$. The corresponding scalar product and norm are given by

$$(u, w)_{L^2(\mathcal{E})} = \sum\nolimits_{e \in \mathcal{E}} (u, w)_{L^2(0,\ell_e)} \qquad \text{and} \qquad \|u\|^2_{L^2(\mathcal{E})} = (u, u)_{L^2(\mathcal{E})},$$

and we will make use of the short-hand notation $(u, w)_{\mathcal{E}} = (u, w)_{L^2(\mathcal{E})}$. Other L^p spaces on networks can be defined in the same way. Occasionally, we abbreviate

$$\int_{\mathcal{E}} u(x)\, dx = \sum\nolimits_{e \in \mathcal{E}} \int_0^{\ell_e} u_e(x)\, dx.$$

Similarly, we define by $H^k_{pw}(\mathcal{E}) = \{u : u_e \in H^k(0, \ell_e) \text{ for all } e \in \mathcal{E}\}$ the broken Sobolev spaces on the network with associated scalar products and norms

$$(u, w)_{H^k_{pw}(\mathcal{E})} = \sum\nolimits_{e \in \mathcal{E}} (u, w)_{H^k_{pw}(0,\ell_e)}, \qquad \|u\|^2_{H^k_{pw}(\mathcal{E})} = (u, u)_{H^k_{pw}(\mathcal{E})}.$$

By standard embedding theory for fractional Sobolev spaces [28], functions in $H^k_{pw}(\mathcal{E})$ are continuous along edges for $k > 1/2$ but may be discontinuous at network junctions. We thus denote by $H^1(\mathcal{E})$ the corresponding space of functions in $H^1_{pw}(\mathcal{E})$ that are additionally continuous across junctions. Each $u \in H^1(\mathcal{E})$ then takes a unique value $u(v)$ at $v \in \mathcal{V}$ which belongs to the space $\ell_2(\mathcal{V})$ of possible vertex values.

Transformation of model equations

In the following, we transform the rescaled isothermal gas transport model (3.10)–(3.11) into a system having the structure of a dissipative Hamiltonian system. By the chain rule

of differentiation, it holds that

$$\begin{aligned}\varepsilon^2\partial_\tau w = \varepsilon^2\partial_\tau\Big(\frac{m}{a\rho}\Big) &= \frac{\varepsilon^2}{a\rho}\partial_\tau m - \frac{\varepsilon^2}{a\rho^2}m\partial_\tau\rho \\ &= -\frac{1}{a\rho}\Big(\partial_x\big(\varepsilon^2 a\rho w^2 + ap(\rho)\big) + \gamma|m|w\Big) + \frac{\varepsilon^2}{a^2\rho^2}m\partial_x m \\ &= -\frac{\varepsilon^2}{a\rho}\partial_x(wm) + \frac{\varepsilon^2}{a\rho}w\partial_x m - \frac{1}{\rho}\partial_x p(\rho) - \gamma|w|w \\ &= -\frac{\varepsilon^2}{2}\partial_x w^2 - \frac{1}{\rho}\partial_x p(\rho) - \gamma|w|w,\end{aligned}$$

where we used (3.10)–(3.11) and the fact that $\partial_x(wm) = w\partial_x m + \partial_x wm$, as well as $w\partial_x w = \frac{1}{2}\partial_x w^2$. We further introduce the pressure potential

$$P : \mathbb{R}_+ \to \mathbb{R}, \qquad P(\rho) := \rho\int_1^\rho \frac{p(r)}{r^2}\,dr,$$

for which we find that

$$\partial_x P'(\rho) = \partial_x\Big(\int_1^\rho \frac{p(r)}{r^2}\,dr + \frac{p(\rho)}{\rho}\Big) = \frac{p(\rho)}{\rho^2}\partial_x\rho + \frac{\partial_x p(\rho)}{\rho} - \frac{p(\rho)}{\rho^2}\partial_x\rho = \frac{\partial_x p(\rho)}{\rho}.$$

We can then replace (3.11) by

$$\varepsilon^2\partial_\tau w + \partial_x\big(\frac{\varepsilon^2}{2}w^2 + P'(\rho)\big) = -\gamma|w|w.$$

By introducing a new variable $h = h^\varepsilon := \frac{\varepsilon^2}{2}w^2 + P'(\rho)$ being the total specific enthalpy of the system, we finally obtain the following reformulated equations

$$a\partial_\tau\rho + \partial_x m = 0, \tag{3.13}$$

$$\varepsilon^2\partial_\tau w + \partial_x h^\varepsilon = -\gamma|w|w. \tag{3.14}$$

For solutions that are sufficiently regular, both systems (3.10)–(3.11) and (3.13)–(3.14) are equivalent.

3.1.2. Model problem

We assume that (3.13)–(3.14) hold on each pipe $e \in \mathcal{E}$ of the network, i.e.,

$$a_e\partial_\tau\rho_e + \partial_x m_e = 0, \tag{3.15}$$

$$\varepsilon^2\partial_\tau w_e + \partial_x h_e^\varepsilon = -\gamma_e|w_e|w_e \tag{3.16}$$

for $0 < x < \ell_e,\ e \in \mathcal{E}$, and $\tau > 0$ with

$$m_e = a_e\rho_e w_e \qquad \text{and} \qquad h_e^\varepsilon = \frac{\varepsilon^2}{2}w_e^2 + P'(\rho_e). \tag{3.17}$$

At the boundary vertices, we prescribe Dirichlet data for the total specific enthalpy, i.e.,

$$h_e^\varepsilon(v,\tau) = \hat{h}_\partial^v(\tau), \qquad v \in \mathcal{V}_\partial,\ e \in \mathcal{E}(v),\ \tau > 0. \tag{3.18}$$

In order to couple the solutions across the network junctions, we require that

$$\sum\nolimits_{e\in\mathcal{E}(v)} m_e(v,\tau)n_e(v) = 0, \qquad v\in\mathcal{V}_0,\ \tau>0, \tag{3.19}$$

$$h_e^\varepsilon(v,\tau) = \hat{h}_v^\varepsilon(\tau), \qquad v\in\mathcal{V}_0,\ e\in\mathcal{E}(v),\ \tau>0. \tag{3.20}$$

An additional degree of freedom $\hat{h}_v^\varepsilon$ has been introduced at all junctions $v\in\mathcal{V}_0$ in order to enforce continuity of the total specific enthalpy h^ε. The coupling conditions (3.19)–(3.20) ensure the conservation of mass and energy at interior vertices. A pair of functions

$$\rho,\, w \in C^1([0,\tau_{max}]; L^2(\mathcal{E})) \cap C^0([0,\tau_{max}]; H^1_{pw}(\mathcal{E}))$$

is called a *classical solution* of (3.15)–(3.20) up to time $\tau_{max}>0$ if the above equations are satisfied in a pointwise sense. Note that the mass flux $m(\tau)$ lies in the space

$$H(\mathrm{div};\mathcal{E}) = \{r\in H^1_{pw}(\mathcal{E}) : \sum\nolimits_{e\in\mathcal{E}(v)} r_e(v)n_e(v) = 0 \ \ \forall\, v\in\mathcal{V}_0\} \tag{3.21}$$

of functions in $H^1_{pw}(\mathcal{E})$ that are additionally conserved at network junctions for all $\tau>0$.

3.1.3. Weak formulation

The analysis and numerical approximation of the model problem (3.15)–(3.20) is based on the following weak characterization of solutions.

Lemma 3.1. *Let (ρ,w) be a classical solution to* (3.15)–(3.20)*. Then,*

$$(a\partial_\tau\rho(\tau),q)_{\mathcal{E}} + (\partial_x m(\tau),q)_{\mathcal{E}} = 0, \tag{3.22}$$

$$(\varepsilon^2\partial_\tau w(\tau),r)_{\mathcal{E}} - (h^\varepsilon(\tau),\partial_x r)_{\mathcal{E}} + (\gamma|w(\tau)|w(\tau),r)_{\mathcal{E}} = -\sum\nolimits_{v\in\mathcal{V}_\partial} \hat{h}^v_\partial(\tau)r_e(v)n_e(v) \tag{3.23}$$

holds for all $q\in L^2(\mathcal{E}),\ r\in H(\mathrm{div};\mathcal{E})$ and $\tau>0$.

Proof. Multiplying (3.15)–(3.16) with suitable test functions $q\in L^2(\mathcal{E})$ and $r\in H(\mathrm{div};\mathcal{E})$, integrating over each edge $e\in\mathcal{E}$, and summing up immediately yields the first equation (3.22). In order to verify the second equation (3.23), we additionally apply integration-by-parts to the second term, i.e.,

$$(\partial_x h^\varepsilon, r)_{\mathcal{E}} = -(h^\varepsilon,\partial_x r)_{\mathcal{E}} + \sum\nolimits_{v\in\mathcal{V}}\sum\nolimits_{e\in\mathcal{E}(v)} h_e^\varepsilon(v)r_e(v)n_e(v).$$

The contributions at interior vertices $v\in\mathcal{V}_0$ vanish due to the continuity condition (3.20) for h^ε and the fact that $r\in H(\mathrm{div};\mathcal{E})$. □

Note that the coupling condition (3.19) for the mass flux is strongly enforced in the space $H(\mathrm{div};\mathcal{E})$, whereas the coupling condition (3.20) for the total specific enthalpy is weakly imposed in the variational formulation (3.22)–(3.23) via integration-by-parts.

3.1.4. Basic properties

The associated physical energy of the system (3.15)–(3.20) is given by the functional

$$\mathcal{H}^\varepsilon(\rho, w) := \sum\nolimits_{e\in\mathcal{E}} \int_0^{\ell_e} a_e\Big(\frac{\varepsilon^2}{2}\rho_e(x)w_e^2(x) + P(\rho_e(x))\Big)\, dx. \tag{3.24}$$

The *state variables* (ρ, w) and *co-state variables* (h^ε, m), also called *energy* and *co-energy variables*, are linked via the variational derivatives of the energy functional, i.e.,

$$\delta_\rho \mathcal{H}^\varepsilon(\rho, w) = ah^\varepsilon \qquad \text{and} \qquad \delta_w \mathcal{H}^\varepsilon(\rho, w) = \varepsilon^2 m. \tag{3.25}$$

This reveals the underlying "energy structure" of the system (3.22)–(3.23), which can also be written in the following abstract form

$$\mathcal{C}^\varepsilon \partial_\tau u + (\mathcal{J} + \mathcal{R}(u))\boldsymbol{z}^\varepsilon(u) = \boldsymbol{b}_\partial, \tag{3.26}$$

$$\boldsymbol{z}^\varepsilon(u) = (\mathcal{C}^\varepsilon)^{-1}(\mathcal{H}^\varepsilon)'(u) \tag{3.27}$$

with *state variables* $u = (\rho, w)$, *co-state variables* $\boldsymbol{z}^\varepsilon(u) = (h^\varepsilon, m)$, and operators

$$\langle \mathcal{C}^\varepsilon u, v\rangle := (a\rho, q)_\mathcal{E} + (\varepsilon^2 w, r)_\mathcal{E}, \qquad \langle \mathcal{J}\boldsymbol{z}^\varepsilon(u), v\rangle := (\partial_x m, q)_\mathcal{E} - (h^\varepsilon, \partial_x q)_\mathcal{E},$$

$$\langle \mathcal{R}(u)\boldsymbol{z}^\varepsilon(u), v\rangle := (\gamma|w|w, r)_\mathcal{E}, \qquad \langle \boldsymbol{b}_\partial, v\rangle := -\sum\nolimits_{v\in\mathcal{V}_\partial} \hat{h}_\partial^v r_e(v) n_e(v).$$

Here, $v = (q, r)$ is a time-independent test function and $\langle\cdot,\cdot\rangle$ denotes the duality bracket for the corresponding function spaces. The operator $\mathcal{C}^\varepsilon$ is positive definite, $\mathcal{J}$ is skew-symmetric, and $\mathcal{R}(u)$ is positive semi-definite. This structure turns out to be essential for our analysis and can be preserved under Galerkin projection. Moreover, it allows for a simple proof of the following global balance laws.

Lemma 3.2. *Any classical solution* (ρ, w) *to* (3.15)–(3.20) *satisfies*

$$\frac{d}{d\tau}\int_\mathcal{E} a\rho(x,\tau)\, dx = -\sum\nolimits_{v\in\mathcal{V}_\partial} m_e(v,\tau) n_e(v), \tag{3.28}$$

$$\frac{d}{d\tau}\mathcal{H}^\varepsilon(\rho(\tau), w(\tau)) + \mathcal{D}(\rho(\tau), w(\tau)) = -\sum\nolimits_{v\in\mathcal{V}_\partial} \hat{h}_\partial^v(\tau)\, m_e(v,\tau) n_e(v) \tag{3.29}$$

with dissipation functional

$$\mathcal{D}(\rho, w) := \int_\mathcal{E} a\gamma\rho(x)|w(x)|^3\, dx. \tag{3.30}$$

Consequently, mass is conserved up to flux over the network boundary and a change in total energy is only caused by friction at pipe walls and flux over the boundary.

Proof. The mass balance (3.28) immediately follows by testing (3.22) with $q = 1$. The contributions at interior vertices then vanish since $m \in H(\mathrm{div}; \mathcal{E})$. By formal differentiation of the energy functional and exploiting the identities (3.25), we find that

$$\begin{aligned}\frac{d}{d\tau}\mathcal{H}^\varepsilon(\rho, w) &= (\delta_\rho \mathcal{H}^\varepsilon, \partial_\tau \rho)_\mathcal{E} + (\delta_w \mathcal{H}^\varepsilon, \partial_\tau w)_\mathcal{E} = (ah^\varepsilon, \partial_\tau\rho)_\mathcal{E} + (\varepsilon^2 m, \partial_\tau w)_\mathcal{E} \\ &= (h^\varepsilon, \partial_x m)_\mathcal{E} - (\gamma|w|w, m)_\mathcal{E} - \sum\nolimits_{v\in\mathcal{V}_\partial} \hat{h}_\partial^v r_e(v) n_e(v) - (\partial_x m, h^\varepsilon)_\mathcal{E},\end{aligned}$$

where we used (3.22)–(3.23) in the third identity. The first and the last term on the right-hand side cancel. This yields the energy identity (3.29). □

3.1.5. Main assumptions

For the analysis of the isothermal gas transport, we make the following assumptions.

(A1) The pressure potential $P : \mathbb{R}_+ \to \mathbb{R}$ is smooth and strongly convex with

$$P''(\rho) \geq c_P, \tag{3.31}$$

which holds for all relevant densities $\underline{\rho} \leq \rho \leq \bar{\rho}$ for constants $\bar{\rho}$, $\underline{\rho} > 0$.

(A2) The parameters a and γ are edgewise constant and bounded by $0 < \underline{a} \leq a_e \leq \bar{a}$ and $0 < \underline{\gamma} \leq \gamma_e \leq \bar{\gamma}$ for all $e \in \mathcal{E}$. Moreover, ε is constant and bounded by $0 \leq \varepsilon \leq \bar{\varepsilon}$. It further holds that

$$\rho P''(\rho) \geq 4\bar{\varepsilon}^2 |w|^2 \tag{3.32}$$

for all $\underline{\rho} \leq \rho \leq \bar{\rho}$ and $|w| \leq 3\bar{w}/2$.

(A3) For all $0 \leq \varepsilon \leq \bar{\varepsilon}$ there exists a classical solution (ρ, w) of (3.15)–(3.20) that satisfies

$$0 < \underline{\rho} \leq \rho_e(x,\tau) \leq \bar{\rho} \quad \text{and} \quad |w_e(x,\tau)| \leq \bar{w}$$

for all $0 \leq x \leq \ell_e,\ e \in \mathcal{E}$ and $0 \leq \tau \leq \tau_{max}$. We call such solutions *subsonic bounded state solutions.*

In order to obtain quantitative convergence rates, we additionally assume higher regularity of the solution in the analysis of the numerical scheme in Section 3.2.

(A4) The solutions in (A3) are bounded independently of ε in $W^{2,\infty}(0, \tau_{max}; L^2(\mathcal{E}))^2$ and $W^{1,\infty}(0, \tau_{max}; H^1(\mathcal{E}))^2$.

Remark 3.3. Assumption (A1) implies strict monotonicity of the pressure function $p(\rho)$ since $P''(\rho) = p'(\rho)/\rho$, which is a natural thermodynamic requirement and guarantees that the isothermal Euler equations are a hyperbolic system [26, Ch. 4.8]. The speed of sound is defined as $c(\rho) = \sqrt{p'(\rho)} = \sqrt{\rho P''(\rho)}$; see [58, Ch.III.1]. Hence, the assumptions (A2) and (A3) ensure that the flow is subsonic. Note that (3.32) is automatically satisfied for $\bar{\varepsilon} \leq \frac{1}{3\bar{w}}\sqrt{\underline{\rho} c_P}$. Moreover, the densities are bounded away from the vacuum. In this case, exactly one boundary condition at each end of every pipe is needed; see [123]. Consequently, (3.18)–(3.20) give the correct number of boundary and coupling conditions. Under standard operating conditions in a gas network, solutions are assumed to be sufficiently smooth. Moreover, the scaling suggests that solutions are close to the parabolic model for which solutions exist under suitable assumptions on parameters and data; we refer to [113]. Assumptions (A3)–(A4) can thus be considered reasonable.

3.1.6. Relative energy

Under the assumptions (A1)–(A2), the energy functional $\mathcal{H}^\varepsilon$ defined in (3.24) is uniformly convex with respect to an ε-weighted L^2-norm, which will be shown in Lemma 3.4 below.

This important property allows us to use the concept of relative energy in order to measure the distance between exact and perturbed solutions to (3.15)–(3.20). Let $u = (\rho, w)$ and $\hat{u} = (\hat{\rho}, \hat{w})$ be two pairs of functions. The relative energy is then defined as

$$\mathcal{H}^\varepsilon(u|\hat{u}) := \mathcal{H}^\varepsilon(u) - \mathcal{H}^\varepsilon(\hat{u}) - \langle (\mathcal{H}^\varepsilon)'(\hat{u}), u - \hat{u}\rangle \tag{3.33}$$

and equals the second-order remainder of the Taylor expansion of $\mathcal{H}^\varepsilon$. Before we collect important properties, we introduce the following ε-weighted norms

$$\|u\|_\varepsilon^2 := \|\rho\|_{L^2(\mathcal{E})}^2 + \varepsilon^2 \|w\|_{L^2(\mathcal{E})}^2 \qquad \text{and} \qquad \|u\|_{\varepsilon,\infty} := \|\rho\|_{L^\infty(\mathcal{E})} + \varepsilon \|w\|_{L^\infty(\mathcal{E})} \tag{3.34}$$

that will be used throughout this chapter.

Lemma 3.4. *Let assumptions (A1)–(A2) hold. Then, the energy functional $\mathcal{H}^\varepsilon$ defined in* (3.24) *is well-defined, smooth and uniformly convex on the* set of admissible states

$$\mathcal{AS} := \{(\rho, w) \in L^\infty(\mathcal{E})^2 : \underline{\rho} \le \rho \le \bar{\rho},\ |w| \le 3\bar{w}/2\}$$

with respect to the ε-weighted L^2-norm defined in (3.34)*. It further holds that*

$$c_{rel}\|u - \hat{u}\|_\varepsilon^2 \le \mathcal{H}^\varepsilon(u|\hat{u}) \le C_{rel}\|u - \hat{u}\|_\varepsilon^2 \qquad \text{for all } u, \hat{u} \in \mathcal{AS}, \tag{3.35}$$

i.e., the relative energy is positive and introduces a distance measure that is equivalent to $\|\cdot\|_\varepsilon^2$. Moreover, for all $x \in L^\infty(\mathcal{E})^2,\ y \in L^2(\mathcal{E})^2$ it holds that

$$\big\langle ((\mathcal{H}^\varepsilon)''(u) - (\mathcal{H}^\varepsilon)''(\hat{u}))x, y\big\rangle \le C\|u - \hat{u}\|_\varepsilon \|x\|_{\varepsilon,\infty}\|y\|_\varepsilon. \tag{3.36}$$

The constants c_{rel}, C_{rel}, C only depend on the bounds in the assumptions (A1)–(A2).

Proof. Let us first prove that $\mathcal{H}^\varepsilon$ is uniformly convex and that the lower bound in (3.35) holds. In order to show the latter, we define $F(s) := \mathcal{H}^\varepsilon(su + (1-s)\hat{u})$ for $0 \le s \le 1$. By Taylor's theorem and the chain rule, we find that

$$\mathcal{H}^\varepsilon(u|\hat{u}) = F(1) - F(0) - F'(0) = \tfrac{1}{2}F''(s^*) = \tfrac{1}{2}\langle (\mathcal{H}^\varepsilon)''(u^*)(u - \hat{u}), (u - \hat{u})\rangle \tag{3.37}$$

holds for some $0 < s^* < 1$ and $u^* := s^* u + (1 - s^*)\hat{u}$, which lies in the set $\mathcal{AS}$ due to its convexity. An closer investigation of $(\mathcal{H}^\varepsilon)''$ reveals that

$$(\mathcal{H}^\varepsilon)''(u) = \begin{pmatrix} \delta_{\rho\rho}\mathcal{H}^\varepsilon & \delta_{\rho w}\mathcal{H}^\varepsilon \\ \delta_{w\rho}\mathcal{H}^\varepsilon & \delta_{ww}\mathcal{H}^\varepsilon \end{pmatrix} = \begin{pmatrix} aP''(\rho) & a\varepsilon^2 w \\ a\varepsilon^2 w & a\varepsilon^2 \rho \end{pmatrix}. \tag{3.38}$$

Using this, Young's inequality, and the assumptions (A1)–(A2), we can estimate

$$\begin{aligned}
(u - \hat{u})^\top (\mathcal{H}^\varepsilon)''(u^*)(u - \hat{u}) &= aP''(\rho^*)(\rho - \hat{\rho})^2 + 2a\varepsilon^2 w^*(\rho - \hat{\rho})(w - \hat{w}) + a\varepsilon^2\rho^*(w - \hat{w})^2 \\
&\ge aP''(\rho^*)(\rho - \hat{\rho})^2 - \nu a\varepsilon^2 \tfrac{|w^*|^2}{\rho^*}(\rho - \hat{\rho})^2 - \tfrac{1}{\nu}a\varepsilon^2\rho^*(w - \hat{w}) + a\varepsilon^2\rho^*(w - \hat{w})^2 \\
&\ge (1 - \tfrac{\nu}{4})aP''(\rho^*)(\rho - \hat{\rho})^2 + (1 - \tfrac{1}{\nu})a\varepsilon^2\rho^*(w - \hat{w})^2 \\
&\ge (1 - \tfrac{\nu}{4})\underline{a}c_P(\rho - \hat{\rho})^2 + (1 - \tfrac{1}{\nu})\underline{a}\varepsilon^2\underline{\rho}(w - \hat{w})^2.
\end{aligned}$$

By integrating over all edges $e \in \mathcal{E}$ and choosing $\nu = 2$ we obtain the uniform convexity of $\mathcal{H}^\varepsilon$ with respect to $\|\cdot\|_\varepsilon$ as well as the lower bound in (3.35) with $c_{rel} = \min(\underline{a}c_P/2, \underline{a}\underline{\rho}/2)$. The upper bound in (3.35) readily follows from (3.37)–(3.38) using the fact that P is smooth, the bounds in $\mathcal{AS}$, and Hölder's and Young's inequality. It remains to prove the second assertion (3.36). It holds that

$$\begin{aligned}\langle(\mathcal{H}^\varepsilon)''(u) - (\mathcal{H}^\varepsilon)''(\hat{u}))x, y\rangle &= (a(P''(\rho) - P''(\hat{\rho}))x_1, y_1)_{\mathcal{E}} + (a\varepsilon^2(w - \hat{w})x_1, y_2)_{\mathcal{E}} \\ &\quad + (a\varepsilon^2(w - \hat{w})x_2, y_1)_{\mathcal{E}} + (a\varepsilon^2(\rho - \hat{\rho})x_2, y_2)_{\mathcal{E}} \\ &\leq C\bar{a}\|\rho - \hat{\rho}\|_{L^2(\mathcal{E})}\|x_1\|_{L^\infty(\mathcal{E})}\|y_1\|_{L^2(\mathcal{E})} + \bar{a}\|\varepsilon(w - \hat{w})\|_{L^2(\mathcal{E})}\|x_1\|_{L^\infty(\mathcal{E})}\|\varepsilon y_2\|_{L^2(\mathcal{E})} \\ &\quad + \bar{a}\|\varepsilon(w - \hat{w})\|_{L^2(\mathcal{E})}\|\varepsilon x_2\|_{L^\infty(\mathcal{E})}\|y_1\|_{L^2(\mathcal{E})} + \bar{a}\|\rho - \hat{\rho}\|_{L^2(\mathcal{E})}\|\varepsilon x_2\|_{L^\infty(\mathcal{E})}\|\varepsilon y_2\|_{L^2(\mathcal{E})},\end{aligned}$$

where we used that P is smooth and its derivatives are bounded on $\mathcal{AS}$. By the definition of the ε-weighted norms, we can conclude (3.36). □

3.1.7. Asymptotic analysis

For completeness and later reference, let us recall the main result of [37], where the general stability of solutions to (3.15)–(3.20) with respect to perturbations in model parameters and initial and boundary data was studied. We present the asymptotic estimate, which is a special case of the more general stability estimate given in [37, Thm. 18], and provide a brief sketch of the proof since similar techniques will later be used for the convergence analysis of the proposed numerical method in Section 3.2.

Theorem 3.5. *Let (A1)–(A3) hold and let $(\rho^\varepsilon, w^\varepsilon)$ and (ρ^0, w^0) be classical solutions to (3.15)–(3.20) for $\varepsilon > 0$ and $\varepsilon = 0$, respectively, having the same boundary data h_∂ and initial data $\rho^\varepsilon(0) = \rho^0(0)$ and $w^\varepsilon(0) = w^0(0)$. Moreover, let (ρ^0, w^0) be bounded in $W^{1,\infty}(0, \tau_{max}; L^\infty(\mathcal{E}))^2$ and let additionally w^0 be bounded in $L^\infty(0, \tau_{max}; H^1_{pw}(\mathcal{E}))$. Then,*

$$\|\rho^\varepsilon(\tau) - \rho^0(\tau)\|^2_{L^2(\mathcal{E})} + \varepsilon^2\|w^\varepsilon(\tau) - w^0(\tau)\|^2_{L^2(\mathcal{E})} + \int_0^\tau \|w^\varepsilon(s) - w^0(s)\|^3_{L^3(\mathcal{E})}\, ds \leq C_0 e^{c_0\tau}\varepsilon^3$$

holds for all $0 < \tau < \tau_{max}$. Moreover, if $|w^\varepsilon|$, $|w^0| \geq \underline{w} > 0$, then

$$\|\rho^\varepsilon(\tau) - \rho^0(\tau)\|^2_{L^2(\mathcal{E})} + \varepsilon^2\|w^\varepsilon(\tau) - w^0(\tau)\|^2_{L^2(\mathcal{E})} + \int_0^\tau \|w^\varepsilon(s) - w^0(s)\|^2_{L^2(\mathcal{E})}\, ds \leq C_0' e^{c_0'\tau}\varepsilon^4.$$

All constants only depend on the bounds in (A1)–(A3) and the bounds on (ρ^0, w^0).

Sketch of the proof. We only sketch the main ideas of the proof, which is based on the abstract energy structure (3.26)–(3.27) that allows us to use the relative energy introduced in (3.33) for measuring the distance between the two solutions $(\rho^\varepsilon, w^\varepsilon)$ and (ρ^0, w^0). We can understand the solution to the parabolic limit problem as a perturbed solution to (3.26)–(3.27) for $\varepsilon > 0$, i.e., $u^0 = (\rho^0, w^0)$ solves

$$\mathcal{C}^\varepsilon\partial_\tau u^0 + (\mathcal{J} + \mathcal{R}(u^0))\boldsymbol{z}^\varepsilon(u^0) = \boldsymbol{b}_\partial + \boldsymbol{res}^0, \tag{3.39}$$

$$\boldsymbol{z}^\varepsilon(u^0) = (\mathcal{C}^\varepsilon)^{-1}(\mathcal{H}^\varepsilon)'(u^0) \tag{3.40}$$

with residual

$$\langle \boldsymbol{res}^0, v\rangle := (\varepsilon^2\partial_\tau w^0, r)_{\mathcal{E}} - (\tfrac{\varepsilon^2}{2}(w^0)^2, \partial_x r)_{\mathcal{E}} \tag{3.41}$$

defined for test functions $v = (q, r) \in L^2(\mathcal{E}) \times H(\mathrm{div}; \mathcal{E})$. Now, formally differentiating the relative energy $\mathcal{H}^\varepsilon(u^\varepsilon|u^0)$ with respect to time yields

$$\begin{aligned}\frac{d}{d\tau}\mathcal{H}^\varepsilon(u^\varepsilon|u^0) &= \langle (\mathcal{H}^\varepsilon)'(u^\varepsilon) - (\mathcal{H}^\varepsilon)'(u^0), \partial_\tau u^\varepsilon - \partial_\tau u^0\rangle \\ &\quad + \langle (\mathcal{H}^\varepsilon)'(u^\varepsilon) - (\mathcal{H}^\varepsilon)'(u^0) - (\mathcal{H}^\varepsilon)''(u^0)(u^\varepsilon - u^0), \partial_\tau u^0\rangle.\end{aligned} \tag{3.42}$$

Using the fact that u^ε and u^0 solve (3.26)–(3.27) and (3.39)–(3.40), respectively, the first term equals

$$\begin{aligned}\langle (\mathcal{H}^\varepsilon)'(u^\varepsilon) - (\mathcal{H}^\varepsilon)'(u^0), \partial_\tau u^\varepsilon - \partial_\tau u^0\rangle &= \langle \mathcal{C}^\varepsilon\partial_\tau u^\varepsilon - \mathcal{C}^\varepsilon u^0, \boldsymbol{z}^\varepsilon(u^\varepsilon) - \boldsymbol{z}^\varepsilon(u^0)\rangle \\ &= -\langle \mathcal{R}(u^\varepsilon) - \mathcal{R}(u^0), \boldsymbol{z}^\varepsilon(u^\varepsilon) - \boldsymbol{z}^\varepsilon(u^0)\rangle + \langle \boldsymbol{res}^0, \boldsymbol{z}^\varepsilon(u^\varepsilon) - \boldsymbol{z}^\varepsilon(u^0)\rangle,\end{aligned}$$

where we used the skew-symmetry of $\mathcal{J}$ and the fact that both problems have the same boundary data. The statements of Theorem 3.5 then immediately follow from the norm equivalence for the relative energy (3.35) and by applying Grönwall's Lemma, see e.g. [116, Lemma 2.7], to (3.42) under the following three assumptions:

(E1) $\langle (\mathcal{H}^\varepsilon)'(u^\varepsilon) - (\mathcal{H}^\varepsilon)'(u^0) - (\mathcal{H}^\varepsilon)''(u^0)(u^\varepsilon - u^0), \partial_\tau u^0\rangle \le C_1\mathcal{H}^\varepsilon(u^\varepsilon|u^0)$,

(E2) $-\langle \mathcal{R}(u^\varepsilon) - \mathcal{R}(u^0), \boldsymbol{z}^\varepsilon(u^\varepsilon) - \boldsymbol{z}^\varepsilon(u^0)\rangle \le C_2\mathcal{H}^\varepsilon(u^\varepsilon|u^0) - 2\mathcal{D}(u^\varepsilon|u^0)$,

(E3) $\langle \boldsymbol{res}^0, \boldsymbol{z}^\varepsilon(u^\varepsilon) - \boldsymbol{z}^\varepsilon(u^0)\rangle \le C_3\mathcal{H}^\varepsilon(u^\varepsilon|u^0) + \mathcal{D}(u^\varepsilon|u^0) + C_4\varepsilon^3$

with relative dissipation functional defined by

$$\mathcal{D}(u^\varepsilon|u^0) := \tfrac{1}{8}\sum_{e\in\mathcal{E}}\int_0^{\ell_e} a_e\gamma_e\rho_e^0(|w_e^\varepsilon| + |w_e^0|)(w_e^\varepsilon - w_e^0)^2\, dx \ge \tfrac{1}{8}\underline{a}\underline{\gamma}\underline{\rho}\|w^\varepsilon - w^0\|^3_{L^3(\mathcal{E})}. \tag{3.43}$$

Let us note that if $|w^\varepsilon|$, $|w^0| \ge \underline{w} > 0$, then $\mathcal{D}(u^\varepsilon|u^0)$ can alternatively be estimated by

$$\mathcal{D}(u^\varepsilon|u^0) \ge \tfrac{1}{4}\underline{a}\underline{\gamma}\underline{\rho}\underline{w}\|w^\varepsilon - w^0\|^2_{L^2(\mathcal{E})}. \tag{3.44}$$

The estimate (E3) of the residual can then be improved to $C_5\varepsilon^4$ instead of $C_4\varepsilon^3$ leading to the better asymptotic estimate stated in Theorem 3.5. Let us stress that the additional dissipation provided by friction is crucial for the stability of the problem. For the sake of completeness the verification of (E1)–(E3) is presented in Appendix A.1. □

3.2. Numerical approximation

For the discretization of the isothermal gas transport model (3.15)–(3.20), we propose a mixed finite element method for the spatial semi-discretization complemented by an implicit Euler time-stepping. As we will see, this allows to preserve the underlying energy structure of the problem. The content of this section is based on our publication [38].

3.2.1. Mesh and approximation spaces

On every edge $e \in \mathcal{E}$ we define the spatial grid points by $x_e^i = ih_e$ for $i = 0, \dots, M_e$ with local and global mesh sizes $h_e = \ell_e/M_e$ and $h = \max_{e\in\mathcal{E}} h_e$, respectively. The complete spatial mesh is then given by

$$\mathcal{T}_h = \{T_e^i = (x_e^{i-1}, x_e^i) : i = 1, \dots, M_e,\ e \in \mathcal{E}\}$$

and we introduce the approximation spaces on $\mathcal{T}_h$ by

$$Q_h = \mathcal{P}_0(\mathcal{T}_h) \qquad \text{and} \qquad R_h = \mathcal{P}_1(\mathcal{T}_h) \cap H(\mathrm{div}; \mathcal{E})$$

with $\mathcal{P}_k$ being the space of piecewise polynomials of degree $\leq k$. The space Q_h consists of piecewise constant densities, whereas the space R_h contains all piecewise linear fluxes that are continuous within edges and satisfy the conservation condition (3.19) at network junctions. We further denote by $\Pi_h : L^2(\mathcal{E}) \to Q_h$ and $I_h : H(\mathrm{div}; \mathcal{E}) \to R_h$ the L^2-orthogonal projection and the linear interpolation operator, which are defined via

$$\begin{aligned} \int_T q - \Pi_h q \, dx &= 0 && \text{for all } T \in \mathcal{T}_h,\ q \in L^2(\mathcal{E}), \\ I_h r(x_e^i) &= r(x_e^i) && \text{for all } i = 0, \dots, M_e,\ e \in \mathcal{E},\ r \in H(\mathrm{div}; \mathcal{E}). \end{aligned}$$

Let us note that the conservation property (3.19) is preserved under linear interpolation, i.e., $I_h r \in H(\mathrm{div}; \mathcal{E})$. For the time discretization, we make use of the discrete time points $\tau^n = n\Delta\tau,\ n = 0, \dots, N$ with $\Delta\tau = \tau_{max}/N$. The backward difference quotient is denoted by $\bar{d}_\tau u^n = (u^n - u^{n-1})/\Delta\tau$, where we abbreviate $u^n = u(\tau^n)$.

3.2.2. Structure-preserving discretization scheme

For the approximation of the solution to (3.15)–(3.20), we propose the following method.

Problem 3.6. Let $\rho_h^0 = \Pi_h \rho(0),\ m_h^0 = I_h m(0)$. Then, for $n = 1, \dots, N$ find $\rho_h^n \in Q_h$, $m_h^n \in R_h$ so that

$$(a\bar{d}_\tau \rho_h^n, q_h)_{\mathcal{E}} + (\partial_x m_h^n, q_h)_{\mathcal{E}} = 0, \tag{3.45}$$

$$(\varepsilon^2 \bar{d}_\tau w_h^n, r_h)_{\mathcal{E}} - (h_h^n, \partial_x r_h)_{\mathcal{E}} + (\gamma |w_h^n| w_h^n, r_h)_{\mathcal{E}} = -\sum\nolimits_{v\in\mathcal{V}_\partial} \hat{h}_\partial^v(\tau) r_e(v) n_e(v) \tag{3.46}$$

holds for all $q_h \in Q_h$ and $r_h \in R_h$. For abbreviation, we introduced

$$w_h^n = w_h(\rho_h^n, m_h^n) = \frac{m_h^n}{a\rho_h^n} \quad \text{and} \quad h_h^n = h_h^\varepsilon(\rho_h^n, m_h^n) = \frac{\varepsilon^2}{2}\Big(\frac{m_h^n}{a\rho_h^n}\Big)^2 + P'(\rho_h^n). \tag{3.47}$$

Remark 3.7. The above scheme (3.45)–(3.47) preserves the energy structure of the weak formulation (3.22)–(3.23) and can thus be written as an abstract system of the form (3.26)–(3.27). Basic properties like the balance laws in Lemma 3.2 are thus conserved as we will see below. The coupling conditions at network junctions are incorporated just like in the weak formulation, i.e., the conservation condition (3.19) on the mass flux m is

strongly enforced in the space R_h whereas the continuity condition (3.20) on the enthalpy h is weakly imposed in (3.46). Moreover, by formally setting $\varepsilon = 0$ we obtain a viable scheme for the parabolic limit problem, which, however, does not coincide with the method proposed in [113] that is based on a reformulation of the model equations into a single parabolic equation of second-order.

For the rest of this section, we make the following additional assumption.

(A3h) There exists a discrete solution $(\rho_h^n, m_h^n)_{0\le n\le N}$ to Problem 3.6 that satisfies

$$\underline{\rho} \le \rho_h^n(x) \le \bar{\rho} \qquad \text{and} \qquad |w_h^n(x)| \le 3\bar{w}/2$$

for all $0 \le x \le \ell_e,\ e \in \mathcal{E}$ and $n = 0, \dots, N$ with $w_h = \frac{m_h}{a\rho_h}$.

This assumption allows us to estimate distances between discrete solutions via the relative energy since $(\rho_h^n, w_h^n) \in \mathcal{AS}$, i.e., the statements of Lemma 3.4 are valid. Moreover, global balance laws immediately hold for the discrete solution.

Lemma 3.8. *Let (A1)–(A2) and (A3h) hold with $(\rho_h^n, m_h^n)_{0\le n\le N}$ being a corresponding solution to Problem 3.6. Then,*

$$\int_{\mathcal{E}} a\bar{d}_\tau \rho_h^n(x)\ dx = -\sum\nolimits_{v\in\mathcal{V}_\partial} m_h^n(v) n_e(v), \tag{3.48}$$

$$\bar{d}_\tau \mathcal{H}^\varepsilon(\rho_h^n, w_h^n) + \mathcal{D}(\rho_h^n, w_h^n) \le -\sum\nolimits_{v\in\mathcal{V}_\partial} \hat{h}_\partial^v(\tau^n) m_h^n(v) n_e(v) \tag{3.49}$$

holds for all $n = 1, \dots, N$ with dissipation functional defined in (3.30).

Proof. The discrete mass balance (3.48) immediately follows by testing (3.45) with $q_h = 1$. The contributions for interior vertices vanish since $m_h^n \in H(\mathrm{div}; \mathcal{E})$. Let us abbreviate $u_h^n = (\rho_h^n, w_h^n)$ in the following. Due to the convexity of $\mathcal{H}^\varepsilon$ on $\mathcal{AS}$ we have

$$\mathcal{H}^\varepsilon(u_h^n) - \mathcal{H}^\varepsilon(u_h^{n-1}) \le \langle (\mathcal{H}^\varepsilon)'(u_h^n), u_h^n - u_h^{n-1}\rangle.$$

From this we can conclude that

$$\begin{aligned}
\bar{d}_\tau \mathcal{H}^\varepsilon(\rho_h^n, w_h^n) &\le (\delta_\rho \mathcal{H}^\varepsilon(\rho_h^n, w_h^n), \bar{d}_\tau \rho_h^n)_{\mathcal{E}} + (\delta_w \mathcal{H}^\varepsilon(\rho_h^n, w_h^n), \bar{d}_\tau w_h^n)_{\mathcal{E}} \\
&= (h_h^n, a\bar{d}_\tau \rho_h^n)_{\mathcal{E}} + (m_h^n, \varepsilon^2 \bar{d}_\tau w_h^n)_{\mathcal{E}} \\
&= -(h_h^n, \partial_x m_h^n)_{\mathcal{E}} + (h_h^n, \partial_x m_h^n)_{\mathcal{E}} - (\gamma |w_h^n| w_h^n, m_h^n)_{\mathcal{E}} - \sum\nolimits_{v\in\mathcal{V}_\partial} \hat{h}_\partial^v(\tau^n) m_h^n(v) n_e(v) \\
&= -\mathcal{D}(\rho_h^n, w_h^n) - \sum\nolimits_{v\in\mathcal{V}_\partial} \hat{h}_\partial^v(\tau^n) m_h^n(v) n_e(v).
\end{aligned}$$

Here, we used the variational identities (3.25) for the energy as well as the equations (3.45)–(3.46). Since $\bar{d}_\tau \rho_h^n$ and $\partial_x m_h^n$ are piecewise constant, $\bar{d}_\tau \rho_h^n = \partial_x m_h^n$ holds pointwise due to (3.45), i.e., we can test (3.45) with any L^2-function. This proves (3.49). □

3.2.3. Uniform error estimate

We are now in the position to state the main result of this section.

Theorem 3.9. *Let (A1)–(A4) hold with (ρ, w) being a corresponding subsonic bounded state solution to* (3.15)–(3.20) *and $m = a\rho w$. Moreover, let (A3h) hold with (ρ_h^n, m_h^n) being a corresponding discrete solution to Problem 3.6. Then,*

$$\|\rho(\tau^n) - \rho_h^n\|_{L^2(\mathcal{E})}^2 + \varepsilon^2 \|m(\tau^n) - m_h^n\|_{L^2(\mathcal{E})}^2 + \sum_{k=1}^{n} \Delta\tau \|m(\tau^k) - m_h^k\|_{L^3(\mathcal{E})}^3 \leq C(h^2 + \Delta\tau^2)$$

holds for all $n = 1, \ldots, N$ with a constant C that only depends on the bounds in the assumptions, but not on ε, h or $\Delta\tau$.

Remark 3.10. Since the constant C in the above statement is independent of ε, the error estimate holds uniformly in ε, in particular also in the limit $\varepsilon = 0$. We thus obtain optimal convergence behavior which is asymptotically preserved. The validity of the Theorem, however, is conditional on the existence of a subsonic bounded state solution to (3.15)–(3.20) and a discrete solution to Problem 3.6 satisfying Assumption (A3h). In practical computations, the latter can be checked explicitly.

3.2.4. Proof of the uniform error estimate

The proof of Theorem 3.9 is based on relative energy estimates exploiting the preserved energy structure of the numerical method, which allows us to proceed similarly as in the proof of Theorem 3.5. Let us first give the key steps (Step 1 – Step 3). The proofs of Lemma 3.13 and Lemma 3.15 stated in Step 3, which are quite technical, are postponed to Section 3.2.5.

Step 1 (Error splitting). Following the standard procedure in the error analysis for Galerkin methods, we introduce projections

$$\hat{\rho}_h^n = \hat{\rho}_h(\tau^n) := \Pi_h \rho(\tau^n) \quad \text{and} \quad \hat{m}_h^n = \hat{m}_h(\tau^n) := I_h m(\tau^n)$$

of the exact solution (ρ, m). Recall that Π_h is the L^2-orthogonal projection onto Q_h and I_h the piecewise linear interpolation onto R_h. By applying the triangle inequality we can then split the error into a *projection error* and a *discrete error component*, i.e.,

$$\|\rho(\tau^n) - \rho_h^n\|_{L^p(\mathcal{E})} \leq \|\rho(\tau^n) - \hat{\rho}_h^n\|_{L^p(\mathcal{E})} + \|\hat{\rho}_h^n - \rho_h^n\|_{L^p(\mathcal{E})}, \tag{3.50}$$

$$\|m(\tau^n) - m_h^n\|_{L^p(\mathcal{E})} \leq \|m(\tau^n) - \hat{m}_h^n\|_{L^p(\mathcal{E})} + \|\hat{m}_h^n - m_h^n\|_{L^p(\mathcal{E})} \tag{3.51}$$

for $1 \leq p \leq \infty$. Both components are now estimated separately in Step 2 and Step 3.

Step 2 (Estimation of the projection error). The following estimates can be derived by standard arguments; see e.g. [12, Ch. 4] or [72, App. C].

Lemma 3.11. *Let $z \in W^{1,p}(T)$ for $T \in \mathcal{T}_h$ and $1 \le p \le \infty$. Then,*

$$\partial_x(I_h z) = \Pi_h(\partial_x z), \quad \|\Pi_h z\|_{L^\infty(T)} \le \|z\|_{L^\infty(T)}, \quad \text{and} \quad \|I_h z\|_{L^\infty(T)} \le \|z\|_{L^\infty(T)}. \tag{3.52}$$

Furthermore,

$$\|z - \Pi_h z\|_{L^p(T)} \le Ch\|\partial_x z\|_{L^p(T)} \quad \text{and} \quad \|z - I_h z\|_{L^p(T)} \le C'h\|\partial_x z\|_{L^p(T)} \tag{3.53}$$

hold with constants C, C' that are independent of z, p and h.

Proof. The first property in (3.52), also known as *commuting diagram property*, follows from the properties of the projections and the fundamental theorem of calculus, i.e.,

$$\Pi_h(\partial_x z) = h_T^{-1} \int_T \Pi_h(\partial_x z)\, dx = h_T^{-1} \int_T \partial_x z\, dx = h_T^{-1}\big(z(x^i) - z(x^{i-1})\big) = \partial_x(I_h z)$$

with $T = (x^{i-1}, x^i)$ and $h_T = x^i - x^{i-1}$. Since $\Pi_h z$ is constant, it holds that $\Pi_h z = z(\xi)$ for some $\xi \in T$. Due to the definition of I_h we have $|I_h z(x)| \le \max(|z(x^i)|, |z(x^{i-1})|)$ for $x \in T$. From this, we can immediately deduce the L^∞-bounds on the projections. The error estimates (3.53) can be shown by standard arguments and found in the references stated above. □

From the previous lemma, we can derive estimates for the projection error components.

Lemma 3.12. *Let (A1)–(A4) hold. Then, for all $n = 1, \dots, N$ it holds that*

$$\|\rho(\tau^n) - \hat{\rho}_h^n\|_{L^2(\mathcal{E})}^2 + \varepsilon^2\|m(\tau^n) - \hat{m}_h^n\|_{L^2(\mathcal{E})}^2 + \sum_{k=1}^n \Delta\tau\|m(\tau^k) - \hat{m}_h^k\|_{L^3(\mathcal{E})}^3 \le Ch^2 \tag{3.54}$$

with a constant C that only depends on the bounds in the assumptions but not on ε, h or $\Delta\tau$. Moreover, the projections are bounded by $\underline{\rho} \le \hat{\rho}_h^n \le \bar{\rho}$ and $|\hat{m}_h^n| \le \bar{a}\bar{\rho}\bar{w}$. For any $0 < h \le h_0$ sufficiently small it further holds that $|\hat{w}_h^n| \le 3\bar{w}/2$ with $\hat{w}_h^n = \hat{m}_h^n / a\hat{\rho}_h^n$.

Proof. Since the network is the sum of the elements $T \in \mathcal{T}_h$, the first two terms in (3.54) can immediately be estimated by the previous lemma using the extra regularity of the exact solution provided by (A4) as well as the bounds in (A3). For the third term in (3.54) we see that

$$\begin{aligned}\sum\nolimits_{k=1}^n \Delta\tau\|m(\tau^k) - \hat{m}_h^k\|_{L^3(\mathcal{E})}^3 &\le \sum\nolimits_{k=1}^n \|m(\tau^k) - \hat{m}_h^k\|_{L^\infty(\mathcal{E})}\|m(\tau^k) - \hat{m}_h^k\|_{L^2(\mathcal{E})}^2 \\ &\le 2C\tau_{max}\bar{a}\bar{\rho}\bar{w}h^2,\end{aligned}$$

where we exploit the fact that $\sum_{k=1}^n \Delta\tau = \tau_{max}$ as well as the bounds on m and $\hat{m}_h^n$ and the projection error estimates (3.53). The bounds on $\hat{\rho}_h^n$ and $\hat{m}_h^n$ immediately follow from the construction of the projections, the bounds (3.52), and assumption (A3). Using the triangle inequality, we can estimate $\hat{w}_h^n$ by

$$\|\hat{w}_h^n\|_{L^\infty(\mathcal{E})} \le \|w(\tau^n) - \hat{w}_h^n\|_{L^\infty(\mathcal{E})} + \|w(\tau^n)\|_{L^\infty(\mathcal{E})},$$

where the latter term is bounded by $\bar{w}$ due to (A3). For the former term, we find that

$$\|w(\tau^n) - \hat{w}_h^n\|_{L^\infty(\mathcal{E})} \le \frac{1}{\underline{a}\underline{\rho}}\|m(\tau^n) - \hat{m}_h^n\|_{L^\infty(\mathcal{E})} + \frac{\bar{a}\bar{\rho}\bar{w}}{\underline{\rho}^2}\|\rho(\tau^n) - \hat{\rho}_h^n\|_{L^\infty(\mathcal{E})} \le Ch$$

by (3.53) and (A3)–(A4). For sufficiently small h we obtain the desired bounds on $\hat{w}_h^n$. □

Step 3 (Estimation of the discrete error). The main challenge for our analysis is the estimation of the discrete error components. We proceed similarly to the proof of the asymptotic estimates in Theorem 3.5. We use the relative energy (3.33) to measure the distance between (ρ_h^n, m_h^n) and the projections $(\hat{\rho}_h^n, \hat{m}_h^n)$, which are both in the set $\mathcal{AS}$ of admissible states for sufficiently small $0 < h \leq h_0$ due to (A3h) and the bounds in Lemma 3.12. We understand the projections as perturbed solutions to Problem 3.6 satisfying (3.45)–(3.46) with residuals on the right-hand side defined by

$$\langle \mathrm{res}_1^n, q_h \rangle := (a\bar{d}_\tau \hat{\rho}_h^n, q_h)_{\mathcal{E}} + (\partial_x \hat{m}_h^n, q_h)_{\mathcal{E}}, \tag{3.55}$$

$$\langle \mathrm{res}_2^n, r_h \rangle := (\varepsilon^2 \bar{d}_\tau \hat{w}_h^n, r_h)_{\mathcal{E}} - (\hat{h}_h^n, \partial_x r_h)_{\mathcal{E}} + (\gamma |\hat{w}_h^n| \hat{w}_h^n, r_h)_{\mathcal{E}} + \sum_{v \in \mathcal{V}_\partial} \hat{h}_\partial^v(\tau^n) q_h(v) n_e(v) \tag{3.56}$$

for $q_h \in Q_h,\ r_h \in R_h$ with $\hat{w}_h^n = \hat{m}_h^n / a\hat{\rho}_h^n$ and $\hat{h}_h^n = \frac{1}{2}\varepsilon^2 (\hat{w}_h^n)^2 + P'(\hat{\rho}_h^n)$. We now first estimate the discrete time derivative of the relative energy by exploiting the energy structure of the problem. In the second step, we successively give estimates for all appearing terms. Finally, the application of a discrete Grönwall-type lemma yields the desired error estimate.

Lemma 3.13. *Let (A1)–(A2) hold and let $u_h^k,\ \hat{u}_h^k \in \mathcal{AS}$ for $k = n-1, n$. Then,*

$$\begin{aligned} \bar{d}_\tau \mathcal{H}^\varepsilon(u_h^n | \hat{u}_h^n) \leq\ & \langle (\mathcal{H}^\varepsilon)'(u_h^n) - (\mathcal{H}^\varepsilon)'(\hat{u}_h^n) - (\mathcal{H}^\varepsilon)''(\hat{u}_h^n)(u_h^n - \hat{u}_h^n), \bar{d}_\tau \hat{u}_h^n \rangle \\ & + \langle (\mathcal{H}^\varepsilon)'(u_h^n) - (\mathcal{H}^\varepsilon)'(\hat{u}_h^n), \bar{d}_\tau u_h^n - \bar{d}_\tau \hat{u}_h^n \rangle \\ & + C \|\bar{d}_\tau \hat{u}_h^n\|_{\varepsilon,\infty} \big(\mathcal{H}^\varepsilon(u_h^n | \hat{u}_h^n) + \mathcal{H}^\varepsilon(u_h^{n-1} | \hat{u}_h^{n-1}) \big) + C' \|\bar{d}_\tau \hat{u}_h^n\|_{\varepsilon,\infty} \|\hat{u}_h^n - \hat{u}_h^{n-1}\|_\varepsilon^2 \end{aligned} \tag{3.57}$$

is valid with constants C, C' that are independent of ε, $\Delta\tau$ and u_h^k, $\hat{u}_h^k$.

The proof of this technical result is postponed to Section 3.2.5.

Remark 3.14. Note that the first two lines also appeared in the estimate of the continuous time derivative of the relative energy in (3.42). The additional terms in the last line of (3.57) are thus perturbations caused by the time discretization. Let us also mention that the above result only depends on strong convexity and smoothness of the energy functional but not on the particular functions u_h^k, $\hat{u}_h^k$.

It now remains to estimate the terms on the right-hand side of (3.57). The first two lines also appear in (3.42) and we exploit the energy structure of (3.45)–(3.46) as we have done in the proof of Theorem 3.5. This leads to the following estimate. Since the proof is quite technical it will also be postponed in Section 3.2.5.

Lemma 3.15. *Under the assumptions of Theorem 3.9 it holds that*

$$\begin{aligned} \bar{d}_\tau \mathcal{H}^\varepsilon(u_h^n | \hat{u}_h^n) \leq\ & C\mathcal{H}^\varepsilon(u_h^n | \hat{u}_h^n) + C'\mathcal{H}^\varepsilon(u_h^{n-1} | \hat{u}_h^{n-1}) + \tfrac{1}{\Delta\tau}(h - \hat{h}_h, \rho_h - \hat{\rho}_h)_{\mathcal{E}} \Big|_{\tau_{n-1}}^{\tau_n} \\ & + C''(h^2 + \Delta\tau^2) - \tfrac{1}{2}\mathcal{D}(u_h^n | \hat{u}_h^n) \end{aligned} \tag{3.58}$$

for all $0 \leq n \leq N$ with $u_h^n = (\rho_h^n, m_h^n)$, $\hat{u}_h^n = (\hat{\rho}_h^n, \hat{m}_h^n)$, and relative dissipation functional defined in (3.43)*. Note that h is the total specific enthalpy of the exact solution (ρ, w).*

We are now in the position to complete the proof of Theorem 3.9. By multiplying (3.58) with $\Delta\tau$ and summing over the time steps, we obtain

$$\begin{aligned}\mathcal{H}^\varepsilon(u_h^n|\hat{u}_h^n) \leq \mathcal{H}^\varepsilon(u_h^0|\hat{u}_h^0) + \Delta\tau \sum\nolimits_{k=1}^n \Big(C_1\mathcal{H}^\varepsilon(u_h^k|\hat{u}_h^k) + C_2\mathcal{H}^\varepsilon(u_h^{k-1}|\hat{u}_h^{k-1}) \\ + C_3(h^2+\Delta\tau^2) - \tfrac{1}{2}\mathcal{D}(u_h^k|\hat{u}_h^k)\Big) + (h-\hat{h}_h, \rho_h - \hat{\rho}_h)\mathcal{E}\,\big|_0^{\tau_n}.\end{aligned} \tag{3.59}$$

The last term in the second line vanishes at $\tau = 0$ since $\rho_h^0 = \hat{\rho}_h^0$. By Hölder's and Young's inequality, we further deduce that

$$\begin{aligned}(h(\tau^n) - \hat{h}_h^n, \rho_h^n - \hat{\rho}_h^n)\mathcal{E} &\leq \tfrac{1}{2}c_{rel}^{-1}\|h(\tau^n) - \hat{h}_h^n\|_{L^2(\mathcal{E})}^2 + \tfrac{1}{2}c_{rel}\|\rho_h^n - \hat{\rho}_h^n\|_{L^2(\mathcal{E})}^2 \\ &\leq C_4h^2 + \tfrac{1}{2}\mathcal{H}^\varepsilon(u_h^n|\hat{u}_h^n),\end{aligned} \tag{3.60}$$

where we used the norm equivalence for the relative energy (3.35) as well as the fact that

$$\begin{aligned}\|h(\tau^n) - \hat{h}_h^n\|_{L^2(\mathcal{E})} &\leq C\varepsilon^2\|w(\tau^n) - \hat{w}_h^n\|_{L^2(\mathcal{E})} + C'\|\rho(\tau^n) - \hat{\rho}_h^n\|_{L^2(\mathcal{E})} \\ &\leq C''\varepsilon^2\|m(\tau^n) - \hat{m}_h^n\|_{L^2(\mathcal{E})} + C'''\|\rho(\tau^n) - \hat{\rho}_h^n\|_{L^2(\mathcal{E})} \leq C''''h\end{aligned}$$

holds by the projection error estimates and bounds in Lemma 3.12 as well as (A1)–(A4) with constants that only depend on the bounds in the assumptions. The last term in (3.60) can be absorbed into the left-hand side (3.59). We can now apply the discrete Grönwall Lemma A.1 with

$$a^n = \mathcal{H}^\varepsilon(u_h^n|\hat{u}_h^n),\ b^n = 2\tau_{max}C_3(h^2+\Delta\tau^2) + C_4h^2,\ c = 2\max(C_1, C_2),\ d^n = \mathcal{D}(u_h^n|\hat{u}_h^n).$$

Since $a^0 = 0$ by the choice of initial data, $b^n \geq 0$ and $n\tau \leq \tau_{max}$, we obtain

$$\mathcal{H}^\varepsilon(u_h^n|\hat{u}_h^n) + \Delta\tau\sum\nolimits_{k=1}^n \mathcal{D}(u_h^k|\hat{u}_h^k) \leq C(h^2+\Delta\tau^2)$$

with a constant C that only depends on the bounds in the assumptions and τ_{max} but is independent of ε. The equivalence of norms for the relative energy (3.35) and the estimate for the relative dissipation functional (3.43) then yield

$$\|\rho_h^n - \hat{\rho}_h^n\|_{L^2(\mathcal{E})}^2 + \varepsilon^2\|w_h^n - \hat{w}_h^n\|_{L^2(\mathcal{E})}^2 + \sum\nolimits_{k=1}^n \Delta\tau\|w_h^n - \hat{w}_h^n\|_{L^3(\mathcal{E})}^3 \leq C'(h^2+\Delta\tau^2).$$

Due to the uniform boundedness of ρ_h^n, $\hat{\rho}_h^n$ and w_h^n, $\hat{w}_h^n$, the same estimate holds for w_h^n, $\hat{w}_h^n$ replaced by m_h^n, $\hat{m}_h^n$. Together with the estimate for the projection error in Lemma 3.12, the error splitting (3.50)–(3.51) yields the final error estimate and concludes the proof of Theorem 3.9. □

3.2.5. Proof of the technical results

Let us now present the proofs of Lemma 3.13 and Lemma 3.15.

Proof of Lemma 3.13

For ease of notation, we write $\mathcal{H} = \mathcal{H}^\varepsilon$. In the first step, we rearrange the terms and apply Taylor's theorem leading to

$$\begin{aligned}
\bar{d}_\tau \mathcal{H}(u_h^n|\hat{u}_h^n) &= \tfrac{1}{\Delta\tau}\big(\mathcal{H}(u_h^n) - \mathcal{H}(u_h^{n-1}) - \mathcal{H}(\hat{u}_h^n) + \mathcal{H}(\hat{u}_h^{n-1}) \\
&\qquad - \langle \mathcal{H}'(\hat{u}_h^n), u_h^n - \hat{u}_h^n\rangle + \langle \mathcal{H}'(\hat{u}_h^{n-1}), u_h^{n-1} - \hat{u}_h^{n-1}\rangle\big) \\
&= \langle \mathcal{H}'(u_h^n), \bar{d}_\tau u_h^n\rangle - \tfrac{\Delta\tau}{2}\langle \mathcal{H}''(u_h^*)\,\bar{d}_\tau u_h^n, \bar{d}_\tau u_h^n\rangle - \langle \mathcal{H}'(\hat{u}_h^n), \bar{d}_\tau \hat{u}_h^n\rangle + \tfrac{\Delta\tau}{2}\langle \mathcal{H}''(\hat{u}_h^*)\,\bar{d}_\tau \hat{u}_h^n, \bar{d}_\tau \hat{u}_h^n\rangle \\
&\qquad - \langle \mathcal{H}'(\hat{u}_h^n), \bar{d}_\tau u_h^n - \bar{d}_\tau \hat{u}_h^n\rangle - \tfrac{1}{\Delta\tau}\langle \mathcal{H}'(\hat{u}_h^n) - \mathcal{H}'(\hat{u}_h^{n-1}), u_h^{n-1} - \hat{u}_h^{n-1}\rangle,
\end{aligned}$$

where $u_h^* := \xi u_h^n + (1-\xi)u_h^{n-1}$ and $\hat{u}_h^* := \hat{\xi}\hat{u}_h^n + (1-\hat{\xi})\hat{u}_h^{n-1}$ denote intermediate values for some ξ, $\hat{\xi} \in (0,1)$. Note that $u_h^*, \hat{u}_h^* \in \mathcal{AS}$. As the next step we add and subtract the terms $\langle \mathcal{H}'(u_h^n), \bar{d}_\tau \hat{u}_h^n\rangle$, $\langle \bar{d}_\tau \mathcal{H}'(\hat{u}_h^n), u_h^n - \hat{u}_h^n\rangle$, and $\langle \mathcal{H}''(\hat{u}_h^n)(u_h^n - \hat{u}_h^n), \bar{d}_\tau \hat{u}_h^n\rangle$, which yields

$$\begin{aligned}
\bar{d}_\tau \mathcal{H}(u_h^n|\hat{u}_h^n) &= \langle \mathcal{H}'(u_h^n) - \mathcal{H}'(\hat{u}_h^n), \bar{d}_\tau u_h^n - \bar{d}_\tau \hat{u}_h^n\rangle \\
&\quad + \langle \mathcal{H}'(u_h^n) - \mathcal{H}'(\hat{u}_h^n) - \mathcal{H}''(\hat{u}_h^n)(u_h^n - \hat{u}_h^n), \bar{d}_\tau \hat{u}_h^n\rangle \\
&\quad - \tfrac{\Delta\tau}{2}\langle \mathcal{H}''(u_h^*)\bar{d}_\tau u_h^n, \bar{d}_\tau u_h^n\rangle + \tfrac{\Delta\tau}{2}\langle \mathcal{H}''(\hat{u}_h^*)\,\bar{d}_\tau \hat{u}_h^n, \bar{d}_\tau \hat{u}_h^n\rangle \\
&\quad - \langle \bar{d}_\tau \mathcal{H}'(\hat{u}_h^n) - \mathcal{H}''(\hat{u}_h^n)\,\bar{d}_\tau \hat{u}_h^n, u_h^n - \hat{u}_h^n\rangle + \Delta\tau\langle \bar{d}_\tau \mathcal{H}'(\hat{u}_h^n), \bar{d}_\tau u_h^n - \bar{d}_\tau \hat{u}_h^n\rangle.
\end{aligned} \tag{3.61}$$

The first two lines already appear in the desired estimate (3.57). By applying Taylor's theorem again the last two lines equal

$$\begin{aligned}
(*) &= -\tfrac{\Delta\tau}{2}\langle \mathcal{H}''(u_h^*)\bar{d}_\tau u_h^n, \bar{d}_\tau u_h^n\rangle + \tfrac{\Delta\tau}{2}\langle \mathcal{H}''(\hat{u}_h^*)\,\bar{d}_\tau \hat{u}_h^n, \bar{d}_\tau \hat{u}_h^n\rangle \\
&\quad - \langle (\mathcal{H}''(\hat{u}_h^{**}) - \mathcal{H}''(\hat{u}_h^n))\,\bar{d}_\tau \hat{u}_h^n, u_h^n - \hat{u}_h^n\rangle + \Delta\tau\langle \mathcal{H}''(\hat{u}_h^{**})\bar{d}_\tau \hat{u}_h^n, \bar{d}_\tau u_h^n - \bar{d}_\tau \hat{u}_h^n\rangle
\end{aligned}$$

with $\hat{u}_h^{**} = \xi^{**}\hat{u}_h^n + (1-\xi^{**})\hat{u}_h^{n-1} \in \mathcal{AS}$ for some $\xi^{**} \in (0,1)$. Adding and subtracting the terms $\Delta\tau\langle \mathcal{H}''(u_h^*)\bar{d}_\tau \hat{u}_h^n, \bar{d}_\tau u_h^n\rangle$ and $\frac{\Delta\tau}{2}\langle \mathcal{H}''(u_h^*)\bar{d}_\tau \hat{u}_h^n, \bar{d}_\tau \hat{u}_h^n\rangle$ then leads to

$$\begin{aligned}
(*) &= -\tfrac{\Delta\tau}{2}\langle \mathcal{H}''(u_h^*)\bar{d}_\tau u_h^n, \bar{d}_\tau u_h^n\rangle + \Delta\tau\langle \mathcal{H}''(u_h^*)\bar{d}_\tau \hat{u}_h^n, \bar{d}_\tau u_h^n\rangle - \tfrac{\Delta\tau}{2}\langle \mathcal{H}''(u_h^*)\bar{d}_\tau \hat{u}_h^n, \bar{d}_\tau \hat{u}_h^n\rangle \\
&\quad + \Delta\tau\langle \big(\mathcal{H}''(\hat{u}_h^{**}) - \mathcal{H}''(u_h^*)\big)\bar{d}_\tau \hat{u}_h^n, \bar{d}_\tau u_h^n\rangle + \tfrac{\Delta\tau}{2}\langle \big(\mathcal{H}''(\hat{u}_h^*) - \mathcal{H}''(\hat{u}_h^{**})\big)\bar{d}_\tau \hat{u}_h^n, \bar{d}_\tau \hat{u}_h^n\rangle \\
&\quad + \tfrac{\Delta\tau}{2}\langle \big(\mathcal{H}''(u_h^*) - \mathcal{H}''(\hat{u}_h^{**})\big)\bar{d}_\tau \hat{u}_h^n, \bar{d}_\tau \hat{u}_h^n\rangle - \langle (\mathcal{H}''(\hat{u}_h^{**}) - \mathcal{H}''(\hat{u}_h^n))\,\bar{d}_\tau \hat{u}_h^n, u_h^n - \hat{u}_h^n\rangle.
\end{aligned}$$

Due to the convexity of $\mathcal{H}$ on the set $\mathcal{AS}$, which was shown in Lemma 3.4, the first line is non-positive. The last two lines can then be estimated using (3.36). We obtain

$$\begin{aligned}
(*) &\le C\big(\|\bar{d}_\tau \hat{u}_h^n\|_{\varepsilon,\infty}\|u_h^* - \hat{u}_h^{**}\|_\varepsilon\|u_h^n - u_h^{n-1}\|_\varepsilon + \|\bar{d}_\tau \hat{u}_h^n\|_{\varepsilon,\infty}\|\hat{u}^* - \hat{u}_h^{**}\|_\varepsilon\|\hat{u}_h^n - \hat{u}_h^{n-1}\|_\varepsilon \\
&\quad + \|\bar{d}_\tau \hat{u}_h^n\|_{\varepsilon,\infty}\|u^* - \hat{u}_h^{**}\|_\varepsilon\|\hat{u}_h^n - \hat{u}_h^{n-1}\|_\varepsilon + \|\bar{d}_\tau \hat{u}_h^n\|_{\varepsilon,\infty}\|\hat{u}_h^n - \hat{u}_h^{**}\|_\varepsilon\|u_h^n - \hat{u}_h^n\|_\varepsilon\big).
\end{aligned}$$

The appearing expressions can then be further estimated by

$$\begin{aligned}
\|u_h^* - \hat{u}_h^{**}\|_\varepsilon &\le \|u_h^n - \hat{u}_h^n\|_\varepsilon + \|\hat{u}_h^n - \hat{u}_h^{n-1}\|_\varepsilon + \|u_h^{n-1} - \hat{u}_h^{n-1}\|_\varepsilon, \\
\|u_h^n - u_h^{n-1}\|_\varepsilon &\le \|u_h^n - \hat{u}_h^n\|_\varepsilon + \|\hat{u}_h^n - \hat{u}_h^{n-1}\|_\varepsilon + \|u_h^{n-1} - \hat{u}_h^{n-1}\|_\varepsilon, \\
\|\hat{u}_h^* - \hat{u}_h^{**}\|_\varepsilon &\le \|\hat{u}_h^n - \hat{u}_h^{n-1}\|_\varepsilon, \qquad \|\hat{u}_h^n - \hat{u}_h^{**}\|_\varepsilon \le \|\hat{u}_h^n - \hat{u}_h^{n-1}\|_\varepsilon.
\end{aligned}$$

From the norm equivalence (3.35) for the relative energy we can then deduce the desired estimate (3.57). □

Proof of Lemma 3.15

In the following, we consider the estimate (3.57) for the discrete time derivative of the relative energy in Lemma 3.13 and estimate the three lines on the right-hand side of (3.57) separately. We abbreviate them by

$$
\begin{aligned}
(\ell 1) &:= \langle (\mathcal{H}^\varepsilon)'(u_h^n) - (\mathcal{H}^\varepsilon)'(\hat{u}_h^n) - (\mathcal{H}^\varepsilon)''(\hat{u}_h^n)(u_h^n - \hat{u}_h^n), \bar{d}_\tau \hat{u}_h^n \rangle, \\
(\ell 2) &:= \langle (\mathcal{H}^\varepsilon)'(u_h^n) - (\mathcal{H}^\varepsilon)'(\hat{u}_h^n), \bar{d}_\tau u_h^n - \bar{d}_\tau \hat{u}_h^n \rangle, \\
(\ell 3) &:= C \|\bar{d}_\tau \hat{u}_h^n\|_{\varepsilon,\infty} \big(\mathcal{H}^\varepsilon(u_h^n | \hat{u}_h^n) + \mathcal{H}^\varepsilon(u_h^{n-1} | \hat{u}_h^{n-1}) \big) + C' \|\bar{d}_\tau \hat{u}_h^n\|_{\varepsilon,\infty} \|\hat{u}_h^n - \hat{u}_h^{n-1}\|_\varepsilon^2.
\end{aligned}
$$

Estimation of the first line $(\ell 1)$**.** The definition of $\mathcal{H}^\varepsilon$ in (3.24) yields

$$
(\mathcal{H}^\varepsilon)'(u_h^n) - (\mathcal{H}^\varepsilon)'(\hat{u}_h^n) - (\mathcal{H}^\varepsilon)''(\hat{u}_h^n)(u_h^n - \hat{u}_h^n) = \begin{pmatrix} aP'(\rho_h^n | \hat{\rho}_h^n) + \frac{1}{2} a\varepsilon^2 (w_h^n - \hat{w}_h^n)^2 \\ a\varepsilon^2 (\rho_h^n - \hat{\rho}_h^n)(w_h^n - \hat{w}_h^n) \end{pmatrix}
$$

with $P'(\rho_h^n | \hat{\rho}_h^n) := P'(\rho_h^n) - P'(\hat{\rho}_h^n) - P''(\hat{\rho}_h^n)(\rho_h^n - \hat{\rho}_h^n)$. By Taylor's theorem, we can estimate

$$
P'(\rho_h^n | \hat{\rho}_h^n) \le |P'''(\rho_h^*)| (\rho_h^n - \hat{\rho}_h^n)^2 \le C(\rho_h^n - \hat{\rho}_h^n)^2
$$

with intermediate value $\rho_h^* = \xi \rho_h^n + (1-\xi)\hat{\rho}_h^n$ for some $\xi \in (0,1)$. The latter inequality holds since the pressure potential P is smooth due to (A1) and ρ_h^n and $\hat{\rho}_h^n$ are bounded due to (A3h) and Lemma 3.12, respectively. Moreover, by Young's inequality we have

$$
a\varepsilon^2 (\rho_h^n - \hat{\rho}_h^n)(w_h^n - \hat{w}_h^n) \le \tfrac{1}{2} \bar{a} \varepsilon |\rho_h^n - \hat{\rho}_h^n|^2 + \tfrac{1}{2} \bar{a} \varepsilon^3 |w_h^n - \hat{w}_h^n|^2.
$$

This enables us to estimate

$$
(\ell 1) \le C' \|u_h^n - \hat{u}_h^n\|_\varepsilon^2 \|\bar{d}_\tau \hat{u}_h^n\|_{\varepsilon,\infty} \le C'' \mathcal{H}^\varepsilon(u_h^n | \hat{u}_h^n),
$$

where we used that

$$
\|\bar{d}_\tau \hat{u}_h^n\|_{\varepsilon,\infty} \le \|\partial_\tau \hat{u}_h\|_{L^\infty(0,\tau_{max}; L^\infty(\mathcal{E}; \|\cdot\|_{\varepsilon,\infty}))} \le \|\partial_\tau u\|_{L^\infty(0,\tau_{max}; L^\infty(\mathcal{E}; \|\cdot\|_{\varepsilon,\infty}))} \le C'''
$$

by the construction of the projections, Lemma 3.11, and assumption (A4).

Estimation of the third line $(\ell 3)$**.** Using Taylor's theorem, the properties of the projections, and (A4), we find that

$$
\|\hat{u}_h^n - \hat{u}_h^{n-1}\|_\varepsilon^2 \le C \Delta\tau^2 \|\partial_\tau \hat{u}_h^n\|^2_{L^\infty(t^{n-1}, t^n; \|\cdot\|_\varepsilon)} \le C' \Delta\tau^2 \|\partial_\tau u\|^2_{L^\infty(t^{n-1}, t^n; \|\cdot\|_\varepsilon)} \le C'' \Delta\tau^2.
$$

Together with the estimate for $\|\bar{d}_\tau \hat{u}_h^n\|_{\varepsilon,\infty}$ from above, $(\ell 3)$ can be estimated by

$$
(\ell 3) \le C''(\mathcal{H}^\varepsilon(u_h^n | \hat{u}_h^n) + \mathcal{H}^\varepsilon(u_h^{n-1} | \hat{u}_h^{n-1})) + C''' \Delta\tau^2.
$$

Estimation of the second line $(\ell 2)$**.** The term in the second line of (3.57) also appears in the continuous estimate for the relative energy in (3.42). Hence, we proceed

similarly as in the proof of Theorem 3.5 and exploit the energy structure of (3.45)–(3.46). As before, the relations (3.25) for the variational derivatives of the energy yield

$$\begin{aligned}(\ell 2) &= (a\bar{d}_\tau \rho_h^n - a\bar{d}_\tau \hat{\rho}_h^n, h_h^n - \hat{h}_h^n)_{\mathcal{E}} + (\varepsilon^2 \bar{d}_\tau w_h^n - \varepsilon^2 \bar{d}_\tau \hat{w}_h^n, m_h^n - \hat{m}_h^n)_{\mathcal{E}} \\ &= -(\partial_x m_h^n - \partial_x \hat{m}_h^n, h_h^n - \hat{h}_h^n)_{\mathcal{E}} - \langle \mathrm{res}_1^n, h_h^n - \hat{h}_h^n\rangle + (h_h^n - \hat{h}_h^n, \partial_x m_h^n - \partial_x \hat{m}_h^n)_{\mathcal{E}} \\ &\quad - (\gamma|w_h^n|w_h^n - \gamma|\hat{w}_h^n|\hat{w}_h^n, m_h^n - \hat{m}_h^n)_{\mathcal{E}} - \langle \mathrm{res}_2^n, m_h^n - \hat{m}_h^n\rangle \\ &= -(\gamma|w_h^n|w_h^n - \gamma|\hat{w}_h^n|\hat{w}_h^n, m_h^n - \hat{m}_h^n)_{\mathcal{E}} - \langle \mathrm{res}_1^n, h_h^n - \hat{h}_h^n\rangle - \langle \mathrm{res}_2^n, m_h^n - \hat{m}_h^n\rangle \\ &= (\ell 2.1) + (\ell 2.2) + (\ell 2.3),\end{aligned}$$

where we used that (ρ_h^n, m_h^n) solves (3.45)–(3.46) and $(\hat{\rho}_h^n, \hat{m}_h^n)$ can be understood as perturbed solution with residuals given by (3.55)–(3.56). Note that since $\bar{d}_\tau \rho_h^n$ and $\partial_x m_h^n$ as well as $\bar{d}_\tau \hat{\rho}_h^n$ and $\partial_x \hat{m}_h^n$ are all piecewise constant, (3.45) and the corresponding perturbed equation can be tested with any L^2-function. Let us now estimate the three terms $(\ell 2.1)$, $(\ell 2.2)$, and $(\ell 2.3)$ separately.

Estimation of $(\ell 2.1)$. We observe that

$$\gamma|w_h^n|w_h^n - \gamma|\hat{w}_h^n|\hat{w}_h^n = 2\gamma \int_0^1 |\hat{w}_h^n + \xi(w_h^n - \hat{w}_h^n)|\, d\xi\, (w_h^n - \hat{w}_h^n),$$

since $(|\xi|\xi)' = 2|\xi|$. The integral can further be estimated from below and above by

$$\frac{|w_h^n| + |\hat{w}_h^n|}{4} \le \int_0^1 |\hat{w}_h^n + \xi(w_h^n - \hat{w}_h^n)|\, d\xi \le \frac{|w_h^n| + |\hat{w}_h^n|}{2}. \tag{3.62}$$

The upper estimate follows directly from the triangle inequality. The lower estimate can be shown by minimizing the functional $F(w_h^n) := \int_0^1 |\hat{w}_h^n + \xi(w_h^n - \hat{w}_h^n)|\, d\xi$ for fixed $\hat{w}_h^n$. Since F takes its minimum for $w_h^n = -\hat{w}_h^n$, it holds that

$$\int_0^1 |\hat{w}_h^n + \xi(w_h^n - \hat{w}_h^n)|\, d\xi \ge \min F(w_h^n) = \tfrac{1}{4}|\hat{w}_h^n| + \tfrac{1}{4}|w_h^n|.$$

We can further write

$$m_h^n - \hat{m}_h^n = a\rho_h^n w_h^n - a\hat{\rho}_h^n \hat{w}_h^n = a(\rho_h^n - \hat{\rho}_h^n) w_h^n + a\hat{\rho}_h^n (w_h^n - \hat{w}_h^n),$$

which together with the previous considerations leads to

$$\begin{aligned}(\gamma|w_h^n|w_h^n - \gamma|\hat{w}_h^n|\hat{w}_h^n)(m_h^n - \hat{m}_h^n) &= 2a\gamma w_h^n \int_0^1 |\hat{w}_h^n + \xi(w_h^n - \hat{w}_h^n)|\, d\xi\, (\rho_h^n - \hat{\rho}_h^n)(w_h^n - \hat{w}_h^n) \\ &\quad + 2a\gamma\hat{\rho}_h^n \int_0^1 |\hat{w}_h^n + \xi(w_h^n - \hat{w}_h^n)|\, d\xi\, (w_h^n - \hat{w}_h^n)^2 = (i) + (ii).\end{aligned}$$

Using (3.62) and Young's inequality we deduce that

$$\begin{aligned}(i) &\ge -\tfrac{1}{4}a\gamma\hat{\rho}_h^n(|w_h^n| + |\hat{w}_h^n|)(w_h^n - \hat{w}_h^n)^2 - 2a\gamma\tfrac{(w_h^n)^2}{\hat{\rho}_h^n}(|w_h^n| + |\hat{w}_h^n|)(\rho_h^n - \hat{\rho}_h^n)^2, \\ (ii) &\ge \tfrac{1}{2}a\gamma\hat{\rho}_h^n(|w_h^n| + |\hat{w}_h^n|)(w_h^n - \hat{w}_h^n)^2.\end{aligned}$$

With the bounds in (A3h), Lemma 3.12, and assumption (A3), this finally yields

$$\begin{aligned}(\ell 2.1) &\leq -\sum\nolimits_{e\in\mathcal{E}} \int_0^{\ell_e} (i) + (ii)\ dx \\ &\leq -\tfrac{1}{4}\sum\nolimits_{e\in\mathcal{E}} \int_0^{\ell_e} a_e\gamma_e\hat{\rho}_h^n(|w_h^n| + |\hat{w}_h^n|)(w_h^n - \hat{w}_h^n)^2\ dx + 5\bar{a}\bar{\gamma}\tfrac{\bar{w}^3}{\underline{\rho}}\|\rho_h^n - \hat{\rho}_h^n\|_{\mathcal{E}}^2 \\ &\leq -2\mathcal{D}(u_h^n|\hat{u}_h^n) + C\mathcal{H}^\varepsilon(u_h^n|\hat{u}_h^n)\end{aligned}$$

with relative dissipation functional $\mathcal{D}(\cdot|\cdot)$ defined in (3.43).

Estimation of $(\ell 2.2)$. From the definition of res_1 in (3.55) and the fact that $\bar{d}_\tau\hat{\rho}_h^n$ and $\partial_x\hat{m}_h^n$ are piecewise constant we conclude that $res_1^n = a\bar{d}_\tau\hat{\rho}_h^n + \partial_x\hat{m}_h^n$ holds pointwise and can thus be tested with any L^2-function. We find that

$$\begin{aligned}(\ell 2.2) &= -\langle res_1^n, h_h^n - \hat{h}_h^n\rangle = -(a\bar{d}_\tau\hat{\rho}_h^n + \partial_x\hat{m}_h^n, h_h^n - \hat{h}_h^n)_{\mathcal{E}} \\ &= -(a\bar{d}_\tau\hat{\rho}_h^n - a\partial_\tau\hat{\rho}_h^n, h_h^n - \hat{h}_h^n)_{\mathcal{E}} - (a\partial_\tau\hat{\rho}_h^n + \partial_x\hat{m}_h^n, h_h^n - \hat{h}_h^n)_{\mathcal{E}}.\end{aligned}$$

The last term vanishes due to the definition of the projections and the commuting diagram property in (3.52) as well as equation (3.22), which imply that

$$(a\partial_\tau\hat{\rho}_h^n, q)_{\mathcal{E}} + (\partial_x\hat{m}_h^n, q)_{\mathcal{E}} = 0 \qquad \text{for all } q \in L^2(\mathcal{E}). \tag{3.63}$$

Applying Hölder's and Young's inequality to the first term yields

$$-(a\bar{d}_\tau\hat{\rho}_h^n - \partial_\tau\hat{\rho}_h^n, h_h^n - \hat{h}_h^n)_{\mathcal{E}} \leq \tfrac{\bar{a}^2}{2}\|\bar{d}_\tau\hat{\rho}_h^n - \partial_\tau\hat{\rho}_h^n\|_{L^2(\mathcal{E})}^2 + \tfrac{1}{2}\|h_h^n - \hat{h}_h^n\|_{L^2(\mathcal{E})}^2.$$

Taylor's theorem allows us to estimate the first term by

$$\begin{aligned}\tfrac{\bar{a}^2}{2}\|\bar{d}_\tau\hat{\rho}_h^n - \partial_\tau\hat{\rho}_h^n\|_{L^2(\mathcal{E})}^2 &\leq \tfrac{\bar{a}^2}{4}\Delta\tau^2\|\partial_{\tau\tau}\hat{\rho}_h^n\|_{L^\infty(\tau^{n-1},\tau^n;L^2(\mathcal{E}))}^2 \\ &\leq \tfrac{\bar{a}^2}{4}\Delta\tau^2\|\partial_{\tau\tau}\rho(\tau^n)\|_{L^\infty(\tau^{n-1},\tau^n;L^2(\mathcal{E}))}^2 \leq C\Delta\tau^2,\end{aligned}$$

where we used the property of the projection Π_h in (3.52) as well as assumption (A4). In order to handle the second term, we observe that

$$|h_h^n - \hat{h}_h^n| = \left|\tfrac{\varepsilon^2}{2}(|w_h^n|^2 - |\hat{w}_h^n|^2) + P'(\rho_h^n) - P'(\hat{\rho}_h^n)\right| \leq C\varepsilon^2|w_h^n - \hat{w}_h^n| + C'|\rho_h^n - \hat{\rho}_h^n|$$

with constants that only depend on the bounds in the assumptions, where we used (A3h), the bounds on the projections in Lemma 3.12, and the fact that P is smooth by (A1). By the norm equivalence of the relative energy (3.35) it then holds that

$$\|h_h^n - \hat{h}_h^n\|_{L^2(\mathcal{E})}^2 \leq C''\mathcal{H}^\varepsilon(u_h^n|\hat{u}_h^n).$$

In summary, the term $(\ell 2.2)$ can be estimated by

$$(\ell 2.2) \leq C\Delta\tau^2 + C'\mathcal{H}^\varepsilon(u_h^n|\hat{u}_h^n).$$

Estimation of $(\ell 2.3)$. By definition of res_2 in (3.56) it holds that

$$\begin{aligned}(\ell 2.3) = &-\langle res_2^n, m_h^n - \hat{m}_h^n\rangle = -(\varepsilon^2\bar{d}_\tau\hat{w}_h^n, m_h^n - \hat{m}_h^n)_{\mathcal{E}} + (\hat{h}_h^n, \partial_x m_h^n - \partial_x\hat{m}_h^n)_{\mathcal{E}} \\ &- (\gamma|\hat{w}_h^n|\hat{w}_h^n, m_h^n - \hat{m}_h^n)_{\mathcal{E}} - \sum\nolimits_{v\in\mathcal{V}_\partial} \hat{h}_\partial^v(\tau^n)(m_h^n(v) - \hat{m}_h^n(v))n_e(v).\end{aligned}$$

Since (ρ, w) solves (3.22)–(3.23), we can add (3.23) tested with $r = m_h^n - \hat{m}_h^n$ to (ℓ2.3) and obtain

$$\begin{aligned}(\ell 2.3) &= (\varepsilon^2 \partial_\tau w^n - \varepsilon^2 \bar{d}_\tau \hat{w}_h^n, m_h^n - \hat{m}_h^n)_{\mathcal{E}} - (h^n - \hat{h}_h^n, \partial_x m_h^n - \partial_x \hat{m}_h^n)_{\mathcal{E}} \\ &\quad + (\gamma |w^n| w^n - \gamma |\hat{w}_h^n| \hat{w}_h^n, m_h^n - \hat{m}_h^n)_{\mathcal{E}} = (i) + (ii) + (iii).\end{aligned} \tag{3.64}$$

Here, we abbreviate $\rho^n = \rho(\tau^n)$, $w^n = w(\tau^n)$, $m^n = m(\tau^n)$ and $h^n = h(\tau^n)$. In the following, we estimate the terms $(i) - (iii)$ separately and exploit the projection error estimates (3.53) in order to get convergence rates. By applying Hölder's and Young's inequality, the first term can be estimated by

$$(i) \leq \tfrac{\varepsilon^2}{2} \|\partial_\tau w^n - \bar{d}_\tau \hat{w}_h^n\|_{L^2(\mathcal{E})}^2 + \tfrac{\varepsilon^2}{2} \|m_h^n - \hat{m}_h^n\|_{L^2(\mathcal{E})}^2.$$

The second term on the right-hand side can be further estimated by $C\mathcal{H}^\varepsilon(u_h^n | \hat{u}_h^n)$ due to the norm equivalence (3.35). The constant C only depends on the bounds in the assumptions and Lemma 3.12. For the first term in this expansion, applying the triangle inequality and the projection error estimates (3.53), we deduce that

$$\begin{aligned}\tfrac{\varepsilon^2}{2} \|\partial_\tau w^n - \bar{d}_\tau \hat{w}_h^n\|_{L^2(\mathcal{E})}^2 &\leq \varepsilon^2 \|\partial_\tau w^n - \partial_\tau \hat{w}_h^n\|_{L^2(\mathcal{E})}^2 + \varepsilon^2 \|\partial_\tau \hat{w}_h^n - \bar{d}_\tau \hat{w}_h^n\|_{L^2(\mathcal{E})}^2 \\ &\leq C\big(\|\rho^n - \hat{\rho}_h^n\|_{L^2(\mathcal{E})}^2 + \|\partial_\tau \rho^n - \partial_\tau \hat{\rho}_h^n\|_{L^2(\mathcal{E})}^2 + \|m^n - \hat{m}_h^n\|_{L^2(\mathcal{E})}^2 + \|\partial_\tau m^n - \partial_\tau \hat{m}_h^n\|_{L^2(\mathcal{E})}^2\big) \\ &\quad + C' \Delta\tau^2 \|\varepsilon \partial_{\tau\tau} \hat{w}\|_{L^\infty(\tau^{n-1}, \tau^n; L^2(\mathcal{E}))}^2 \leq C'' h^2 + C''' \Delta\tau^2\end{aligned}$$

with constants that only depend on the bounds in the assumptions and Lemma 3.12. In summary, we find that

$$(i) \leq C\mathcal{H}^\varepsilon(u_h^n | \hat{u}_h^n) + C'(h^2 + \Delta\tau^2).$$

Using the fact that (3.45) can be tested with any L^2-function as well as (3.63) we find for the second term in (3.64) that

$$\begin{aligned}(ii) &= (h^n - \hat{h}_h^n, a\bar{d}_\tau \rho_h^n - a\partial_\tau \hat{\rho}_h^n)_{\mathcal{E}} \\ &= (h^n - \hat{h}_h^n, a\bar{d}_\tau \rho_h^n - a\bar{d}_\tau \hat{\rho}_h^n)_{\mathcal{E}} + (h^n - \hat{h}_h^n, a\bar{d}_\tau \hat{\rho}_h^n - a\partial_\tau \hat{\rho}_h^n)_{\mathcal{E}}.\end{aligned}$$

The second term in this expansion can be estimated by Hölder's and Young's inequality

$$(h^n - \hat{h}_h^n, a\bar{d}_\tau \hat{\rho}_h^n - a\partial_\tau \hat{\rho}_h^n)_{\mathcal{E}} \leq \tfrac{1}{2} \|h^n - \hat{h}_h^n\|_{L^2(\mathcal{E})}^2 + \tfrac{\bar{a}^2}{2} \|\bar{d}_\tau \hat{\rho}_h^n - \partial_\tau \hat{\rho}_h^n\|_{L^2(\mathcal{E})}^2 \leq C(h^2 + \Delta\tau^2),$$

since $|h^n - \hat{h}_h^n| \leq C|\varepsilon w^n - \varepsilon \hat{w}_h^n| + C'|\rho^n - \hat{\rho}_h^n|$ holds due to the fact that P is smooth by assumption (A1). All constants only depend on the bounds in the assumptions and in Lemma 3.12. The rates follow from the projection error estimates (3.53). For the first term, we utilize the discrete integration-by-parts formula

$$\bar{d}_\tau u^n v^n = -u^{n-1} \bar{d}_\tau v^n + \tfrac{1}{\Delta\tau}(u^n v^n - u^{n-1} v^{n-1}),$$

which yields

$$\begin{aligned}(h^n - \hat{h}_h^n, a\bar{d}_\tau \rho_h^n - a\bar{d}_\tau \hat{\rho}_h^n)_{\mathcal{E}} &= -(\bar{d}_\tau h^n - \bar{d}_\tau \hat{h}_h^n, a\rho_h^{n-1} - a\hat{\rho}_h^{n-1})_{\mathcal{E}} \\ &\quad + \tfrac{1}{\Delta\tau}(h - \hat{h}_h, a\rho_h - a\hat{\rho}_h)_{\mathcal{E}}\Big|_{\tau^{n-1}}^{\tau^n}.\end{aligned}$$

By Hölder's and Young's inequality, we further deduce that

$$-(\bar{d}_\tau h^n - \bar{d}_\tau \hat{h}_h^n, a\rho_h^{n-1} - a\hat{\rho}_h^{n-1})_{\mathcal{E}} \leq \tfrac{1}{2}\|\bar{d}_\tau h^n - \bar{d}_\tau \hat{h}_h^n\|_{L^2(\mathcal{E})}^2 + \tfrac{\bar{a}^2}{2}\|\rho_h^{n-1} - \hat{\rho}_h^{n-1}\|_{L^2(\mathcal{E})}^2.$$

The second term can be estimated by $C\mathcal{H}^\varepsilon(u_h^{n-1}|\hat{u}_h^{n-1})$ due to the norm equivalence (3.35), whereas the first term can be split into

$$\|\bar{d}_\tau h^n - \bar{d}_\tau \hat{h}_h^n\|_{L^2(\mathcal{E})}^2 \leq 3\big(\|\bar{d}_\tau h^n - \partial_\tau h^n\|_{L^2(\mathcal{E})}^2 + \|\partial_\tau h^n - \partial_\tau \hat{h}_h^n\|_{L^2(\mathcal{E})}^2 + \|\partial_\tau \hat{h}_h^n - \bar{d}_\tau \hat{h}_h^n\|_{L^2(\mathcal{E})}^2\big).$$

By Taylor's theorem, the projection error estimates (3.53) and the bounds in the assumptions, the individual terms can be estimated by

$$\begin{aligned}
\|\bar{d}_\tau h^n - \partial_\tau h^n\|_{L^2(\mathcal{E})}^2 &\leq C\Delta\tau^2 \|\partial_{\tau\tau} h\|_{L^\infty(\tau^{n-1},\tau^n;L^2(\mathcal{E}))}^2 \leq C'\Delta\tau^2,\\
\|\partial_\tau h^n - \partial_\tau \hat{h}_h^n\|_{L^2(\mathcal{E})}^2 &\leq C'h^2 \|\partial_\tau h^n\|_{H^1(\mathcal{E})}^2 \leq C'h^2,\\
\|\partial_\tau \hat{h}_h^n - \bar{d}_\tau \hat{h}_h^n\|_{L^2(\mathcal{E})}^2 &\leq C\Delta\tau^2 \|\partial_{\tau\tau} \hat{h}_h\|_{L^\infty(\tau^{n-1},\tau^n;L^2(\mathcal{E}))}^2 \leq C'\Delta\tau^2,
\end{aligned}$$

where we used that $\|\partial_{\tau\tau} h_h\|$ and $\|\partial_{\tau\tau} \hat{h}_h\|$ can be estimated by the bounds for the time derivatives of ρ and m in (A4). Overall, we find that

$$(ii) \leq C\mathcal{H}^\varepsilon(u_h^n|\hat{u}_h^n) + C'(h^2 + \Delta\tau^2) + \tfrac{1}{\Delta\tau}(h - \hat{h}_h, a\rho_h - a\hat{\rho}_h)\big|_{\tau^{n-1}}^{\tau^n}.$$

It remains to estimate the third term (iii) in (3.64). Note that we need to be careful with the asymptotic parameter ε and are going to exploit the extra stability provided by the relative dissipation functional in (ℓ2.1). First, we expand

$$\begin{aligned}
(iii) &= (\gamma(|w^n| - |\hat{w}_h^n|)(w^n - \hat{w}_h^n), m_h^n - \hat{m}_h^n)_{\mathcal{E}} + (\gamma|\hat{w}_h^n|(w^n - \hat{w}_h^n), m_h^n - \hat{m}_h^n)_{\mathcal{E}}\\
&\quad + (\gamma(|w^n| - |\hat{w}_h^n|)\hat{w}_h^n, m_h^n - \hat{m}_h^n)_{\mathcal{E}} = (iii.1) + (iii.2) + (iii.3).
\end{aligned}$$

Hölder's and Young's inequality as well as the bounds in the assumptions and in Lemma 3.12 enable us to estimate

$$\begin{aligned}
(iii.1) &\leq \bar{a}\bar{\gamma}\bar{\rho}\|(w^n - \hat{w}_h^n)^2\|_{L^{3/2}(\mathcal{E})}\|w_h^n - \hat{w}_h^n\|_{L^3(\mathcal{E})} + \bar{a}\bar{\gamma}\bar{\rho}\|(w^n - \hat{w}_h^n)^2\|_{L^2(\mathcal{E})}\|\rho_h^n - \hat{\rho}_h^n\|_{L^2(\mathcal{E})}\\
&\leq \tfrac{2}{3}(\bar{a}\bar{\gamma}\bar{\rho})^{3/2}\delta^{-3/2}\|w^n - \hat{w}_h^n\|_{L^3(\mathcal{E})}^3 + \tfrac{1}{3}\delta^3\|w_h^n - \hat{w}_h^n\|_{L^3(\mathcal{E})}^3 + Ch^2 + C'\mathcal{H}^\varepsilon(u_h^n|\hat{u}_h^n)\\
&\leq C''(\delta)h^3 + \tfrac{1}{4}\mathcal{D}(u_h^n|\hat{u}_h^n) + Ch^2 + C'\mathcal{H}^\varepsilon(u_h^n|\hat{u}_h^n)
\end{aligned}$$

for some $\delta > 0$ sufficiently small so that the second term in the second line can be bounded by the relative dissipation functional (3.43). Here, we used the projection error estimates (3.53) and the norm equivalence for the relative energy (3.35). Similarly, we estimate

$$(iii.2) + (iii.3) \leq \tfrac{1}{2\delta'}\bar{\gamma}\bar{w}\|w_h^n - \hat{w}_h^n\|_{L^2(\mathcal{E})}^2 + \tfrac{1}{2}\delta'\|(m_h^n - \hat{m}_h^n)|\hat{w}_h^n|^{1/2}\|_{L^2(\mathcal{E})}^2.$$

By the projection error estimates (3.53) the first term can be bounded by $C(\delta')h^2$. The second term equals

$$\begin{aligned}
\tfrac{1}{2}\delta'\|(m_h^n - \hat{m}_h^n)|\hat{w}_h^n|^{1/2}\|_{L^2(\mathcal{E})}^2 &= \delta'\bar{a}\bar{\rho}\sum_{e\in\mathcal{E}}\int_0^{\ell_e}(w_h^n - \hat{w}_h^n)^2\hat{\rho}_h^n|\hat{w}_h^n|\,dx + C(\delta')\|\rho_h^n - \hat{\rho}_h^n\|_{L^2(\mathcal{E})}^2\\
&\leq \tfrac{1}{4}\mathcal{D}(u_h^n|\hat{u}_h^n) + C'(\delta')\mathcal{H}^\varepsilon(u_h^n|\hat{u}_h^n),
\end{aligned}$$

which holds for $\delta' > 0$ small enough due to the definition of $\mathcal{D}(\cdot|\cdot)$ in (3.43). In summary, we obtain

$$(\ell 2.3) \leq C\mathcal{H}^\varepsilon(u_h^n|\hat{u}_h^n) + C'\mathcal{H}^\varepsilon(u_h^{n-1}|\hat{u}_h^{n-1}) + C''(h^2 + \Delta\tau^2) + \tfrac{1}{\Delta\tau}(h - \hat{h}_h, a\rho_h - a\hat{\rho}_h)\big|_{\tau^{n-1}}^{\tau^n}.$$

The final estimate for $(\ell 2)$ then follows from the separate estimates for $(\ell 2.1) - (\ell 2.3)$, which then together with the estimates for the other two lines $(\ell 1)$ and $(\ell 2)$ yields the assertion of Lemma 3.15. □

This completes the proof of Theorem 1.23 and closes our investigations for the isothermal gas transport in pipe networks.

3.3. Non-isothermal gas transport

In this section, we aim to extend some of the ideas and results from the previous sections to the non-isothermal gas transport in pipe networks. In particular, we derive a reformulation of the governing equations (3.5)–(3.7) and propose a suitable set of coupling conditions at interior junctions. It turns out that the resulting system has a similar "energy structure" allowing for a simple proof of global balance laws.

3.3.1. Preliminaries

We make use of the notation introduced in Section 3.1.1 and again start with deriving a different set of equations that allows us to alternatively characterize smooth solutions of (3.5)–(3.7) on a single pipe. As a first step, we observe that the variational derivatives of the total energy density $E^\varepsilon(\rho, w, s) := \frac{1}{2}\varepsilon^2 a\rho w^2 + a\rho e$ are given by

$$\delta_\rho E^\varepsilon = ah^\varepsilon, \qquad \delta_w E^\varepsilon = \varepsilon^2 m, \qquad \delta_s E^\varepsilon = a\rho\theta, \tag{3.65}$$

where we used the constitutive equations (3.4) and introduced the total specific enthalpy $h^\varepsilon = \frac{\varepsilon^2}{2}w^2 + e + \frac{p}{\rho}$. By (3.5)–(3.6) we further find that

$$\varepsilon^2\partial_\tau w = \varepsilon^2\partial_\tau(\tfrac{m}{a\rho}) = \tfrac{\varepsilon^2}{a\rho}\partial_\tau m - \tfrac{\varepsilon^2}{a\rho^2}m\partial_\tau\rho = -\tfrac{1}{\rho}\partial_x(\varepsilon^2\rho w^2 + p) - \gamma|w|w + \tfrac{\varepsilon^2}{a^2\rho^2}m\partial_x m.$$

Using the relations for the specific internal energy (3.4), one can see that

$$\tfrac{1}{\rho}\partial_x p = \partial_x(\tfrac{p}{\rho}) + \tfrac{p}{\rho^2}\partial_x\rho = \partial_x(\tfrac{p}{\rho}) + \delta_\rho e\partial_x\rho = \partial_x(\tfrac{p}{\rho} + e) - \theta\partial_x s.$$

We further observe that

$$\tfrac{1}{\rho}\partial_x(\rho w^2) - \tfrac{m}{a^2\rho^2}\partial_x m = \tfrac{w}{a\rho}\partial_x m + \tfrac{\rho w}{\rho}\partial_x w - \tfrac{w}{a\rho}\partial_x m = w\partial_x w = \tfrac{1}{2}\partial_x(w^2).$$

In summary, this shows that

$$\varepsilon^2\partial_\tau w + \partial_x h^\varepsilon - \theta\partial_x s = -\gamma|w|w.$$

From (3.5), (3.65), and the above equation we deduce

$$\begin{aligned}\frac{d}{d\tau}E^\varepsilon &= \delta_\rho E^\varepsilon \partial_\tau \rho + \delta_w E^\varepsilon \partial_\tau w + \delta_s E^\varepsilon \partial_\tau s \\ &= a h^\varepsilon \partial_\tau \rho + \varepsilon^2 m \partial_\tau w + a\rho\theta\partial_\tau s \\ &= -h^\varepsilon \partial_x m - m\partial_x h^\varepsilon - \gamma m|w|w + m\theta\partial_x s + a\rho\theta\partial_\tau s \\ &= -\partial_x(mh^\varepsilon) - \gamma|m|w^2 + m\theta\partial_x s + a\theta\rho\partial_\tau s.\end{aligned}$$

By (3.7) we know that

$$\begin{aligned}\varepsilon^3\frac{d}{d\tau}E^\varepsilon &= -\varepsilon^3\partial_x(w(E^\varepsilon + ap)) - \beta(\theta-\theta^0) - \varepsilon^3\gamma|m|w^2 \\ &= -\varepsilon^3\partial_x\big(\tfrac{\varepsilon^2}{2}mw^2 + a\rho we + awp\big) - \beta(\theta-\theta^0) - \varepsilon^3\gamma|m|w^2 \\ &= -\varepsilon^3\partial_x(mh^\varepsilon) - \beta(\theta-\theta^0) - \varepsilon^3\gamma|m|w^2.\end{aligned}$$

Comparing the two equations for $\frac{d}{d\tau}E^\varepsilon$ shows that

$$\varepsilon^3 a\rho\partial_\tau s + \varepsilon^3 m\partial_x s = -\beta\frac{\theta-\theta^0}{\theta}$$

must hold and we can replace (3.7) by this equation, leading to the following system

$$a\partial_t\rho + \partial_x m = 0, \tag{3.66}$$

$$\varepsilon^2\partial_\tau w + \partial_x g^\varepsilon - (\theta-\theta^0)\partial_x s = -\gamma|w|w, \tag{3.67}$$

$$\varepsilon^3 a\rho\partial_\tau s + \varepsilon^3 m\partial_x s = -\beta\frac{\theta-\theta^0}{\theta}, \tag{3.68}$$

where we introduced a new variable, the specific free enthalpy or specific Gibb's free energy

$$g^\varepsilon := h^\varepsilon - \theta^0 s = \frac{\varepsilon^2}{2}w^2 + \frac{p}{\rho} + e - \theta^0 s. \tag{3.69}$$

For sufficiently smooth solutions the system (3.66)–(3.68) is equivalent to the original system (3.5)–(3.7) with constitutive equations (3.4).

3.3.2. Model problem

We now turn to describing the full model on the pipe network. Let (3.66)–(3.68) be satisfied on each edge $e \in \mathcal{E}$, i.e.,

$$a_e\partial_\tau\rho_e + \partial_x m_e = 0, \tag{3.70}$$

$$\varepsilon^2\partial_\tau w_e + \partial_x g_e^\varepsilon - (\theta_e-\theta^0)\partial_x s_e = -\gamma_e|w_e|w_e, \tag{3.71}$$

$$\varepsilon^3 a_e\rho_e\partial_\tau s_e + \varepsilon^3 m_e\partial_x s_e = -\beta_e\frac{\theta_e-\theta^0}{\theta_e} \tag{3.72}$$

for all $0 < x < \ell_e,\ e \in \mathcal{E}$ and $\tau > 0$ with

$$m_e = a_e\rho_e w_e, \quad g_e^\varepsilon = \frac{\varepsilon^2}{2}w_e^2 + \frac{p(\rho_e,s_e)}{\rho_e} + e(\rho_e,s_e) - \theta^0 s_e, \quad \theta_e = \theta(\rho_e,s_e). \tag{3.73}$$

Figure 3.2.: Number of boundary conditions that are needed for different flow situations. The arc direction corresponds to the flow direction.

The system has to be complemented by suitable boundary and coupling conditions. In the subsonic regime, which is assumed to be of relevance in gas pipelines, two boundary conditions have to be prescribed at the inflow boundary of each pipe, while only one condition is needed at the outflow boundary [123]; see Figure 3.2 for an illustration. Let us thus introduce the sets

$$\mathcal{V}_\partial^{in}(\tau) = \{v \in \mathcal{V}_\partial : m_e(v,\tau)n_e(v) < 0\} \quad \text{and} \quad \mathcal{V}_\partial^{out}(\tau) = \{v \in \mathcal{V}_\partial : m_e(v,\tau)n_e(v) > 0\}$$

of inflow and outflow boundary vertices at time $\tau \geq 0$. Moreover, for each interior vertex $v \in \mathcal{V}_0$ we define the sets

$$\begin{aligned} \mathcal{E}^{in}(v,\tau) &= \{e \in \mathcal{E}(v) : m_e(v,\tau)n_e(v) > 0\}, \\ \mathcal{E}^{out}(v,\tau) &= \{e \in \mathcal{E}(v) : m_e(v,\tau)n_e(v) < 0\} \end{aligned}$$

of edges carrying flow into or out of the vertex. Note that the above spaces depend on the time τ in comparison to the corresponding spaces introduced in Chapter 1.1.2. The choice of appropriate boundary conditions that give rise to a well-posed problem is in general not an easy task; a review can be found in [123]. At the network boundary, we prescribe

$$g_e^\varepsilon(v,\tau) = \hat{g}_\partial^v(\tau), \qquad v \in \mathcal{V}_\partial,\ e \in \mathcal{E}(v),\ \tau > 0, \tag{3.74}$$

$$s_e(v,\tau) = \hat{s}_\partial^v(\tau), \qquad v \in \mathcal{V}_\partial^{in}(\tau),\ e \in \mathcal{E}(v),\ \tau > 0. \tag{3.75}$$

In order to ensure basic physical principles at network junctions, we impose the following coupling conditions

$$\sum\nolimits_{e\in\mathcal{E}(v)} m_e(v,\tau)n_e(v) = 0, \qquad v \in \mathcal{V}_0,\ \tau > 0, \tag{3.76}$$

$$g_e^\varepsilon(v,\tau) = \hat{g}_v^\varepsilon(\tau), \qquad v \in \mathcal{V}_0,\ e \in \mathcal{E}(v),\ \tau > 0, \tag{3.77}$$

$$s_e(v,\tau) = \hat{s}_v(\tau) \qquad v \in \mathcal{V}_0,\ e \in \mathcal{E}^{out}(v,\tau),\ \tau > 0 \tag{3.78}$$

with mixing value

$$\hat{s}_v(\tau) = \frac{\sum_{e\in\mathcal{E}^{in}(v,\tau)} m_e(v,\tau)s_e(v,\tau)n_e(v)}{\sum_{e\in\mathcal{E}^{in}(v,\tau)} m_e(v,\tau)n_e(v)}, \qquad v \in \mathcal{V}_0,\ \tau > 0. \tag{3.79}$$

The first coupling condition (3.76) guarantees conservation of mass at junctions and ensures that $m \in H(\mathrm{div};\mathcal{E})$ defined in (3.21). By introducing additional degrees of freedom $\hat{g}_v^\varepsilon$ and $\hat{s}_v$ at interior vertices $v \in \mathcal{V}_0$, the second condition (3.77) enforces continuity of the free enthalpy, wheres the third condition (3.78) ensures outflow continuity of the specific

entropy which ultimately guarantees conservation of entropy at junctions. We then call any triple of functions

$$\rho, w, s \in C^1([0, \tau_{max}]; L^2(\mathcal{E})) \cap C^0([0, \tau_{max}]; H^1_{pw}(\mathcal{E}))$$

a *classical solution* of (3.70)–(3.79) if the model equations are satisfied in a pointwise sense up to some $\tau_{max} > 0$.

Remark 3.16. The fact that entropy is conserved at network junctions might not be physically correct since we would expect that entropy is produced due to the mixing. The coupling condition (3.78)–(3.79) for the entropy could be replaced by

$$\eta(s_e(v, \tau)) = \hat{\eta}_v(\tau) \qquad v \in \mathcal{V}_0,\ e \in \mathcal{E}^{out}(v, \tau),\ \tau > 0 \tag{3.80}$$

with mixing value

$$\hat{\eta}_v(\tau) = \frac{\sum_{e \in \mathcal{E}^{in}(v,\tau)} m_e(v, \tau)\eta(s_e(v, \tau))n_e(v)}{\sum_{e \in \mathcal{E}^{in}(v,\tau)} m_e(v, \tau)n_e(v)}, \qquad v \in \mathcal{V}_0,\ \tau > 0 \tag{3.81}$$

for some convex and strictly monotonically increasing function $\eta : \mathbb{R} \to \mathbb{R}$. This condition now allows for entropy production at junctions if $\eta \neq \mathrm{id}$.

Example 3.17 (Ideal gas)**.** Let us consider the case of a simple ideal gas that fulfills the following thermodynamic relations

$$p = R\rho\theta, \qquad e = c_v\theta = \frac{R}{\gamma - 1}\theta$$

with specific heat at constant volume $c_v = \frac{R}{\gamma-1}$, specific gas constant $R = \mu\mathcal{R}$, where $\mathcal{R} = 8.314\frac{J}{mol\,K}$ is the universal gas constant and μ the mole-mass fraction, as well as $1 < \gamma \leq 5/3$; see [58, Ch. III.1]. Let us note that $\gamma = 5/3$ corresponds to a monatomic gas in dimension 3. From (3.4) we deduce that

$$e(\rho, s) = \rho^{\gamma-1}e^{s/c_v} \qquad \text{and} \qquad \theta(\rho, s) = c_v^{-1}e(\rho, s) = c_v^{-1}\rho^{\gamma-1}e^{s/c_v}.$$

The latter relation can be transformed to

$$s(\rho, \theta) = c_v \log\left(\frac{c_v\theta}{\rho^{\gamma-1}}\right).$$

The function $\eta : \mathbb{R} \to \mathbb{R},\ s \mapsto e^{s/c_v}$ is convex and strictly monotonically increasing. For this choice the coupling conditions (3.80)–(3.81) correspond to a mixing of the quantity $c_v\theta/\rho^{\gamma-1}$ and entropy will be produced at network junctions.

3.3.3. Weak formulation

Our analysis and numerical approximation for the non-isothermal gas transport in pipe networks are again based on a weak characterization of classical solutions.

Lemma 3.18. *Any classical solution* (ρ, w, s) *of* (3.70)–(3.79) *satisfies*

$$(a\partial_\tau \rho, q)_{\mathcal{E}} + (\partial_x m, q)_{\mathcal{E}} = 0, \tag{3.82}$$

$$(\varepsilon^2 \partial_\tau w, r)_{\mathcal{E}} - (g^\varepsilon, \partial_x r)_{\mathcal{E}} - ((\theta - \theta^0)\partial_x s, r)_{\mathcal{E}} + (\gamma |w| w, r)_{\mathcal{E}} = -\sum_{v \in \mathcal{V}_\partial} \hat{g}^v_\partial r_e(v) n_e(v), \tag{3.83}$$

$$(\varepsilon^3 a\rho \partial_\tau s, z)_{\mathcal{E}} + (\varepsilon^3 m \partial_x s, z)_{\mathcal{E}} = -(\beta \frac{\theta - \theta^0}{\theta}, z)_{\mathcal{E}} \tag{3.84}$$

for all q, $z \in L^2(\mathcal{E})$, $r \in H(\mathrm{div}; \mathcal{E})$ *and* $0 < \tau < \tau_{max}$.

Proof. The weak formulation immediately follows from multiplying (3.70)–(3.72) with q, r, z, integrating over each edge $e \in \mathcal{E}$ and summing up. In the second equation, we further apply integration-by-parts to the second term, i.e.,

$$(\partial_x g^\varepsilon, r)_{\mathcal{E}} = -(g^\varepsilon, \partial_x r)_{\mathcal{E}} + \sum\nolimits_{v \in \mathcal{V}} \sum\nolimits_{e \in \mathcal{E}(v)} g^\varepsilon_e(v) r_e(v) n_e(v).$$

The contributions at interior vertices $v \in \mathcal{V}_0$ vanish due to the continuity of g^ε by (3.77) and the fact that $r \in H(\mathrm{div}; \mathcal{E})$. □

3.3.4. Basic properties

Let us now derive some properties of solutions to the non-isothermal gas transport problem.

Energy structure and formal asymptotics to the parabolic limit

We associate the following *exergy* or *ballistic free energy* functional

$$\mathcal{H}^\varepsilon(\rho, w, s) = \sum\nolimits_{e \in \mathcal{E}} \int_0^{\ell_e} a_e \Big(\frac{\varepsilon^2}{2} \rho_e w_e^2 + \rho_e e(\rho_e, s_e) - \rho_e s_e \theta^0 \Big) \, dx \tag{3.85}$$

to the system (3.70)–(3.79); see [47, Ch. 1.3]. The variational derivatives are given by

$$\delta_\rho \mathcal{H}^\varepsilon = a g^\varepsilon, \qquad \delta_w \mathcal{H}^\varepsilon = \varepsilon^2 m, \qquad \delta_s \mathcal{H}^\varepsilon = a\rho(\theta - \theta^0). \tag{3.86}$$

Similar to the isothermal case, we call (ρ, w, s) the *state* and $(g^\varepsilon, m, \rho(\theta - \theta^0))$ the corresponding *co-state variables*; these will play an important role in the following considerations. By formally setting $\varepsilon = 0$ in (3.72) we observe that $\theta(\rho, s) = \theta^0$ is constant. Consequently, $s = s(\rho; \theta^0)$ is a function of ρ only. The inversion of this equation is always possible since $\partial_s \theta(\rho, s) > 0$ holds under the assumption that the gas is in a local thermodynamic equilibrium, which implies that $\theta(\rho, s)$ is invertible w.r.t. s; see [58, Ch. III.1.1]. Moreover, the pressure $p = p(\rho)$ then also depends on ρ only. We further deduce from (3.4) that

$$e(\rho, s) = \int_1^\rho \frac{p(r)}{r^2} \, dr + \theta^0 s. \tag{3.87}$$

The exergy functional thus becomes

$$\mathcal{H}^0(\rho, w) = \sum\nolimits_{e\in\mathcal{E}} \int_0^{\ell_e} a_e\rho_e \int_1^{\rho_e} \frac{p(r)}{r^2}\, dr\, dx = \sum\nolimits_{e\in\mathcal{E}} \int_0^{\ell_e} aP(\rho_e)\, dx$$

with pressure potential $P(\rho) = \rho \int_1^\rho \frac{p(r)}{r^2}\, dr$ that was already introduced in Section 3.1.1. In the limit $\varepsilon = 0$, the system (3.70)–(3.72) thus reduces to the transformed parabolic gas transport model that on each edge $e \in \mathcal{E}$ is given by

$$\begin{aligned} a_e\partial_\tau\rho_e + \partial_x m_e &= 0, \\ \partial_x P'(\rho_e) &= -\gamma_e|w_e|w_e, \end{aligned}$$

with $s = s(\rho; \theta^0)$ and associated energy $\mathcal{H}^0$. Here, we used that for $\varepsilon = 0$ we have

$$g^0 = \frac{p}{\rho} + e(\rho, s) - \theta^0 s = \frac{p}{\rho} + \int_1^\rho \frac{p(r)}{r^2}\, dr = P'(\rho)$$

by (3.87). The coupling conditions for the mass flux m and the free enthalpy g in (3.76)–(3.77) reduce to the corresponding ones for the parabolic limit problem, i.e., $m \in H(\mathrm{div}; \mathcal{E})$ and ρ being continuous across junctions; compare with (3.15)–(3.20) for $\varepsilon = 0$ and [113].

From the previous considerations, we see that the system (3.82)–(3.84) has an "energy structure" and can be written as the following abstract system

$$\mathcal{C}^\varepsilon\partial_\tau u + \mathcal{J}(u)\boldsymbol{z}^\varepsilon(u) + \mathcal{R}^\varepsilon(u)\boldsymbol{z}^\varepsilon(u) = \boldsymbol{b}_\partial, \tag{3.88}$$

$$\boldsymbol{z}^\varepsilon(u) = (\mathcal{C}^\varepsilon)^{-1}(\mathcal{H}^\varepsilon)'(u) \tag{3.89}$$

with *state variables* $u = (\rho, w, s)$, *co-state variables* $\boldsymbol{z}^\varepsilon(u) = (g^\varepsilon, m, \rho(\theta - \theta^0))$, and operators defined by

$$\begin{aligned} \langle \mathcal{C}^\varepsilon u, v\rangle &:= (a\partial_\tau\rho, q)_\mathcal{E} + (\varepsilon^2\partial_\tau w, r)_\mathcal{E} + (a\partial_\tau s, z)_\mathcal{E}, \\ \langle \mathcal{J}(u)\boldsymbol{z}^\varepsilon(u), v\rangle &:= (\partial_x m, q)_\mathcal{E} - (g^\varepsilon, \partial_x r)_\mathcal{E} - (\frac{\partial_x s}{\rho}\rho(\theta - \theta^0), r)_\mathcal{E} + (\frac{\partial_x s}{\rho} m, z)_\mathcal{E}, \\ \langle \mathcal{R}^\varepsilon(u)\boldsymbol{z}^\varepsilon(u), v\rangle &:= (\gamma\frac{|w|}{\rho} m, r)_\mathcal{E} + (\frac{\beta}{\varepsilon^3\rho^2\theta}\rho(\theta - \theta^0), z)_\mathcal{E}, \\ \langle \boldsymbol{b}_\partial, v\rangle &:= -\sum\nolimits_{v\in\mathcal{V}_\partial} \hat{g}_\partial^v r_e(v) n_e(v), \end{aligned}$$

where $v = (q, r, z) \in L^2(\mathcal{E}) \times H(\mathrm{div}; \mathcal{E}) \times L^2(\mathcal{E})$ is a test function. Note that the third equation (3.84) was divided by ρ. The operator $\mathcal{C}^\varepsilon$ is positive definite, $\mathcal{R}^\varepsilon(u)$ is positive semi-definite, and $\mathcal{J}(u)$ is skew-symmetric. In comparison to the abstract form (3.26)–(3.27) of the isothermal gas equations, both systems have a similar structure, but the operator $\mathcal{J}$ now depends on the state variable u.

Global balance laws

Based on the weak formulation of the equations and the above relations between state and co-state variables, one can immediately derive the following global balance laws.

Lemma 3.19. *Let* (ρ, w, s) *be a classical solution to* (3.70)–(3.79)*. Then,*

$$\frac{d}{d\tau}\int_{\mathcal{E}} a\rho\, dx = -\sum\nolimits_{v\in\mathcal{V}_\partial} m_e(v)n_e(v) \tag{3.90}$$

$$\frac{d}{d\tau}\mathcal{H}^\varepsilon(\rho, w, s) = -\sum_{v\in\mathcal{V}_\partial} \hat{g}^v_\partial m_e(v)n_e(v) - \int_{\mathcal{E}} \gamma|m|w^2\, dx - \int_{\mathcal{E}} \frac{\beta}{\varepsilon^3}\frac{(\theta-\theta^0)^2}{\theta}\, dx, \tag{3.91}$$

$$\frac{d}{d\tau}\int_{\mathcal{E}} a\rho s\, dx = -\sum\nolimits_{v\in\mathcal{V}_\partial} m_e(v)s_e(v)n_e(v) - \int_{\mathcal{E}} \frac{\beta}{\varepsilon^3}\frac{\theta-\theta^0}{\theta}\, dx. \tag{3.92}$$

If the coupling conditions for the entropy are replaced by (3.80)–(3.81)*, it holds that*

$$\frac{d}{d\tau}\int_{\mathcal{E}} a\rho s\, dx \le -\sum\nolimits_{v\in\mathcal{V}_\partial} m_e(v)s_e(v)n_e(v) - \int_{\mathcal{E}} \frac{\beta}{\varepsilon^3}\frac{\theta-\theta^0}{\theta}\, dx. \tag{3.93}$$

Remark 3.20. The total mass of the system is conserved up to flux over the network boundary. The change in total exergy of the system is only caused by flux over the network boundary and dissipation by friction at pipe walls and by heat exchange with the ambient medium. The total entropy changes only due to flux over the network boundary and temperature exchange with the ambient medium. Depending on the choice of coupling conditions (3.78)–(3.79) or (3.80)–(3.81), entropy is either conserved or produced at network junctions.

Proof. The conservation of mass (3.90) immediately follows from equation (3.82) by testing with $q = 1$. The appearing contributions at interior junctions vanish due to the coupling condition on the mass flux (3.76). In order to prove the energy identity (3.91), we use that

$$\frac{d}{d\tau}\mathcal{H}^\varepsilon(\rho, w, s) = (\partial_\tau\rho, ag^\varepsilon)_{\mathcal{E}} + (\partial_\tau w, \varepsilon^2 m)_{\mathcal{E}} + (\partial_\tau s, a\rho(\theta-\theta^0))_{\mathcal{E}}$$

holds due to the relations in (3.86). Using the test functions $q = g^\varepsilon$, $r = m$, $z = \varepsilon^{-3}(\theta-\theta^0)$ in the variational identities (3.82)–(3.84) then leads to

$$\begin{aligned}\frac{d}{d\tau}\mathcal{H}^\varepsilon(\rho, w, s) = &-(\partial_x m, g^\varepsilon)_{\mathcal{E}} + (g^\varepsilon, \partial_x m)_{\mathcal{E}} + ((\theta-\theta^0)\partial_x s, m)_{\mathcal{E}} - (\gamma|w|w, m)_{\mathcal{E}}\\ &- \sum_{v\in\mathcal{V}_\partial} \hat{g}^v_\partial m_e(v)n_e(v) - (m\partial_x s, \theta-\theta^0)_{\mathcal{E}} - (\beta\frac{\theta-\theta^0}{\theta}, \varepsilon^{-3}(\theta-\theta^0))_{\mathcal{E}}.\end{aligned}$$

By canceling the terms with opposite sign, we obtain equation (3.91). Choosing $q = s$, $r = 0$, and $z = \varepsilon^{-3}$ in (3.82)–(3.84) directly leads to

$$\begin{aligned}\frac{d}{d\tau}\int_{\mathcal{E}} a\rho s\, dx &= (a\partial_\tau\rho, s)_{\mathcal{E}} + (\varepsilon^3 a\rho\partial_\tau s, \varepsilon^{-3})_{\mathcal{E}}\\ &= -(\partial_x m, s)_{\mathcal{E}} - (\varepsilon^3 m\partial_x s, \varepsilon^{-3})_{\mathcal{E}} - (\beta\frac{\theta-\theta^0}{\theta}, \varepsilon^{-3})_{\mathcal{E}}\\ &= -\sum\nolimits_{v\in\mathcal{V}}\sum\nolimits_{e\in\mathcal{E}(v)} m_e(v)s_e(v)n_e(v) - \int_{\mathcal{E}} \frac{\beta}{\varepsilon^3}\frac{\theta-\theta^0}{\theta}\, dx.\end{aligned}$$

The contributions at $v \in \mathcal{V}_0$ vanish due to (3.78)–(3.79), more precisely

$$\begin{aligned}\sum_{e\in\mathcal{E}(v)} m_e(v,\tau)s_e(v,\tau)n_e(v) &= \sum_{e\in\mathcal{E}^{out}(v,\tau)} m_e(v)\hat{s}_v(\tau)n_e(v) + \sum_{e\in\mathcal{E}^{in}(v,\tau)} m_e(v,\tau)s_e(v,\tau)n_e(v)\\ &= \sum\nolimits_{e\in\mathcal{E}^{out}(v,\tau)} m_e(v,\tau)n_e(v)\frac{\sum_{e'\in\mathcal{E}^{in}(v,\tau)} m_{e'}(v,\tau)s_{e'}(v,\tau)n_{e'}(v)}{\sum_{e'\in\mathcal{E}^{in}(v,\tau)} m_{e'}(v,\tau)n_{e'}(v)}\\ &\quad + \sum\nolimits_{e\in\mathcal{E}^{in}(v,\tau)} m_e(v,\tau)s_e(v,\tau)n_e(v) = 0.\end{aligned}$$

Here, we additionally used the fact that by (3.76) we have

$$\sum\nolimits_{e\in\mathcal{E}^{in}(v,\tau)} m_e(v,\tau)n_e(v) = -\sum\nolimits_{e\in\mathcal{E}^{out}(v,\tau)} m_e(v,\tau)n_e(v).$$

If the entropy coupling conditions are replaced by (3.80)–(3.81), it holds that

$$\begin{aligned}-\sum\nolimits_{e\in\mathcal{E}(v)} m_e(v,\tau)s_e(v,\tau)n_e(v) &= -\sum\nolimits_{e\in\mathcal{E}^{out}(v,\tau)} m_e(v,\tau)\eta^{-1}(\hat{\eta}_v(\tau))n_e(v)\\ &\quad - \sum\nolimits_{e\in\mathcal{E}^{in}(v,\tau)} m_e(v,\tau)s_e(v,\tau)n_e(v)\\ &= -\sum\nolimits_{e\in\mathcal{E}^{out}(v,\tau)} m_e(v,\tau)n_e(v)\,\eta^{-1}\Big(\frac{\sum_{e'\in\mathcal{E}^{in}(v,\tau)} m_{e'}(v,\tau)\eta(s_{e'}(v,\tau))n_{e'}(v)}{\sum_{e'\in\mathcal{E}^{in}(v,\tau)} m_{e'}(v,\tau)n_{e'}(v)}\Big)\\ &\quad - \sum\nolimits_{e\in\mathcal{E}^{in}(v,\tau)} m_e(v,\tau)s_e(v,\tau)n_e(v)\\ &\geq -\sum\nolimits_{e\in\mathcal{E}^{out}(v,\tau)} m_e(v,\tau)n_e(v)\frac{\sum_{e'\in\mathcal{E}^{in}(v,\tau)} m_{e'}(v,\tau)\eta^{-1}(\eta(s_{e'}(v,\tau)))n_{e'}(v)}{\sum_{e'\in\mathcal{E}^{in}(v,\tau)} m_{e'}(v,\tau)n_{e'}(v)}\\ &\quad - \sum\nolimits_{e\in\mathcal{E}^{in}(v,\tau)} m_e(v,\tau)s_e(v,\tau)n_e(v) = 0,\end{aligned}$$

where we applied Jensen's inequality and used the fact that η^{-1} exists and is concave since η is convex and strictly monotonically increasing. □

3.4. Numerical approximation

For the discretization of the system (3.70)–(3.79), we extend the mixed finite element method proposed in Section 3.2 and in [38] for the isothermal gas transport to the non-isothermal regime. A hybrid discontinuous Galerkin approach with upwinding is used to approximate the additional transport equation (3.72) for the entropy. Such methods have shown to be especially suitable for handling the coupling conditions at network junctions; see Chapter 1.3 and [39].

3.4.1. Mesh and approximation spaces

We approximate the density ρ and the entropy s by piecewise constant and the mass flux m by piecewise linear, edgewise continuous functions in space on the spatial mesh

$$\mathcal{T}_h = \{T_e^i = (x_e^{i-1}, x_e^i) : i = 1,\dots,M_e,\ x_e^0 = 0,\ x_e^{M_e} = \ell_e,\ e \in \mathcal{E}\}.$$

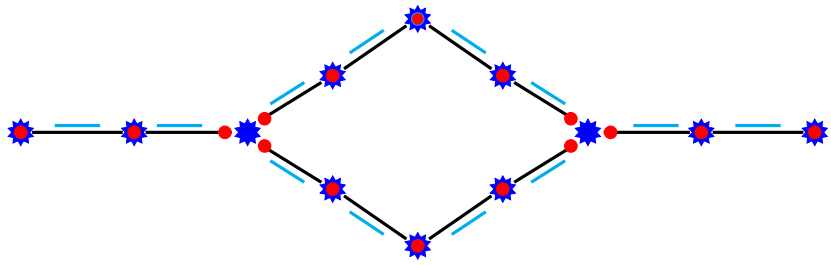

Figure 3.3.: A simple spatial mesh with two sub-intervals per pipe for the network given in Figure 3.1. The degrees of freedom for density and entropy are depicted in (cyan, bar) and for the mass flux in (red, dot). The placement of the hybrid variables is illustrated in (blue, star).

The grid points are given by $x_e^i = ih_e$, $i = 0, \dots, M_e$ with local and global mesh sizes denoted by $h_e = \ell_e/M_e$ and $h = \max_{e\in\mathcal{E}} h_e$. Interior grid points are collected in the set

$$\mathcal{X}_h = \{x_e^i : i = 1, \dots, M_e - 1\}.$$

We further introduce the outward normal n on the mesh $\mathcal{T}_h$ that takes the values

$$n|_{T_e^i}(x_e^{i-1}) = -1 \qquad \text{and} \qquad n|_{T_e^i}(x_e^i) = 1 \qquad \text{for } i = 1, \dots, M_e,\ e \in \mathcal{E}.$$

The spatial approximation spaces are defined by

$$Q_h = \mathcal{P}_0(\mathcal{T}_h), \qquad R_h = \mathcal{P}_1(\mathcal{T}_h) \cap H(\mathrm{div}; \mathcal{E}), \qquad \text{and} \qquad Z_h = \mathcal{P}_0(\mathcal{T}_h)$$

with $\mathcal{P}_k(\mathcal{T}_h)$ denoting the space of piecewise polynomials of degree $\leq k$ on the mesh. Moreover, we introduce additional degrees of freedom called *hybrid variables* at all vertices and interior grid points that lie in the space $\hat{Z}_h = \ell_2(\mathcal{V} \cup \mathcal{X}_h)$; compare with Chapter 1.3. In Figure 3.3 we present an illustration of the degrees of freedom for density, mass flux, entropy, and the hybrid variables. The discrete time steps are given by $\tau^n = n\Delta\tau$, $n = 0, \dots, N$ with $\Delta\tau = \tau_{max}/N$ and we abbreviate $u^n = u(\tau^n)$. In order to approximate the time derivative, we will make use of the backward difference quotient $\bar{d}_\tau u^n = (u^n - u^{n-1})/\Delta\tau$. Let us further introduce the following grid- and time-dependent scalar products

$$(u, w)_{\mathcal{T}_h} = \sum\nolimits_{T\in\mathcal{T}_h} (u, w)_{L^2(T)}, \quad \langle u, w\rangle_{\partial\mathcal{T}_h} = \sum\nolimits_{T\in\mathcal{T}_h} \sum\nolimits_{x\in\partial T} u|_T(x) w|_T(x)$$

with $\partial T_e^i = \{x_e^{i-1}, x_e^i\}$ being the element boundary of $T_e^i = (x_e^{i-1}, x_e^i)$, as well as

$$\langle u, w\rangle_{\partial\mathcal{T}_h^{in,n}} = \sum\nolimits_{T\in\mathcal{T}_h} \sum\nolimits_{x\in\partial T^{in,n}} u^n\big|_T(x) w^n\big|_T(x),$$
$$\langle u, w\rangle_{\partial\mathcal{T}_h^{out,n}} = \sum\nolimits_{T\in\mathcal{T}_h} \sum\nolimits_{x\in\partial T^{out,n}} u^n\big|_T(x) w^n\big|_T(x),$$

where the in- and outflow boundary of $T \in \mathcal{T}_h$ at time τ^n is defined by

$$\partial T^{in,n} = \{x \in \partial T : m_h^n(x) n|_T(x) \leq 0\} \quad \text{and} \quad \partial T^{out,n} = \{x \in \partial T : m_h^n(x) n|_T(x) > 0\}.$$

Note that m_h^n is edgewise continuous. Similarly, the network inflow and outflow boundary at time τ^n will be denoted by $\mathcal{V}_\partial^{in,n}$ and $\mathcal{V}_\partial^{out,n}$, respectively, i.e., for $v \in \mathcal{V}_\partial$ it holds that $v \in \mathcal{V}_\partial^{in,n}$ if $m_h^n(v) n_e(v) < 0$ and $v \in \mathcal{V}_\partial^{out,n}$ if $m_h^n(v) n_e(v) > 0$.

3.4.2. Structure-preserving discretization scheme

For the approximation of solutions to (3.70)–(3.79), we propose the following method.

Problem 3.21. Let $\rho_h^0 \in Q_h,\ m_h^0 \in R_h$, and $s_h^0 \in Z_h$ be given. Then, for $n = 1, \dots, N$ find $\rho_h^n \in Q_h,\ m_h^n \in R_h,\ s_h^n \in Z_h,\ \hat{s}_h^n \in \hat{Z}_h$ so that $\hat{s}_h^n(v) = \hat{s}_\partial^v(\tau^n)$ at $v \in \mathcal{V}_\partial^{in,n}$ and

$$(a\bar{d}_\tau \rho_h^n, q_h)_{\mathcal{T}_h} + (\partial_x m_h^n, q_h)_{\mathcal{T}_h} = 0, \tag{3.94}$$

$$(\varepsilon^2 \bar{d}_\tau w_h^n, r_h)_{\mathcal{T}_h} - (g_h^{\varepsilon,n}, \partial_x r_h)_{\mathcal{T}_h} - \langle (\theta_h^n - \theta^0)(\hat{s}_h^n - s_h^n), r_h n\rangle_{\partial \mathcal{T}_h^{in,n}} \tag{3.95}$$
$$+ (\gamma |w_h^n| w_h^n, r_h)_{\mathcal{T}_h} + \sum\nolimits_{v \in \mathcal{V}_\partial} g_\partial^v(\tau^n) r_h(v) n_e(v) = 0,$$

$$(\varepsilon^3 a \rho_h^{n-1} \bar{d}_\tau s_h^n, z_h)_{\mathcal{T}_h} + \langle \varepsilon^3 m_h^n (\hat{s}_h^n - s_h^n), z_h^{dw} n\rangle_{\partial \mathcal{T}_h} + (\beta \frac{\theta_h^n - \theta^0}{\theta_h^n}, z_h)_{\mathcal{T}_h} = 0 \tag{3.96}$$

for all $q_h \in Q_h,\ r_h \in R_h$ and $z_h \in Z_h,\ \hat{z}_h \in \hat{Z}_h$ with $w_h^n,\ g_h^{\varepsilon,n}$, and θ_h^n being functions of the discrete approximations ρ_h^n, m_h^n, and s_h^n, i.e.,

$$w_h^n = \frac{m_h^n}{a\rho_h^n}, \quad g_h^{\varepsilon,n} = \frac{\varepsilon^2}{2}(w_h^n)^2 + \frac{p(\rho_h^n, s_h^n)}{\rho_h^n} + e(\rho_h^n, s_h^n) - \theta^0 s_h^n \quad \text{and} \quad \theta_h^n = \theta(\rho_h^n, s_h^n).$$

The convective downwind flux is defined by $m_h^n z_h^{dw} n = \max(m_h^n n, 0)\hat{z}_h + \min(m_h^n n, 0) z_h$.

Let us note that the structure of the weak formulation (3.82)–(3.84) is preserved by the above scheme. Moreover, by formally setting $\varepsilon = 0$ we obtain a viable method for the parabolic limit problem, which equals the method provided by Problem 3.6 for $\varepsilon = 0$. The coupling condition for the mass flux (3.76) is strongly included in the approximation space R_h, whereas the continuity of the free enthalpy (3.77) is weakly included in (3.46). The mixing condition for the entropy at junctions (3.78)–(3.79) is enforced by the additional hybrid variables $\hat{s}_h$ and $\hat{z}_h$ and thus naturally included in the method. More precisely, by formally testing (3.96) with $z_h = 0$ and $\hat{z}_h = \chi_v$ for $v \in \mathcal{V}_0$, we find that

$$\hat{s}_h^n(v) = \frac{\sum_{e \in \mathcal{E}^{in}(v,\tau^n)} m_{h,e}^n(v) s_{h,e}^n(v) n_e(v)}{\sum_{e \in \mathcal{E}^{in}(v,\tau^n)} m_{h,e}^n(v) n_e(v)}, \tag{3.97}$$

i.e., $\hat{s}_h^n(v)$ equals the mixing value (3.79) and serves as upwind value for all outgoing pipes.

Remark 3.22. When one wants to replace the coupling conditions for the entropy by (3.80)–(3.81), the method can be modified as follows: We replace equation (3.95) by

$$(\varepsilon^2 \bar{d}_\tau w_h^n, r_h)_{\mathcal{T}_h} - (g_h^{\varepsilon,n}, \partial_x r_h)_{\mathcal{T}_h} - \langle (\theta_h^n - \theta^0) \frac{\eta(\hat{s}_h^n) - \eta(s_h^n))}{\eta'(s_h^n)}, r_h n\rangle_{\partial \mathcal{T}_h^{in,n}} \tag{3.98}$$
$$+ (\gamma |w_h^n| w_h^n, r_h)_{\mathcal{T}_h} + \sum\nolimits_{v \in \mathcal{V}_\partial} g_\partial^v(\tau^n) r_h(v) n_e(v) = 0$$

and equation (3.96) by

$$(\varepsilon^3 a \rho_h^{n-1} \eta'(s_h^n) \bar{d}_\tau s_h^n, z_h)_{\mathcal{T}_h} + \langle \varepsilon^3 m_h^n (\eta(\hat{s}_h^n) - \eta(s_h^n)), z_h^{dw} n\rangle_{\partial \mathcal{T}_h} \tag{3.99}$$
$$+ (\beta \eta'(s_h^n) \frac{\theta_h^n - \theta^0}{\theta_h^n}, z_h)_{\mathcal{T}_h} = 0.$$

Note that since η is a strictly monotonically increasing function, it holds that $\eta'(s) > 0$ for all s. Again, testing (3.99) with $z_h = 0,\ \hat{z}_h = \chi_v,\ v \in \mathcal{V}_0$, we find that

$$\eta(\hat{s}_h^n(v)) = \frac{\sum_{e\in\mathcal{E}^{in}(v,\tau^n)} m_{h,e}^n(v)\eta(s_{h,e}^n(v))n_e(v)}{\sum_{e\in\mathcal{E}^{in}(v,\tau^n)} m_{h,e}^n(v)n_e(v)}, \tag{3.100}$$

which equals the mixing value (3.81).

3.4.3. Discrete balance laws

Next, we show that the solution (ρ_h^n, m_h^n, s_h^n) of Problem 3.21 satisfies discrete global balance laws. In order to do so, we make the following assumptions:

(B1) There exist constants $\underline{\rho}$, $\bar{\rho} > 0$ so that $\underline{\rho} \le \rho_h^n \le \bar{\rho}$ for all $n = 0, \dots, N$.

(B2) The function $(\nu, s) \mapsto \tilde{e}(\nu, s)$ with $\nu = 1/\rho$ and $\tilde{e}(\nu, s) := e(\rho, s)$ is strictly convex and there exists a constant $0 < \zeta \le 1$ so that

$$(\tilde{e}''(\nu, s)(x, y), (x, y)) \ge \zeta\, \delta_{\nu\nu}\tilde{e}(\nu, s)x^2$$

for all x, y, and all $\rho = 1/\nu$ and s.

(B3) The flow satisfies the subsonic condition

$$\tfrac{1}{2}\varepsilon^2(\rho_h^n w_h^n)^2 \le \zeta\, \delta_{\nu\nu}\tilde{e}(\nu_h^*, s_h^*)$$

for all $\nu_h^* = \xi_1 \frac{1}{\rho_h^n} + (1-\xi_1)\frac{1}{\rho_h^{n-1}}$, $s_h^* = \xi_2 s_h^n + (1-\xi_2)s_h^{n-1}$ with ξ_1, $\xi_2 \in (0, 1)$ and all $n = 0, \dots, N$.

Remark 3.23. Following common practice, see e.g. [17, 58], we write the internal energy in terms of the specific volume $\nu = 1/\rho$ instead of the density ρ. It then holds that

$$\delta_\nu\tilde{e}(\nu, s) = -\tilde{p}(\nu, s) = -p(\rho, s), \qquad \delta_s\tilde{e}(\nu, s) = \tilde{\theta}(\nu, s) = \theta(\rho, s). \tag{3.101}$$

Assumption (B2) corresponds to one of the basic assumptions in thermodynamics, namely that the flow is in a local thermodynamic equilibrium. Assumption (B3) enforces the flow to be subsonic since the speed of sound c is defined by

$$c = \nu\sqrt{\delta_{\nu\nu}\tilde{e}(\nu, s)}.$$

We refer to [58, Ch. III.1.1] for details. The assumptions are reasonable for flow in pipe networks, which is supposed to be subsonic, and for the example of an ideal gas, which will be demonstrated in the following example.

Example 3.24. Let us revisit the case of a simple ideal gas from Example 3.17 which fulfills the following thermodynamic relations

$$p = R\rho\theta \qquad \text{and} \qquad e = c_v\theta = \frac{R}{\gamma - 1}\theta.$$

From (3.4) and (3.101) we deduce that

$$e(\rho, s) = \rho^{\gamma-1} e^{s/c_v} \qquad \text{and} \qquad \tilde{e}(\nu, s) = \nu^{1-\gamma} e^{s/c_v}.$$

Differentiating $\tilde{e}$ twice with respect to ν and s shows that

$$(x, y)^\top \tilde{e}''(\nu, s)(x, y) = (\gamma - 1)\gamma\nu^{-1-\gamma} e^{s/c_v} x^2 - 2(\gamma - 1)c_v^{-1}\nu^{-\gamma} e^{s/c_v} xy + c_v^{-2}\nu^{1-\gamma} e^{s/c_v} y^2.$$

By applying Young's inequality, the second term on the right-hand side can then further be estimated by

$$2(\gamma - 1)c_v^{-1}\nu^{-\gamma} e^{s/c_v} xy \geq -(1-\zeta)(\gamma - 1)\gamma\nu^{-1-\gamma} e^{s/c_v} x^2 - \tfrac{1}{1-\zeta}\tfrac{\gamma-1}{\gamma} c_v^{-2}\nu^{1-\gamma} e^{s/c_v} y^2.$$

We now require that $\frac{1}{1-\zeta}\frac{\gamma-1}{\gamma} < 1$ and $0 < \zeta \leq 1$, which is satisfied for $0 < \zeta < \frac{1}{\gamma}$. Consequently, $\tilde{e}$ is a strongly convex function that satisfies assumption (B2).

Theorem 3.25. *Let the assumptions (B1)–(B3) hold. Then, a solution (ρ_h^n, m_h^n, s_h^n) of Problem 3.21 satisfies the following discrete global balance laws*

$$\int_{\mathcal{E}} a\rho_h^n \, dx = \int_{\mathcal{E}} a\rho_h^{n-1} \, dx - \Delta\tau \sum\nolimits_{v\in\mathcal{V}_\partial} m_h^n(v) n_e(v), \tag{3.102}$$

$$\begin{aligned}\mathcal{H}^\varepsilon(\rho_h^n, m_h^n, s_h^n) \leq \mathcal{H}^\varepsilon(\rho_h^{n-1}, m_h^{n-1}, s_h^{n-1}) - \Delta\tau \sum\nolimits_{v\in\mathcal{V}_\partial} \hat{g}_\partial^v(\tau^n) m_h^n(v) n_e(v) \\ - \Delta\tau \int_{\mathcal{E}} a\gamma\rho_h^n |w_h^n|^3 \, dx - \Delta\tau \int_{\mathcal{E}} \frac{\beta}{\varepsilon^3} \frac{(\theta_h^n - \theta^0)^2}{\theta_h^n} \, dx,\end{aligned} \tag{3.103}$$

$$\begin{aligned}\int_{\mathcal{E}} a\rho_h^n s_h^n \, dx = \int_{\mathcal{E}} a\rho_h^{n-1} s_h^{n-1} \, dx - \Delta\tau \int_{\mathcal{E}} \frac{\beta}{\varepsilon^3} \frac{\theta_h^n - \theta^0}{\theta_h^n} \, dx \\ - \Delta\tau \Big(\langle m_h^n, s_h^n n\rangle_{\mathcal{V}_\partial^{out,n}} + \langle m_h^n, s_\partial(\tau^n) n\rangle_{\mathcal{V}_\partial^{in,n}} \Big).\end{aligned} \tag{3.104}$$

If the equations (3.95)–(3.96) *in Problem 3.21 are replaced by* (3.98)–(3.99)*, the corresponding solution (ρ_h^n, m_h^n, s_h^n) satisfies the mass and energy balance* (3.102) *and* (3.103) *as well as the following entropy balance*

$$\begin{aligned}\int_{\mathcal{E}} a\rho_h^n s_h^n \, dx \geq \int_{\mathcal{E}} a\rho_h^{n-1} s_h^{n-1} \, dx - \Delta\tau \int_{\mathcal{E}} \frac{\beta}{\varepsilon^3} \frac{\theta_h^n - \theta^0}{\theta_h^n} \, dx \\ - \Delta\tau \Big(\langle m_h^n, s_h^n n\rangle_{\mathcal{V}_\partial^{out,n}} + \langle m_h^n, \hat{s}_\partial(\tau^n) n\rangle_{\mathcal{V}_\partial^{in,n}} \Big),\end{aligned} \tag{3.105}$$

i.e., entropy at junctions is produced instead of conserved.

Proof. Conservation of mass. The first identity (3.102) follows directly from testing (3.94) with $q_h = 1$, i.e.,

$$\int_{\mathcal{E}} a\bar{d}_\tau \rho_h^n \, dx = -\int_{\mathcal{E}} \partial_x m_h^n \, dx = -\sum\nolimits_{v\in\mathcal{V}} \sum\nolimits_{e\in\mathcal{E}(v)} m_h^n(v) n_e(v).$$

The contributions at interior vertices vanish since $m_h^n \in R_h \subset H(\mathrm{div}; \mathcal{E})$.

Dissipation of exergy. By definition of the exergy in (3.85) it holds that

$$\begin{aligned}
\bar{d}_\tau \mathcal{H}^\varepsilon(\rho_h^n, w_h^n, s_h^n) &= \tfrac{1}{\Delta\tau}\int_{\mathcal{E}} a\tfrac{\varepsilon^2}{2}(\rho_h^n(w_h^n)^2 - \rho_h^{n-1}(w_h^{n-1})^2) \\
&\qquad + a\rho_h^n e(\rho_h^n, s_h^n) - a\rho_h^{n-1}e(\rho_h^{n-1}, s_h^{n-1}) - (a\rho_h^n s_h^n - a\rho_h^{n-1}s_h^{n-1})\theta^0 \; dx \\
&= (a\bar{d}_\tau\rho_h^n, \tfrac{\varepsilon^2}{2}(w_h^n)^2 + e(\rho_h^n, s_h^n) - s_h^n\theta^0)_{\mathcal{T}_h} + \tfrac{1}{\Delta\tau}\int_{\mathcal{E}} a\tfrac{\varepsilon^2}{2}\rho_h^{n-1}((w_h^n)^2 - (w_h^{n-1})^2)\; dx \\
&\quad + \tfrac{1}{\Delta\tau}\int_{\mathcal{E}} a\rho_h^{n-1}(e(\rho_h^n, s_h^n) - e(\rho_h^{n-1}, s_h^{n-1}))\; dx - \tfrac{1}{\Delta\tau}\int_{\mathcal{E}} a\rho_h^{n-1}(s_h^n - s_h^{n-1})\theta^0\; dx \\
&= (i) + (ii) + (iii) + (iv).
\end{aligned}$$

Let us first consider the term (iii). By assumption (B2) and (3.101) we observe that

$$\begin{aligned}
e_h^n - e_h^{n-1} &\le \delta_\nu \tilde{e}_h^n(\nu_h^n - \nu_h^{n-1}) + \delta_s\tilde{e}_h^n(s_h^n - s_h^{n-1}) - \zeta\delta_{\nu\nu}\tilde{e}(\nu_h^*, s_h^*)(\nu_h^n - \nu_h^{n-1})^2 \\
&\le \tfrac{p_h^n}{\rho_h^n\rho_h^{n-1}}(\rho_h^n - \rho_h^{n-1}) + \theta_h^n(s_h^n - s_h^{n-1}) - \tfrac{\zeta\delta_{\nu\nu}\tilde{e}_h^*}{(\rho_h^n\rho_h^{n-1})^2}(\rho_h^n - \rho_h^{n-1})^2
\end{aligned}$$

with $\nu_h^* = \xi_1\frac{1}{\rho_h^n} + (1-\xi_1)\frac{1}{\rho_h^{n-1}}$, $s_h^* = \xi_2 s_h^n + (1-\xi_2)s_h^{n-1}$ for some ξ_1, $\xi_2 \in (0,1)$, where we abbreviated $e_h^n = e(\rho_h^n, s_h^n)$ and $\tilde{e}_h^* = \tilde{e}(\rho_h^*, s_h^*)$. From this we directly deduce that

$$\begin{aligned}
(iii) &\le (a\bar{d}_\tau\rho_h^n, \tfrac{p_h^n}{\rho_h^n})_{\mathcal{T}_h} + (a\rho_h^{n-1}\bar{d}_\tau s_h^n, \theta_h^n)_{\mathcal{T}_h} - \tfrac{1}{\Delta\tau}\int_{\mathcal{E}} a\tfrac{\zeta\delta_{\nu\nu}\tilde{e}_h^*}{(\rho_h^n)^2\rho_h^{n-1}}(\rho_h^n - \rho_h^{n-1})^2\; dx \\
&= (iii.1) + (iii.2) + (iii.3).
\end{aligned}$$

We observe that

$$(i) + (iii.1) = (a\bar{d}_\tau\rho_h^n, g_h^{\varepsilon,n})_{\mathcal{T}_h} \qquad \text{and} \qquad (iv) + (iii.2) = (a\rho_h^{n-1}\bar{d}_\tau s_h^n, \theta_h^n - \theta^0)_{\mathcal{T}_h}.$$

It remains to estimate the last term $(iii.3)$ together with (ii), i.e.,

$$(ii) + (iii.3) = \tfrac{1}{\Delta\tau}\int_{\mathcal{E}} a\tfrac{\varepsilon^2}{2}\rho_h^{n-1}((w_h^n)^2 - (w_h^{n-1})^2) - \tfrac{1}{\Delta\tau}\int_{\mathcal{E}} a\tfrac{\zeta\delta_{\nu\nu}\tilde{e}_h^*}{(\rho_h^n)^2\rho_h^{n-1}}(\rho_h^n - \rho_h^{n-1})^2\; dx.$$

Let us note that

$$\begin{aligned}
a\tfrac{\varepsilon^2}{2}\rho_h^{n-1}((w_h^n)^2 - (w_h^{n-1})^2) &= a\varepsilon^2\rho_h^n w_h^n(w_h^n - w_h^{n-1}) \\
&\qquad - a\varepsilon^2(\rho_h^n - \rho_h^{n-1})w_h^n(w_h^n - w_h^{n-1}) - a\tfrac{\varepsilon^2}{2}\rho_h^{n-1}(w_h^n - w_h^{n-1})^2.
\end{aligned}$$

The first term equals $\Delta\tau\varepsilon^2\bar{d}_\tau w_h^n m_h^n$. Under assumption (B3) and using Young's inequality, we can show that the remaining terms are negative, i.e,

$$\begin{aligned}
&-\tfrac{\zeta\delta_{\nu\nu}\tilde{e}_h^*}{(\rho_h^n)^2\rho_h^{n-1}}(\rho_h^n - \rho_h^{n-1})^2 - \varepsilon^2(\rho_h^n - \rho_h^{n-1})w_h^n(w_h^n - w_h^{n-1}) - \tfrac{\varepsilon^2}{2}\rho_h^{n-1}(w_h^n - w_h^{n-1})^2 \\
&\qquad \le -\tfrac{\varepsilon^2}{2}\tfrac{(\rho_h^n w_h^n)^2}{(\rho_h^n)^2\rho_h^{n-1}}(\rho_h^n - \rho_h^{n-1})^2 + \tfrac{\varepsilon^2}{2}\tfrac{(w_h^n)^2}{\rho_h^{n-1}}(\rho_h^n - \rho_h^{n-1})^2 \\
&\qquad\qquad + \tfrac{\varepsilon^2}{2}\rho_h^{n-1}(w_h^n - w_h^{n-1})^2 - \tfrac{\varepsilon^2}{2}\rho_h^{n-1}(w_h^n - w_h^{n-1})^2 = 0,
\end{aligned}$$

which allows us to estimate $(ii) + (iii.3) \le (\varepsilon^2\bar{d}_\tau w_h^n, m_h^n)_{\mathcal{T}_h}$. Overall, we obtain

$$\bar{d}_\tau\mathcal{H}^\varepsilon(\rho_h^n, w_h^n, s_h^n) \le \; (a\bar{d}_\tau\rho_h^n, g_h^{\varepsilon,n})_{\mathcal{T}_h} + (\varepsilon^2\bar{d}_\tau w_h^n, m_h^n)_{\mathcal{T}_h} + (a\rho_h^{n-1}\bar{d}_\tau s_h^n, \theta_h^n - \theta^0)_{\mathcal{T}_h}. \quad (3.106)$$

Testing (3.94) with $g_h^{\varepsilon,n} \in L^2(\mathcal{E})$, (3.95) with $m_h^n \in R_h$, and (3.96) with $\varepsilon^{-3}(\theta_h^n - \theta^0) \in Z_h$ then yields

$$\begin{aligned}
\bar{d}_\tau \mathcal{H}^\varepsilon(\rho_h^n, w_h^n, s_h^n) \leq & -(\partial_x m_h^n, g_h^{\varepsilon,n})_{\mathcal{T}_h} + (g_h^{\varepsilon,n}, \partial_x m_h^n)_{\mathcal{T}_h} + \langle (\theta_h^n - \theta^0)(\hat{s}_h^n - s_h^n), m_h^n n\rangle_{\partial \mathcal{T}_h^{in,n}} \\
& - (\gamma |w_h^n| w_h^n, m_h^n)_{\mathcal{T}_h} - \sum\nolimits_{v \in \mathcal{V}_\partial} \hat{g}_\partial^v(\tau^n) m_h^n(v) n_e(v) \\
& - \langle m_h^n(\hat{s}_h^n - s_h^n), (\theta_h^n - \theta^0) n\rangle_{\partial \mathcal{T}_h^{in,n}} - (\beta \frac{\theta_h^n - \theta^0}{\theta_h^n}, \varepsilon^{-3}(\theta_h^n - \theta^0))_{\mathcal{T}_h} \\
= & - \sum_{v \in \mathcal{V}_\partial} \hat{g}_\partial^v(\tau^n) m_h^n(v) n_e(v) - \int_{\mathcal{E}} \gamma a \rho_h^n |w_h^n|^3 \, dx - \int_{\mathcal{E}} \frac{\beta}{\varepsilon^3} \frac{(\theta_h^n - \theta^0)^2}{\theta_h^n} \, dx.
\end{aligned}$$

Let us note that (3.94) can formally be tested with L^2-functions since $\bar{d}_\tau \rho_h^n$ as well as $\partial_x m_h^n$ are piecewise constant and (3.94) thus holds pointwise.

Balance of entropy. By formally testing (3.94) with $r_h = s_h^n \in Q_h$ and (3.96) with $z_h = \varepsilon^{-3} \in Z_h$, $\hat{z}_h = 0$, we estimate

$$\begin{aligned}
\tfrac{1}{\Delta\tau} \int_{\mathcal{E}} a\rho_h^n s_h^n - a\rho_h^{n-1} s_h^{n-1} \, dx = & (a\bar{d}_\tau \rho_h^n, s_h^n)_{\mathcal{T}_h} + (a\varepsilon^3 \rho_h^{n-1} \bar{d}_\tau s_h^n, \varepsilon^{-3})_{\mathcal{T}_h} \\
= & -(\partial_x m_h^n, s_h^n)_{\mathcal{T}_h} - \langle m_h^n(\hat{s}_h^n - s_h^n), n\rangle_{\partial \mathcal{T}_h^{in,n}} - (\beta \frac{\theta_h^n - \theta^0}{\theta_h^n}, \varepsilon^{-3})_{\mathcal{T}_h} \\
= & -\langle m_h^n s_h^n, n\rangle_{\partial \mathcal{T}_h} - \langle m_h^n(\hat{s}_h^n - s_h^n), n\rangle_{\partial \mathcal{T}_h^{in,n}} - (\beta \frac{\theta_h^n - \theta^0}{\theta_h^n}, \varepsilon^{-3})_{\mathcal{T}_h} \\
= & -\langle m_h^n s_h^n, n\rangle_{\mathcal{V}_\partial^{out,n}} - \langle m_h^n \hat{s}_\partial^v(\tau^n), n\rangle_{\mathcal{V}_\partial^{in,n}} - (\beta \frac{\theta_h^n - \theta^0}{\theta_h^n}, \varepsilon^{-3})_{\mathcal{T}_h},
\end{aligned}$$

where the contributions at interior vertices and grid points cancel due to the fact that $\hat{s}_h$ equals the upwind value within pipes and the mixing value (3.97) at junctions, and m_h^n is continuous, from which we can conclude that $\langle m_h^n \hat{s}_h^n, n\rangle_{\partial \mathcal{T}_h^{in,n} \setminus \mathcal{V}_\partial} = -\langle m_h^n s_h^n, n\rangle_{\partial \mathcal{T}_h^{out,n} \setminus \mathcal{V}_\partial}$.

Balance laws for η. Conservation of mass trivially holds since the first equation (3.94) is unchanged. In order to prove that the energy balance (3.91) is still valid, we start from (3.106) and test (3.94) with $g_h^{\varepsilon,n} \in L^2(\mathcal{E})$ which is an admissible test function, (3.98) with $m_h^n \in R_h$ and (3.99) with $\varepsilon^{-3}(\theta_h^n - \theta^0)/\eta'(s_h^n) \in Z_h$ and $\hat{z}_h = 0$. This leads to

$$\begin{aligned}
\frac{d}{d\tau} \mathcal{H}^\varepsilon(\rho_h^n, w_h^n, s_h^n) \leq & -(\partial_x m_h^n, g_h^{\varepsilon,n})_{\mathcal{T}_h} + (g_h^{\varepsilon,n}, \partial_x m_h^n)_{\mathcal{T}_h} - (\gamma |w_h^n| w_h^n, m_h^n)_{\mathcal{T}_h} \\
& + \langle (\theta_h^n - \theta^0)(\eta(\hat{s}_h^n) - \eta(s_h^n))/\eta'(s_h^n), m_h^n \, n\rangle_{\partial \mathcal{T}_h^{in,n}} - \sum\nolimits_{v \in \mathcal{V}_\partial} \hat{g}_\partial^v(\tau^n) m_h^n(v) n_e(v) \\
& - \langle m_h^n(\eta(\hat{s}_h^n) - \eta(s_h^n)), (\theta_h^n - \theta^0)/\eta'(s_h^n) \, n\rangle_{\partial \mathcal{T}_h^{in,n}} - (\varepsilon^{-3}\beta(\theta_h^n - \theta^0)/\theta_h^n, \theta_h^n - \theta^0)_{\mathcal{T}_h}.
\end{aligned}$$

By canceling the terms with opposite signs, we already obtain the energy balance (3.91). Similarly as above, we find

$$\begin{aligned}
\tfrac{1}{\Delta\tau} \int_{\mathcal{E}} a\rho_h^n s_h^n - a\rho_h^{n-1} s_h^{n-1} \, dx = & (a\bar{d}_\tau \rho_h^n, s_h^n)_{\mathcal{T}_h} + (a\rho_h^{n-1} \eta'(s_h^n) \bar{d}_\tau s_h^n, \eta'(s_h^n)^{-1})_{\mathcal{T}_h} \\
= & -(\partial_x m_h^n, s_h^n)_{\mathcal{T}_h} - \langle m_h^n(\eta(\hat{s}_h^n) - \eta(s_h^n)), \eta'(s_h^n)^{-1} n\rangle_{\partial \mathcal{T}_h^{in,n}} - (\beta \frac{\theta_h^n - \theta^0}{\theta_h^n}, \varepsilon^{-3})_{\mathcal{T}_h}
\end{aligned}$$

Since s_h^n is piecewise constant, the first term equals $-\langle m_h^n, s_h^n\, n\rangle_{\partial\mathcal{T}_h}$. Using that $m_h^n n < 0$ at $\partial\mathcal{T}_h^{in,n}$ and that η is convex, i.e., $\eta(\hat{s}_h^n)-\eta(s_h^n) \geq \eta'(s_h^n)(\hat{s}_h^n - s_h^n)$, and strictly monotonically increasing, i.e., $\eta'(s_h^n) > 0$, we can estimate the second term by

$$-\langle m_h^n(\eta(\hat{s}_h^n) - \eta(s_h^n)), \eta'(s_h^n)^{-1} n\rangle_{\partial\mathcal{T}_h^{in,n}} \geq -\langle m_h^n(\hat{s}_h^n - s_h^n), n\rangle_{\partial\mathcal{T}_h^{in,n}}.$$

At interior grid points $\mathcal{X}_h$ it holds that $\hat{s}_h^n$ is given by the upwind value and m_h^n is continuous within edges, we can thus conclude that $-\langle m_h^n \hat{s}_h^n, n\rangle_{\partial\mathcal{T}_h^{in,n}\setminus\mathcal{V}} = \langle m_h^n s_h^n, n\rangle_{\partial\mathcal{T}_h^{out,n}\setminus\mathcal{V}}$. At interior junctions $v \in \mathcal{V}_0$, however, it holds that

$$\begin{aligned}
&-\sum\nolimits_{e\in\mathcal{E}^{out}(v,\tau^n)} m_{h,e}^n(v)\hat{s}_{h,e}^n(v)n_e(v) \\
&\quad = -\sum\nolimits_{e\in\mathcal{E}^{out}(v,\tau^n)} m_{h,e}^n(v)n_e(v)\eta^{-1}\Big(\frac{\sum_{e'\in\mathcal{E}^{in}(v,\tau^n)} m_{h,e'}^n(v)\eta(s_{h,e'}^n(v))n_{e'}(v)}{\sum_{e'\in\mathcal{E}^{in}(v,\tau^n)} m_{h,e'}^n(v)n_{e'}(v)}\Big) \\
&\quad \geq \sum\nolimits_{e\in\mathcal{E}^{in}(v,\tau^n)} m_{h,e}^n(v)s_{h,e}^n(v)n_e(v),
\end{aligned}$$

where we used the fact that $\eta(\hat{s}_h^n)$ is given by the mixing value (3.100), that η^{-1} is concave, as well as Jensen's inequality. In summary, we thus find that

$$-\langle m_h^n \hat{s}_h^n, n\rangle_{\partial\mathcal{T}_h^{in,n}\setminus\mathcal{V}_\partial} \geq \langle m_h^n s_h^n, n\rangle_{\partial\mathcal{T}_h^{out,n}\setminus\mathcal{V}_\partial}.$$

Together with the previous considerations we can thus estimate

$$\begin{aligned}
-(\partial_x m_h^n, s_h^n)_{\mathcal{T}_h} - \langle m_h^n(\hat{s}_h^n - s_h^n), \eta'(s_h^n)^{-1} n\rangle_{\partial\mathcal{T}_h^{in,n}} \\
&\geq -\langle m_h^n, s_h^n\, n\rangle_{\partial\mathcal{T}_h} - \langle m_h^n(\hat{s}_h^n - s_h^n), n\rangle_{\partial\mathcal{T}_h^{in,n}} \\
&\geq -\langle m_h^n, s_h^n n\rangle_{\mathcal{V}_\partial^{out,n}} - \langle m_h^n, \hat{s}_\partial(\tau^n)n\rangle_{\mathcal{V}_\partial^{in,n}},
\end{aligned}$$

i.e., additional entropy is produced at junctions due to mixing. This yields (3.93). □

This concludes our theoretical investigations for the non-isothermal gas transport in pipe networks. Open questions that occurred will be discussed at the end of this chapter.

3.5. Numerical illustration

Let us conclude this chapter with some numerical experiments illustrating our theoretical findings. We again consider the GasLib-11 network from Chapter 1.4 depicted in Figure 3.4. This network consists of 11 pipes and vertices from which 5 are boundary vertices. We assume that all pipes have the rescaled length $\ell = 1$, diameter $d = 1$, and cross-sectional area $a = \pi/4$. According to the data in [112] that corresponds to the GasLib-11 network, the length of the pipes is about $55\,km$ with diameters of $0.5\,m$. Relevant time scales range from hours to days and usual mass fluxes are $10 - 20\,m/s$ [98]. This corresponds to a scaling parameter $\varepsilon \approx 0.1 - 0.01$.

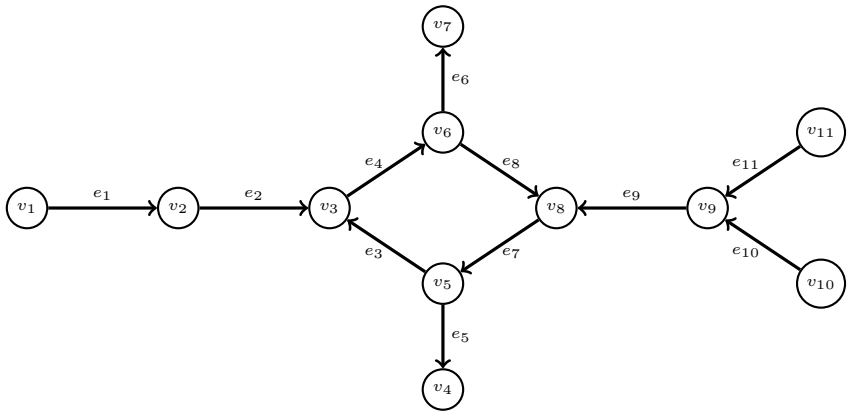

Figure 3.4.: GasLib-11 network from [112].

3.5.1. Isothermal gas transport

We first consider the isothermal gas transport and choose $\gamma = 1$ as the friction coefficient. We assume that the pressure-to-density relation is given by $p(\rho) = c^2\rho$, which holds for an ideal gas in the isothermal regime, with the rescaled speed of sound $c = 1$. As boundary conditions, we prescribe the enthalpy at the network boundary vertices by

$$h_\partial^{v_1}(\tau) = 0.2\sin(2\pi\tau/\tau_{max})^3 + 1, \quad h_\partial^{v_4}(\tau) = 0.3\sin(2\pi\tau/\tau_{max})^3 + 1,$$
$$h_\partial^{v_7}(\tau) = h_\partial^{v_{10}}(\tau) = h_\partial^{v_{11}}(\tau) = 1$$

for a time horizon $\tau_{max} = 5$. The initial conditions are given by the stationary states corresponding to the boundary data at $\tau = 0$. Let us note that for $\varepsilon \ll 1$, fixing the enthalpy at the boundary vertices is more or less equivalent to fixing the density since $h^\varepsilon = \frac{\varepsilon^2}{2}w^2 + P'(\rho) \approx P'(\rho)$. We solve the nonlinear system of equations, which we obtain from (3.45)–(3.46) after choosing suitable basis functions for the discrete spaces, using Newton's method. In our computations, we obtained convergence within $4 - 5$ steps up to a tolerance of 10^{-12}.

Asymptotic convergence

In order to illustrate the asymptotic estimate from Theorem 3.5, we compare the solutions for different $\varepsilon > 0$ with the solution to the parabolic limit problem $\varepsilon = 0$. Since we cannot explicitly compute the exact solutions, we approximate them using the method proposed in Problem 3.6 for small mesh sizes h and $\Delta\tau$. Our results are shown in Table 3.1. The distances depicted therein are computed as

$$\mathrm{dist}(u) = \max_{n=0,\dots,N} \|u_h^{\varepsilon,n} - u_h^{0,n}\|_{L^2(\mathcal{E})}$$

with $u = \rho$ or $u = m$. For ε sufficiently small, we obtain second-order convergence with respect to ε in density and also in mass flux. These observations are in accordance with the theoretical findings from Theorem 3.5, where a second-order convergence in ε was proven if the velocities are bounded away from zero. Although in our scenario velocities change sign, we still observe this convergence.

ε	1	10^{-1}	10^{-2}	10^{-3}	10^{-4}	10^{-5}	10^{-6}
dist(ρ)	1.22e-1	6.62e-3	6.92e-5	6.98e-7	6.98e-9	6.98e-11	6.98e-13
rate	–	1.27	1.98	2.00	2.00	2.00	2.00
dist(m)	5.35	8.32e-1	6.56e-2	9.20e-4	9.54e-6	9.54e-8	9.56e-10
rate	–	0.81	1.10	1.85	1.98	2.00	2.00

Table 3.1.: Distance to the parabolic limit and convergence rate with respect to ε. The mesh sizes are chosen as $h = \Delta\tau = 2^{-6}$.

$\varepsilon = 1$	$\mathrm{err}_h(\rho)$	5.41e-2	4.55e-2	3.41e-2	2.38e-2	1.57e-2	9.89e-3
	rate	–	0.25	0.42	0.52	0.60	0.66
	$\mathrm{err}_h(m)$	3.90e-2	3.35e-2	2.35e-2	1.64e-2	1.10e-2	7.06e-3
	rate	–	0.22	0.51	0.52	0.58	0.64
$\varepsilon = 10^{-1}$	$\mathrm{err}_h(\rho)$	1.07e-2	5.76e-3	3.02e-3	1.56e-3	7.99e-4	4.06e-4
	rate	–	0.90	0.93	0.95	0.96	0.97
	$\mathrm{err}_h(m)$	4.03e-2	2.41e-2	1.38e-2	7.61e-3	4.06e-3	2.11e-3
	rate	–	0.74	0.81	0.85	0.91	0.94
$\varepsilon = 10^{-2}$	$\mathrm{err}_h(\rho)$	9.34e-3	4.78e-3	2.46e-3	1.25e-3	6.30e-4	3.17e-4
	rate	–	0.97	0.96	0.98	0.99	0.99
	$\mathrm{err}_h(m)$	3.53e-2	2.10e-2	1.53e-2	7.88e-3	4.40e-3	2.39e-3
	rate	–	0.75	0.45	0.96	0.84	0.88
$\varepsilon = 10^{-3}$	$\mathrm{err}_h(\rho)$	9.34e-3	4.77e-3	2.46e-3	1.25e-3	6.30e-4	3.16e-4
	rate	–	0.97	0.96	0.98	0.99	0.99
	$\mathrm{err}_h(m)$	3.53e-2	2.19e-2	1.89e-2	1.06e-2	9.76e-3	4.84e-3
	rate	–	0.69	0.21	0.83	0.12	1.01
$\varepsilon = 0$	$\mathrm{err}_h(\rho)$	9.34e-3	4.77e-3	2.46e-3	1.25e-3	6.30e-4	3.16e-4
	rate	–	0.97	0.96	0.98	0.99	0.99
	$\mathrm{err}_h(m)$	3.53e-2	2.20e-2	1.89e-2	1.08e-2	9.95e-3	5.27e-3
	rate	–	0.68	0.22	0.81	0.12	0.92

Table 3.2.: Error and convergence rates with respect to h for different values of ε. Space and time discretization with $h = \Delta\tau = 2^{-3-r}$ in refinement $r = 0, \dots, 5$.

Error estimates

We also investigate the simulation errors and convergence rates of the numerical scheme given in Problem 3.6 for different scaling parameters $\varepsilon \geq 0$. Since the exact solution to (3.15)–(3.20) is not known, the numerical errors are approximated by

$$\mathrm{err}_h(u) = \max_{n=1,\dots,N} \|u_h^n - u_{h/2}^n\|_{L^2(\mathcal{E})}$$

with $u = \rho$ or $u = m$ and $u_{h/2}^n$ denoting the solution on a finer mesh with $h = h/2$ and $\Delta\tau = \Delta\tau/2$ at the same time point $\tau_n = n\Delta\tau$ in time. The results are depicted in Table 3.2. As theoretically proven in Theorem 3.9, we observe linear convergence for the

density for all choices of the scaling parameter ε sufficiently small, in particular also for the parabolic limit $\varepsilon = 0$. Linear convergence can also be seen for the mass flux for ε sufficiently small, but not too close to the limit $\varepsilon = 0$, which is also in accordance with Theorem 3.9. Let us further highlight that the observed errors in the density are more or less identical for $\varepsilon = 10^{-2}, 10^{-3}$ and $\varepsilon = 0$, which underlines the asymptotic convergence behavior of the exact solutions to the parabolic limit.

3.5.2. Non-isothermal gas transport

Let us now focus on the non-isothermal gas transport in pipe networks. We consider a simple ideal gas, see Example 3.17 and 3.24, and choose $\gamma = 5/3$ which corresponds to a monatomic gas in dimension 3. Let us recall that $e(\rho, s) = \rho^{\gamma-1} e^{s/c_v}$ with $c_v = \frac{R}{\gamma-1}$ and $R = \mu\mathcal{R}$ with $\mathcal{R} = 8.314 \frac{J}{mol\,K}$ being the universal gas constant. As rescaled mole-mass fraction we choose $\mu = 1\,\frac{mol}{kg}$. Similarly, we can write the entropy s as function of density ρ and temperature θ, i.e., $s(\rho, \theta) = c_v \log(c_v\theta) - R\log(\rho)$. We choose the rescaled parameters $\ell_e = 1,\ d_e = 1,\ a_e = \pi^2/4,\ \beta_e = 1,\ \gamma_e = 1$ for all $e \in \mathcal{E}$, a constant ambient temperature of $\theta^0 = 1$ and a time horizon of $\tau_{max} = 5$. As boundary conditions we set

$$\begin{aligned}
[g_\partial^{v_1}(\tau),\, g_\partial^{v_4}(\tau),\, g_\partial^{v_7}(\tau),\, g_\partial^{v_{10}}(\tau),\, g_\partial^{v_{11}}(\tau)] &= [0.2\sin(2\pi\tau/\tau_{max})^3 + 1,\ 0.3\sin(2\pi\tau/\tau_{max})^3 + 1, \\
&\quad 1,\ 1,\ 1] \cdot \big(e(1, s(1,1)) + \partial_\rho e(1, s(1,1)) - s(1,1)\big), \\
\hat{s}_\partial^v(\tau) &= s(1,1) \quad \text{for all } v \in \mathcal{V}_\partial^{in}(\tau).
\end{aligned}$$

The initial condition is given by the corresponding stationary solution to the boundary conditions at time $\tau = 0$. By choosing a suitable basis for the discrete spaces Q_h, R_h and Z_h, we solve in each time step $n = 1, \ldots, N$ the system (3.94)–(3.96) using Newton's method, which usually converged within 4 steps using a tolerance up to 10^{-10} in our simulation.

Discrete balance laws

As a first step, we illustrate the validity of the discrete balance laws (3.102)–(3.104) for various choices of $0 < \varepsilon \leq 1$, which corresponds to different time and length scales. The results are displayed in Table 3.3 with

$$\begin{aligned}
\Delta M_h(\tau^n) &:= \int_{\mathcal{E}} a\rho_h^n - a\rho_h^0 \, dx + \Delta\tau \sum\nolimits_{j=1}^n \sum\nolimits_{v\in\mathcal{V}_\partial} m_h^j(v) n_e(v), \\
\Delta\mathcal{H}_h^\varepsilon(\tau^n) &:= \mathcal{H}^\varepsilon(\rho_h^n, w_h^n, s_h^n) - \mathcal{H}^\varepsilon(\rho_h^0, w_h^0, s_h^0) + \Delta\tau \sum\nolimits_{j=1}^n \sum\nolimits_{v\in\mathcal{V}_\partial} \hat{g}_\partial^v(\tau^j) m_h^j(v) n_e(v) \\
&\qquad + \Delta\tau \sum\nolimits_{j=1}^n \int_{\mathcal{E}} \gamma a \rho_h^j |w_h^j|^3 + \frac{\beta}{\varepsilon^3} \frac{(\theta_h^j - \theta^0)^2}{\theta_h^j} \, dx, \\
\Delta S_h^\varepsilon(\tau^n) &:= \int_{\mathcal{E}} a\rho_h^n s_h^n - a\rho_h^0 s_h^0 \, dx + \Delta\tau \sum\nolimits_{j=1}^n \int_{\mathcal{E}} \frac{\beta}{\varepsilon^3} \frac{\theta_h^j - \theta^0}{\theta_h^j} \, dx \\
&\qquad + \Delta\tau \sum\nolimits_{j=1}^n \Big(\langle m_h^j, s_h^j n\rangle_{\mathcal{V}_\partial^{out,j}} + \langle m_h^j, s_\partial^j n\rangle_{\mathcal{V}_\partial^{in,j}} \Big).
\end{aligned}$$

ε	1	2^{-1}	2^{-2}	2^{-3}	2^{-4}
$\Delta M_h(\tau_{max})$	-3.33e-16	1.47e-15	2.22e-15	0	-1.55e-15
$\Delta \mathcal{H}_h^\varepsilon(\tau_{max})$	-1.82e-1	-6.03e-2	-6.06e-2	-6.06e-2	-6.06e-2
$\Delta S_h^\varepsilon(\tau_{max})$	2.49e-14	4.17e-14	4.03e-11	1.66e-8	1.99e-5

Table 3.3.: Differences $\Delta M_h(\tau_{max})$, $\Delta \mathcal{H}_h^\varepsilon(\tau_{max})$, $\Delta S_h^\varepsilon(\tau_{max})$ in total mass, exergy and entropy at time $\tau_{max} = 5$ for $h = \Delta\tau = 2^{-6}$.

ε	1	2^{-1}	2^{-2}	2^{-3}	2^{-4}
$\Delta M_h(\tau_{max})$	-2.11e-15	-2.22e-15	1.89e-15	-1.22e-15	-6.12e-16
$\Delta \mathcal{H}_h^\varepsilon(\tau_{max})$	-1.82e-1	-6.01e-2	-6.06e-2	-6.06e-2	-6.06e-2
$\Delta S_h^\varepsilon(\tau_{max})$	5.89e-5	1.13e-1	6.66e-1	6.70e-1	6.70e-1

Table 3.4.: Differences $\Delta M_h(\tau_{max})$, $\Delta \mathcal{H}_h^\varepsilon(\tau_{max})$, $\Delta S_h^\varepsilon(\tau_{max})$ in total mass, exergy and entropy at time $\tau_{max} = 5$ for $h = \Delta\tau = 2^{-6}$ for coupling conditions (3.80)–(3.81) with η chosen as in Example 3.17.

They are in accordance with our theoretical findings from Theorem 3.25. In a second experiment, we changed to coupling conditions for the entropy to (3.80)–(3.81) with function $\eta(s) = e^{s/c_v}$ chosen as in Example 3.17. The method described in Problem 3.6 is changed according to Remark 3.22. Our findings are depicted in Table 3.4. Let us stress that entropy is now produced at junctions in comparison to the previous test.

Asymptotic convergence

Although a rigorous asymptotic analysis is not yet available, let us present a numerical test. We compare the solutions for different $\varepsilon > 0$ with the solution to the parabolic limit $\varepsilon = 0$. We measure the distance by

$$\operatorname{dist}(u) = \max_{n=0,\dots,N} \|u_h^{\varepsilon,n} - u_h^{0,n}\|_{L^2(\mathcal{E})}$$

for $u = \rho, m, s$ on a fine mesh. Our results are depicted in Table 3.5. For ε sufficiently

ε	1	10^{-1}	10^{-2}	10^{-3}	10^{-4}	10^{-5}	10^{-6}
dist(ρ)	2.67e-1	4.98e-2	2.31e-4	7.82e-7	8.24e-9	8.28e-11	8.29e-13
rate	–	0.73	2.33	2.47	1.98	2.00	2.00
dist(m)	3.28	2.86e-1	1.49e-2	1.19e-3	3.17e-5	3.19e-7	3.19e-9
rate	–	1.06	1.28	1.10	1.57	2.00	2.00
dist(s)	4.57	5.32e-1	1.81e-3	6.22e-6	6.17e-8	6.17e-10	6.17e-12
rate	–	0.93	2.47	2.46	2.00	2.00	2.00

Table 3.5.: Distance to the parabolic limit and convergence rate with respect to ε. The mesh sizes are chosen as $h = \Delta\tau = 2^{-6}$.

small the solutions are very close. We also displayed the convergence rates which for small ε indicate a second-order convergence.

3.6. Discussion and outlook

To conclude this chapter, we discuss our results and open questions and give an outlook on possible future research directions.

Isothermal gas transport. The first part of this chapter was dedicated to the isothermal gas transport in pipe networks. For an appropriate numerical approximation, we proposed the mixed finite element method given in Problem 3.6 using basis functions of the lowest order. The extension to higher-order polynomials and, in particular, the analysis of the discretization error by using similar techniques based on relative energy estimates could be of interest. We also see a lot of potential in analyzing structure-preserving Galerkin methods for other nonlinear problems that have an underlying "energy structure" by relative energy techniques.

Another topic that might be worth investigating is concerned with an alternative proof of the well-posedness of the parabolic gas model. In [113], the existence of weak solutions is shown based on the reformulation of the problem to the degenerate second-order parabolic equation. A Galerkin approximation of the corresponding weak formulation yields convergent subsequences whose limits turn out to be weak solutions. It would be of interest to alternatively consider the approximation of the parabolic problem provided by our method for $\varepsilon = 0$. It might then be possible to show that the limit also yields a weak solution to the corresponding variational formulation (3.22)–(3.23).

Finally, the application of our method to calibration and optimal control problems arising in the context of gas networks leaves room for future research [78].

Non-isothermal gas transport. We proposed a suitable transformation of the model equations. The corresponding weak formulation (3.82)–(3.84) turned out to have an energy structure that could be written as an abstract system of the form (3.88)–(3.89). In particular, the problem had a similar structure as the reformulated isothermal gas transport model (3.26)–(3.27), but with one crucial difference, namely the skew-symmetric matrix $\mathcal{J}$ depended on the state u. However, a rigorous asymptotic analysis is not yet available. It might be possible to estimate the difference between the solution $u^\varepsilon = (\rho^\varepsilon, w^\varepsilon, s^\varepsilon)$ to the non-isothermal gas transport (3.70)–(3.79) and the parabolic limit solution $u^0 = (\rho^0, w^0, s^0 = s^0(\rho^0))$, which can again be understood as a perturbed solution to (3.82)–(3.84), with similar techniques as for the isothermal case in Section 3.1.7. In order to use the relative exergy that is given by

$$\mathcal{H}^\varepsilon(u^\varepsilon|u^0) := \mathcal{H}^\varepsilon(u^\varepsilon) - \mathcal{H}^\varepsilon(u^0) - \langle \mathcal{H}^\varepsilon(u^0), u^\varepsilon - u^0 \rangle$$

with exergy functional defined in (3.85) as a distance measure, we have to ensure that $\mathcal{H}^\varepsilon(\cdot|\cdot)$ is equivalent to some norm, i.e., the exergy $\mathcal{H}^\varepsilon$ is strongly convex with respect to a norm. In the isothermal case, this was true under a subsonic condition, and we expect

that under similar conditions like (B1)–(B3), i.e., close to the parabolic limit, this also holds in the non-isothermal case. For research in similar directions, we refer to [16, 51] where the exergy was used to investigate the weak-strong uniqueness for the Navier-Stokes and the full Euler system, respectively.

The next step could then be a rigorous error analysis of the method proposed in Problem 3.21. Since the energy structure is preserved by the discretization scheme, it might be possible to investigate the error and convergence with similar techniques as in the isothermal case presented in Section 3.2.

Conclusion

In this thesis, we considered three examples of partial differential equations on networks that each contained an asymptotic parameter ε describing either a singular perturbation, different modeling scales, or different physical regimes. The problem type and the type of asymptotics differed forcing us to use various techniques and approaches for the analysis. Let us summarize the focus areas and main tools, as well as comment on some open questions and possible next steps. A detailed discussion and outlook for each of the three model problems can be found at the end of the corresponding chapter.

Existence of solutions. In Chapter 1 and 2 we provided existence results of solutions to the corresponding problems under consideration. As a main tool, we exploited semigroup theory, which turned out to be particularly well-suited for problems on networks. Energy estimates based on weak characterizations of solutions and fixed point arguments in the case of nonlinear equations then enabled us to derive the existence and uniqueness of solutions uniformly in the scaling parameter ε. For the kinetic chemotaxis model in Chapter 2, however, we could only prove local existence. The extension to global results is a possible next step for our research; we expect the need for other techniques.

Asymptotic analysis. One main focus of this work was the investigation of the behavior of solutions for $\varepsilon \to 0$. Different techniques were applied for the asymptotic analysis. In Chapter 1 and 2 we made use of suitable boundary layer functions and asymptotic expansions in order to derive quantitative estimates. A-priori bounds on solutions uniformly in the scaling parameter ε were crucial for the analysis of the kinetic chemotaxis model. The investigation of more general coupling conditions, as well as nonlinear models in the context of traffic flow or cross-diffusion systems and other kinetic equations (on networks) opens up further research fields. For the isothermal gas transport model in Chapter 3, however, we needed different tools. Based on a suitable transformation of the equations and a weak characterization of solutions having an "energy structure", we exploited relative energy estimates to obtain an asymptotic estimate. The extension to the non-isothermal model, which has a similar "energy structure", seems possible, but remains to be studied.

Numerical approximation. Based on weak characterizations of solutions, we considered Galerkin methods that preserved the underlying structure and the basic properties of the model problems. Moreover, methods were still viable in the asymptotic limit $\varepsilon = 0$. A special emphasis was on the proper handling of the coupling conditions at network junctions. Introducing additional hybrid variables at vertices and grid points turned out to be particularly well-suited. The application of similar methods to other (nonlinear)

problems on networks is of great interest. Moreover, a suitable numerical approximation of the kinetic chemotaxis model on networks, that is still viable in the diffusion limit $\varepsilon = 0$, has not been considered yet and is thus a possible next step for our research.

Error analysis. In order to analyze the error of the proposed numerical methods, we faced different challenges. In Chapter 1 boundary and internal layers made the use of layer-adapted meshes on the edges of the network necessary, leading to ε-uniform error estimates. The particular construction and proposed approximation strategy could be applied to other problems (on networks) forming layers for small scalings. A completely different error analysis was performed for the isothermal gas transport in Chapter 3. Based on the "energy structure" of our model problem that was inherited by the mixed finite element method for the isothermal gas transport, we used relative energy estimates to measure the discretization error. We further hope to analyze the error of the numerical method for the non-isothermal gas transport with similar techniques. This is, however, left for future research. In general, relative energy estimates are an extremely useful tool for the error analysis of (structure-preserving) discretization schemes and could be applied to other nonlinear problems having an "energy structure".

A

Appendix

A.1. Verification of (E1)–(E3) in the proof of Theorem 3.5

For the sake of completeness, we show that the estimates (E1)–(E3) are valid for $u^\varepsilon = (\rho^\varepsilon, w^\varepsilon)$ and $u^0 = (\rho^0, w^0)$ solving (3.26)–(3.27) and (3.39)–(3.40), respectively.

Verification of (E1). By definition of $\mathcal{H}^\varepsilon$ in (3.24) it holds that

$$(\mathcal{H}^\varepsilon)'(u^\varepsilon) - (\mathcal{H}^\varepsilon)'(u^0) - (\mathcal{H}^\varepsilon)''(u^0)(u^\varepsilon - u^0) = \begin{pmatrix} aP'(\rho^\varepsilon|\rho^0) + \frac{1}{2}a\varepsilon^2(w^\varepsilon - w^0)^2 \\ a\varepsilon^2(\rho^\varepsilon - \rho^0)(w^\varepsilon - w^0) \end{pmatrix}$$

with $P'(\rho^\varepsilon|\rho^0) := P'(\rho^\varepsilon) - P'(\rho^0) - P''(\rho^0)(\rho^\varepsilon - \rho^0)$. Applying Taylor's theorem then yields

$$P'(\rho^\varepsilon|\rho^0) \leq |P'''(\rho^*)|(\rho^\varepsilon - \rho^0)^2 \leq C(\rho^\varepsilon - \rho^0)^2$$

with intermediate value $\rho^* := \xi\rho^\varepsilon + (1-\xi)\rho^0$ for some $\xi \in (0,1)$. The latter inequality holds since the pressure potential P is smooth and ρ is bounded due to (A1) and (A3). Young's inequality further enables us to estimate

$$a\varepsilon^2(\rho^\varepsilon - \rho^0)(w^\varepsilon - w^0) \leq \tfrac{1}{2}\bar{a}\varepsilon|\rho^\varepsilon - \rho^0|^2 + \tfrac{1}{2}\bar{a}\varepsilon^3|w^\varepsilon - w^0|^2,$$

which then leads to

$$\begin{aligned} \langle (\mathcal{H}^\varepsilon)'(u^\varepsilon) - (\mathcal{H}^\varepsilon)'(u^0) - (\mathcal{H}^\varepsilon)''(u^0)(u^\varepsilon - u^0), \partial_\tau u^0 \rangle \\ \leq C'\|\partial_\tau u^0\|_{\varepsilon,\infty}\|u^\varepsilon - u^0\|_\varepsilon^2 \leq C_1\mathcal{H}^\varepsilon(u^\varepsilon|u^0) \end{aligned}$$

with ε-weighted norms defined in (3.34). In the last step we used the norm equivalence (3.35) for the relative energy and the fact that u^0 is bounded in $W^{1,\infty}(0,\tau_{max}; L^\infty(\mathcal{E}))^2$.

Verification of (E2). Since $(|\xi|\xi)' = 2|\xi|$, it holds that

$$\gamma|w^\varepsilon|w^\varepsilon - \gamma|w^0|w^0 = 2\gamma\int_0^1 |w^0 + \xi(w^\varepsilon - w^0)|\, d\xi\ (w^\varepsilon - w^0).$$

The integral can further be estimated from below and above by

$$\frac{|w^\varepsilon| + |w^0|}{4} \leq \int_0^1 |w^0 + \xi(w^\varepsilon - w^0)|\, d\xi \leq \frac{|w^\varepsilon| + |w^0|}{2}. \tag{A.1}$$

The upper estimate is an immediate consequence of the triangle inequality. The lower estimate can be shown by minimizing the functional $F(w^\varepsilon) := \int_0^1 |w^0 + \xi(w^\varepsilon - w^0)|\, d\xi$ for fixed w^0. Since F takes its minimum for $w^\varepsilon = -w^0$, we have

$$\int_0^1 |w^0 + \xi(w^\varepsilon - w^0)|\, d\xi \geq \min F(w^\varepsilon) = \tfrac{1}{4}|w^0| + \tfrac{1}{4}|w^\varepsilon|.$$

We can further write

$$m^\varepsilon - m^0 = a\rho^\varepsilon w^\varepsilon - a\rho^0 w^0 = a(\rho^\varepsilon - \rho^0)w^\varepsilon + a\rho^0(w^\varepsilon - w^0),$$

which together with the previous considerations yields

$$\begin{aligned}(\gamma|w^\varepsilon|w^\varepsilon - \gamma|w^0|w^0)(m^\varepsilon - m^0) &= 2a\gamma w^\varepsilon \int_0^1 |w^0 + \xi(w^\varepsilon - w^0)|\, d\xi\ (\rho^\varepsilon - \rho^0)(w^\varepsilon - w^0) \\ &\quad + 2a\gamma\rho^0 \int_0^1 |w^0 + \xi(w^\varepsilon - w^0)|\, d\xi\ (w^\varepsilon - w^0)^2 = (i) + (ii).\end{aligned}$$

From (A.1) and Young's inequality we deduce that

$$\begin{aligned}(i) &\geq -\tfrac{1}{4}a\gamma\rho^0(|w^\varepsilon| + |w^0|)(w^\varepsilon - w^0)^2 - 2a\gamma\tfrac{(w^\varepsilon)^2}{\rho^0}(|w^\varepsilon| + |w^0|)(\rho^\varepsilon - \rho^0)^2, \\ (ii) &\geq \tfrac{1}{2}a\gamma\rho^0(|w^\varepsilon| + |w^0|)(w^\varepsilon - w^0)^2.\end{aligned}$$

With the bounds in (A2)–(A3), we finally obtain

$$\begin{aligned}-\langle \mathcal{R}(u^\varepsilon) - \mathcal{R}(u^0), \boldsymbol{z}^\varepsilon(u^\varepsilon) - \boldsymbol{z}^\varepsilon(u^0)\rangle &\leq -\sum\nolimits_{e\in\mathcal{E}} \int_0^{\ell_e} (i) + (ii)\ dx \\ &\leq -\tfrac{1}{4}\sum\nolimits_{e\in\mathcal{E}} \int_0^{\ell_e} a_e\gamma_e\rho^0(|w^\varepsilon| + |w^0|)(w^\varepsilon - w^0)^2\ dx + 4\bar{a}\bar{\gamma}\tfrac{\bar{w}^3}{\underline{\rho}}\|\rho^\varepsilon - \rho^0\|_{\mathcal{E}}^2 \\ &\leq -2\mathcal{D}(u^\varepsilon|u^0) + C_2\mathcal{H}^\varepsilon(u^\varepsilon|u^0)\end{aligned}$$

with relative dissipation functional defined by (3.43).

Verification of (E3). Inserting the definition of the residual in (3.41) yields

$$\langle \boldsymbol{res}^0, \boldsymbol{z}^\varepsilon(u^\varepsilon) - \boldsymbol{z}^\varepsilon(u^0)\rangle = (\varepsilon^2\partial_\tau w^0, m^\varepsilon - m^0)_{\mathcal{E}} - (\tfrac{\varepsilon^2}{2}(w^0)^2, \partial_x(m^\varepsilon - m^0))_{\mathcal{E}} = (iii) + (iv).$$

The first term can be estimated using Hölder's and Young's inequality, the bounds in (A2)–(A3) as well as the fact that $m^\varepsilon - m^0 = a(\rho^\varepsilon - \rho^0)w^\varepsilon + a\rho^0(w^\varepsilon - w^0)$ which leads to

$$\begin{aligned}(iii) \leq\ & \tfrac{1}{2}\bar{a}\bar{w}\big(\varepsilon^4\|\partial_\tau w^0\|_{L^2(\mathcal{E})}^2 + \|\rho^\varepsilon - \rho^0\|_{L^2(\mathcal{E})}^2\big) + \tfrac{8}{3}\tfrac{(\bar{a}\bar{\rho})^{3/2}}{(3\underline{a}\underline{\gamma}\underline{\rho})^{1/2}}\varepsilon^3\|\partial_\tau w^0\|_{L^{3/2}(\mathcal{E})}^{3/2} \\ & + \tfrac{1}{16}\underline{a}\underline{\gamma}\underline{\rho}\|w^\varepsilon - w^0\|_{L^3(\mathcal{E})}^3 \leq C\mathcal{H}^\varepsilon(u^\varepsilon|u^0) + \tfrac{1}{2}\mathcal{D}(u^\varepsilon|u^0) + C'\varepsilon^3,\end{aligned}$$

where the latter inequality follows from (3.35), (3.43), the bounds on $\partial_\tau u^0$, and the finiteness of the network. If $|w^\varepsilon|, |w^0| \geq \underline{w} > 0$, we can alternatively estimate

$$\begin{aligned}(iii) \leq\ & \tfrac{1}{2}\bar{a}\bar{w}\big(\varepsilon^4\|\partial_\tau w^0\|_{L^2(\mathcal{E})}^2 + \|\rho^\varepsilon - \rho^0\|_{L^2(\mathcal{E})}^2\big) + 8\tfrac{\bar{a}^2\bar{\rho}^2}{\underline{a}\underline{\gamma}\underline{\rho}\underline{w}}\varepsilon^4\|\partial_\tau w^0\|_{L^2(\mathcal{E})}^2 \\ & + \tfrac{1}{16}\underline{a}\underline{\gamma}\underline{\rho}\underline{w}\|w^\varepsilon - w^0\|_{L^2(\mathcal{E})}^2 \leq C\mathcal{H}^\varepsilon(u^\varepsilon|u^0) + \tfrac{1}{2}\mathcal{D}(u^\varepsilon|u^0) + C'\varepsilon^4,\end{aligned} \tag{A.2}$$

using (3.44) instead of (3.43). Similarly, by applying integration-by-parts we find that

$$(iv) = (\varepsilon^2 w^0 \partial_x w^0, m^\varepsilon - m^0)_{\mathcal{E}} \leq C\mathcal{H}(u^\varepsilon|u^0) + \tfrac{1}{2}\mathcal{D}(u^\varepsilon|u^0) + C'\varepsilon^3,$$

where C' now depends on $\|\partial_x w^0\|_{L^2(\mathcal{E})}$ which is bounded by assumption. This estimate can again be improved if the velocities are bounded away from zero. In summary, this proves (E3). □

A.2. Discrete Grönwall lemma

In the proof of the uniform convergence result from Theorem 3.9 in Chapter 3, we make use of the following discrete version of the Grönwall lemma.

Lemma A.1. *Let a^n, b^n, $d^n \geq 0$ for $n = 0, \dots, N$, and let $\Delta\tau > 0$ with $c\Delta\tau < 1$ for a given $c > 0$. Moreover, for all $1 \leq n \leq N$ it holds that*

$$a^n + \sum_{k=1}^n \Delta\tau d^k \leq a^0 + b^n + c\sum_{k=1}^n \Delta\tau(a^k + a^{k-1}). \tag{A.3}$$

Then,

$$a^n + \Delta\tau \sum_{k=1}^n d^k \leq a^0 + b^n + c\Delta\tau e^{\frac{2nc\Delta\tau}{1-c\Delta\tau}}\big(a^0 + \sum_{k=1}^n e^{\frac{(1-2k)c\Delta\tau}{1-c\Delta\tau}}(2a_0 + b^k + b^{k-1})\big).$$

Proof. Let us introduce

$$s^n := \sum_{k=1}^n (a^k + a^{k-1}), \quad s^0 = a^0, \quad \text{and} \quad w := \frac{1 - c\Delta\tau}{1 + c\Delta\tau}.$$

and rewrite (A.3) as

$$a^n - c\Delta\tau s^n \leq a^0 + b^n - \sum_{k=1}^n \Delta\tau d^k. \tag{A.4}$$

By defining $\tilde{a}^n := w^n s^n$ we observe that

$$\begin{aligned}
\tilde{a}^n - \tilde{a}^{n-1} &= w^n s^n - w^{n-1}s^{n-1} = w^{n-1}(ws^n - s^{n-1}) \\
&= w^{n-1}(1 + c\Delta\tau)^{-1}(s^n - c\Delta\tau s^n - s^{n-1} - c\Delta\tau s^{n-1}) \\
&= w^{n-1}(1 + c\Delta\tau)^{-1}\big((a^n - c\Delta\tau s^n) + (a^{n-1} - c\Delta\tau s^{n-1})\big) \\
&\leq w^{n-1}(1 + c\Delta\tau)^{-1}(a^0 + b^n - \sum_{k=1}^n \Delta\tau d^k + a^0 + b^{n-1} - \sum_{k=1}^{n-1} \Delta\tau d^k),
\end{aligned}$$

where we used (A.4) for the last inequality. Summing up over n then leads to

$$\tilde{a}^n \leq \tilde{a}^0 + \sum_{k=1}^n w^{k-1}(1 + c\Delta\tau)^{-1}\big(2a^0 + b^k + b^{k-1} - \sum_{j=1}^k \Delta\tau d^j - \sum_{j=1}^{k-1} \Delta\tau d^j\big).$$

Since $\tilde{a}^0 = a^0$ and $\tilde{a}^n = w^n s^n$ as well as $d^j \geq 0$, we see that

$$s^n \leq w^{-n}a^0 + w^{-n}\sum_{k=1}^n w^{k-1}(1 + c\Delta\tau)^{-1}\big(2a^0 + b^k + b^{k-1}\big).$$

In order to estimate the terms on the right-hand side, we make use of the fact that

$$w^{-n} = \left(\tfrac{1+c\Delta\tau}{1-c\Delta\tau}\right)^n = \left(1 + \tfrac{2c\Delta\tau}{1-c\Delta\tau}\right)^n \leq e^{2nc\Delta\tau/(1-c\Delta\tau)},$$

which follows from the exponential series. From this, we immediately conclude that

$$w^{-n}w^{k-1}(1+c\Delta\tau)^{-1} = \left(\tfrac{1+c\Delta\tau}{1-c\Delta\tau}\right)^{n-k}(1-c\Delta\tau)^{-1} \leq e^{\frac{(2(n-k)+1)c\Delta\tau}{1-c\Delta\tau}},$$

where we additionally used that $(1-c\Delta\tau)^{-1} = 1 + \frac{c\Delta\tau}{1-c\Delta\tau} \leq e^{c\Delta\tau/(1-c\Delta\tau)}$. Inserting into (A.4) yields

$$a^n + \Delta\tau \sum\nolimits_{k=1}^{n} d^k \leq a^0 + b^n + c\Delta\tau e^{\frac{2nc\Delta\tau}{1-c\Delta\tau}}\left(a^0 + \sum\nolimits_{k=1}^{n} e^{\frac{(1-2k)c\Delta\tau}{1-c\Delta\tau}}(2a_0 + b^k + b^{k-1})\right),$$

which already proves the assertion. □

Bibliography

[1] G. Akrivis, C. Makridakis, and R. H. Nochetto. Galerkin and Runge-Kutta methods: unified formulation, a posteriori error estimates and nodal superconvergence. *Numer. Math.*, 118(3):429–456, 2011.

[2] M. D. Baker, P. M. Wolanin, and J. B. Stock. Signal transduction in bacterial chemotaxis. *Bioessays*, 28(1):9–22, 2006.

[3] A. Bamberger, M. Sorine, and J. P. Yvon. Analyse et contrôle d'un réseau de transport de gaz. In *Computing methods in applied sciences and engineering (Proc. Third Internat. Sympos., Versailles, 1977), II*, volume 91 of *Lecture Notes in Phys.*, pages 347–359. Springer, Berlin-New York, 1979.

[4] J. A. Bárcena-Petisco, M. Cavalcante, G. M. Coclite, N. de Nitti, and E. Zuazua. Control of hyperbolic and parabolic equations on networks and singular limits. *HAL-report*, 03233211, 2021.

[5] C. Bardos, F. Golse, B. Perthame, and R. Sentis. The nonaccretive radiative transfer equations: existence of solutions and Rosseland approximation. *J. Funct. Anal.*, 77(2):434–460, 1988.

[6] J. Bergh and J. Löfström. *Interpolation spaces. An introduction.* Grundlehren der Mathematischen Wissenschaften, No. 223. Springer-Verlag, Berlin-New York, 1976.

[7] C. Berthon, M. Bessemoulin-Chatard, and H. Mathis. Numerical convergence rate for a diffusive limit of hyperbolic systems: p-system with damping. *SMAI J. Comput. Math.*, 2:99–119, 2016.

[8] L. Bobisud. Second-order linear parabolic equations with a small parameter. *Arch. Rational Mech. Anal.*, 27:385–397, 1967.

[9] R. Borsche, S. Göttlich, A. Klar, and P. Schillen. The scalar Keller-Segel model on networks. *Math. Models Methods Appl. Sci.*, 24(2):221–247, 2014.

[10] R. Borsche, J. Kall, A. Klar, and T. N. H. Pham. Kinetic and related macroscopic models for chemotaxis on networks. *Math. Models Methods Appl. Sci.*, 26(6):1219–1242, 2016.

[11] F. Boyer and P. Fabrie. *Mathematical Tools for the Study of the Incompressible Navier-Stokes Equations and Related Models*, volume 183. Springer Science & Business Media, 2012.

[12] S. C. Brenner and L. R. Scott. *The mathematical theory of finite element methods*, volume 15 of *Texts in Applied Mathematics*. Springer, New York, third edition, 2008.

[13] A. Bressan, S. Čanić, M. Garavello, M. Herty, and B. Piccoli. Flows on networks: recent results and perspectives. *EMS Surv. Math. Sci.*, 1(1):47–111, 2014.

[14] G. Bretti, R. Natalini, and M. Ribot. A hyperbolic model of chemotaxis on a network: a numerical study. *ESAIM Math. Model. Numer. Anal.*, 48(1):231–258, 2014.

[15] J. Brouwer, I. Gasser, and M. Herty. Gas pipeline models revisited: model hierarchies, nonisothermal models, and simulations of networks. *Multiscale Model. Simul.*, 9(2):601–623, 2011.

[16] J. Březina and E. Feireisl. Measure-valued solutions to the complete Euler system. *J. Math. Soc. Japan*, 70(4):1227–1245, 2018.

[17] H. B. Callen. Thermodynamics and an introduction to thermostatistics, 1998.

[18] F. L. Cardoso-Ribeiro, D. Matignon, and L. Lefèvre. A partitioned finite element method for power-preserving discretization of open systems of conservation laws. *IMA J. Math. Control Inform.*, 38(2):493–533, 2021.

[19] F. A. C. C. Chalub, P. A. Markowich, B. Perthame, and C. Schmeiser. Kinetic models for chemotaxis and their drift-diffusion limits. *Monatsh. Math.*, 142(1-2):123–141, 2004.

[20] B. Cockburn, J. Gopalakrishnan, and R. Lazarov. Unified hybridization of discontinuous Galerkin, mixed, and continuous Galerkin methods for second order elliptic problems. *SIAM J. Numer. Anal.*, 47:1319–1365, 2009.

[21] G. M. Coclite and M. Garavello. Vanishing viscosity for traffic on networks. *SIAM J. Math. Anal.*, 42:1761–1783, 2010.

[22] R. M. Colombo and F. Marcellini. Coupling conditions for the 3×3 Euler system. *Netw. Heterog. Media*, 5(4):675–690, 2010.

[23] R. M. Colombo and C. Mauri. Euler system for compressible fluids at a junction. *J. Hyperbolic Differ. Equ.*, 5(3):547–568, 2008.

[24] P. Constantinou and C. Xenophontos. Finite element analysis of an exponentially graded mesh for singularly perturbed problems. *Comput. Methods Appl. Math.*, 15:135–143, 2015.

[25] J. B. Conway. *A course in functional analysis*, volume 96. Springer, 2019.

[26] C. M. Dafermos. *Hyperbolic conservation laws in continuum physics*, volume 325 of *Grundlehren der mathematischen Wissenschaften [Fundamental Principles of Mathematical Sciences]*. Springer-Verlag, Berlin, fourth edition, 2016.

[27] R. Dautray and J.-L. Lions. *Mathematical analysis and numerical methods for science and technology. Vol. 6.* Springer-Verlag, Berlin, 1993. Evolution problems. II, With the collaboration of Claude Bardos, Michel Cessenat, Alain Kavenoky, Patrick Lascaux, Bertrand Mercier, Olivier Pironneau, Bruno Scheurer and Rémi Sentis, Translated from the French by Alan Craig.

[28] E. Di Nezza, G. Palatucci, and E. Valdinoci. Hitchhiker's guide to the fractional Sobolev spaces. *Bull. Sci. Math.*, 136(5):521–573, 2012.

[29] D. A. Di Pietro and A. Ern. *Mathematical aspects of discontinuous Galerkin methods*, volume 69. Springer Science & Business Media, 2011.

[30] J. I. Diaz and F. de Thélin. On a nonlinear parabolic problem arising in some models related to turbulent flows. *SIAM J. Math. Anal.*, 25(4):1085–1111, 1994.

[31] V. Dolejší and M. Feistauer. *Discontinuous Galerkin method*, volume 48 of *Springer Series in Computational Mathematics*. Springer, Cham, 2015. Analysis and applications to compressible flow.

[32] D. Dormann and C. J. Weijer. Chemotactic cell movement during dictyostelium development and gastrulation. *Curr. Opin. Genet. Dev.*, 16(4):367–373, 2006.

[33] B. Dorn, M. Kramar Fijavž, R. Nagel, and A. Radl. The semigroup approach to transport processes in networks. *Phys. D*, 239:1416–1421, 2010.

[34] R. G. Durán and A. L. Lombardi. Finite element approximation of convection diffusion problems using graded meshes. *Appl. Numer. Math.*, 56:1314–1325, 2006.

[35] H. Egger. A robust conservative mixed finite element method for isentropic compressible flow on pipe networks. *SIAM J. Sci. Comput.*, 40(1):A108–A129, 2018.

[36] H. Egger. Structure preserving approximation of dissipative evolution problems. *Numer. Math.*, 143(1):85–106, 2019.

[37] H. Egger and J. Giesselmann. Stability and asymptotic analysis for instationary gas transport via relative energy estimates. *Numer. Math.*, 153(4):701–728, 2023.

[38] H. Egger, J. Giesselmann, T. Kunkel, and N. Philippi. An asymptotic-preserving discretization scheme for gas transport in pipe networks. *IMA J. Numer. Anal.*, 2022.

[39] H. Egger and N. Philippi. A hybrid discontinuous Galerkin method for transport equations on networks. In *Finite volumes for complex applications IX—methods, theoretical aspects, examples—FVCA 9, Bergen, Norway, June 2020*, volume 323 of *Springer Proc. Math. Stat.*, pages 487–495. Springer, Cham, 2020.

[40] H. Egger and N. Philippi. On the transport limit of singularly perturbed convection-diffusion problems on networks. *Math. Methods Appl. Sci.*, 44(6):5005–5020, 2021.

[41] H. Egger and N. Philippi. A hybrid-dG method for singularly perturbed convection-diffusion equations on pipe networks. *ESAIM: M2AN*, 57(4):2077–2095, 2023.

[42] H. Egger and M. Schlottbom. A mixed variational framework for the radiative transfer equation. *Math. Models Methods Appl. Sci.*, 22(3):1150014, 30, 2012.

[43] H. Egger and M. Schlottbom. Diffusion asymptotics for linear transport with low regularity. *Asymptot. Anal.*, 89(3-4):365–377, 2014.

[44] H. Egger and L. Schöbel-Kröhn. Chemotaxis on networks: Analysis and numerical approximation. *ESAIM: M2AN*, 54(4):1339–1372, 2020.

[45] H. Egger and J. Schöberl. A hybrid mixed discontinuous Galerkin finite-element method for convection-diffusion problems. *IMA J. Numer. Anal.*, 30:1206–1234, 2010.

[46] K.-J. Engel and R. Nagel. *One-parameter semigroups for linear evolution equations*, volume 194 of *Graduate Texts in Mathematics*. Springer-Verlag, New York, 2000. With contributions by S. Brendle, M. Campiti, T. Hahn, G. Metafune, G. Nickel, D. Pallara, C. Perazzoli, A. Rhandi, S. Romanelli and R. Schnaubelt.

[47] J. L. Ericksen. *Introduction to the Thermodynamics of Solids*, volume 275. Springer, 1998.

[48] A. Ern and J.-L. Guermond. *Finite elements III—first-order and time-dependent PDEs*, volume 74 of *Texts in Applied Mathematics*. Springer, Cham, [2021] ©2021.

[49] L. C. Evans. *Partial differential equations*, volume 19 of *Graduate Studies in Mathematics*. American Mathematical Society, Providence, RI, second edition, 2010.

[50] E. Feireisl, M. Lukáčová-Medviďová, v. Nečasová, A. Novotný, and B. She. Asymptotic preserving error estimates for numerical solutions of compressible Navier-Stokes equations in the low Mach number regime. *Multiscale Model. Simul.*, 16(1):150–183, 2018.

[51] E. Feireisl and A. Novotný. Weak-strong uniqueness property for the full Navier-Stokes-Fourier system. *Arch. Ration. Mech. Anal.*, 204(2):683–706, 2012.

[52] E. Feireisl and A. Novotný. *Singular limits in thermodynamics of viscous fluids*. Advances in Mathematical Fluid Mechanics. Birkhäuser/Springer, Cham, 2017.

[53] G. Fu, W. Qiu, and W. Zhang. An analysis of HDG methods for convection-dominated diffusion problems. *ESAIM Math. Model. Numer. Anal.*, 49(1):225–256, 2015.

[54] T. Gallouët, R. Herbin, D. Maltese, and A. Novotny. Error estimates for a numerical approximation to the compressible barotropic Navier-Stokes equations. *IMA J. Numer. Anal.*, 36(2):543–592, 2016.

[55] M. Garavello and B. Piccoli. *Traffic flow on networks*, volume 1 of *AIMS Series on Applied Mathematics*. American Institute of Mathematical Sciences (AIMS), Springfield, MO, 2006.

[56] E. C. Gartland, Jr. Graded-mesh difference schemes for singularly perturbed two-point boundary value problems. *Math. Comp.*, 51(184):631–657, 1988.

[57] T. Geveci. On the application of mixed finite element methods to the wave equations. *RAIRO Modél. Math. Anal. Numér.*, 22(2):243–250, 1988.

[58] E. Godlewski and P.-A. Raviart. *Numerical approximation of hyperbolic systems of conservation laws*, volume 118 of *Applied Mathematical Sciences*. Springer-Verlag, New York, [2021] ©2021.

[59] F. R. Guarguaglini and R. Natalini. Global smooth solutions for a hyperbolic chemotaxis model on a network. *SIAM J. Math. Anal.*, 47(6):4652–4671, 2015.

[60] F. R. Guarguaglini and R. Natalini. Vanishing viscosity approximation for linear transport equations on finite star-shaped networks. *J. Evol. Equ.*, 21(2):2413–2447, 2021.

[61] F. R. Guarguaglini, M. Papi, and F. Smarrazzo. Local and global solutions for a hyperbolic-elliptic model of chemotaxis on a network. *Math. Models Methods Appl. Sci.*, 29(8):1465–1509, 2019.

[62] M. Gugat and S. Ulbrich. Lipschitz solutions of initial boundary value problems for balance laws. *Math. Models Methods Appl. Sci.*, 28(5):921–951, 2018.

[63] E. Hairer and G. Wanner. *Solving ordinary differential equations. II*, volume 14 of *Springer Series in Computational Mathematics*. Springer-Verlag, Berlin, second edition, 1996. Stiff and differential-algebraic problems.

[64] S.-A. Hauschild, N. Marheineke, V. Mehrmann, J. Mohring, A. M. Badlyan, M. Rein, and M. Schmidt. Port-Hamiltonian modeling of district heating networks. In *Progress in differential-algebraic equations II*, Differ.-Algebr. Equ. Forum, pages 333–355. Springer, Cham, 2020.

[65] M. Herty. Coupling conditions for networked systems of Euler equations. *SIAM J. Sci. Comput.*, 30(3):1596–1612, 2008.

[66] T. Hillen and K. J. Painter. A user's guide to PDE models for chemotaxis. *J. Math. Biol.*, 58(1-2):183–217, 2009.

[67] T. Hillen, C. Rohde, and F. Lutscher. Existence of weak solutions for a hyperbolic model of chemosensitive movement. *J. Math. Anal. Appl.*, 260(1):173–199, 2001.

[68] T. Hillen and A. Stevens. Hyperbolic models for chemotaxis in 1-d. *Nonlinear Anal. Real World Appl.*, 1, 10 2000.

[69] D. Horstmann. From 1970 until present: the Keller-Segel model in chemotaxis and its consequences. I. *Jahresber. Deutsch. Math.-Verein.*, 105(3):103–165, 2003.

[70] H. J. Hwang, K. Kang, and A. Stevens. Drift-diffusion limits of kinetic models for chemotaxis: a generalization. *Discrete Contin. Dyn. Syst. Ser. B*, 5(2):319–334, 2005.

[71] H. J. Hwang, K. Kang, and A. Stevens. Global existence of classical solutions for a hyperbolic chemotaxis model and its parabolic limit. *Indiana Univ. Math. J.*, 55(1):289–316, 2006.

[72] V. John. *Finite element methods for incompressible flow problems*, volume 51 of *Springer Series in Computational Mathematics*. Springer, Cham, 2016.

[73] P. Joly. Variational methods for time-dependent wave propagation problems. In *Topics in computational wave propagation*, volume 31 of *Lect. Notes Comput. Sci. Eng.*, pages 201–264. Springer, Berlin, 2003.

[74] S. Junca and M. Rascle. Strong relaxation of the isothermal Euler system to the heat equation. *Z. Angew. Math. Phys.*, 53(2):239–264, 2002.

[75] A. Jüngel. *Entropy methods for diffusive partial differential equations*. SpringerBriefs in Mathematics. Springer, [Cham], 2016.

[76] E. F. Keller and L. A. Segel. Initiation of slime mold aggregation viewed as an instability. *J. Theoret. Biol.*, 26(3):399–415, 1970.

[77] R. B. Kellogg and A. Tsan. Analysis of some difference approximations for a singular perturbation problem without turning points. *Math. Comp.*, 32(144):1025–1039, 1978.

[78] T. Koch, B. Hiller, M. E. Pfetsch, and L. Schewe, editors. *Evaluating gas network capacities*, volume 21 of *MOS-SIAM Series on Optimization*. Society for Industrial and Applied Mathematics (SIAM), Philadelphia, PA, 2015.

[79] M. Kramar and E. Sikolya. Spectral properties and asymptotic periodicity of flows in networks. *Math. Z.*, 249:139–162, 2005.

[80] M. Kramar Fijavž, D. Mugnolo, and E. Sikolya. Variational and semigroup methods for waves and diffusion in networks. *Appl. Math. Optim.*, 55(2):219–240, 2007.

[81] D. Kröner. *Numerical schemes for conservation laws*. Wiley-Teubner Series Advances in Numerical Mathematics. John Wiley & Sons, Ltd., Chichester; B. G. Teubner, Stuttgart, 1997.

[82] V. Kumar and G. Leugering. Singularly perturbed reaction-diffusion problems on a k-star graph. *Math. Methods Appl. Sci.*, 44(18):14874–14891, 2021.

[83] V. Kumar and G. Leugering. Convection dominated singularly perturbed problems on a metric graph. *J. Comput. Appl. Math.*, 425:Paper No. 115062, 26, 2023.

[84] Y.-S. Kwon and A. Novotný. Consistency, convergence and error estimates for a mixed finite element-finite volume scheme to compressible Navier-Stokes equations with general inflow/outflow boundary data. *IMA J. Numer. Anal.*, 42(1):107–164, 2022.

[85] C. D. Laird, L. T. Biegler, B. G. van Bloemen Waanders, and R. A. Bartlett. Contamination source determination for water networks. *J. Water Res. Plan. Man.*, 131:125–134, 2005.

[86] J. Lang and P. Mindt. Entropy-preserving coupling conditions for one-dimensional Euler systems at junctions. *Netw. Heterog. Media*, 13(1):177–190, 2018.

[87] C. Lattanzio and A. E. Tzavaras. Relative entropy in diffusive relaxation. *SIAM J. Math. Anal.*, 45(3):1563–1584, 2013.

[88] R. J. LeVeque. *Finite volume methods for hyperbolic problems.* Cambridge Texts in Applied Mathematics. Cambridge University Press, Cambridge, 2002.

[89] Y. Li, C. Mu, and Q. Xin. Global existence and asymptotic behavior of solutions for a hyperbolic-parabolic model of chemotaxis on network. *Math. Methods Appl. Sci.*, 45(11):6739–6765, 2022.

[90] B. Liljegren-Sailer and N. Marheineke. On port-Hamiltonian approximation of a nonlinear flow problem on networks. *SIAM J. Sci. Comput.*, 44(3):B834–B859, 2022.

[91] P. Marcati and A. Milani. The one-dimensional Darcy's law as the limit of a compressible Euler flow. *J. Differential Equations*, 84(1):129–147, 1990.

[92] V. Mehrmann and R. Morandin. Structure-preserving discretization for port-hamiltonian descriptor systems. In *2019 IEEE 58th Conference on Decision and Control (CDC)*, pages 6863–6868. IEEE, 2019.

[93] A. Morin and G. A. Reigstad. Pipe networks: Coupling constants in a junction for the isentropic euler equations. *Energy Procedia*, 64:140–149, 2015.

[94] D. Mugnolo. *Semigroup methods for evolution equations on networks.* Understanding Complex Systems. Springer, Cham, 2014.

[95] A. Novotný and I. Straškraba. *Introduction to the mathematical theory of compressible flow*, volume 27 of *Oxford Lecture Series in Mathematics and its Applications.* Oxford University Press, Oxford, 2004.

[96] S. F. Oppenheimer. A convection-diffusion problem in a network. *Appl. Math. Comput.*, 112:223–240, 2000.

[97] K. Osaki and A. Yagi. Finite dimensional attractor for one-dimensional Keller-Segel equations. *Funkcial. Ekvac.*, 44(3):441–469, 2001.

[98] A. Osiadacz. Simulation of transient gas flows in networks. *Int. J. Numer. Methods Fluids*, 4(1):13–24, 1984.

[99] H. G. Othmer, S. R. Dunbar, and W. Alt. Models of dispersal in biological systems. *J. Math. Biol.*, 26(3):263–298, 1988.

[100] A. Pazy. *Semigroups of linear operators and applications to partial differential equations*, volume 44 of *Applied Mathematical Sciences*. Springer-Verlag, New York, 1983.

[101] B. Perthame. Mathematical tools for kinetic equations. *Bull. Amer. Math. Soc. (N.S.)*, 41(2):205–244, 2004.

[102] B. Perthame. *Transport equations in biology*. Frontiers in Mathematics. Birkhäuser Verlag, Basel, 2007.

[103] B. Perthame, N. Vauchelet, and Z. Wang. The flux limited Keller-Segel system; properties and derivation from kinetic equations. *Rev. Mat. Iberoam.*, 36(2):357–386, 2020.

[104] S. C. S. Rao and V. Srivastava. Parameter-robust numerical method for time-dependent weakly coupled linear system of singularly perturbed convection-diffusion equations. *Differ. Equ. Dyn. Syst.*, 25(2):301–325, 2017.

[105] P. A. Raviart. Sur la résolution de certaines équations paraboliques non linéaires. *J. Functional Analysis*, 5:299–328, 1970.

[106] G. A. Reigstad. Existence and uniqueness of solutions to the generalized Riemann problem for isentropic flow. *SIAM J. Appl. Math.*, 75(2):679–702, 2015.

[107] H.-G. Roos and T. Linß. Sufficient conditions for uniform convergence on layer-adapted grids. *Computing*, 63(1):27–45, 1999.

[108] H.-G. Roos and T. Skalický. A comparison of the finite element method on Shishkin and Gartland-type meshes for convection-diffusion problems. volume 10, pages 277–300. 1997. International Workshop on the Numerical Solution of Thin-layer Phenomena (Amsterdam, 1997).

[109] H.-G. Roos, M. Stynes, and L. Tobiska. *Robust numerical methods for singularly perturbed differential equations*, volume 24 of *Springer Series in Computational Mathematics*. Springer-Verlag, Berlin, second edition, 2008. Convection-diffusion-reaction and flow problems.

[110] H.-G. Roos, L. Teofanov, and Z. Uzelac. Graded meshes for higher order fem. *J. Comput. Math*, 33(1):1–16, 2015.

[111] T. Roubíček. *Nonlinear partial differential equations with applications*, volume 153 of *International Series of Numerical Mathematics*. Birkhäuser/Springer Basel AG, Basel, second edition, 2013.

[112] M. Schmidt, D. Aßmann, R. Burlacu, J. Humpola, I. Joormann, N. Kanelakis, T. Koch, D. Oucherif, M. E. Pfetsch, L. Schewe, R. Schwarz, and M. Sirvent. GasLib – A Library of Gas Network Instances. *Data*, 2(4):article 40, 2017.

[113] L. Schöbel-Kröhn. *Analysis and numerical approximation of nonlinear evolution equations on network structures.* Dr. Hut, 2020.

[114] G. Singh and S. Natesan. Study of the NIPG method for two-parameter singular perturbation problems on several layer adapted grids. *J. Appl. Math. Comput.*, 63:683–705, 2020.

[115] M. Stynes and E. O'Riordan. Uniformly convergent difference schemes for singularly perturbed parabolic diffusion-convection problems without turning points. *Numer. Math.*, 55(5):521–544, 1989.

[116] G. Teschl. *Ordinary differential equations and dynamical systems*, volume 140 of *Graduate Studies in Mathematics.* American Mathematical Society, Providence, RI, 2012.

[117] V. Thomée. *Galerkin finite element methods for parabolic problems*, volume 25 of *Springer Series in Computational Mathematics.* Springer-Verlag, Berlin, second edition, 2006.

[118] A. Van Der Schaft and D. Jeltsema. Port-hamiltonian systems theory: An introductory overview. *Found. Trends Syst. Control.*, 1(2-3):173–378, 2014.

[119] M. Vlasák and F. Roskovec. On Runge-Kutta, collocation and discontinuous Galerkin methods: mutual connections and resulting consequences to the analysis. In *Programs and algorithms of numerical mathematics 17*, pages 231–236. Acad. Sci. Czech Repub. Inst. Math., Prague, 2015.

[120] T. Warburton and J. S. Hesthaven. On the constants in *hp*-finite element trace inverse inequalities. *Comput. Methods Appl. Mech. Engrg.*, 192(25):2765–2773, 2003.

[121] D. Wu. Signaling mechanisms for regulation of chemotaxis. *Cell research*, 15(1):52–56, 2005.

[122] Z. Xie and Z. Zhang. Uniform superconvergence analysis of the discontinuous Galerkin method for a singularly perturbed problem in 1-D. *Math. Comp.*, 79:35–45, 2010.

[123] H. Yee. Numerical approximation of boundary conditions with applications to inviscid equations of gas dynamics. Technical report, 1981.

Wissenschaftlicher Werdegang

Nora Marie Philippi
geboren am 15.3.1994 in Wiesbaden, Deutschland

28.8.2023	Verteidigung der Dissertation, TU Darmstadt
7.2022 – 9.2023	Wissenschaftliche Mitarbeiterin am Johann Radon Institute for Computational and Applied Mathematics, Linz, Österreich
7.2019 – 6.2022	Wissenschaftliche Mitarbeiterin am Fachbereich Mathematik, TU Darmstadt
4.2017 – 6.2019	Studium der Mathematik mit Abschluss M.Sc., TU Darmstadt
10.2013 – 4.2017	Studium der Mathematik mit Abschluss B.Sc., TU Darmstadt
2013	Abitur an der Gutenbergschule Wiesbaden